



HAL
open science

Dynamic covalent surfactants for the controlled release of bioactive volatiles

Eric Lutz

► **To cite this version:**

Eric Lutz. Dynamic covalent surfactants for the controlled release of bioactive volatiles. Other. Université de Strasbourg, 2014. English. NNT : 2014STRAF041 . tel-01647226

HAL Id: tel-01647226

<https://theses.hal.science/tel-01647226v1>

Submitted on 24 Nov 2017

HAL is a multi-disciplinary open access archive for the deposit and dissemination of scientific research documents, whether they are published or not. The documents may come from teaching and research institutions in France or abroad, or from public or private research centers.

L'archive ouverte pluridisciplinaire **HAL**, est destinée au dépôt et à la diffusion de documents scientifiques de niveau recherche, publiés ou non, émanant des établissements d'enseignement et de recherche français ou étrangers, des laboratoires publics ou privés.

ÉCOLE DOCTORALE DES SCIENCES CHIMIQUES
ICS - SAMS

THÈSE présentée par :
Eric LUTZ

soutenue le : **15 octobre 2014**

pour obtenir le grade de : **Docteur de l'université de Strasbourg**

Discipline/ Spécialité : Chimie Supramoléculaire

**Dynamic covalent surfactants for the
controlled release of bioactive volatiles**

THÈSE dirigée par :

Pr. Nicolas Giuseppone

Professeur, ICS - Université de Strasbourg

RAPPORTEURS :

Pr. Nicolas WISSINGER

Professeur - Université de Genève, Suisse

Pr. Kay SEVERIN

Professeur - Ecole polytechnique fédérale de Lausanne, Suisse

AUTRES MEMBRES DU JURY :

Dr. Jean-François LUTZ

Docteur, ICS - Université de Strasbourg

Résumé en français:

La chimie combinatoire dynamique (CDC), inspiré de la complexité des systèmes biochimiques, est basée sur l'utilisation de mélanges de molécules ayant la capacité à réagir entre elles via des liaisons covalentes réversibles, et formant des bibliothèques combinatoires virtuelles dont les constituants peuvent former l'ensemble des combinaisons possibles. Selon les conditions dans le milieu (Température, concentrations, pH, autres molécules en présence...), différentes molécules peuvent effectivement être formées et tout changement du milieu provoquera une réorganisation des espèces en présence. Le succès de cette approche dans différents domaines (découverte de substances biologiques actives, de catalyseurs, de nouveaux matériaux) a conduit à un développement rapide de la CDC, ainsi que d'autres domaines de la chimie pouvant tirer parti de cette diversité constitutionnelle et de cette capacité de sélection, telle que la chimie adaptative et la chimie de l'auto-organisation (un exemple étant la chimie des dynablocks).

Les dynablocks sont une nouvelle famille de tensio-actifs issus de la condensation réversible entre un bloc ayant des propriétés hydrophiles et un bloc hydrophobe, résultant en un auto-assemblage en solution aqueuse en mésophases structurées. Ces travaux ont été initiés lors des précédentes études dirigé par le Pr. Giuseppe qui a publié trois articles décrivant le comportement de ces amphiphiles covalents dynamiques basés sur l'association réversible entre un aldéhyde hydrophobe et des dérivés d'amines hydrophiles (Figure 1).

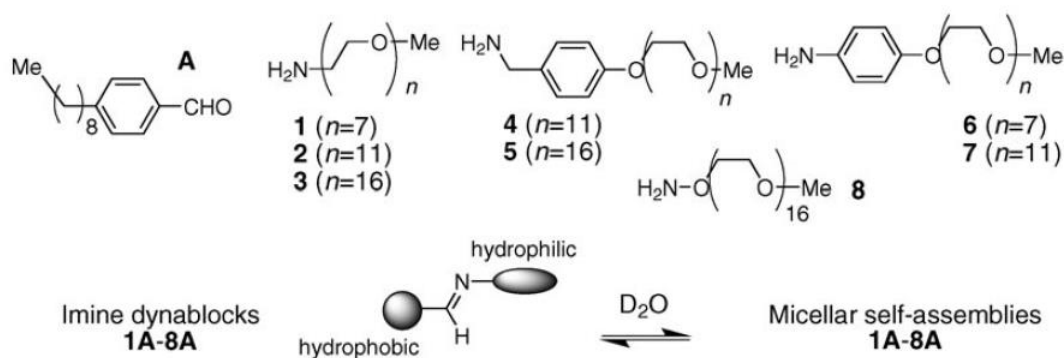


Figure 1. Structure des dynablocks. Les réactions des amines hydrophiles 1–8 avec l'aldéhyde hydrophobe A conduit aux imines 1A–8A.

En plus de l'équilibre thermodynamique au niveau moléculaire lié au caractère dynamique de la fonction chimique reliant les deux blocs du dynablock, un autre équilibre a lieu au sein de l'auto-assemblage micellaire supramoléculaire (Figure 2). Cet équilibre thermodynamique moléculaire supplémentaire confère des opportunités uniques de contrôler la stabilité de la structure entière. Par conséquent, ces objets peuvent être modifiés pour répondre à des stimuli extérieurs qui peuvent provoquer leur agrégation ou leur dissociation, et cela avec un contrôle cinétique poussé. De plus, le cœur hydrophobe de ces micelles fournit un espace suffisant pour solubiliser des molécules volatiles hydrophobes qui sont ensuite libérées en contrôlant la dissociation des micelles. Il a également été possible d'intégrer ces molécules volatiles au sein même des dynablocks, où leur relargage dans le milieu interviendra par déplacement des équilibres moléculaires et supramoléculaires.

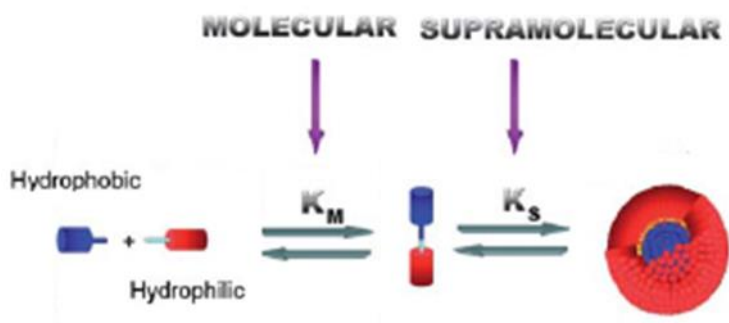


Figure 2. Structure des dynablocks. Les réactions des amines hydrophiles 1–8 avec l'aldéhyde hydrophobe A conduit aux imines 1A–8A.

La diversité des structures pouvant être obtenues (micelles sphériques, cylindriques, vésicules, lamelles...) selon la taille et la nature des différents blocs constituant les dynablocks entraîne un large éventail d'applications possibles, tel que la modification de nanoparticules, la catalyse, la formation de gels stimulables, l'encapsulation, la structuration de composés pour l'optoélectronique, etc.

Le but de ma thèse a été de concevoir, synthétiser et étudier des micelles constituées de dynablocks à la fois biocompatibles et capables de relarguer des molécules volatiles bioactives à partir d'une solution aqueuse sous l'influence de stimuli extérieurs tel que le pH ou la concentration. Cette thèse a été réalisée en collaboration avec Firmenich S.A., entreprise suisse de création d'arômes alimentaires et de parfums fondée en 1895, et leader du marché

mondial de la parfumerie et des arômes juste derrière Givaudan. Elle répond en partie à deux objectifs :

- a) Un objectif académique : Une meilleure compréhension de la chimie combinatoire dynamique appliquée à des systèmes supramoléculaires auto-assemblés.
- b) Un objectif industriel : L'obtention d'une famille de composés biocompatibles et peu onéreux présentant une large gamme de temps de relargage de molécules volatiles pouvant être utilisés dans des applications de parfumerie/cosmétique pour en améliorer les performances.

Mes travaux ont commencé par la synthèse de l'imine 7A et la continuation de l'étude de ses propriétés, notamment de sa cinétique d'hydrolyse en milieu aqueux dans une large gamme de pH (5-13) et de concentrations suivie par RMN, ainsi que de ses capacités à encapsuler différents aldéhydes hydrophobes. Cette dernière étude a été menée grâce à un suivi de la taille des particules par DLS ainsi que par des mesures de DOSY.

Une fois les cinétiques d'hydrolyse de cette imine connues dans une large gamme de pH et de concentration, mon étude s'est portée sur une modification de la stabilité des imines en solution par l'ajout de nouveaux groupes pouvant former des liaisons hydrogènes. Des dérivés du bloc hydrophobe et du bloc hydrophile contenant des groupes amide, carbamate et urée ont donc été synthétisés, et les imines correspondantes formées. Par ces expériences, il a été possible de montrer que les vitesses d'hydrolyse des imines peuvent être augmentées de façon parfois importante par déstabilisation de la structure micellaire. Néanmoins, ces systèmes n'ont que la capacité à augmenter la vitesse d'hydrolyse de l'imine, et nullement à la ralentir. Nous nous sommes donc orientés vers des dynablocks présentant une stabilité accrue pour arriver à cette fin.

La suite des travaux a donc été la synthèse d'oximes amphiphiles, et l'étude de leur stabilité dans l'eau à différents pH selon la taille de la chaîne polyéthylène glycol (PEG) et la nature de l'aldéhyde hydrophobe utilisé. Les oximes se sont révélés très stables, et le pH nécessaire pour détecter les composés issus de l'hydrolyse est très bas (<pH 1). La formation de dynablocks d'oximes présentant un groupe urée dans la partie hydrophobe n'a quant à elle pas été suffisante pour accélérer la vitesse d'hydrolyse, la stabilité du dynablock provenant essentiellement de la stabilité intrinsèque de la fonction oxime et non d'une stabilisation liée à l'autoassemblage supramoléculaire. J'ai donc poursuivi ma recherche dans le développement de nouvelles

structures (dérivés d'oximes) pouvant potentiellement offrir une stabilité intermédiaire entre les imines et les oximes.

Une partie importante des travaux réalisés concerne donc la synthèse et l'étude des cinétiques d'hydrolyse de dérivés de dynablocks possédants différents groupements fonctionnels, et ce dans le but d'avoir une large gamme de vitesses d'hydrolyse, à des pH compris entre 1 et 13. Il en résulte de ses travaux un ensemble de structures formant des micelles et pouvant encapsuler des composés hydrophobes avec des cinétiques d'hydrolyse comprises entre quelques minutes jusqu'à plusieurs mois, certains s'hydrolysant en milieux acide et d'autres en milieux basique voire neutre.

Une autre partie du projet a concerné quant à elle la synthèse de nouveaux dynablocks incorporant dans leur structure les composés à relarguer, et l'étude de leurs cinétiques d'hydrolyse selon la concentration et le pH. Ces nouveaux composés ont ensuite été incorporés dans des formulations industrielles pour comprendre l'influence du milieu (présence et concentration en cotensio-actifs, viscosité,...). Des liens Structure-Propriétés-Performances ont pu être établis, permettant de comprendre les résultats obtenus mais également de choisir la nature des dynablocks selon l'application choisie. Des cinétiques d'hydrolyse en présence de plusieurs dynablocks de nature différente ou en présence d'aldéhydes ont également été réalisées, dans le but de comprendre l'influence des recombinaisons entre constituants du mélange sur les vitesses d'hydrolyse. La dernière étape de ce projet étant une compréhension plus fine des structures en jeu par DOSY et par diffusion de neutrons (SANS), ainsi que par des mesures de performances en conditions réelles réalisées par Firmenich (Head-space).

Lors de ce travail, j'ai pu modifier un système existant (Dynablock) pour créer de nouvelles familles de molécules possédant des propriétés nouvelles (Biocompatibilité, contrôle poussé de la vitesse d'hydrolyse, capacité de relargage de molécules volatiles, faible coût...) grâce à un choix judicieux des blocs hydrophiles, conduisant à une déstabilisation ou à une stabilisation de la fonction imine en solution et donc à une large gamme de vitesse d'hydrolyse. J'ai également compris l'influence de nombreux paramètres du milieu sur la stabilité des imines en solution, pour ensuite appliquer les nouvelles molécules développées à des formulations industrielles, réussissant à avoir une large gamme de temps de relargage.

TABLE OF CONTENTS

ACKNOWLEDGEMENTS	13
ABBREVIATIONS AND SYMBOLS	15
INTRODUCTION	19
Chapter 1: Bibliography	23
1/ Supramolecular chemistry.....	23
2/ Dynamic combinatorial chemistry	24
a) Definitions and concepts.....	24
b) First examples of DCC.....	28
c) Functional materials and devices	34
3/ Surfactants	39
a) Low molecular weight amphiphiles.....	42
b) Block copolymer amphiphiles.....	44
c) Dynablocks.....	46
4/ Profragrances	51
a) Definitions and concepts.....	51
b) Non-dynamic profragrances	54
c) Dynamic profragrances	65
d) Use of precursors in marketed products.....	70
Chapter 2: Synthesis and characterization of dynablocks	73
1/ Chemistry of dynablocks.....	75
a) Choice of the reversible bond	75
b) Choice of the hydrophilic block	77
c) Choice of the hydrophobic block.....	79
d) Design of dynablocks	80
2/ Synthesis of the hydrophilic amine derivatives.....	81
a) General synthetic scheme for PEG functionalisations.....	81
b) Tosylation of PEGs.....	82
c) Substitution of tosylated PEGs and deprotection	83
d) Synthesis of PEGs with hydrogen bonding abilities.....	87
3/ Synthesis of aldehydes.....	91
a) Hydrophobic benzaldehyde derivative.....	91
b) Hydrophilic benzaldehyde derivative	92
4/ Synthesis of imine derivatives	93
a) Oximes.....	95
b) Semicarbazone	97
c) Imines for encapsulation	98
d) Imines for the study of hydrophobic chain length on micellisation.....	101
e) Aliphatic imines as profragrances	103
f) Acyloximes	105

Chapter 3: Kinetics of hydrolysis and encapsulation properties of dynablocks109

1/ Hydrolysis of imine derivatives (for encapsulation applications)	110
a) Study of aromatic imines.....	110
b) Study of aliphatic imines	121
c) Hydrolysis of oximes	134
d) Hydrolysis of semicarbazone 30	135
e) Hydrolysis of acyloximes	136
2/ Characterisation of micelles and of their encapsulation properties	139
a) Encapsulation followed by DLS.....	139
b) Encapsulation followed by DOSY NMR.....	142
c) TEM	145
3/ Conclusion.....	147

Chapter 4: Study of dynamic profragrances and their kinetics of hydrolysis151

1/ Hydrolysis of amphiphilic hexylcinnamal-based profragrances.....	152
a) Hydrolysis at 10 mM.....	152
b) Influence of concentration	157
c) Influence of pH	159
d) Kinetic considerations	162
2/ Hydrolysis of amphiphilic citral-based profragrances	165
a) Hydrolysis at 10 mM.....	165
b) Influence of concentration	167
c) Influence of pH	169
3/ Hydrolysis of non-amphiphilic profragrances	170
a) Hydrolysis of M1000 Vanillin	170
b) Hydrolysis of M600-based profragrances	171
4/ Mixture of several imines/aldehydes.....	173
a) Mixture of imines	173
b) Mixture of imine and aldehyde.....	174
5/ Influence of hydrophobic chain length, co-surfactants and viscosity	177
a) Influence of the hydrophobic chain length	177
b) Influence of the presence of co-surfactants.....	180
c) Influence of the concentration of co-surfactants	194
d) Influence of the concentration of salt in liquid body wash	195
6/ Hydrolysis of profragrances in formulations.....	197
a) Liquid body-wash.....	198
b) Liquid Detergent	203
c) Solid Soap	207
7/ Conclusion.....	210

Conclusions and Perspectives213

EXPERIMENTAL PART.....215

Syntheses and characterization of organic compounds.....217

1/ Background on the experimental methods for the analyses of dynablocks	217
2/ General Procedures	223

a) Solvent and chemical reagents	223
b) Chromatographic methods.....	223
c) Analytical methods and instruments.....	223
3/ Synthesis of hydrophilic amine derivatives.....	226
4/ Synthesis of aldehydes.....	235
5/ Synthesis of dynablocks	237
a) Oximes.....	237
b) Semicarbazone	240
c) Imines	241
6/ Acyloxime.....	250
7/ Kinetic experiments of dynablocks hydrolysis followed by ¹ H NMR.....	251
8/ Kinetic experiments of dynablocks hydrolysis in formulations followed by ¹ H NMR	251
9/ Competition experiments of dynablocks studied by ¹ H NMR	252

ACKNOWLEDGEMENTS

I would like to thank my PhD advisor Nicolas Giuseppone, who has chosen me for this important project and who always had confidence in me. I will not forget all the interesting discussions we had during the (long) ways between Strasbourg and Geneva. I also thank Dr. Andreas Herrmann, for guiding me in this project and for his warm welcomes at Firmenich in Geneva, as well as all the other members of Firmenich who followed my work and gave me very useful advices (Daniel, Damien, Vera and Wolfgang).

I would like then to thank Dr. Emilie Moulin, who has continuously helped me from the beginning to the end of my thesis. I am grateful to celine, melodie and odile for their technical support and to Dr. Gad Fuks for sharing with me his vision of an alternative world. I also thank all the people who helped me for the characterisations, notably Vincent bruno for DOSY measurements and Eric Buhler for neutron scattering.

I greatly appreciated to work in the SAMS team and would like to thank all the PhDs and post-docs who make or made this team so lively. A special thank you to Dr. "Master" Busseron and to Dr. Yves Ruff for their extensive teaching about chemistry and life. A very special thank you to Dr. Zanirati for his teaching of patience. I also would like to thank all the very nice people in the institute and especially all my friends from the Schaff team. You all have made these three years very special.

A huge thank you to my Solnyshko and to my family, who were and will always be by my side.

Finally, I thank Prof. Kay Severin, Prof. Nicolas Wissing and Dr. Jean-françois Lutz for examining my work and I am honoured by their attention.

Acknowledgements

ABBREVIATIONS AND SYMBOLS

Å	Angström
ATP	Adenosine triphosphate
aq	aqueous
a.u.	Arbitrary unit
BCC	Body Centred Cubic
Boc	<i>tert</i> -butyloxycarbonyl
C	Concentration
°C	Celsius Degree
CDI	1,1'-Carbonyldiimidazole
C _{eq}	Concentration at equilibrium
CMC	Critical micellar concentration
D	Diffusion coefficient
d.	Day
DCA	Dynamic Covalent Amphiphiles
DCC	Dynamic Combinatorial Chemistry
DCL	Dynamic Combinatorial Library
DIBAL-H	Diisobutylaluminium hydride
DLS	Dynamic Light Scattering
DMSO	Dimethylsulfoxide
DNA	Deoxyribonucleic acid
DOSY	Diffusion-Ordered Spectroscopy
EDC	1-Ethyl-3-[3-dimethylaminopropyl]carbodiimide hydrochloride
EO	Ethylene oxide
eq., equiv.	Equivalent
ESI-MS	Mass Spectrometry with Electrospray Ionisation

Abbreviations and symbols

EtOAc	Ethyl Acetate
f	Friction factor
G	Gyroid
h.	Hour
h	Planck Constant
H _{1/2}	Half-time of hydrolysis
HEPES	4-(2-hydroxyethyl)-1-piperazineethanesulfonic acid
HEX	Hexagonally packed cylinders
HPLC	High Performance Liquid Chromatography
Hr	Hydrodynamic radius
<i>J</i>	Coupling Constant
k	Boltzmann Constant
K	Kelvin
K _d	Dissociation Constant
LAM	Lamellae
LC/MS	Liquid Chromatography coupled to Mass Spectrometry
LogP	Octanol-water partition coefficient
λ _{max}	Incident and scattered wavelength
M	Molarity (g.mol ⁻¹)
M1000	Huntsman Jeffamine M1000
M2070	Huntsman Jeffamine M2070
min.	minute
mL	Millilitre
MS	Mass Spectrometry
η	viscosity
nM	nanomolar
nm	nanometer

Abbreviations and symbols

NMR	Nuclear Magnetic Resonance
ν	Frequency
PEG	poly(ethylene glycol)
pm	picometer
PO	Propylene oxide
ppm	Parts per million
RT	Room Temperature
SANS	Small Angle Neutron Scattering
SAS	Small Angle Scattering
SAXS	Small Angle X-ray Scattering
SLS	Static Light Scattering
T	Temperature
TEA	Triethylamine
TEM	Transmission Electronic Microscopy
T_g	Glass transition temperature
T_s	Tosyl (p-CH ₃ C ₆ H ₄ SO ₂)
TLC	Thin Layer Chromatography
Tyr	Tyramine
UPLC	Ultra Performance Liquid Chromatography
V_0	Initial speed of hydrolysis
VCL	Virtual Combinatorial Library
wt%	Percentage in weight

Introduction

INTRODUCTION

Fragrances are volatile and mostly hydrophobic bioactive compounds employed in numerous products in our everyday life. To perceive the odour of these compounds they should evaporate from various surfaces to be transported via diffusion through the air, to reach the olfactory receptors in our nose. Efficient evaporation of these compounds is obtained by high vapour pressures of the fragrances which, at the same time, limits the duration of perception. To increase the performance of flavours and fragrances in consumer products there is a need for innovative, efficient delivery systems, either based on encapsulation^{[1][2]} or on the preparation of cleavable precursors (profragrances).^[3] In this context, the use of dynamic combinatorial chemistry (DCC) might be promising to control the release of mixtures of fragrance aldehydes and ketones in typical applications of functional perfumery.

As fragrance applications are typically water-based systems formulated in the presence of surfactants, the reversible assembly of surfactant/fragrance micelles could be an interesting way to proceed.

In previous studies in our group, we described the behaviour of a new kind of amphiphilic dynamic objects constructed by the reversible association between a hydrophobic aldehyde and a series of hydrophilic amines or hydroxylamines.^[4] The structures of the molecules were chosen to be as simple as possible (aliphatic chains combined with polyethyleneglycol chains (PEG)), and are thus biocompatible and readily accessible in large quantities. The nature of the reversible linkage, namely the imine bond, was chosen for its reliability in the condensation reaction, and also for further studies concerning the influence of the supramolecular structure stabilization on the amphiphile molecular association (Figure 1).

Indeed, an imine bond can be hydrolysed by a molecule of water and as a consequence, imines are usually not stable in water and mostly dissociate. However, he has shown that the coupling of this imine formation in water, together with a level of supramolecular organization (i.e. the formation of micelles), can produce much more stable imines that would be otherwise fully hydrolysed in the absence of this hierarchical assembly. Moreover, it has

^[1] Augustin, M. A.; Hemar, Y., Nano- and micro-structured assemblies for encapsulation of food ingredients. *Chem Soc Rev*, **38** (4), 902-912 (2009)

^[2] Park, S.-J. Arshady, R., Microcapsules for fragrances and cosmetics, *Microspheres, Microcapsules, Liposomes*, **6**, 157-198 (2003)

^[3] Herrmann, A. Controlled release of volatiles under mild reaction conditions: from nature to everyday products, *Angew. Chem. Int. Ed.*, **46**, 5836–5863 (2007).

^[4] Rémi Nguyen, Ph.D. Thesis “Dynamic Combinatorial Mesophases and Self-Replicating Systems”, University of Strasbourg (2010).

been seen that an aldehyde could be incorporated inside the micellar self-assembly, increasing its local concentration and preventing it from separating from the aqueous solution.

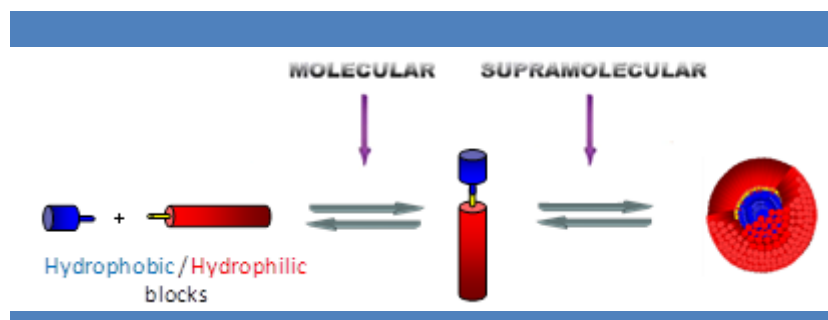


Figure 1 | Schematic representation of a Dynamic Covalent Amphiphile (DCA) that produces micellar structures.

Based on the previous observations, our objective was to understand and to control the kinetics of hydrolysis of chemically different imine derivatives upon various external conditions. The influence of the imine concentration and the pH was systematically measured, and the structural stabilisation of the imine bond was tuned by the creation of additional reversible covalent bonds within the micelles. This work has led us to have families of molecules with a broad range of half-time of hydrolysis. In parallel, the possibility to dissolve hydrophobic fragrances in the micellar core was assessed, furnishing information about the ability of the dynablocks to incorporate fragrances, but also on their kinetics of release.

The study of profragrances was then envisaged. They result from the reversible condensation of fragrance aldehydes with both synthesised and commercial amine derivatives. The incorporation of aldehyde inside the dynablock structure was expected to give several interesting results, from the protection of the aldehyde moiety from hydrolysis or degradation to its slow release in the environment. The influence of the conditions used for further application, such as the presence of co-surfactants, was also studied for the *in fine* incorporation of these profragrance into consumer products.

Although it would have been interesting to also present in this thesis some results already obtained in industrial applications, it was unfortunately not possible; the possible applications are still under investigation, and unveiling early information will prevent the protection of the intellectual property. Our work during the whole Ph.D. was focused on the development of these applications, and some directions taken for my investigation were driven by their

Introduction

preliminary results. Nevertheless, I hope that I managed to make this manuscript clear enough to understand our approach without this information.

My manuscript is composed of four chapters. The first one gives a bibliographic overview of the scientific fields featured by the project: supramolecular chemistry, dynamic combinatorial chemistry, surfactants, and profragrances.

The second chapter concerns the molecular design of the dynablocks and their synthesis. The distinction was made between the different amphiphiles according to the proposed applications: encapsulating systems and profragrances.

The third chapter describes the kinetics of hydrolysis of various imine-type amphiphiles. It starts with aromatic and aliphatic imines and continues with more stable bonds, namely oximes and semicarbazones. The study of several dynablocks based on acyloxime is also proposed. In a second part of this chapter, the micelles and their encapsulation properties are measured using DLS and DOSY NMR.

The fourth chapter deals with the kinetics of hydrolysis of citral and hexylcinnamal-based profragrances, and the effects of several parameters such as the CMC, the viscosity, or the presence of co-surfactants. Finally, these profragrances were incorporated into model applications and their performance were assessed.

Chapter 1: Bibliography

Chapter 1: Bibliography

1/ Supramolecular chemistry

Supramolecular chemistry,^[5] defined as « chemistry beyond the molecule »^{[6][7]} by Jean-Marie Lehn (Nobel Prize of Chemistry 1987) constitutes a very active research field that has evolved toward a multitude of subfields, at the crossroad between chemistry, biology and physics. For a century, research in chemistry has mainly been dedicated to studies on the structure of molecules and to covalent bonding; nowadays, chemistry is also strongly focused on the study of non-covalent bonds.

Supramolecular chemists are interested by the study of self-assembled systems obtained thanks to non-covalent interactions like hydrogen bonds, ionic bonds, π - π interactions, metal-ligands interactions, electrostatic interactions, Van-der-Waals forces and hydrophobic interactions^{[8][9]}. The detailed comprehension of intermolecular bonds, from both a theoretical and an experimental point of view, has made possible the programmed formation of a broad variety of supramolecular architectures with the goal to obtain particular properties (magnetic^[10], electronic^[11], optic, rheological...)^[12]. The combination of polymer chemistry with supramolecular chemistry defines the recent field of supramolecular polymer chemistry^{[13][14]}, where molecular interactions and recognition processes are used to generate main-chain (or side-chain) supramolecular polymers through the self-assembly of complementary components.

Through the manipulation of non-covalent intermolecular interactions was developed a chemistry of molecular interactions that implies the storage of information inside its structure at the molecular scale. Its reading, transfer, and processing happens at the supramolecular level by specific interactional algorithms that operate through molecular recognition based on patterns able to form specific interactions (groups of hydrogen bonding, sequences of donor-

^[5] Lehn, J.-M. *Supramolecular Chemistry: Concepts and Perspectives* (VCH, Weinheim, 1995).

^[6] Lehn, J.-M. *Supramolecular Chemistry - Scope and Perspectives. Molecules, Supermolecules, and Molecular Devices* (Nobel Lecture), *Angew.Chem. Int. Ed. Engl.* **27**, 89–112 (1988)

^[7] Desiraju, G. R. Chemistry beyond the molecule. *Nature* **412**, 397–400 (2001).

^[8] Schneider, H.; J. Binding Mechanisms in Supramolecular Complexes. *Angew.Chem. Int. Ed.* **48**, 3924–3977 (2009).

^[9] Steed, J. W.; Atwood, J. L. *Supramolecular Chemistry*, John Wiley & Sons, Chichester (2000)

^[10] Mukherjee, T.; Costa Pessoa, J.; Kumar, A.; Sarkar, A. R., Synthesis, structure, magnetic properties and biological activity of supramolecular copper(ii) and nickel(ii) complexes with a Schiff base ligand derived from vitamin B6. *Dalton Trans.*, **42** (7), 2594–2607 (2013)

^[11] Jortner, J.; Ratner, M. Eds., *Molecular Electronics*, Blackwell, Oxford (1997).

^[12] Lehn, J.-M. Toward Self-Organization and Complex Matter. *Science* **295**, 2400–2403 (2002).

^[13] Ciferri, A. Ed., *Supramolecular Polymers*, Dekker, New York (2000).

^[14] Brunsveld, L.; Folmer, B. J. B.; Meijer, E. W.; Sijbesma, R. P. *Chem. Rev.* **101**, 4071 (2001).

acceptor interactions, sites of ionic coordination).^[15] Based on kinetically labile and energetically weak bonds, supramolecular systems are dynamic and reversible, providing them with a multitude of potential properties including an ability to self-organise into more complex architectures^[16] as well as self-healing properties^[17] linked to an error-correcting process to reach an energetic minimum. Since biological processes take place in an aqueous environment, water is of interest to study supramolecular systems,^{[18][19]} where it weakens polar interactions by favouring hydrophobic effects. Since the emergence of supramolecular chemistry, supramolecular systems with increased complexity have been created in order to reach the complexity level achieved in biological mechanisms^{[20][12]}. This ever increasing complexity has given birth to multi-component systems able to adapt to the environmental stimuli. The combination of the concept of supramolecular chemistry, namely molecular recognition and self-assemblies processes, linked to the possibility to create libraries of components that can give rise to many different possible combinations has given birth during the 90s to the new concept of «dynamic combinatorial chemistry».

2/ Dynamic combinatorial chemistry

a) Definitions and concepts

Dynamic combinatorial chemistry (DCC), while continuing to use the concepts of supramolecular chemistry, offers new possibilities by expanding its scope to the use of dynamic combinatorial libraries (DCLs), within which reversible bonds are created between various building blocks (Figure 2).^{[21][22][23][24]} These systems, that contain only building blocks with different complementary functionalities at initial time, present at equilibrium both the unreacted reactants and a mixture of all possible products that could have been formed

^[15] Lehn, J.-M. Programmed Chemical Systems: Multiple Subprograms and Multiple Processing/Expression of Molecular Information. *Chem. Eur. J.* **6**, 2097–2102 (2000).

^[16] Lehn, J.-M. Toward complex matter: Supramolecular chemistry and self-organization. *Proc. Nat. Acad. Sci. USA* **99**, 4763–4768 (2002).

^[17] Furlan, R. L. E.; Otto, S.; Sanders, J. K. M. Supramolecular templating in thermodynamically controlled synthesis. *Proc. Natl. Acad. Sci. USA* **99**, 4801–4804 (2002).

^[18] Oshovsky, G.V.; Reinhoudt, D. N.; Verboom, W. Supramolecular Chemistry in Water. *Angew. Chem., Int. Ed.* **46**, 2366–2393 (2007)

^[19] Zayed, J. M.; Nouvel, N.; Rauwald, U.; Scherman, O. A. Chemical complexity-supramolecular self-assembly of synthetic and biological building blocks in water. *Chem. Soc. Rev.* **39**, 2806–2816 (2010)

^[20] Lehn, J.-M., Perspectives in Chemistry—Steps towards Complex Matter. *Angew. Chem., Int. Ed.* **52**, 2836–2850 (2013)

^[21] Lehn, J.-M. Dynamic Combinatorial Chemistry and Virtual Combinatorial Libraries. *Chem. Eur. J.* **5**, 2455–2463 (1999).

^[22] Miller, B. L. Dynamic Combinatorial Chemistry: In Drug Discovery, Bioorganic Chemistry, and Materials Science, John Wiley & Sons (2010)

^[23] Reek, J. N. H.; Otto, S. Dynamic Combinatorial Chemistry, John Wiley & Sons (2010)

^[24] Corbett, P. T.; Leclaire, J.; Vial, L.; West, K. R.; Wietor, J. L.; Sanders, J. K. M.; Otto, S., Dynamic combinatorial chemistry. *Chem Rev*, **106**, 3652–3711 (2006)

between the complementary reactants. The existence of various species as well as the relative proportions of the different components is determined by thermodynamics. Therefore, it becomes possible to modify this equilibrium by changing internal or external parameters, and thus shifting the equilibria toward the amplification of given products after an adaptation process that will occur through an *in situ* screening of these species.

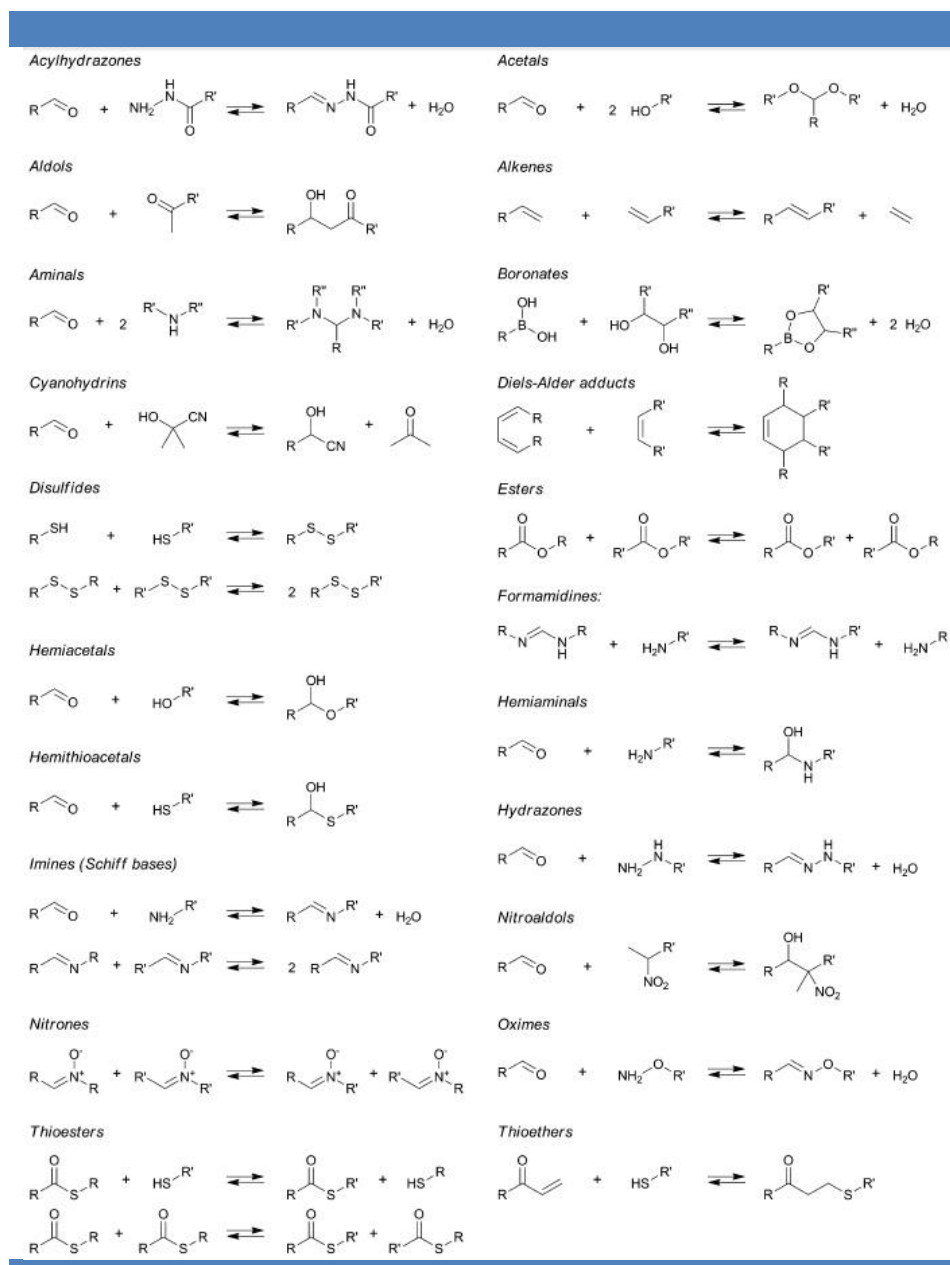


Figure 2 | Reversible reactions explored in DCC to read, generate or modulate the bioactivity of compounds.^[25]

^[25] Herrmann, A., Dynamic combinatorial/covalent chemistry: a tool to read, generate and modulate the bioactivity of compounds and compound mixtures. *Chem Soc Rev.* **43.** 1899-1933 (2014)

The concept of Dynamic Combinatorial Chemistry can be illustrated through the lock and key representation (Figure 3):

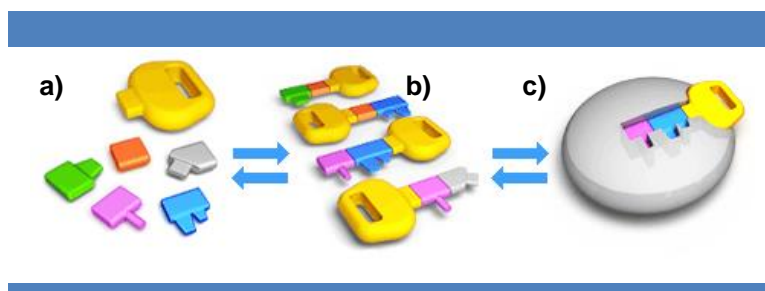


Figure 3 | Schematic representation of the basic principles of dynamic combinatorial chemistry in the framework of a guest/host interaction.^[15]

The process is composed of two distinct equilibria: the first one that takes place at the molecular or supramolecular level between the building blocks and the self-assembled building blocks, and the second one at the supramolecular level between the self-assembled entities and a substrate.

For the first equilibrium a) \leftrightarrow b), building blocks, capable of reversibly interacting together, form a library of higher molecular weight molecules or self-assemblies arising from all the possible reactions.

For the second equilibrium b) \leftrightarrow c): the best fitted member(s) of the library interact with a given substrate, leading to their amplification and selection due to an equilibrium shift.

The amplification process will depend on the strength of the interaction between the substrate and the library members. A direct comparison between the concentrations of the different species in presence or absence of substrate will then directly show which molecules interact more preferably with the substrate. This approach has been used for the selection of ligands in catalysis^[26] or the screening of inhibitors in drug discovery.^[27]

However, in some precise conditions, the amplification process does not furnish the best binder to a substrate. This phenomenon has been described by Severin, who has found out that an increasing quantity of target could lead to a decrease in concentration of the species having

^[26] Brouwer, A. J.; Linden, H.; Liskamp, R. M. J. Combinatorial Chemistry for Ligand Development in Catalysis: Synthesis and Catalysis Screening of Peptidosulfonamide Tweezers on the Solid Phase *J. Org. Chem.* **65**, 1750-1757 (2000)

^[27] Ramström, O., Lehn, J.-M. Drug Discovery by Dynamic Combinatorial Libraries. *Nat. Rev. Drug Disc.* **1**, 26-36 (2002).

the higher thermodynamic stability.^[28] Following this observation by Severin, other theoretical work by Sanders has revealed that the risk of false positive is decreasing when the size of the library is increasing.^[29]

Since the first achievements, DCC has evolved and triggers other than guest/host interactions have been studied. Nowadays, systems developed for DCC achieve amplification through variations between coupled equilibria induced by modifying chemical (pH,^{[30][31]} solvent, metal ions concentration^[32]) and physical parameters (temperature,^{[31][33]} shearing,^{[34][35]} electric fields^{[36][37]}).

DCC presents great assets to become one of the main tools for the design of “smart” materials^{[38][39]}:

- Systems in the framework of DCC are sensitive to initial compositions of the system, and will evolve over time.
- A reversible change of the properties (chemical, physical) of the system is possible by using external perturbations.
- A large choice of building blocks is available leading to an infinite number of combinations.

^[28] Saur, I.; Severin, K. Selection experiments with dynamic combinatorial libraries: the importance of the target concentration. *Chem. Commun.* 1471–1473 (2005).

^[29] Corbett, P. T.; Otto, S.; Sanders, J. K. M. Correlation between host-guest binding and host amplification in simulated dynamic combinatorial libraries. *Chem. Eur. J.* **10**, 3139–3143 (2004).

^[30] Tauk, L.; Schroder, A. P.; Decher, G.; Giuseppone, N., Hierarchical functional gradients of pH-responsive self-assembled monolayers using dynamic covalent chemistry on surfaces. *Nat Chem*, **1** (9), 739-739 (2009)

^[31] Giuseppone, N.; Lehn, J.-M. Protonic and temperature modulation of constituent expression by component selection in a dynamic combinatorial library of imines. *Chem. Eur. J.* **12**, 1715–1722 (2006).

^[32] Giuseppone, N.; Lehn, J. M., Constitutional dynamic self-sensing in a zinc(II)/polyiminofluorenes system. *J Am Chem Soc*, **126** (37), 11448-11449 (2004)

^[33] Giuseppone, N.; Fuks, G.; Lehn, J.-M. Tunable Fluorene-Based Dynamers through Constitutional Dynamic Chemistry. *Chem. Eur. J.* **12**, 1723–1735 (2006).

^[34] Carnall, J. M. A.; Waudby, C. A.; Belenguer, A. M.; Stuart, M. C. A.; Peyralans, J. J. P.; Otto, S., Mechanosensitive Self-Replication Driven by Self-Organization. *Science*, **327** (5972), 1502-1506 (2010)

^[35] Li, J.; Carnall, J. M. A.; Stuart, M. C. A.; Otto, S., Hydrogel Formation upon Photoinduced Covalent Capture of Macrocyclic Stacks from Dynamic Combinatorial Libraries. *Angew. Chem. Int. Ed.*, **50** (36), 8384-8386 (2011)

^[36] Giuseppone, N.; Lehn, J.-M. Electric-Field Modulation of Component Exchange in Constitutional Dynamic Liquid Crystals. *Angew. Chem. Int. Ed.* **45**, 4619–4624 (2006).

^[37] Herrmann, A.; Giuseppone, N.; Lehn, J.-M. Imine Based Liquid Crystals for the Controlled Release of Bioactive Materials. *Chem. Eur. J.* **15**, 117–124 (2009).

^[38] Mann, S. Life as a Nanoscale Phenomenon. *Angew. Chem. Int. Ed.* **47**, 5306–5320 (2008).

^[39] Herrmann A. Dynamic mixtures and combinatorial libraries: imines as probes for molecular evolution at the interface between chemistry and biology. *Org. Biomol. Chem.* **7**, 3195–3204 (2009).

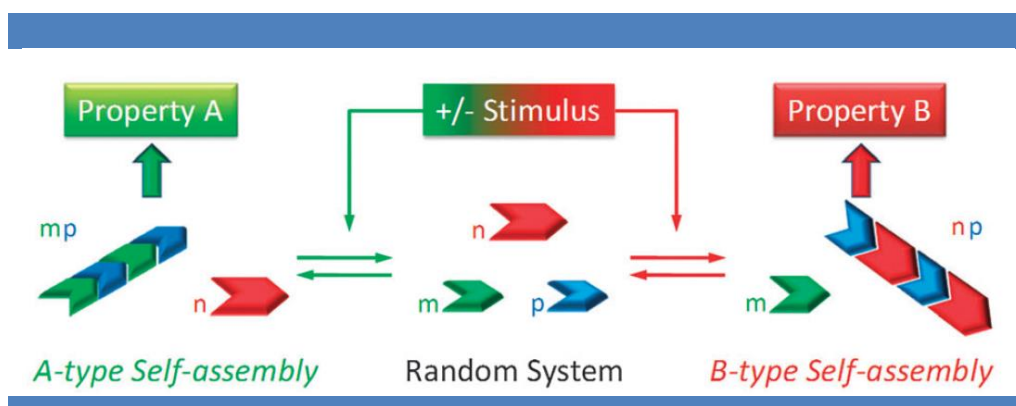


Figure 4 | General functioning principle of a dynamic combinatorial material.^[40]

In Figure 4, a representation of such smart material based on DCC is displayed. Here, depending on a selection process mediated by an external stimulation, either the red or the green molecular unit can be self-assembled with the blue one, among all the other possible intermediate combinations. As a result, and based on an external control, the overall system expresses a given property originating from the selected self-assembly.^[33]

Since the conceptualisation of supramolecular chemistry and DCC, a broad variety of chemical systems have been developed, based on a variety of different interactions and possibly leading to new functional materials. The next part of this chapter will be dedicated to the short and non-exhaustive presentation of some of these systems.

b) First examples of DCC

One of the first examples describing the reshuffling of supramolecular entities as a dynamic combinatorial system was published by Lehn *et al.* in 1996.^[41] A mixture of trisbipyridine ligands and iron(II) ions (Figure 5) in an equimolar ratio was shown to produce a mixture of circular helicates of variable sizes (tetrameric, pentameric...).

^[40] Moulin, E.; Cormos, G.; Giuseppone, N. Dynamic combinatorial chemistry as a tool for the design of functional materials and devices. *Chem. Soc. Rev.* **41**, 1031–1049 (2012)

^[41] Hasenknopf, B.; Lehn, J.-M.; Kneisel, B. O.; Baum, G.; Fenske, D. Self-Assembly of a circular Double Helicate. *Angew. Chem. Int. Ed.* **35**, 1838–1840 (1996).

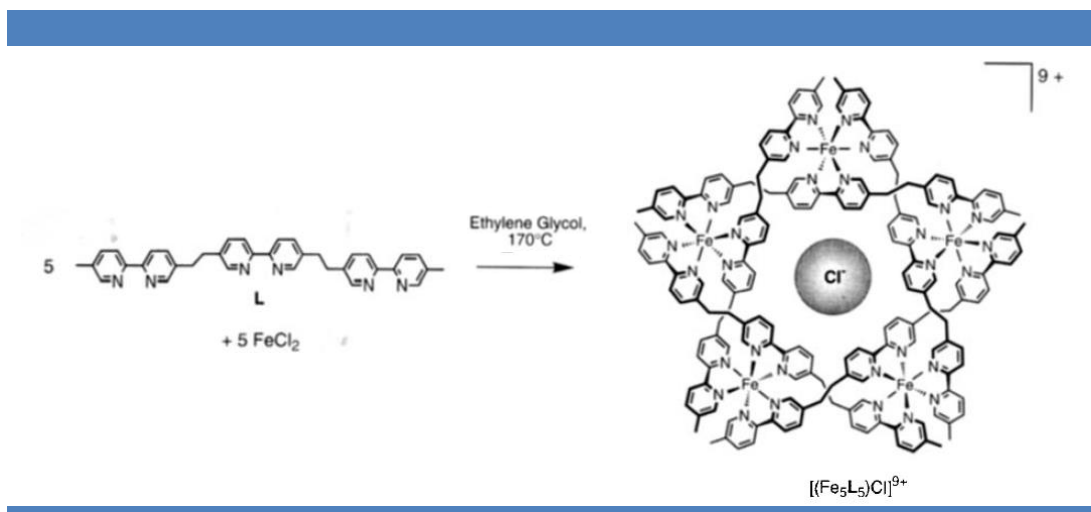


Figure 5 | Self-assembly of circular helicate [(Fe₅L₅)Cl]⁹⁺ from five trisbipyridine ligands and five equivalents of FeCl₂ (Hasenknopf *et al.*).^[41]

It was found that the counter-ions associated to iron(II) and which are complexed within the cavity of the cyclic structures induce the size of the helicates, as proved by the amplification of the pentameric structure in the presence of FeCl₂ and of the hexameric one in the presence of FeSO₄.^[42]

In 1997, Brady and Sanders reported the thermodynamically-controlled cyclisation and interconversion of oligocholates.^[43] This “living macrolactonisation”, obtained through a reversible transesterification, leads to the formation of macrocycles, from dimers up to pentamers (Figure 6).^[44]

^[42] Hasenknopf, B.; Lehn, J.-M.; Boumediene, N.; Dupont-Gervais, A.; VanDorsselaer, A.; Kneisel, B.; Fenske, D. Self-Assembly of Tetra- and Hexanuclear Circular Helicates. *J. Am. Chem. Soc.* **119**, 10956-10962 (1997).

^[43] Brady, P. A.; Sanders, J. K. M. Thermodynamically-controlled cyclisation and interconversion of oligocholates: Metal-ion templated 'living' macrolactonisation. *J. Chem. Soc. Perkin Trans I* 3237-3254 (1997).

^[44] Brady, P. A.; Bonar-Law, R. P.; Rowan, S. J.; Suckling, C. J.; Sanders, J. K. M. "Living" macrolactonisation: thermodynamically-controlled cyclisation and interconversion of oligocholates. *J. Chem. Soc. Chem. Commun.* 319-320 (1996).

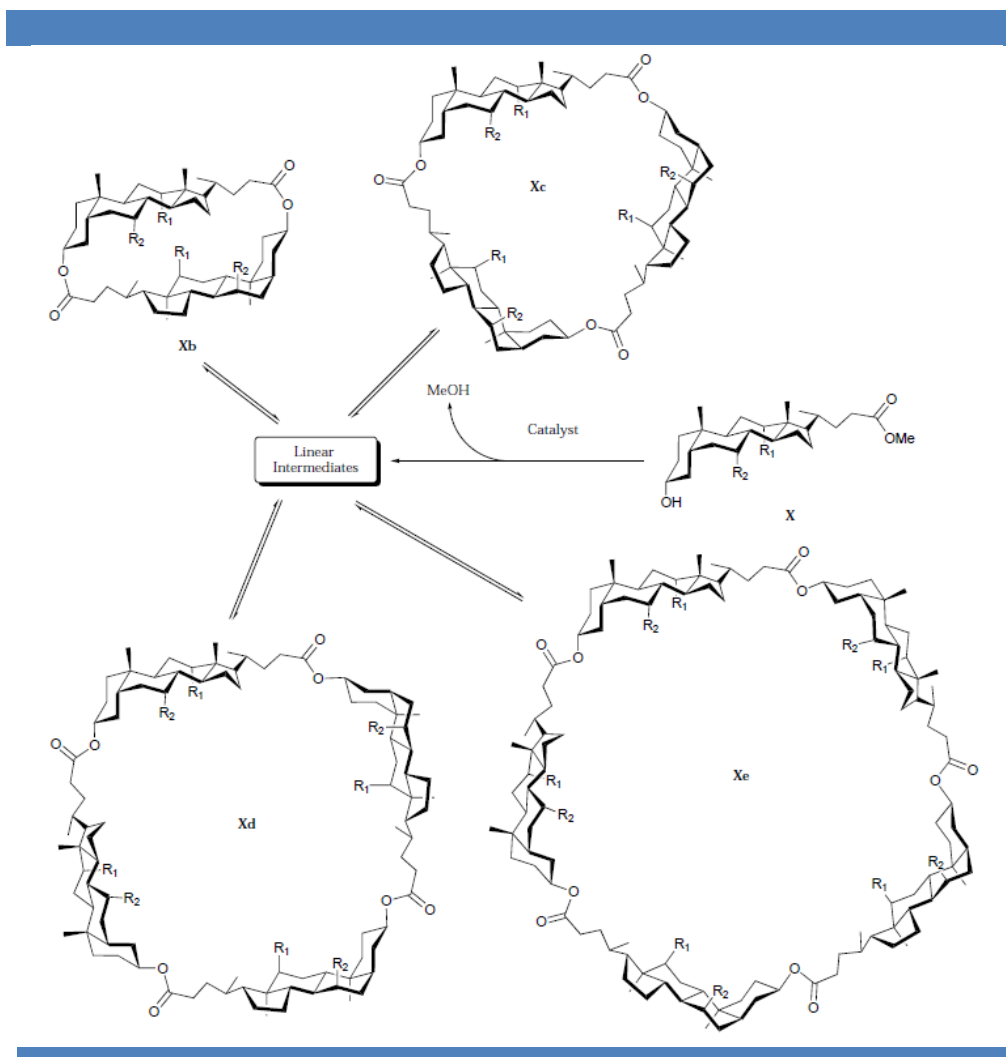


Figure 6 | An equilibrating mixture of cyclic steroid oligomers (Sanders *et al.*).^[43]

Ion-binding side chains were then grafted to the backbone of the cholate in order to change the relative proportion of the different oligomers. When different iodine salts of several metals, including lithium, sodium, potassium, and cesium were tested, only sodium had an important templating effect on the macrocycles, which result in doubling the quantity of tetramer.

The same year, Huc and Lehn published a key article for the development of DCC, in which concepts and experiments met in the framework of the synthesis of carbonic anhydrase inhibitors (Figure 7).^[45]

^[45] Huc, I.; Lehn, J.-M. Virtual combinatorial libraries: dynamic generation of molecular and supramolecular diversity by self-assembly. *Proc. Nat. Acad. Sci. USA* **94**, 2106–2110 (1997).

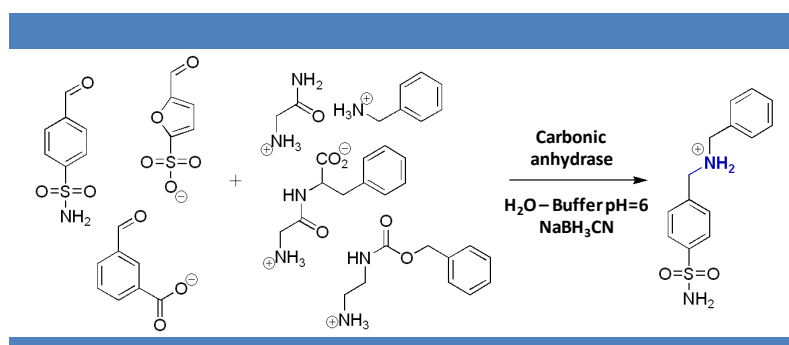


Figure 7 | DCL of imines that interact with carbonic anhydrase ; the structure shown after reduction is that amplified in the presence of the enzymatic target (Huc and Lehn).^[45]

In that case, the reaction of formation and exchange of imines is used for the generation of diversity in a library owing to its fast kinetics of recombination in water. The mixture of three primary amines and of four distinct substituted aldehydes leads to the formation of 12 discrete constituents. The substituents were chosen to mimic known inhibitors of carbonic anhydrase, namely capable of interactions with the Zn^{2+} chelation site (sulphonamide group), and also with the neighbouring hydrophobic pocket. An excess of amine was used to overcome the presence of lysine residues at the surface of the enzyme and in addition, reaction conditions involved sodium cyanoborohydride to reduce the formed imines, during the course of the reaction, as isolable amines. One of the possible combinations was amplified and satisfyingly corresponded to the structure known as carbonic anhydrase inhibitor. Carbonic anhydrase is still nowadays studied to build DCLs.^[46]

Nicolaou *et al.* have also reported the use of a target-accelerated combinatorial synthesis to discover highly potent antibiotics effective against vancomycin-resistant bacteria.^[47] A library of vancomycin analogues was incubated with their target (Ac₂-L-Lys-D-Ala-D-Ala). The formation constant of vancomycin dimers being greater in the presence of target, the target-bound assembly ligated faster than its nontarget-bound counterpart (Figure 8). This enabled correlation between the reaction rate enhancement for the ligation reaction and the ability of vancomycin analogues to bind to the target, and thus their antibiotic ability. This strategy proved useful in predicting biological properties at a pre-screening stage.

^[46] Nasr, G.; Petit, E.; Vullo, D.; Winum, J.-Y.; Supuran, C. T.; Barboiu, M., Carbonic Anhydrase-Encoded Dynamic Constitutional Libraries: Toward the Discovery of Isozyme-Specific Inhibitors. *J Med Chem*, **52** (15), 4853-4859 (2009)

^[47] Nicolaou, K. C.; Hughes, R.; Cho, S. Y.; Winssinger, N.; Smethurst, C.; Labischinski, H.; Endermann, R., Target-accelerated combinatorial synthesis and discovery of highly potent antibiotics effective against vancomycin-resistant bacteria. *Angew. Chem. Int. Ed.*, **39** (21), 3823 (2000)

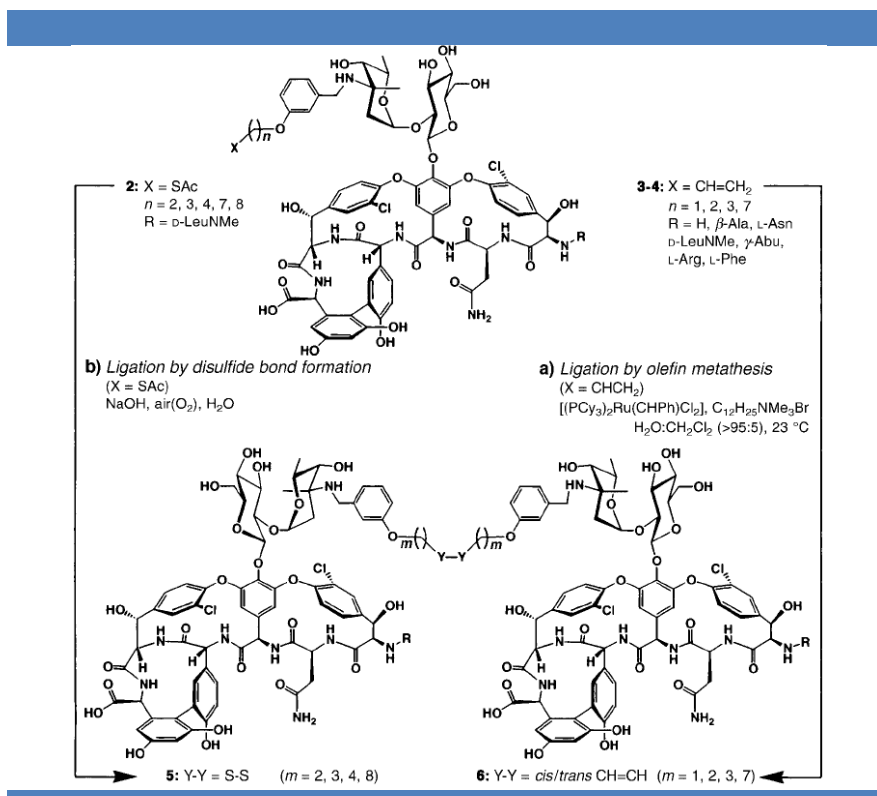


Figure 8 | Dimerisation of monomeric vancomycin thioacetates (**2**) and vancomycin derivatives with terminal olefins (**3, 4**) to form disulfide (**5**) and olefinic dimers (**6**) respectively (Nicolaou *et al.*).^[47]

Another achievement of DCC was its successful use for the design of sensors.^[48] An early example of the use of DCL as sensors has been demonstrated by K. Severin and A. Buryak^[49]. Three commercially available dyes (**1, 2** and **3** Figure 9) were mixed with CuCl₂ and NiCl₂ in buffered aqueous solution to form a dynamic combinatorial library of complexes that were able to differentiated dipeptide analytes.

^[48] Busseron, E.; Ruff, Y.; Moulin, E.; Giuseppone, N., Supramolecular self-assemblies as functional nanomaterials. *Nanoscale*, **5** (16), 7098-7140 (2013)

^[49] Buryak, A.; Severin, K., Dynamic combinatorial libraries of dye complexes as sensors. *Angew. Chem. Int. Ed.* **44** (48), 7935-7938 (2005).

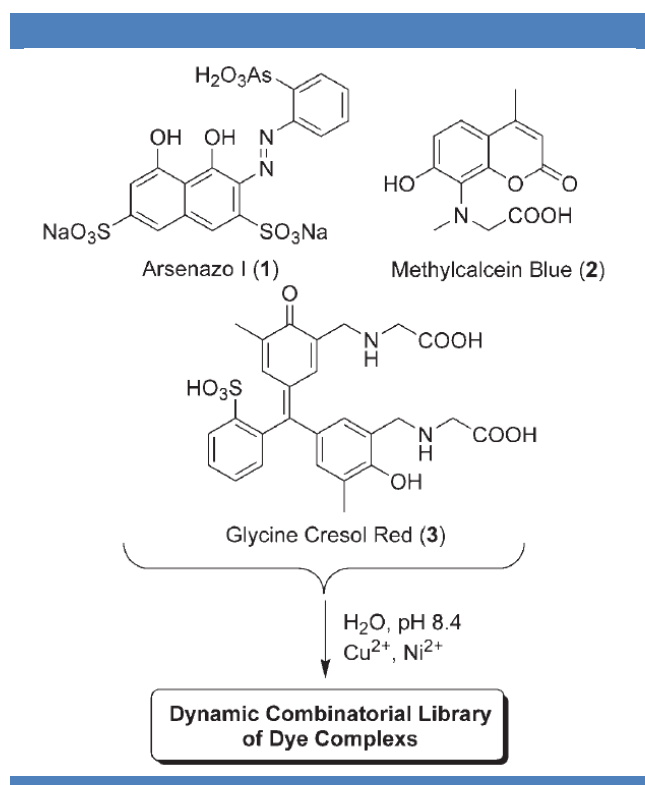


Figure 9 | Generation of a DCL of metal–dye complexes by mixing dyes **1**, **2** and **3** with CuCl_2 and NiCl_2 in buffered aqueous solution (Severin *et al.*).^[50]

Dyes and metal salts are in a dynamic equilibrium with metal-dyes complexes. Therefore, any addition of dipeptide displaces some of the dyes from the metal ions leading to an increase of free dye concentration.^{[51][52]} This re-equilibration of the remaining metal–dye complexes, creating a distinctive change of colour of the system, was efficient to differentiate related analytes such as the stereoisomers Phe-Ala and d-Phe-Ala. In this case, only a single optical measurement was necessary for determining and quantifying the analyte, making this system convenient to use. A large variety of analytes were used to prove the validity of this approach, including dipeptides,^{[50][53]} tripeptides,^[54] nucleotides and phosphates,^[55] peptide hormones,^[56] and sulphated glycosaminoglycans.^[57]

^[50] Otto, S.; Severin, K., Dynamic combinatorial libraries for the development of synthetic receptors and sensors. *Creative Chemical Sensor Systems*, **277**, 267-288 (2007)

^[51] L. Fabbri; M.Licchelli; A.Taglietti, The design of fluorescent sensors for anions: taking profit from the metal–ligand interaction and exploiting two distinct paradigms. *Dalton Trans.* 3471 – 3479 (2003)

^[52] S.L. Wiskur, H. Ait-Haddou, J.J. Lavigne, E.V. Anslyn, Teaching Old Indicators New Tricks, *Acc. Chem. Res.* **34**, 963 – 972 (2001).

^[53] Rochat, S.; Severin, K., Pattern-Based Sensing with Metal-Dye Complexes: Sensor Arrays versus Dynamic Combinatorial Libraries. *J Comb Chem*, **12** (4), 595-599 (2010)

^[54] Buryak, A.; Severin, K., Easy to optimize: Dynamic combinatorial libraries of metal-dye complexes as flexible sensors for tripeptides. *J Comb Chem*, **8** (4), 540-543 (2006)

^[55] Buryak, A.; Pozdnoukhov, A.; Severin, K., Pattern-based sensing of nucleotides in aqueous solution with a multicomponent indicator displacement assay. *Chem Commun*, (23), 2366-2368 (2007)

^[56] Zaubitzer, F.; Riis-Johannessen, T.; Severin, K., Sensing of peptide hormones with dynamic combinatorial libraries of metal-dye complexes: the advantage of time-resolved measurements. *Org Biomol Chem*, **7** (22), 4598-4603 (2009)

DCLs, that were initially used to generate a large set of compounds to screen for biological activity and as a tool to modulate bioactivity and to impact function within a more complex environment,^[25] has now fields of applications spreading from receptor design,^{[58][59]} drug discovery,^{[60][61]} dynamic resolution,^[62] self-sorting,^[63] self-replication,^{[64][65]} DNA-templated synthesis,^{[66][67]} catalysis,^{[68][69]} sensing^{[50][70]} to materials science.^{[71][72]}

In the next part of this introduction, a few examples have been selected to illustrate some use of DCC for the creation of functional materials and devices. The examples have been chosen to be as diverse as possible with a high focus on systems containing imine derivatives.

c) Functional materials and devices

Rapidly after the emergence of the field, DCC has been considered as a possible tool to build functional materials and devices with practical applications. An important work at the crossroad of DCC and material science was developed by Lehn *et al.* and concerns the templated formation of dynamic hydrogels based on the self-assembly of guanine quartets (Figure 10).^[73]

-
- ^[57] Muller-Graff, P. K.; Szelke, H.; Severin, K.; Kramer, R., Pattern-based sensing of sulfated glycosaminoglycans with a dynamic mixture of iron complexes. *Org Biomol Chem*, **8** (10), 2327-2331 (2010)
- ^[58] Li, J.; Nowak, P.; Otto, S. *J. Am. Chem. Soc.* **135**,9222–9239 (2013)
- ^[59] Fuchs, B.; Tetraheterodecalin Podands, Their Linkers, and Resulting Macrocycles: A Hoard of Constitutionally and Stereochemically Dynamic Systems *Isr. J. Chem.* **53**, 45–52 (2013)
- ^[60] Ganesan, A., Strategies for the Dynamic Integration of Combinatorial Synthesis and Screening. *Angew Chem, Int Ed*, **37** (20), 2828-2831 (1998)
- ^[61] Ramstrom, O.; Bunyapaiboonsri, T.; Lohmann, S.; Lehn, J. M., Chemical biology of dynamic combinatorial libraries. *Biochim Biophys Acta*, **1572** (2-3), 178-186 (2002)
- ^[62] Sakulsombat, M.; Zhang, Y.; Ramstrom, O., Dynamic Systemic Resolution. *Top Curr Chem*, **322**, 55-86 (2012)
- ^[63] Osowska, K.; Miljanic, O. S., Kinetic and Thermodynamic Self-Sorting in Synthetic Systems. *Synlett*, **12**, 1643-1648 (2011)
- ^[64] Moulin, E.; Giuseppone, N., Dynamic Combinatorial Self-Replicating Systems. *Top Curr Chem*, **322**, 87-105 (2012)
- ^[65] Hunt, R. A. R.; Otto, S., Dynamic combinatorial libraries: new opportunities in systems chemistry. *Chem Commun*, **47** (3), 847-858 (2011)
- ^[66] Nguyen, R.; Huc, I., Using an enzyme's active site to template inhibitors. *Angew Chem Int Edit*, **40** (9), 1774-1776 (2001)
- ^[67] Rozenman, M. M.; McNaughton, B. R.; Liu, D. R., Solving chemical problems through the application of evolutionary principles. *Curr Opin Chem Biol*, **11** (3), 259-268 (2007)
- ^[68] Luning, U., Macrocycles in supramolecular chemistry: from dynamic combinatorial chemistry to catalysis. *Pol J Chem*, **82** (6), 1161-1174 (2008)
- ^[69] Gasparini, G.; Dal Molin, M.; Prins, L. J., Dynamic Approaches towards Catalyst Discovery. *Eur J Org Chem*, **13**, 2429-2440 (2010)
- ^[70] Otto, S.; Severin, K., Dynamic combinatorial libraries for the development of synthetic receptors and sensors. *Creative Chemical Sensor Systems*, **277**, 267-288 (2007)
- ^[71] Ciesielski, A.; Samori, P., Supramolecular assembly/reassembly processes: molecular motors and dynamers operating at surfaces. *Nanoscale*, **3** (4), 1397-1410 (2011)
- ^[72] Kloxin, C. J.; Bowman, C. N., Covalent adaptable networks: smart, reconfigurable and responsive network systems. *Chem Soc Rev*, **42** (17), 7161-7173 (2013)
- ^[73] Sreenivasachary, N.; Lehn, J.-M. Gelation-driven component selection in the generation of constitutional dynamic hydrogels based on guanine-quartet formation. *Proc. Nat. Acad. Sci. USA*, **102**, 5938–5943 (2005).

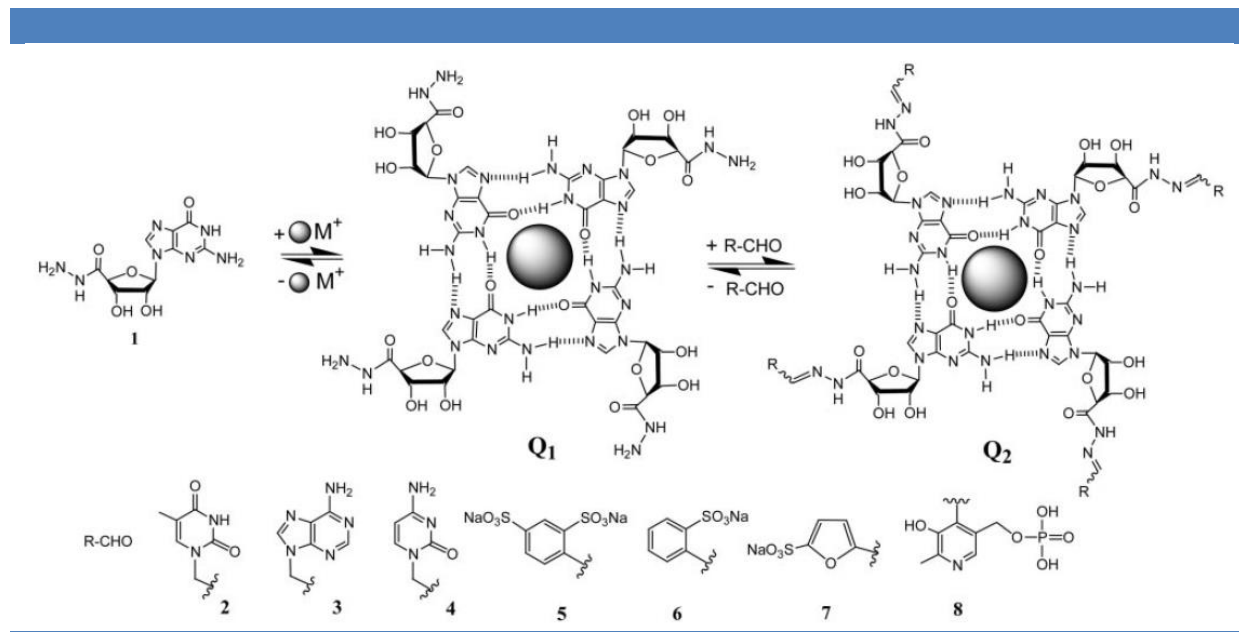


Figure 10 | Dynamic hydrogels based on guanine quartets (Lehn *et al.*).^[73]

Three levels of reversible self-assembly are here represented, the first one being molecular and the last two supramolecular:

- Formation of hydrazones in the presence of aldehydes
- Formation of G-quartets of hydrazino-guanines in the presence of metal ions
- Stacking of the quartets to form columnar fibres, thus leading to hydrogels

In the presence of two different hydrazide and two aldehydes (Figure 11), a self-organization by selection occurs. The choice of the aldehyde for the formation of the hydrazone operates through the formation of the most stable gel. There is a direct analogy between self-sorting of dynamic mixtures driven by gelation in this case and self-sorting by crystallisation obtained by Barboiu *et al.*^[74] This kind of system can find useful applications in the field of smart materials and medicinal chemistry, especially in the case where new gelators would bear biologically relevant recognition groups, forming aqueous gels. These systems can also be used for the controlled release of bioactive volatiles.^{[75][76]}

^[74] Barboiu, M.; Dumitru, F.; Legrand, Y.-M.; Petit, E.; Van Der Lee, A. Self-Sorting of Equilibrating Metallosupramolecular DCLs via Constitutional Crystallization. *Chem. Commun.* 2192–2194 (2009).

^[75] Buchs, B.; Fieber, W.; Vigouroux-Elie, F.; Sreenivasachary, N.; Lehn, J. M.; Herrmann, A., Release of bioactive volatiles from supramolecular hydrogels: influence of reversible acylhydrazone formation on gel stability and volatile compound evaporation. *Org. Biomol. Chem.* **9** (8), 2906–2919 (2011).

^[76] Sreenivasachary, N.; Lehn, J.-M. Structural Selection in G-Quartet-Based Hydrogels and Controlled Release of Bioactive Molecules. *Chem – Asian J.* **3** (1), 134–139 (2008)

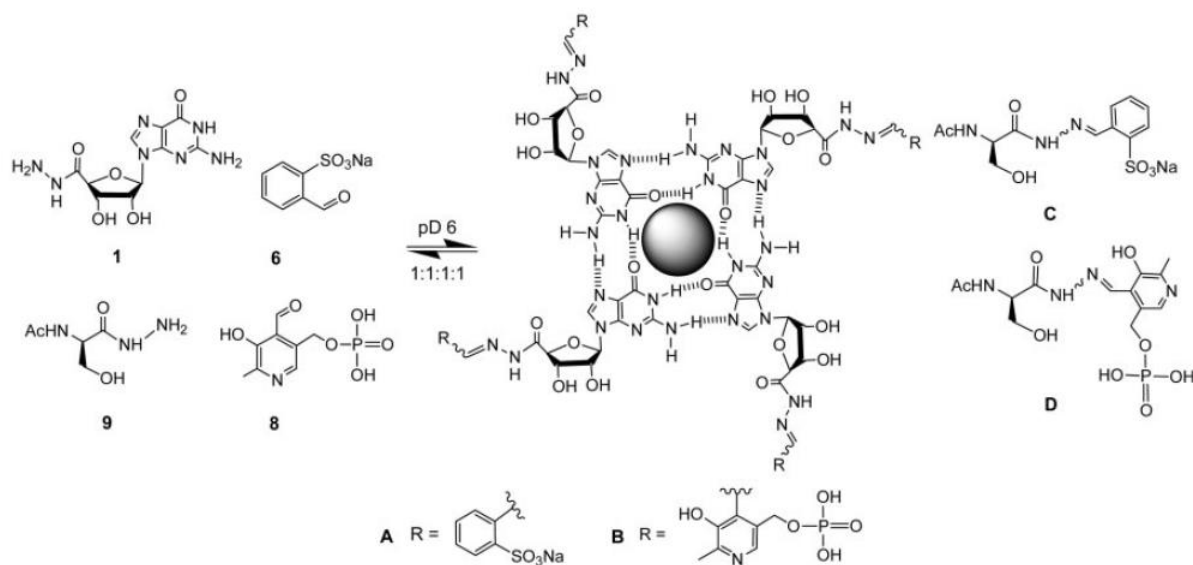


Figure 11 | Generation of a dynamic library of acylhydrazones **C**, **D** and of the acylhydrazone G-quartets **A** and **B** from hydrazides **1**, **9** and aldehydes **6** and **8**. (Lehn *et al.*).^[73]

Giuseppone and Lehn have produced extensive work on the creation of smart materials that undergo constitutional reorganization as an adaptive response under the pressure of external conditions. After having shown that pH and temperature can influence libraries of imines,^[31] they studied the dynamic rearrangement of functional dynamers using metal ions as a stimuli and potentially producing variable fluorescence intensities depending on the reshuffling of the constituents (Figure 12).^[77] When mixing dialdehyde **A** with dialiphatic amine **B** and diaromatic amine **C** (Figure 11), the diimine formed from the aliphatic amine was preferably expressed due to its higher nucleophilicity. Addition of increasing amounts of $\text{Zn}(\text{BF}_4) \cdot 8\text{H}_2\text{O}$ in CD_3CN led to fast and total conversion of the aliphatic polyimine into the aromatic one (orange solution). The constitutional modifications observed may be attributed to the preferential coordination of $\text{Zn}(\text{II})$ to the most basic amine (aliphatic diamine). The possibility to reverse the coordination of $\text{Zn}(\text{II})$ to the aliphatic amine by trapping the $\text{Zn}(\text{II})$ ions with hexamethylhexacyclen was also demonstrated. It is therefore possible to tune the system to provide a given fluorescent response between two extrema that are the responses of either the aliphatic or the aromatic polyimine, by adjusting the quantity of coordinating $\text{Zn}(\text{II})$.

^[77] Giuseppone, N.; Lehn, J.-M. Constitutional Dynamic Self-Sensing in a Zinc(II) Polyiminofluorenes System. *J. Am. Chem. Soc.* **126**, 11448–11449 (2004).

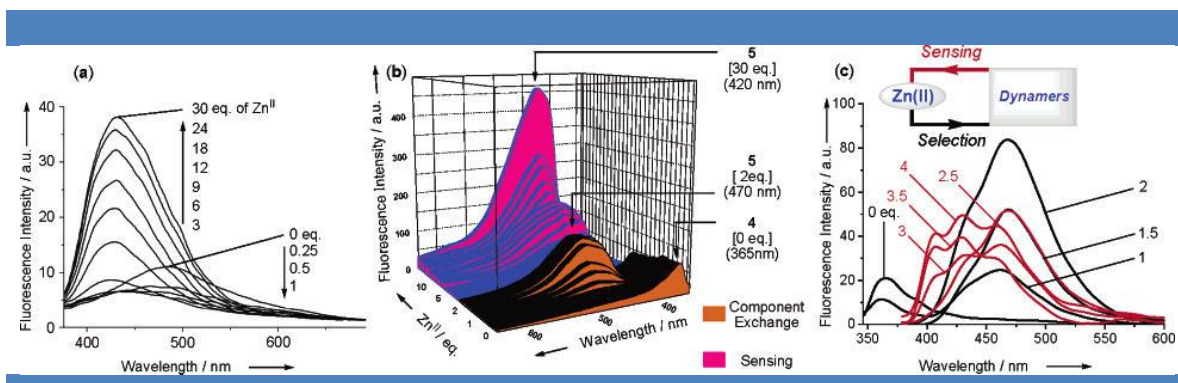


Figure 12 | Fluorescent dynamers and their optical responses as a function of Zn^{2+} ions concentration in solution. (a) Fluorescence spectra at 298 K in CHCl_3 of a pure fluorene polyimine ($c = 4.05 \cdot 10^{-6}$ M) on addition of increasing amounts of $\text{Zn}(\text{BF}_4)_2 \cdot 8\text{H}_2\text{O}$ (equivalent with respect to initial A in 5) solubilized in CH_3CN ; excitation at 350 nm. (b) Fluorescence spectra at 298 K in CHCl_3 of the CDL II of fluorene polyimines, on addition of increasing amounts of $\text{Zn}(\text{BF}_4)_2 \cdot 8\text{H}_2\text{O}$ (equivalent with respect to initial A in CDL II) solubilized in CH_3CN ; excitation at 320 nm. (c) Partial titration (0 to 4 equiv Zn^{II}) in the same conditions as (b), illustrating the self sensing occurring after the component exchange process (sensor formation) is completed, i.e., beyond 2 equiv of Zn^{II} . (Giuseppone and Lehn).^[77]

Another example of tuning the response of a smart material thanks to an external trigger has been demonstrated by Giuseppone and Lehn, who studied the influence of an electric field on the composition of a dynamic mixture.^[36] Small molecules capable of component exchange were mixed, with one of the combinations presenting a high dielectric anisotropy and thus liquid crystal properties (EBBA, Figure 13).

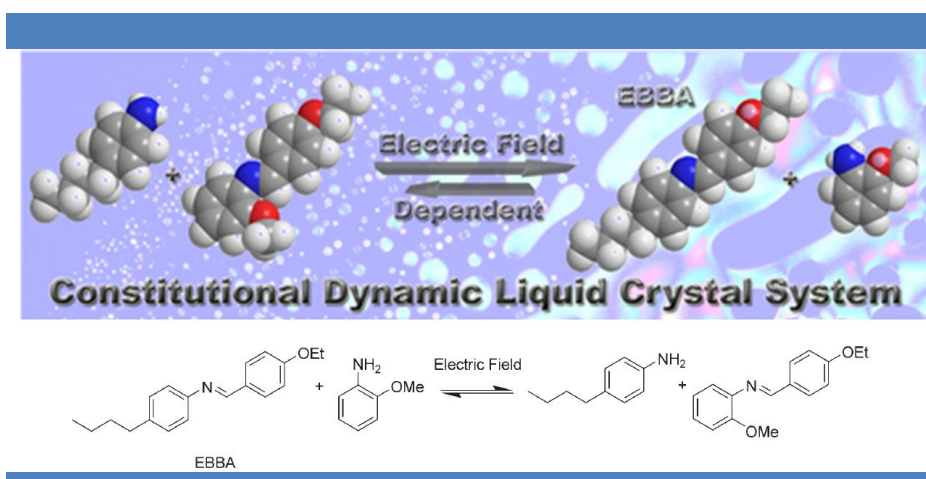


Figure 13 | Dynamic combinatorial liquid crystals upon electric field modulation (Giuseppone and Lehn).^[36]

The authors demonstrated that a macroscopic response (liquid crystal formation) can be obtained when an electric field of high voltage is applied, and that the formation of the imine that interact with the electric field (the liquid crystal imine) is favoured. Such a system can find applications for the fine-tuning of smart material, for example for display technology.^[78] This system was also further used for the controlled release of bioactive volatiles by Herrmann, Giuseppone and Lehn.^[37] Interestingly, when an electric field was applied to liquid crystalline film-forming imines, volatile compounds that do not participate in the formation of the liquid crystalline phase were expelled (**a** and **b**, Figure 14).

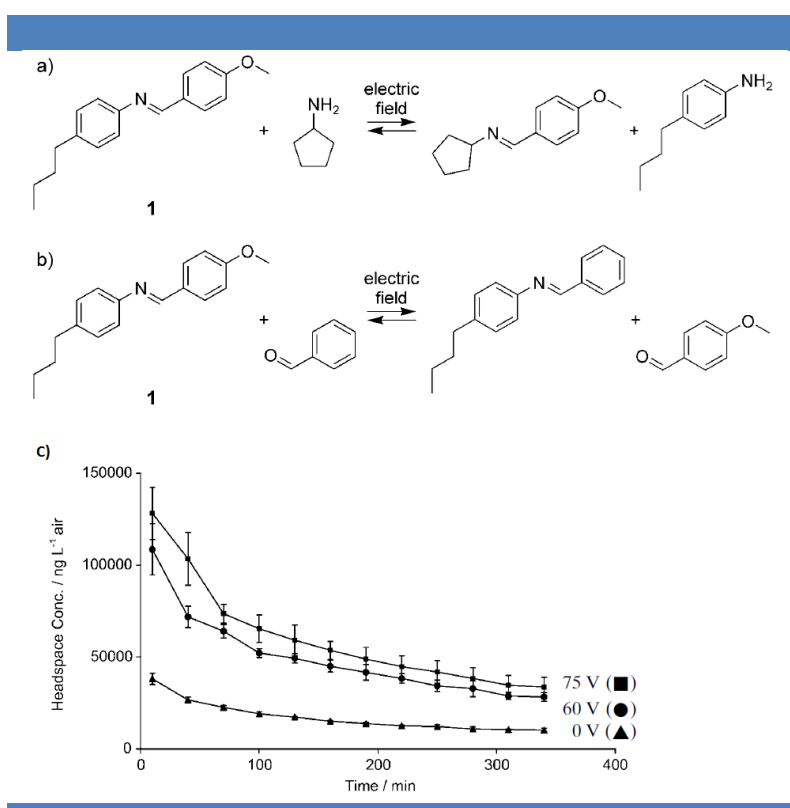


Figure 14 | Principle of constitutional reorganisation by component exchange of MBBA (**1**) with cyclopentylamine a) or benzaldehyde b) in the presence of an electric field. c) Comparison of average headspace concentrations measured for the evaporation of cyclopentanol from a liquid crystalline film of **1** after application of different voltages (Herrmann, Giuseppone and Lehn).^[37]

The concentration of volatile molecules obtained by headspace measurements was higher in presence of the electric field (**c**, Figure 14). This is an example of controlled release of volatiles. Another example of the use of dynamic combinatorial chemistry in the area of

^[78] Kirsch, P.; Bremer, M. Liquid crystals for active matrix displays: molecular design and synthesis, *Angew. Chem. Int. Ed.*, **112**, 4384 (2000)

fragrances has recently been reviewed by Herrmann,^[79] and a noteworthy contribution in this field can be attributed to the group of Matile.^{[80][81]}

Since my PhD work was dedicated to the study of covalent dynamic amphiphiles at the crossroad between DCC and soft materials, I would like in the next chapter to present some of the main properties of surfactants, as well as previous work that have been performed in our group regarding dynamic amphiphilic block copolymers (dynablocks).

3/ Surfactants

Surfactants, contraction of “surface-active agents”, are compounds that possess hydrophobic (the tail) and hydrophilic (the head) moieties and have the property to lower the surface tension between two phases (liquid/liquid, liquid/solid, liquid/gas). When they are dissolved in a suitable solvent, they preferably join interfaces to limit unfavored interactions between the solvent and their non-soluble blocks. If present at high enough concentration in water, these amphiphilic molecules produce microphase separation due to the high contribution of the hydrophobic effect.^[82] Depending on their concentration, surfactants can form a broad variety of structures, ranging from spherical and worm-like micelles to multilayers and organized mesophases (Figure 15).^{[83][84][85]}

^[79] Herrmann, A., Dynamic Mixtures: Challenges and Opportunities for the Amplification and Sensing of Scents. *Chem-Eur J*, **18** (28), 8568-8577 (2012)

^[80] Montenegro, J.; Bonvin, P.; Takeuchi, T.; Matile, S., Dynamic Octopus Amphiphiles as Powerful Activators of DNA Transporters: Differential Fragrance Sensing and Beyond. *Chem-Eur J*, **16** (47), 14159-14166 (2010)

^[81] Montenegro, J.; Fin, A.; Matile, S., Comprehensive screening of octopus amphiphiles as DNA activators in lipid bilayers: implications on transport, sensing and cellular uptake. *Org Biomol Chem*, **9** (8), 2641-2647 (2011)

^[82] Tanford, C. The hydrophobic effect, Formation of Micelles and biological membranes. Wiley Interscience, New-York (1973).

^[83] Israelachvili, J. N. Intermolecular & surface forces. Academic, New York, Academic press, 2nd edition (1992).

^[84] Israelachvili, J. N.; Mitchell, D. J.; Ninham, B. W. Theory of self-assembly of hydrocarbon amphiphiles into micelles and bilayers. *J. Chem. Soc., Faraday Trans. 2* **72**, 1525-1568 (1976).

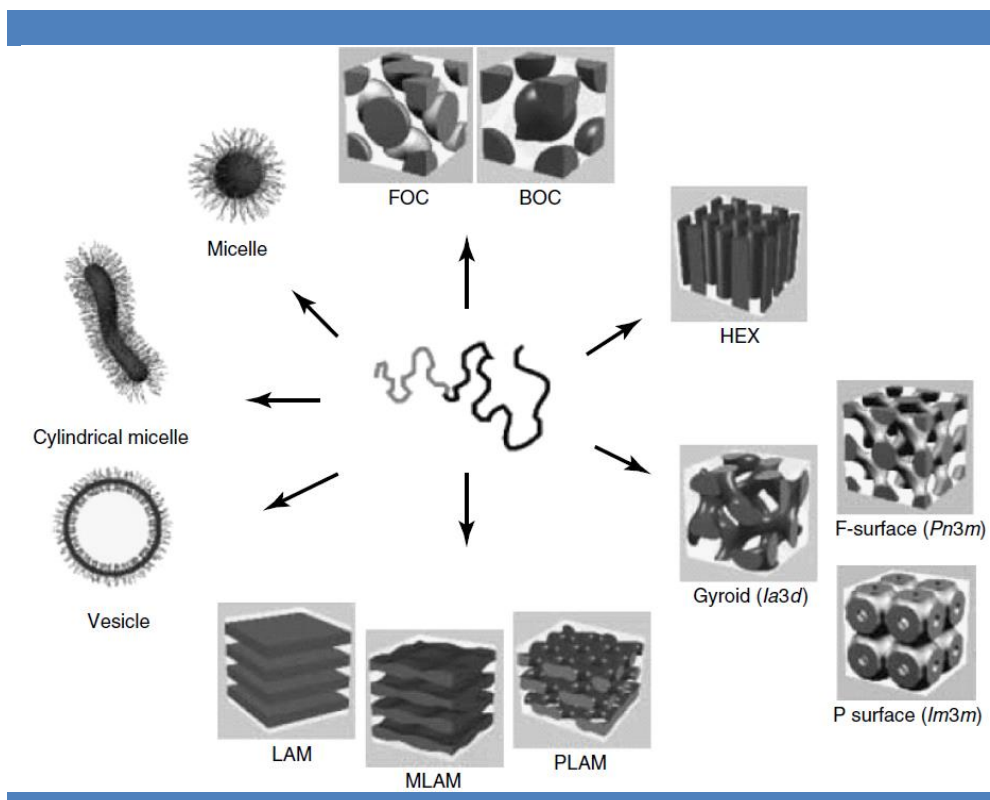


Figure 15 | Self-organization structures of block copolymers and surfactants: spherical micelles, cylindrical micelles, vesicles, fcc and bcc-packed spheres (FCC, BCC), hexagonally packed cylinders (HEX), various minimal surfaces (gyroid, F surface, P surface), simple lamellae (LAM), as well as modulated lamellae (MLAM) and perforated lamellae (PLAM). (Forster and Antonietti)^[85]

An important concept that has been developed to understand the self-assembly of surfactants is the packing parameter^[86], that helps to understand possible changes of shape of a micellar aggregate when a geometrical parameter is modified. For several decades, improvements of this theory have been made, taking into account an increasing number of parameters such as the size of the surfactant tail.^[87] In Table 1, it can be seen that the shape of the aggregate depends on the packing parameter defined as $V_0/(a \cdot l_0)$; V_0 and l_0 being the volume and the extended length of the surfactant tail, and “a” the mean surface occupied by the hydrophilic head at equilibrium in an aggregate. Two additional parameters are extremely important when considering micellisation:

- The Krafft temperature, above which micellisation can only happen and below which surfactants precipitate.

^[85] Forster, S.; Antonietti, M., Amphiphilic block copolymers in structure-controlled nanomaterial hybrids. *Adv Mater*, **10** (3), 195 (1998)

^[86] Israelachvili, J. N.; Mitchell, D. J.; Ninham, B. W., Theory of Self-Assembly of Hydrocarbon Amphiphiles into Micelles and Bilayers. *J. Chem. Soc., Faraday Trans. 2*, **72**, 1525-1568 (1976)

^[87] Nagarajan, R. Molecular Packing Parameter and Surfactant Self-Assembly: The Neglected Role of the Surfactant Tail. *Langmuir*, **18**, 31–38 (2002).

- The second parameter is the CMC (Critical micellar concentration), that marks the transition from the surfactant present only as unimers in solution ($C < C_{MC}$) to the state where unimers are in constant number ($C = C_{MC}$) and coexist with aggregated surfactants ($C > C_{MC}$).

Table 1 | Geometrical Relations for Spherical, Cylindrical, and Bilayer Aggregates (Nagarajan)^[87]

variable	sphere	cylinder	bilayer
volume of core $V = gv_o$	$4\pi R^3/3$	πR^2	$2R$
surface area of core $A = ga$	$4\pi R^2$	$2\pi R$	2
area per molecule a	$3v_o/R$	$2v_o/R$	v_o/R
packing parameter v_o/al_o	$v_o/al_o \leq 1/3$	$v_o/al_o \leq 1/2$	$v_o/al_o \leq 1$
largest aggregation number g_{max}	$4\pi l_o^3/3v_o$	$\pi l_o^2/v_o$	$2l_o/v_o$
aggregation number g	$g_{max} (3v_o/al_o)^3$	$g_{max} (2v_o/al_o)^2$	$g_{max}(v_o/al_o)$

Surfactants are engaged in a dynamic equilibrium between unimers in solution and their aggregated forms, with a timescale ranging from microseconds to kinetically blocked systems. CMC depends on many external parameters such as temperature, pH, ionic force of the dispersion media and nature and length of the surfactant hydrophobic tail and hydrophilic head. This CMC decreases rapidly when the size of the hydrophobic tail increases (**b**, Table 2).

Table 2 | a) CMC for different types of surfactants b) CMC as a function of alkyl chain length for several ethoxylated C₄-C₁₆ fatty acids. Adapted from “les techniques de l’ingénieur”.^[88]

a)	Type of surfactant	Chemical formula	Temperature (°C)	CMC (mM)
	Anionic	C ₁₂ H ₂₅ SO ₄ Na ⁺	40	8.6
		C ₁₂ H ₂₅ C ₆ H ₄ SO ₃ Na ⁺	60	1.2
	Cationic	C ₁₂ H ₂₅ N ⁺ (CH ₃) ₃ Br ⁻	25	20
	Amphoteric	C ₁₂ H ₂₅ N ⁺ H ₂ CH ₂ COO ⁻	27	1.3
	Non-ionic	C ₁₂ H ₂₅ O(CH ₂ CH ₂ O) ₄ H	25	0.04
		C ₁₂ H ₂₅ O(CH ₂ CH ₂ O) ₃ H	25	0.05

b)	Alkyl chain length	Temperature (°C)	CMC (mM)
Hydrophilic block is composed of 6 Ethylene oxide units			
	C4	20	800
	C6	20	74
	C8	20	11.3
	C10	20	0.92 to 0.96
	C12	20	0.074 to 0.100
	C14	25	0.010
	C16	25	10 ⁻³ to 1.7.10 ⁻³

^[88] Bognolo, G. Tensioactifs non ioniques - Propriétés : tableaux comparatifs, *Techniques de l’ingénieur*, j2266 (2004)

a) Low molecular weight amphiphiles

When considering low molecular weight amphiphiles, four different types of surfactant exist: anionic, cationic, zwitter-ionic and non-ionic. The most used category, anionic surfactants, are negatively charged in solution and are usually constituted of carboxylate, sulphate, sulfonate, or phosphate groups, and cannot be used at low pH (below their pKa). Cationic surfactants are mostly protonated amines and quaternary ammonium salts and are unstable in very basic conditions. Zwitterionic (with both a cationic and an anionic part) and non-ionic surfactants (non-charged but rich in polar groups) are stable at all pH. Usually, non-ionic surfactants have lower CMC than charged ones (a, Table 2).

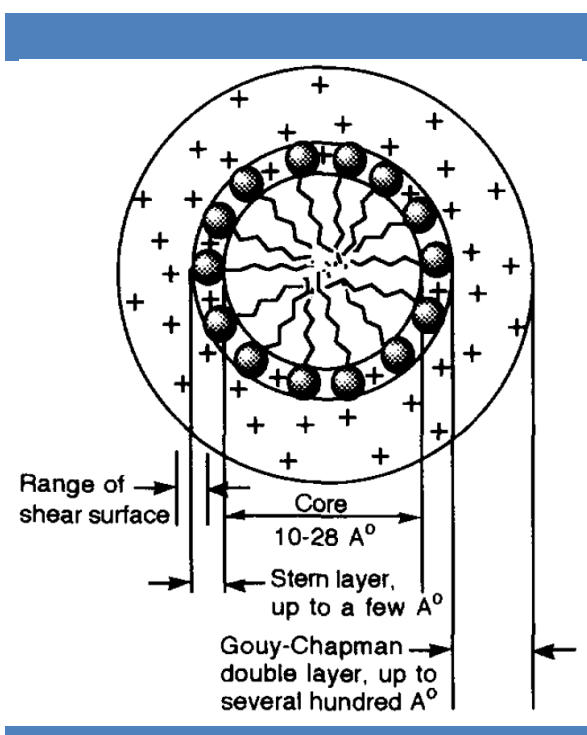


Figure 16 | A two dimensional schematic representation of the regions of a spherical ionic micelle in aqueous solution. The counterions (+), head groups (●) and the hydrocarbon chains (~~~~) are schematically indicated to denote their relative locations (Ramesh and Ramamurthy).^[89]

For ionic surfactants, electrical charges on a micelle are neutralized by counterions in a surrounding electrical double layer (Gouy-Chapman).^[89] The first layer immediately adjacent to its surface is called the Stern Layer (Figure 16), where counterions are adsorbed so strongly

^[89] Tascioglu, S. Micellar solutions as reaction media, *Tetrahedron*, **52** (34), 11113-11152 (1996)

that they migrate together with the colloidal micelle in an electrical field. According to the most widely accepted model, head groups of surfactant molecules are also located in this layer. The decrease in counterion concentration with the distance from the micellar surface follows an exponential decay.^[90] The core radius of the micellar aggregate is about the length of the fully extended alkyl chain of the amphiphile and consists of two regions, the inner and outer core, which contains approximately the first four methylene groups. Finally, another defined region within micelles is called palisade layer (mantle) which includes the head groups and the first few methylene groups.

Hydrocarbon chains in micelles are generally considered as disordered, so as the hydrophobic core constitutes a small fraction of a hydrophobic solvent. Evidence of their liquid-like nature comes from their ability to dissolve hydrocarbons and other hydrophobic substances. Thus, unlike homogeneous solvents, the inherently microheterogeneous micellar solutions provide a variety of solubilisation environments, ranging from “hydrocarbon-like” core to bulk water.^[91] Indeed, one particular property of micelles as solvents is that they can provide not only different micro-environments for different molecules but also different micro-environments for distinct parts of a same molecule (Figure 17).

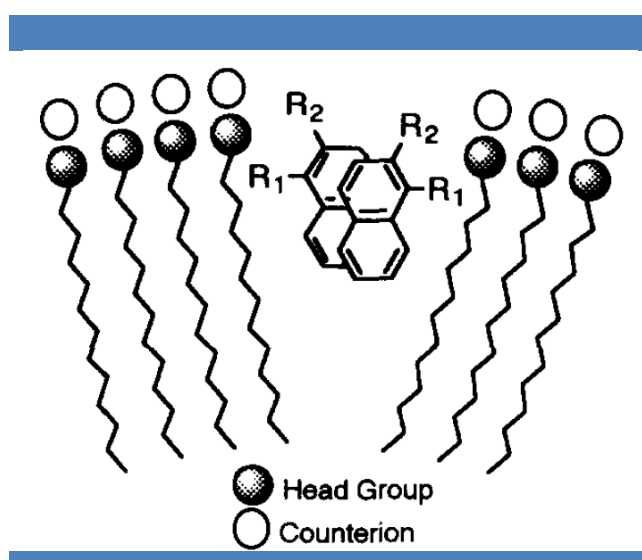


Figure 17 | The role of hydrophilic groups R_2 in preorientating substrate molecules at the micellar interface (Ramesh and Ramamurthy).^[92]

^[90] Bravo, C.; Leis, J. R.; Pena, M. E., Effect of Alcohols on Catalysis by Dodecyl-Sulfate Micelles. *J. Phys. Chem.*, **96** (4), 1957-1961 (1992)

^[91] Schamm, M. P.; Hooley, R. J.; Rebek, J. Guest . Recognition with micelle-bound cavitands. *J. Am. Chem. Soc.* **129**, 9773-9779 (2007).

^[92] Ramesh, V., Ramamurthy, V. Z. Control of Regiochemistry in Photodimerization through Micellar Preorientational Effect: 2-Substituted Naphthalenes. *Org. Chem.*, **49**, 536 (1984)

The ability to solubilize hydrophobic compounds is not the only attribute of micelles. They can also change pathways and reaction rates, by increasing the concentration of reactants inside the micellar core but also stabilise transition states by electrostatic interactions.^{[93][94]} Some quantitative treatments of micellar rate effects in terms of pseudophase model were initially developed by Menger and Portnoy^[95] and reviewed extensively for uni- and bimolecular reactions.^[96]

b) Block copolymer amphiphiles

Block copolymers in the bulk have similar morphologies to those observed for small molecule surfactants, including micelles and vesicles, but with more extensions in condensed mesophases and at much lower CMC.^[97] In dilute solutions, the principle of aggregation of the amphiphilic block copolymers is close to that observed for low molecular weight amphiphiles (Figure 18).

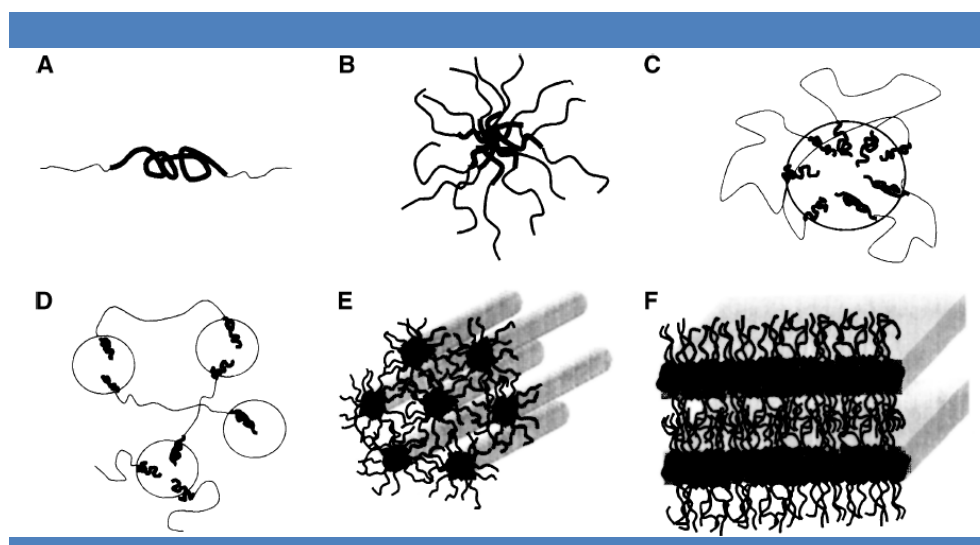


Figure 18 | Schematic representation of aggregated structures formed by block copolymers in solution: (A) copolymer unimer, (B) spherical micelle in a solvent selective for end-blocks, (C)

^[93] Cordes, E. H.; Dunlap, R. B. Kinetics of organic reactions in micellar systems. *Acc. Chem. Res.* **2**, 329-337 (1969).

^[94] Moulin, E.; Giuseppone, N., Reactions in Dynamic Self-Assemblies. In *Supramol, Chem*, Chichester, England John Wiley & Sons (2012).

^[95] Menger, F. M.; Portnoy, C. E. Chemistry of reactions proceeding inside molecular aggregates. *J. Am. Chem. Soc.* **89**, 4698-4703 (1967).

^[96] Tascioglu, S. Micellar solutions as reaction media. *Tetrahedron* **52**, 11113-11152 (1996).

^[97] Hamley, I. W. *Block copolymers in solution, fundamentals and applications*, Chichester, England, Wiley & Sons (2005)

spherical micelle in a solvent selective for middle blocks, (D) network formation in solvent selective for the middle block, (E) hexagonal arrangement of cylindrical micelles, and (F) lamellar structure.^[98]

For condensed mesophases, the organisation depends on the hydrophilic/hydrophobic ratio, with usually a continuous phase made of the longest block and inclusions (spheres, rods, lamellae) made by the shortest one.^{[99][100][101]} Most of the experimental work in this regard has been carried out on polystyrene-*b*-poly(isoprene) (PS-*b*-PI) and polystyrene-*b*-polybutadiene (PS-*b*-PBD). As an example, with increasing volume fraction of PI, the morphology transitions go from body centred cubic (BCC) spheres of PI in a PS matrix, through hexagonally packed cylinders of PI in PS (HEX), gyroid (G), metastable hexagonally perforated layers (HPLs), and finally lamellae (LAM) form when the volume fraction of the two blocks approach equality (Figure 18). As the PI volume fraction increases further, phase inversion occurs, and HPL, G, HEX, and finally BCC morphologies are observed where PI forms the continuous phase.^[94]

The dynamics of chain exchange between micelles are also different for block copolymers due to a number of factors including their high molecular weight, their lower CMC, and their possible entanglement and low mobility of the chains in the core. The lifetime of block copolymer micelles is very broad, from seconds to hours, and even to extremely long times when the glass transition temperature of the core-forming chains is very high ($T_g > 100^\circ\text{C}$). These properties yield notable differences for the preparation of the aggregates compared to surfactants.^[102] As a consequence, block copolymers can extend surfactant applications in many heterophase stabilization problems such as for emulsion polymerisation,^[103] stabilization of pigments,^[104] formulation of cosmetics and drugs,^[105] or patterning of optoelectronic devices.^[106]

All the work done until recently has been focused on the study of well-defined amphiphiles that can dynamically form different types of aggregates. However, it would also be interesting

^[98] Loh, W. Block copolymer micelles, *Encyclopedia of Surface and Colloid Science*, Taylor and Francis group, Broken sound parkway, USA. (2002)

^[99] Blanz, A.; Armes, S. P.; Ryan, A. J., Self-Assembled Block Copolymer Aggregates: From Micelles to Vesicles and their Biological Applications. *Macromol Rapid Comm*, **30** (4-5), 267-277 (2009)

^[100] Mahmud, A.; Xiong, X. B.; Lavasanifar, A., Development of novel polymeric micellar drug conjugates and nano-containers with hydrolyzable core structure for doxorubicin delivery. *Eur J Pharm Biopharm*, **69** (3), 923-934 (2008)

^[101] Qin, S. H.; Geng, Y.; Discher, D. E.; Yang, S., Temperature-controlled assembly and release from polymer vesicles of poly(ethylene oxide)-block-poly(N-isopropylacrylamide). *Adv Mater*, **18** (21), 2905 (2006)

^[102] Förster, S.; Antonietti, M. Amphiphilic block copolymers in structure-controlled Nanomaterial hybrids. *Adv. Mater.* **10**, 195-217 (1998).

^[103] Charleux, B.; D'Agosto, F.; Delaitre, G., Preparation of Hybrid Latex Particles and Core-Shell Particles Through the Use of Controlled Radical Polymerization Techniques in Aqueous Media. *Adv. Polym. Sci.* **233**, 125-183 (2010)

^[104] Zeno, W. W.; Jones, F. N.; Pappas, S. P.; Wicks, D. A. *Organic coatings: science and technology*. Wiley (2007).

^[105] Liu, J.; Lee, H.; Allen, C. Formulation of Drugs in Block Copolymer Micelles: Drug Loading and Release. *Curr. Pharm. Design*. **12**, 4685-4701 (2006).

^[106] Segalman, R. A.; McCulloch, B.; Kirmayer, S.; Urban, J. J. Block copolymers for organic optoelectronic. *Macromolecules* **42**, 9205-9216 (2009).

to add a new dynamic dimension to these self-assembly, by adding reversible bonds to amphiphiles in order to make their molecular constitution responsible to external stimuli.

c) Dynablocks

Giuseppone and co-workers were the first ones to use DCC to form libraries of dynamic amphiphilic block copolymers (dynablocks)^[107]. Dynablocks are constituted of both a hydrophilic and a hydrophobic block linked by a labile imine derivative bond and can form dynamic combinatorial libraries with interesting properties for material science. These systems possess two levels of hierarchical organization, one at the molecular level with the reversible junctions within the block copolymer chains and another one at the mesophase level with the self-assembly of the block copolymers into various kind of micelles and vesicles (**b**, Figure 29). The destruction of the aggregates can be triggered by several environmental changes, like a change of pH^[108] or temperature^[109] and dilution.

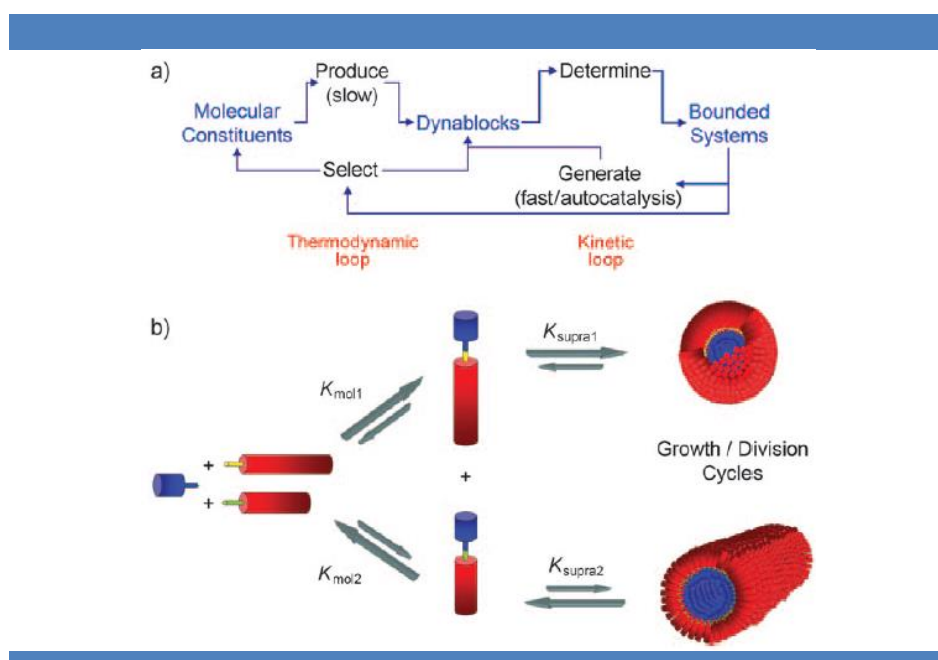


Figure 19 | a) Synergistic constitutional relationships observed at two length scales within b) a model minimal self-replicating DCL. For clarity, the growth/division cycles of micellar structures are not represented. (Giuseppone *et al.*)^[107]

^[107] Nguyen, R.; Allouche, L.; Buhler, E.; Giuseppone, N., Dynamic Combinatorial Evolution within Self-Replicating Supramolecular Assemblies. *Angew Chem Int Edit*, **48** (6), 1093-1096 (2009)

^[108] Minkenberg, C. B.; Li, F.; van Rijn, P.; Florusse, L.; Boekhoven, J.; Stuart, M. C. A.; Koper, G. J. M.; Eelkema, R.; van Esch, J. H., Responsive Vesicles from Dynamic Covalent Surfactants. *Angew Chem, Int Ed*, **50** (15), 3421-3424 (2011)

^[109] Minkenberg, C. B.; Florusse, L.; Eelkema, R.; Koper, G. J. M.; van Esch, J. H., Triggered Self-Assembly of Simple Dynamic Covalent Surfactants. *J Am Chem Soc*, **131** (32), 11274-11275 (2009)

In their first article about dynablocks, Giuseppone *et al.* described the formation of several imines in water which were produced by mixing aldehyde **A** with amine derivatives **1**...**8**^[107] (Figure 20). The imine bond was found out to be surprisingly stable under these conditions with high concentrations of imine at equilibrium. Scattering techniques (DLS, SANS) and DOSY NMR proved that this enhanced stability comes from the formation of supramolecular structures, namely spherical and cylindrical micelles for most of the imines.

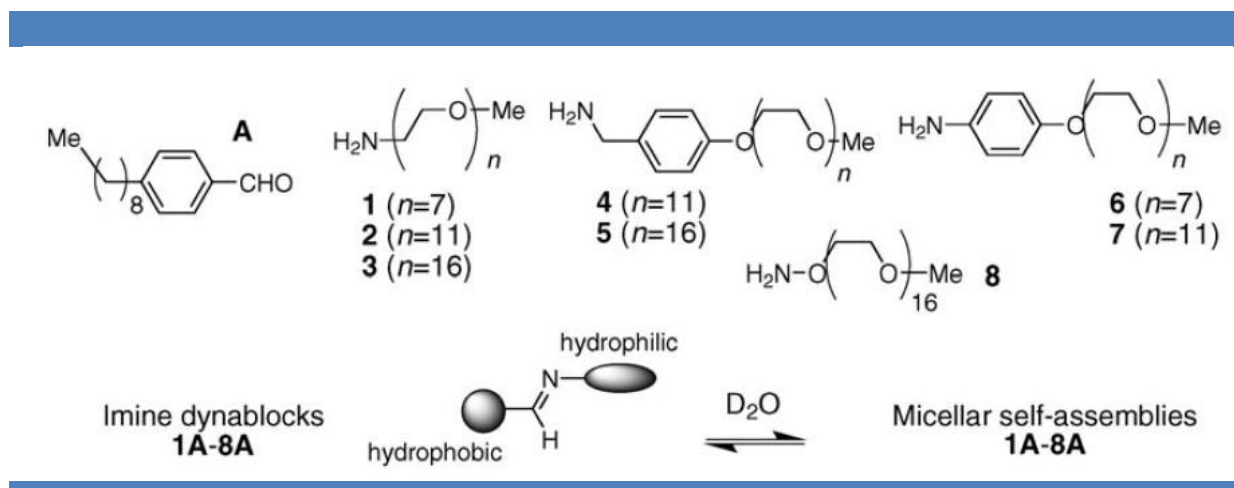


Figure 20 | Structures of dynablocks. The individual reactions of hydrophilic amines **1–8** with hydrophobic aldehyde **A** lead to imines **1A–8A**. In D_2O , these dynablocks self-assemble into supramolecular micellar structures. (Giuseppone *et al.*)^[107]

DOSY NMR measurements also revealed the presence of free aldehyde inside the micellar core of aromatic imine **7A**, and thus the possible use of this system for the encapsulation of hydrophobic compounds. The study of the formation of imine **1A** displayed by 1H NMR a sigmoid concentration-time profile for the condensation of the PEG₇Aliphatic amine **1** and octylbenzaldehyde **A**, which is characteristic of an autocatalytic system. Furthermore, the size of the micelle was decreasing over time. In the case of the formation of the aromatic imine **7A** followed by DOSY NMR, the first detected micellar structure had a hydrodynamic radius of around 16 nm which then decreased until equilibrium to 7 nm. This phenomenon is attributed to a growth/division cycles (Figure 21, as in the case of vesicle growth and division).

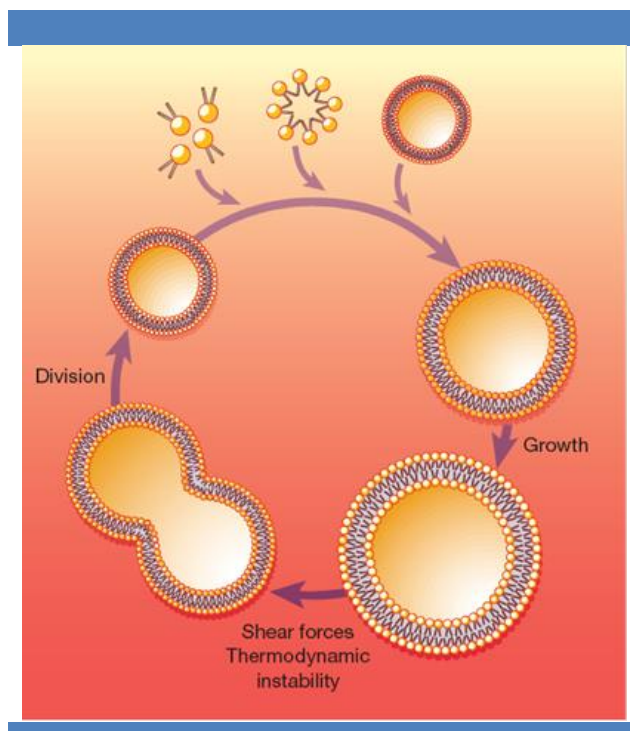


Figure 21 | Mode of vesicle growth and division (Szostak *et al.*)^[110]

Competition experiments between aromatic amine **7**, aliphatic amine **1** and 4-octylbenzaldehyde **A** revealed that aliphatic imine **1A** is preferably formed in acetonitrile due to the higher nucleophilicity of the aliphatic amine, but if the solvent is switched to water the concentration of aliphatic imine will decrease and that of aromatic imine will increase (Figure 22). This is due to the lower stability of the aliphatic imine **1A** which will preferably be hydrolysed in water, and thus release octylbenzaldehyde **A** that will further react with the free aromatic amine to form the most stable aromatic imine.

^[110] Szostak, J. W., Bartel, D. P., Luisi, P. L. Synthesizing life. *Nature* **409**, 387-390 (2001).

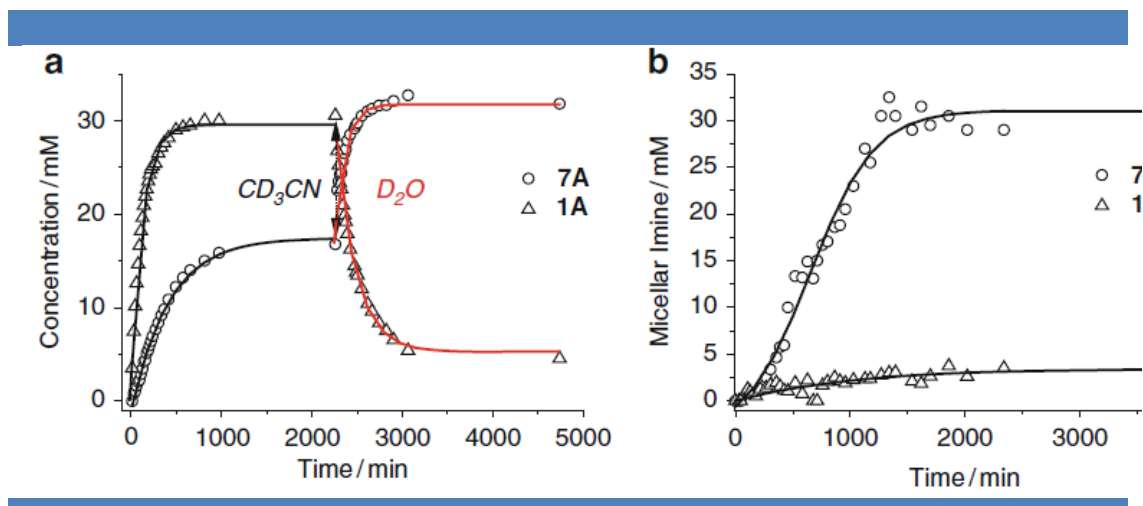


Figure 22 | Molecular selection in coupled equilibria through the self-replication of a specific mesostructure. a) Concentration of imines **1A** and **7A** versus time starting from an equimolar mixture of **1**, **7**, and **A** ($c=50$ mM each) in CD_3CN and, after reaching the thermodynamic equilibrium, by changing the solvent to pure D_2O . b) Concentration of imines **1A** and **7A** versus time starting from an equimolar mixture of **1**, **7**, and **A** in D_2O ($c=50$ mM each). (Giuseppone *et al.*)^[107]

After having described the selection of the best self-replicating nanostructures at mesoscale, the team of Giuseppone extended this work to the study of the structural modulation of several micellar and vesicular dynamic assemblies using pH as an external trigger^{[111][112]} and core-shell inversion by pH modulation in dynamic covalent micelles.^[113] Hydrophilic amines **4** and **6** were chosen because they present a large difference of pKa (4.5 for the aromatic amine and 9.5 for the benzylic one) and form cylindrical micelles when they react with **A** (a, Figure 23). When the pD value is higher than the pKa of **6** (4.5) and lower than the pKa of **4** (9.5), the formation of **6A** is favoured because the benzylic amine is protonated (b, Figure 23). For pDs above 9.5, the benzylic imine is preferentially obtained due to the higher nucleophilicity of benzylic amine **4**. All self-assemblies in this reshuffling pool present a rod like shape for all the pD range used, as shown by SANS experiments (c, Figure 23). It can also be noted that higher molecular weights were observed at low pD due to the more important Π -stacking effect of the aromatic imine over the benzylic one.

^[111] Nguyen, R.; Buhler, E.; Giuseppone, N., Dynablocks: Structural Modulation of Responsive Combinatorial Self-Assemblies at Mesoscale. *Macromolecules*, **42** (16), 5913-5915 (2009)

^[112] Jouault, N.; Nguyen, R.; Rawiso, M.; Giuseppone, N.; Buhler, E., SANS, SAXS, and light scattering investigations of pH-responsive dynamic combinatorial mesophases. *Soft Matter*, **7** (10), 4787-4800 (2011)

^[113] Nguyen, R.; Jouault, N.; Zanirati, S.; Rawiso, M.; Allouche, L.; Fuks, G.; Buhler, E.; Giuseppone, N., Core-shell inversion by pH modulation in dynamic covalent micelles. *Soft Matter*, **10** (22), 3926-3937 (2014)

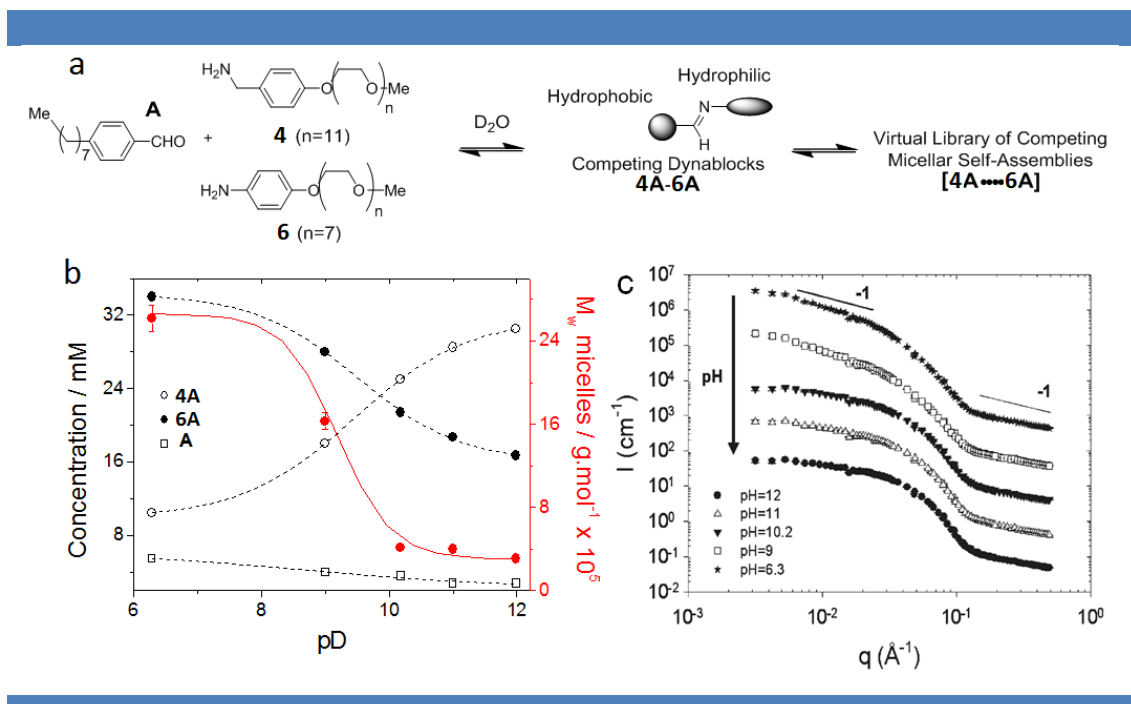


Figure 23 | a) Set of constituents reversibly competing at the molecular level for the reversible covalent condensation of imine dynablocks **1A-2A** b) Concentration plot of **A**, **4A**, and **6A**, as a function of pD, and determined by 1H NMR spectroscopy in D_2O at thermodynamic equilibrium ($T = 293 K$). c) Neutron scattering data showing, as a function of pD and at thermodynamic equilibrium, the structuring of the micellar self-assemblies made of competing dynablocks **4A** and **6A** in D_2O , at $T=293K$. For clarity, the curves are shifted with respect to each other by one log unit. (Giuseppone *et al.*)^[111]

All these results on dynablocks prove that dynamic covalent amphiphiles can be used as a very versatile tool to encapsulate hydrophobic compounds, and that, with a smart engineering of the environment of the imine bond it should be possible to tune the stability of these micellar aggregates. If sufficient stabilisation of an imine in solution made of an aliphatic amine can be achieved, it would be possible to develop releasing systems with performance close to the already developed aromatic imines or hydrazones, but without using potentially carcinogenic aromatic amines^[114] or hydrazine or hydrazide derivatives,^[115] whose use in cosmetic products is banned.^[116] However, encapsulation is not the only technique that could take advantage of the dynablocks, and profragrances could also benefit from this concept.

^[114] He, L.; Jiang, Y.; Tu, C. L.; Li, G. L.; Zhu, B. S.; Jin, C. Y.; Zhu, Q.; Yan, D. Y.; Zhu, X. Y., Self-assembled encapsulation systems with pH tunable release property based on reversible covalent bond. *Chem. Commun.* **46** (40), 7569-7571. (2005)

^[115] Gannett, P.M.; Powell, J.H. *J. Environ. Pathol. Toxicol. Oncol.* **21**(1), 1-31 (2002)

^[116] Regulation (EC) No 1223/2009 of the European parliament and of the council of 30 November 2009 on cosmetic products, Annex II list of substances prohibited in cosmetic products

4/ Profragrances

a) Definitions and concepts

Volatile organic compounds, present in nature and mainly used for inter-species communication through molecules like pheromones, are used by humans since antiquity to produce perfumes and other cosmetic products.^{[117][118]} In order to reach their biological target, they must possess a unique molecular structure, since they have to be detected by specific probes to deliver their biochemical signals. Such volatile compounds must also be easy to evaporate and transport through air by diffusion and convection, which implies low molecular mass and vapour pressure. This ease of evaporation also means that molecules should present a short lifetime in the air at the concentration needed to have a biological role, even if the detection threshold for the human nose is low for most fragrances.^[119]

To avoid high speed dispersion of volatile molecules, strategies have been developed to control the release of fragrances.^[3] Since the performance of perfume ingredients is often correlated to their persistence, the field of controlled release has become vital for perfume and aroma industries. Two main methods have been used to reach this effect:

- Encapsulation, which consists in producing a matrix or a capsule that is specific to the compound to release and to trap, so it can slowly free itself thanks to diffusion phenomena.
- The use of fragrance precursors called profragrances that are analogues of drug precursors used by the pharmaceutical industry, and which present a very different releasing mode.

In profragrances, the active molecule is covalently linked to a substrate to form a higher molecular mass compound, which has a decreased vapour pressure and possibly no smell (Figure 24).^[3] The substrate must be chosen to form an easily cleavable bond with the fragrances, in order to be released under « mild » conditions, i.e. typical conditions used for the targeted product. Various kinds of stimuli can be used to trigger the release: change of temperature, hydrolysis by change of concentration or pH, exposition to light or UV, or enzymatic degradations caused by bacteria and micro-organisms.

^[117] Rowe, D. J. *Chemistry and Technology of Flavors and Fragrances*, Blackwell Publishing Ltd., Oxford, (2005)

^[118] S. Arctander, *Perfume and Flavor Chemicals*, published by the author, Montclair (1969)

^[119] Devos, M.; Patte, F.; Rouault, J.; Laffort, P.; VanGemert, L. J. *Standardized Human Olfactory Thresholds*, Oxford University Press, Oxford (1990)

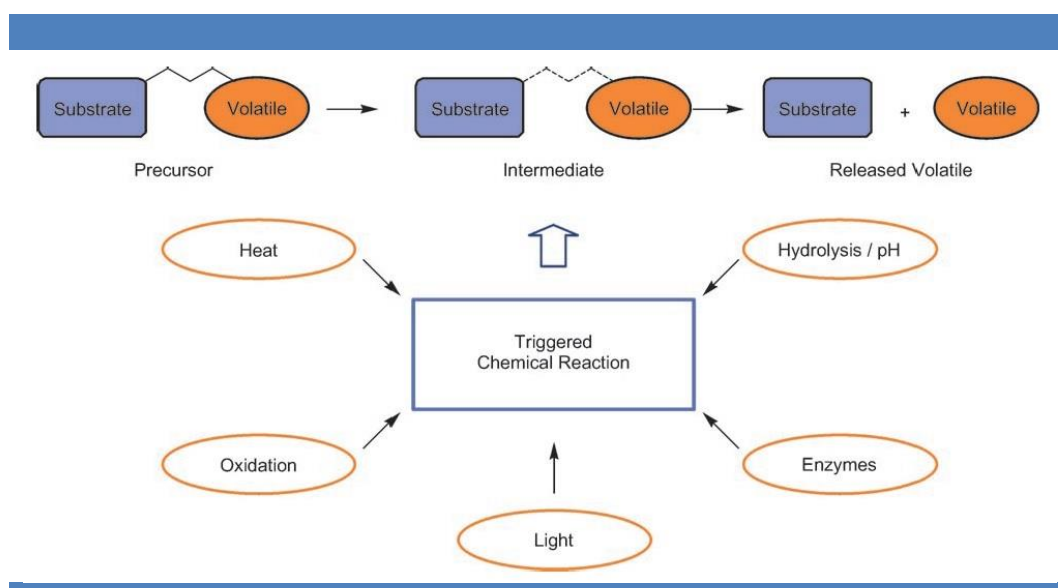


Figure 24 | Principle of the use of profragrances for the controlled release of volatile molecules and external stimuli that can trigger the cleavage of the Substrat-Fragrance bond. (Herrmann)^[3]

Since the release of volatile molecules is based on the breaking of a covalent link between the fragrance and a substrate, the choice of the structure of the precursor is of major importance. Precursors must be able to release a broad variety of chemical functions such as aldehydes, ketones, alcohols, esters etc., (Figure 25), which means *in fine* that a given precursor will only be able to release a single class of chemical compounds. This could be a problem in the field of perfumery, since most of fragrance mixtures are constituted of very diverse compounds, and it would be needed to develop libraries of substrates adapted to all the volatile molecules that have to be released. Hopefully, increasing the performance of a perfume can be reached by focusing only on the most volatile compounds, making the profragrance-based formulations easier to prepare.

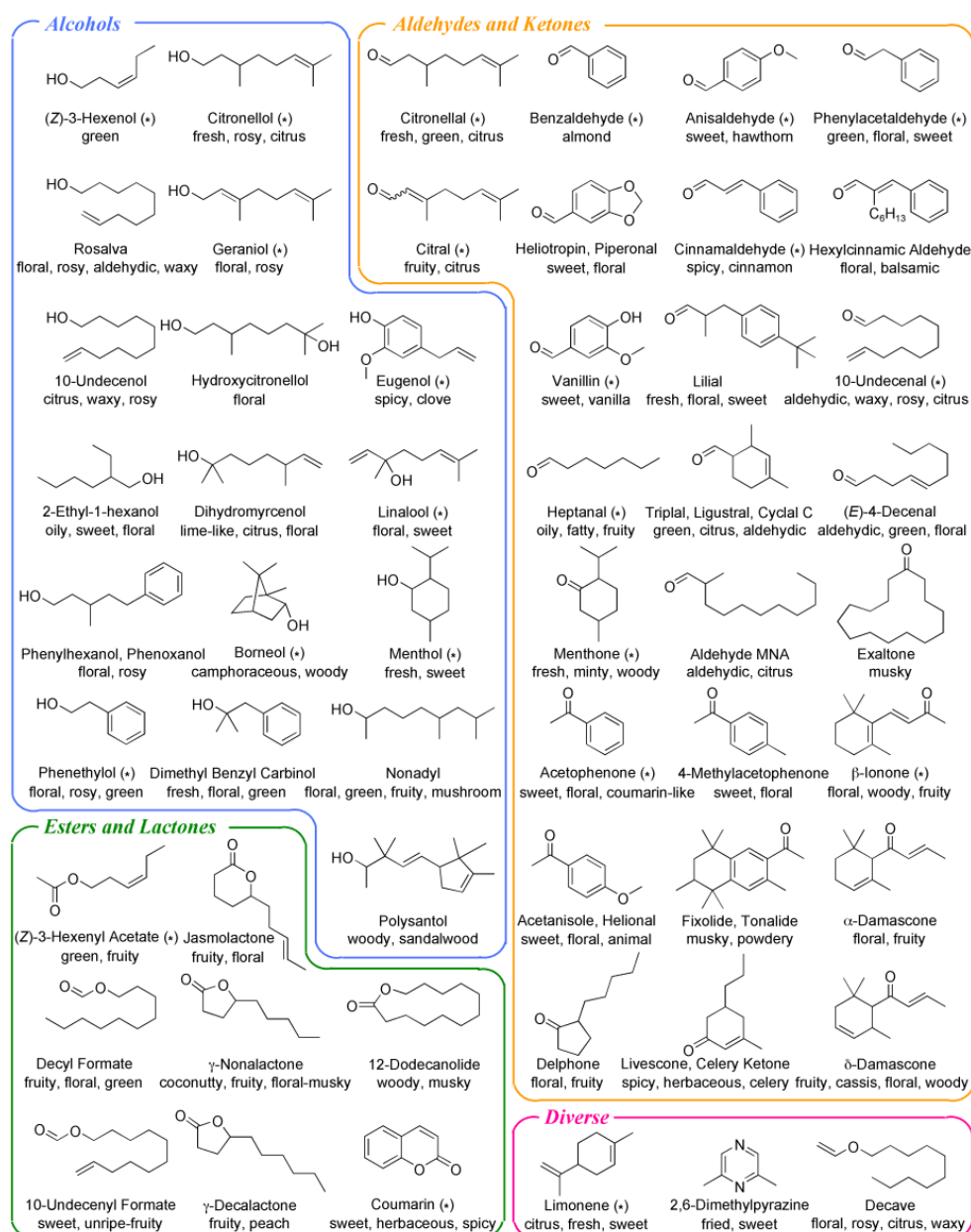


Figure 25 | Selection of groups of volatile compounds that were successfully released from profragrances. (Herrmann)^[3]

The possible chemical links between the substrate and the fragrance are numerous and must be chosen considering the following parameters:

- Molecule(s) to be released
- Environmental conditions
- Trigger
- Desired kinetics of release

Chemical links used so far can be divided in two categories: dynamic and non-dynamic bonds. Whereas dynamic bonds can be formed *in situ* in a fragrance mixture upon addition of an adequate reacting substrate, non-dynamic bonds irreversibly release the volatiles when they are broken, and need specific synthesis.

b) Non-dynamic profragrances

i) Heat

One of the first trigger that has been used to release volatile compounds from profragrances was an increase of the temperature, since it represent the easiest way to have enough energy to break covalent bonds. In everyday's life, plenty of activities require heating, from hair drying and ironing, to smoking and cooking. These wide ranges of temperature enable, according to the chosen application, the use of many different chemical functions in the design of profragrances. One of the oldest applications can be attributed to Teague and Ashburn in 1956 for the release of carboxylic acids during the combustion of a tobacco preparation using galactose, sorbose and poly(vinyl alcohol) polyhydroxy esters (Figure 26).^{[120][121]}

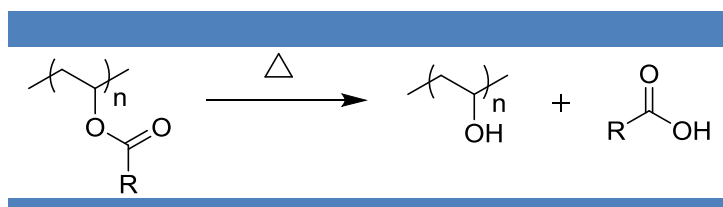


Figure 26 | Principle of the release of carboxylic acids during the combustion of a precursor synthesised from a derivative of poly(vinyl)alcohol. (Ashburn)^[120]

Other molecules with different chemical functions have been released from precursors by pyrolysis at high temperatures (>150°C) such as benzaldehyde or pyrazine derivatives^{[122][123]} (**1**, Figure 27), β-hydroxy acids, esters^[124] (**2**, Figure 27), pinacols^[125] or urea derivatives^[126].

^[120] Ashburn, J. G. (R. J. Reynolds Tobacco Company), US 2766146 (1956)

^[121] Teague, C. E. (R. J. Reynolds Tobacco Company), US 2766150 (1956)

^[122] Houminer, Y., Studies on the Thermolysis of 2-(2-Hydroxy-2-Arylethyl)Pyrazines - Example of a Retro-Ene-Type Reaction. *Journal of Organic Chemistry*, **45** (6), 999-1003 (1980)

^[123] Houminer, Y.; Secor, H. V.; Seeman, J. I. (Philip Morris Products Inc.), EP 0309203 (1989)

^[124] Teng, L. C. (Philip Morris Inc.), US 4036237 (1977)

^[125] Anderson, D. (Givaudan-Roure SA), JP 09003477 (1997)

^[126] Castelmur, H. (Tamag Basel AG), GB 1401099 (1975)

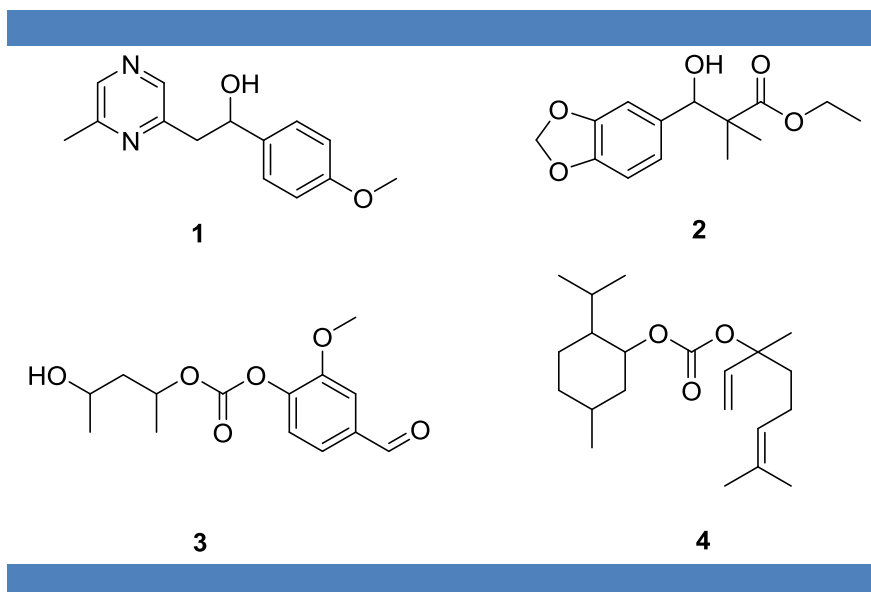


Figure 27 | Thermocleavable precursors for the release of aldehydes (**1**, **2**) and alcohols (**3**, **4**).^{[124][125][127][128]}

Other molecules such as vanillin (**3**, Figure 27)^[127] or menthol (**4**, Figure 27)^[128] can be released at much lower temperatures, mainly thanks to the use of carbonates.

The use of sugar derivatives for the fabrication of profragrances is also widely spread, since they are biocompatible, cheap and easily available from natural sources. They have been used in numerous applications for food industry, which is generally stricter than the cosmetic one from the point of view of toxicity and regulations. Upon heating, sugar derivatives can release alcohols and phenols by cleavage of glycoside bonds^[129] and aldehydes from cyclic acetals.^[130] An interesting example is given by Chan,^[131] with a system that can release both an alcohol and an aldehyde or a ketone (Figure 28).

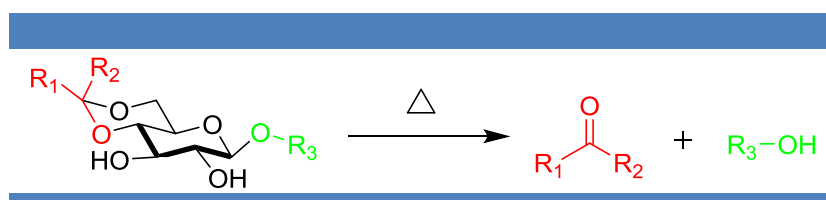


Figure 28 | Example of thermocleavable sugar derivatives. (Chan)^[131]

^[127] Houminer, Y.; Podraza, K. F. (Philip Morris Inc.), US 4509537 (1985)

^[128] Grubbs, H. J.; Auken, T. V.; Johnson, W. R. (PhilipMorris Inc.), DE 2647323 (1977)

^[129] Kallianos, A. G.; Porter, J. F.; Mold, J. D. (Liggett & Myers Inc.),US 3499452 (1970)

^[130] Eilerman, R. G.; Christenson, P. A.; Yurecko, J. M.; Mild, F.; Kucharski, P. E. (BASF K&F Corp.), EP 0413162 (1991)

^[131] Chan, W. G. (Philip Morris Products Inc.), US 5137578 (1992)

ii) Oxidation

Another easy way of breaking covalent bonds to release volatiles is oxidation. In organic chemistry, oxygen is often responsible for the degradation of some functional groups like aldehyde or aromatic amines, or for the generation of side products in organic chemistry or termination reactions in polymer science. However, this trigger could be particularly interesting for designing profragrances that are sensitive to oxidation. Nevertheless, the controlled release of volatiles is not easy to achieve, due to the omnipresence of oxygen that will slowly degrade the profragrance over time. For this reason, oxidation is not the most used trigger for the release of volatiles. Reymond and co-workers^[132] developed a system for releasing aldehydes and ketones based on the oxidation of β -amino alcohols (Figure 29) that have to be mixed with oxidants such as sodium bismuthate to trigger their release in the presence of atmospheric humidity (mechanism of the reaction not described).

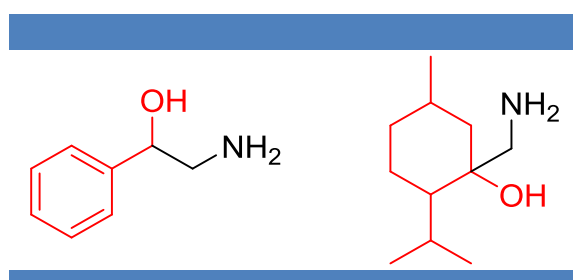


Figure 29 | β -amino alcohols for fragrance release by oxidative bond cleavage. (Raymond *et al.*)^[132]

Another interesting example of profragrance concerns the release of aldehydes by autoxidation of divinyl ethers (Figure 30).^[133] Autoxidation is a free radical process by which organic compounds react with molecular oxygen under ambient condition. The presence of a vinyl ether group in the structure of the profragrance makes it prone to react with oxygen to produce hydroperoxides, which decomposition is expected to yield the desired fragrance.

- Volatiles resulting from the decomposition of divinyl ethers by oxidation were investigated using total ion chromatography of headspace samples collected from profragrance-treated towels. It was found that the major compound released was the

^[132] Yang, Y.; Wahler, D.; Reymond, J.-L. β -Aminoalcohol properfumes, *Helv. Chim. Acta*, **86**, 2928 – 2936 (2003)

^[133] Indradas, B.; Hansen, C.; Palmer, M.; Womack, G. B., Autoxidation as a trigger for the slow release of volatile perfumery chemicals. *Flavour Frag J.* (2014)

expected parent aldehyde **10**, along with that-carbon shorter carbonyl compound **12** and also often the enol formate ester of the parent aldehyde **21**. Furthermore, these divinyl ethers are stable under acidic (1M HCl) and basic (1M NaOH) conditions and have successfully released aldehydes for several weeks after deposition into cotton clothes.

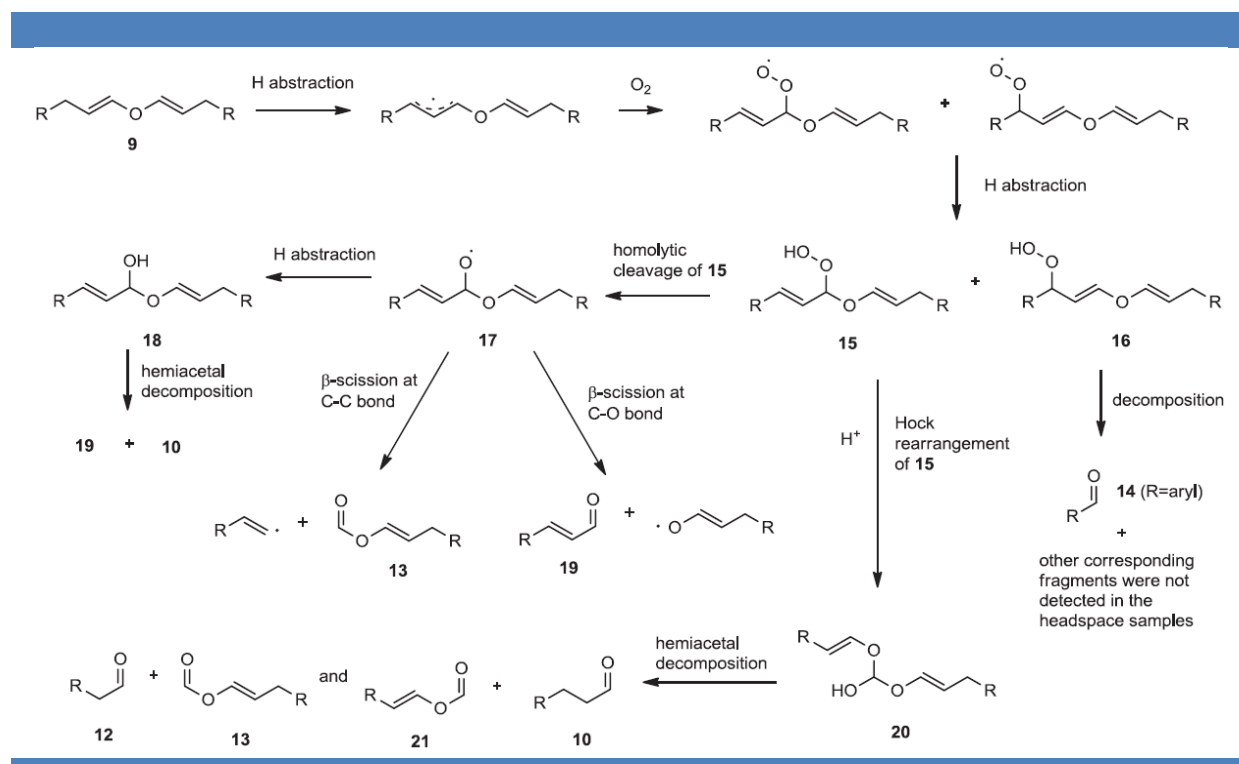


Figure 30 | Potential volatiles generated by homolytic or heterolytic decomposition of divinyl ether allylic hydroperoxides. (Womack et al.)^[133]

iii) Light

Yet, oxygen is not the only trigger present in the environment that can break or create covalent bonds. Sunlight, especially in the UV-B and UV-A wavelength regions of the solar spectrum (280 – 400 nm), can provide sufficient amounts of energy for the cleavage or the isomerization of covalent bonds,^{[134][135]} and this source of energy could be used to release volatiles from profragrances. Photosensitive profragrances have to be deposited directly on targeted surface through coating^[134] or incorporated into formulations like cleaning solutions

^[134] Powell, K.; Benkhoff, J.; Fischer, W.; Fritzsche, K. Secret sensations: novel functionalities triggered by light - Part II: photolabile fragrances *Eur. Coat. J.* **9**, 40 – 49 (2006)

^[135] Roth, H. D. The beginnings of organic photochemistry, *Angew. Chem., Int. Ed. Engl.* **28**, 1193–1207 (1989)

that will deposit the photocleavable molecules on the surface to treat.^{[136][137]} With the continuous development of artificial light sources with high intensities and filters to select efficiently specific wavelengths, it has become possible to perform photochemical reactions in an efficient and selective way.^{[136][138]} Two general ways of releasing molecules will be presented, one based on photocleavage and another one on photochemical E/Z double bond isomerization.

iii.a) Photofragmentation

In 1935, Bamford and Norrish published an early example of photofragmentation of carbonyl derivatives.^[139] This Norrish type II photofragmentation is based on an intramolecular γ -hydrogen abstraction by the oxygen atom of the carbonyl group to form transient 1,4-biradicals, followed by cleavage of the original C(α)-C(β) bond (Figure 31).^{[140][141]} Several functional groups can undergo Norrish type II fragmentation, notably alkyl and aryl α -keto esters and alkyl phenyl ketones. This latter class of compounds can be used to release a wide choice of fragrances, since the reaction can yield carbonyl compounds, alkene derivatives and acids, and even additional derivatives since some side reactions often occur during the photofragmentation of some profragrances (Figure 31).^{[3][142][143]}

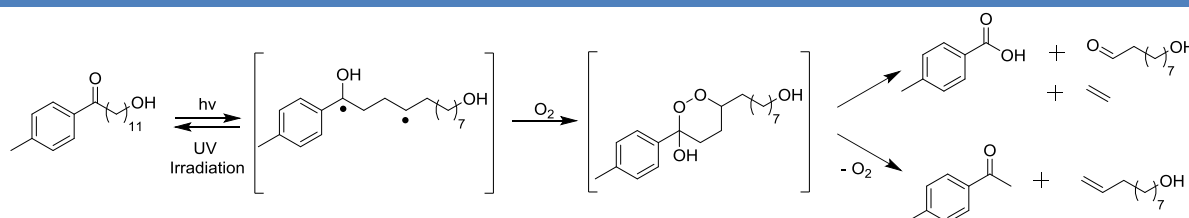


Figure 31 | Norrish type II photofragmentation of 12-hydroxy-1-(p-tolyl)dodecan-1-one (Wagner)^[141]

Another interesting and widely used class of molecules used in photofragmentation processes is based on the 2-nitrobenzyl moiety, that has been widely used as protecting group in

^[136] Herrmann, A. Using photolabile protecting groups for the controlled release of bioactivevolatiles, *Photochem. Photobiol. Sci.*, **11**, 446 (2012)

^[137] Herrmann, A. Photochemical fragrance delivery systems based on the Norrish type II reaction - a review, *Spectrum*, **17** (2), 10–13 (2004)

^[138] Braun, A. M.; Maurette, M.-T.; Oliveros, E. *Photochemical Technology*, John Wiley & Sons, Chichester (1991)

^[139] Bamford, C. H.; Norrish, R. G. H. Primary photochemical reactions. Part VII. Photochemical, decomposition of iso valeraldehyde and di-npropyl ketone, *J. Chem. Soc.*, 1504–1511 (1935)

^[140] Scaiano, J. C.; Lissi, E. A.; Encina, M. V., Chemistry of the biradicals produced in the Norrish Type II reaction. *Reviews of Chemical Intermediates*, **2**, 139-196 (1978)

^[141] Wagner, P. J. Conformational flexibility and photochemistry, *Acc. Chem. Res.*, **16**, 461 – 467 (1983)

^[142] Levrand, B.; Herrmann, A. Light induced controlled release of fragrances by Norrish type II photofragmentation of alkyl phenyl ketones, *Photochem. Photobiol. Sci.*, **1**, 907–919 (2002)

^[143] Griesbeck, A. G.; Hinze, O.; Gerner, H.; Huchel, U.; Kropf, C.; Sundermeier, U.; Gerke, T., Aromatic aldols and 1,5-diketones as optimized fragrance photocages. *Photochem. Photobiol. Sci.*, **11**, 587-592 (2012)

photochemistry.^{[144][145]} It has been efficiently used to release a broad range of alcohols^[146], including volatile alcohols.^[134] For instance the 2-nitrobenzyl ether based profragrance of Figure 32 can release vanillin upon photolysis at 380 nm by photochemical cleavage of the phenyl ether bond.^[136]

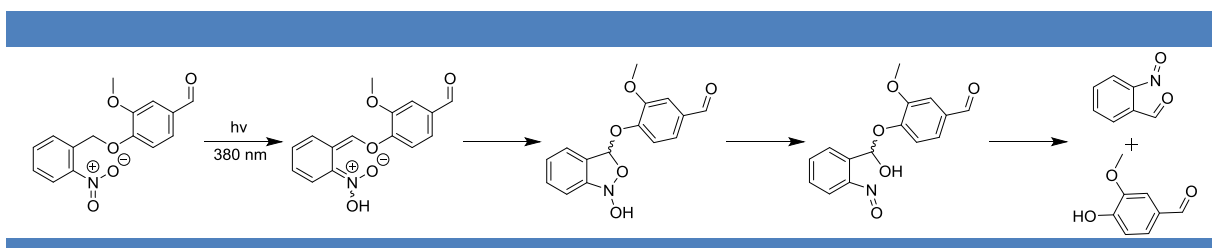


Figure 32 | Mechanism for the light-induced formation of vanillin from a 2-nitrobenzyl ether based profragrance (adaptated from ref. 136)

This profragrance has been successfully tested in coating formulations where it proved to be stable in standard conditions and managed to reduce the bleaching process usually occurring with vanillin.

Besides releasing alcohols, 2-nitrobenzyl group can also be used for the release of aldehydes.^[147] This has been demonstrated by Robles and Bochet who released (R)-citronellal from photolabile ether after photoirradiation at 350 nm for three hours in acetonitrile (Figure 33).

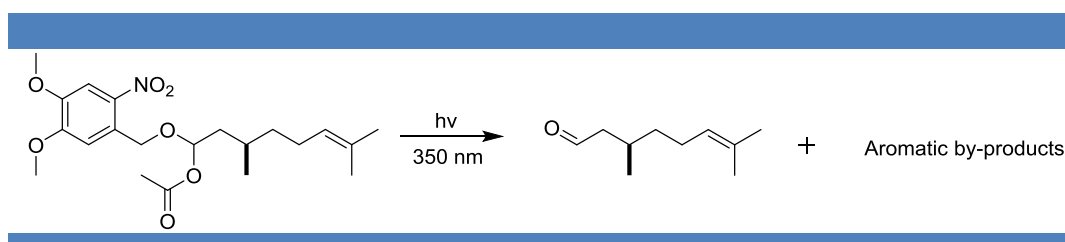


Figure 33 | Photolysis of an acetoxy ether profragrance for the controlled release of citronellal upon UV irradiation (Robles and Bochet).^[147]

^[144] Pillai, V. N. R. Photoremovable protecting groups in organic synthesis, *Synthesis*, 1–26 (1980)

^[145] Pillai, V. N. R. Photolytic deprotection and activation of functional groups, *Org. Photochem.*, **9**, 225–323 (1987)

^[146] Il'ichev, Y. V.; Schwörer, M. A.; Wirz, J. Photochemical reaction mechanisms of 2-nitrobenzyl compounds: methyl ethers and caged ATP, *J. Am. Chem. Soc.*, **126**, 4581–4595 (2004)

^[147] Robles, J. L.; Bochet, C. G. Photochemical liberation of aldehydes, *Org. Lett.* **7**, 3545 – 3547 (2005)

iii.b) Photochemical E/Z double bond isomerization

One of the early work concerning the formation and release of volatiles thanks to the isomerization upon UV irradiation was performed in the 1930s. Dey *et al.* showed that (E)-(2-hydroxyphenyl)acrylates cyclise to coumarins when exposed to sunlight^[148]. A recent development of this approach was conducted by Anderson and Fràter^[149], who successfully synthesised and brought to the market a series of (E)-(2-hydroxyphenyl)acrylates (**a**, Figure 34) which isomerize to (Z)-(2-hydroxyphenyl)acrylates upon irradiation to finally releases coumarins and fragrance alcohols in a 1:1 ratio.

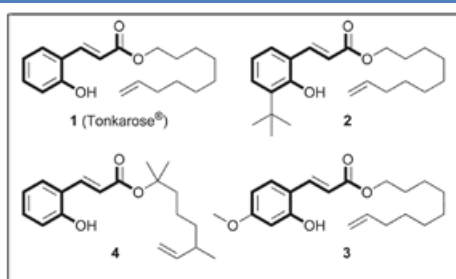


Figure 34 | a) Structure of (E)-(2-hydroxyphenyl)acrylates properfumes^[136] **1-4**.

Precursor **1**, namely Tonkarose, releases coumarin and 9-decenol upon irradiation thanks to an isomerization followed by an intramolecular transesterification.

These few examples of photofragmentation and isomerization represent only a fraction of all the systems that have been developed for decades. A wide range of chemical functions prone to fragmentation upon irradiation exist, and these systems can efficiently release an important number of different chemical functions from profragrances, with the most important concerning the fragrance industry being carbonyl compounds, alcohols, and almost no carboxylic acids.

^[148] Dey, B. B.; Rao, R. H. R.; Seshadri, T. R. Geometrical inversion in the acids derived from the coumarins, *J. Ind. Chem. Soc.*, 743–749 (1934)

^[149] Anderson, D.; Frater, G. Aryl-acrylic acid esters useful as precursors for organoleptic compounds (Givaudan Roure SA), EP 0 936 211 (1999)

iv) Enzymes and microorganisms

Other triggers that can be found everywhere are enzymes and microorganisms, and they are particularly numerous on our skin. These bioorganisms can be used to cleave selective function of deposited profragrances and thus enable the release of fragrances over time. One class of useful enzymes present on skin and in skin bacteria is the family of glycosidases. These enzymes can break glycoside bonds, and are thus efficient at releasing volatiles from mono- or disaccharides. These volatiles can be either mono or sesquiterpenes, aliphatic alcohols, or derivatives of phenylpropane.^[150] Profragrances based on glycosides possess several advantages such as high water solubility (usually fragrances are poorly soluble hydrophobic compounds) and the possibility to release a broad variety of fragrance alcohols. They are therefore interesting for cosmetic or bodycare applications.^{[151][152]} An example is given by T. Ikemoto *et al.*, who synthesised precursor **a**) Figure 35 and confirmed the release of phenylethylol in application conditions on skin and on hair, thanks to GC, HPLC and headspace analysis.^{[151][153]}

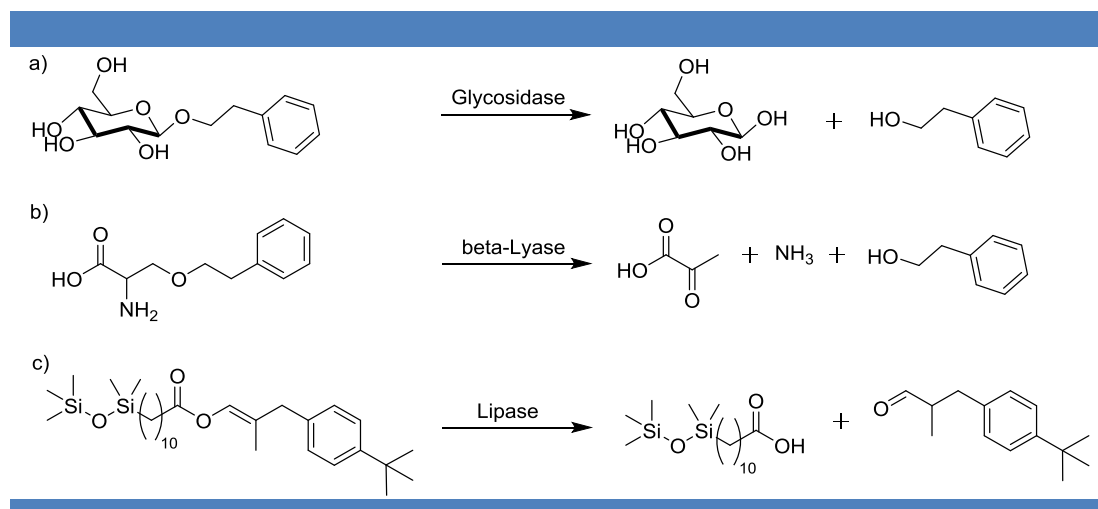


Figure 35 | Enzymatic cleavage of profragrances for the controlled release of volatile alcohol and aldehyde. (T. Ikemoto *et al.*)^{[153][154][158]}

^[150] Sarry, J. E.; Gunata, Z. Plant and microbial glycoside hydrolases : volatile release from glycosidic aroma precursors, *Food Chem.*, **87**, 509 – 521 (2004)

^[151] Ikemoto, T.; Mimura, K.; Kitahara, T. Formation of fragrant materials from odourless glycosidically-bound volatiles on skin microflora (part 2). *Flavour Fragrance J.* **18**, 45 – 47 (2003)

^[152] Jensen, O. R.; Thyge, F. O. (Poalis A/S), WO 2006/087370 (2006)

^[153] Ikemoto, T.; Nakatsugawa, H.; Okabe, B.; Ogino, K.; Inui, S.; Inui, T.; Inui, M.; Inui, J.; Matsui, I.; Wamoto, M.; Fujita, A. (Kanebo Ltd. and T. Hasegawa Co. Ltd.), WO 96/14827 (1996)

A second class of enzymes, so-called β -lyases, present in skin bacteria and known for generating thiols and other bad smells^[154], can be used to cleave precursors. For example, pyridoxal phosphate-dependent amino acid β -lyase was reported to generate a pyruvate, ammonia and either a thiol, an alcohol or a carboxylic acid depending on the precursor.^{[155][156][157]} An example of this type of precursor is described on Figure 36b, a profragrance able to generate phenylethylol after prolonged contact with the skin, and therefore able to reduce the formation of bad smells for deodorant application.^[155]

A third class of enzymes, known as lipase and used to cleave triglycerides, has also been used to cleave various kind of esters. Present on human skin and in skin bacteria, such enzymes can release alcohols and also carbonyl compounds^{[158][159]} from enol esters such as **c** (Figure 36), as well as oximes from oxime carbonates.^[160] Importantly, this enzyme is known to tolerate high pH values, elevated temperatures and the presence of other ingredients in formulations such as detergents.^[161]

v) Hydrolysis

Another compound that is present everywhere and that could be used as trigger is water. Many variety of chemical functions and thus chemical systems are sensitive to hydrolysis and pH variation. I will not give a general overview of all the systems that exist but rather focus on a few of them that will demonstrate the influence of several important parameters like the domains of stability or the influence of surfactants. These observations are important to plan and understand further experiments.

Waite *et al.* have developed an alcohol-releasing profragrance based on an ester bond.^[162] Indeed, monoesters of carboxylic diacids (Figure 36, **a**) display a stability that enables their use for applications in laundry and cleaning compositions. Moreover, the use of these profragrances in such applications proved to have a long-lasting effect, thus performing better than their fragrances counterparts. Various carboxylic diacids can be used, including phthalate (Figure 36, **b**), maleates or succinates. This type of ester can be hydrolysed in different

^[154] Froebe, C.; Simone, A.; Charig, A.; Eigen, E. Axillary malodor production : a new mechanism, *J. Soc. Cosmet.Chem.*, **41**, 173 – 185 (1990)

^[155] Lyon, S. B.; Neal, C. O.; Lee, H. (The Gillette Company), WO 91/11988 (1991)

^[156] Laney, J. W. (The Gillette Company), WO 95/ 07069 (1995).

^[157] Eliot, A. C.; Kirsch, J. F. Pyridoxal phosphate enzymes: mechanistic, structural, and evolutionary considerations, *Annu. Rev. Biochem.* **73**, 383 – 415 (2004)

^[158] Paget, W.; Reichlin, D.; Snowden, R. L.; Walborsky, E. C.; Vial, C. (Firmenich SA), WO 95/04809 (1995)

^[159] Gautschi, M. ; Blondeau, P. ; Derrer, S. (Givaudan-Roure SA), EP 1077251 (2001)

^[160] Anderson, D.; Frater, G. (Givaudan-Roure SA), EP 0980863 (2000)

^[161] Ee, J. H.; Misset, O.; Baas, E. J. Enzymes in Detergency, (Surfactant Sci. Ser., Vol. 69), Marcel Dekker, New York (1997)

^[162] Waite, S. W.; Severns, J.C.; Sivik, M. R.; Hartman, F. A. (The Procter&Gamble Company), WO 97/16523 (1997)

conditions: either by enzymes in neutral conditions when deposited on the skin or in acidic or basic aqueous solutions.

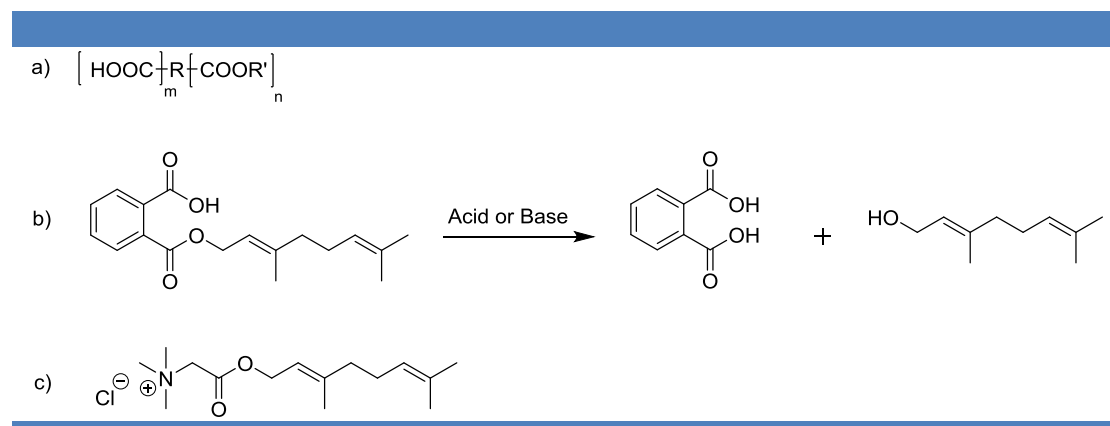


Figure 36 | a) General formula of monoesters of carboxylic diacids ($m = n = 1$). b) Release of geraniol from a profragrance based on an ester bond. (Hartman *et al.*)^[162] c) Betaine ester profragrance for the controlled release of geraniol (Murayama *et al.*)^[163]

Profragrances based on ester links with enhanced properties have also been developed. Murayama *et al.* assessed the performance of betaine ester derivatives in various formulations (Figure 36, c).^[163] These betaine esters can be used as mild hair and skin conditioning agents,^[163] and have surfactant properties as well as properties to interact with anionic centres on the surface of the hair and attach substantively to its surface. However, cationic and amino-functional conditioning agents have cosmetic and odour issues that have to be fixed by the addition of perfume oil. Since betaine esters are stable in basic conditions but readily hydrolyse in neutral conditions^[164] or with an humidity, the design of new formulations that can lead to the deposition of betaine ester profragrances by ionic bonding to the hair and further slowly release fragrances over time can fix this issue.

For some chemicals, controlling the release of the volatile is not the only issue. In the case of aldehydes and, to a lesser extent, ketones, degradation reactions can occur and there is thus a need to stabilise the aldehyde by chemical modification during storage. An easy way to overcome this issue is to react aldehydes with alcohols or polyols^[165] to form hemiacetals or

^[163] Murayama, K.; Tanaka, S.; Katayama, A.; Hirayama, R.; Gema, T. (Kao Corporation), EP 1099689 (2001)

^[164] Struillou, A. P.; Heinzman, S. W.; Gordon, N. J. (The Procter & Gamble Company), EP 0771785 (1997)

^[165] Sharma, A.; Nagarajan, S.; Gurudutt, K. N. Stabilization of Aldehydes as Propylene Glycol Acetals, *J. Agric. Food Chem.* **46**, 654 – 656 (1998)

acetals. An example of the acid-catalysed hydrolysis of an acetal profragrance to give back glycerol and release cinnamal^[166] is given in Figure 37a. Another strategy consists in chemically bonding the profragrance **a** to a polymeric matrix like for **b** to enhance solubilisation properties.

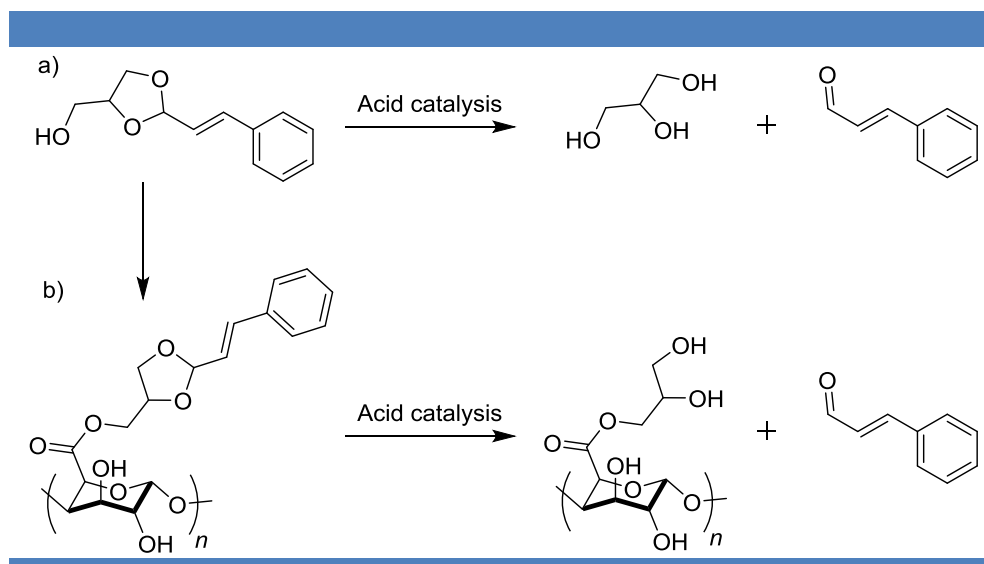


Figure 37 | Release of cinnamal from acetal-based profragrances. (Gurudutt *et al.*)^[165]

The case of acetal-based profragrances is interesting because acetals are usually too stable. However, it is possible to tune the hydrolysis reaction rate by changing substituents at the carbonyl group, polar substituents being preferred to increase the rate of hydrolysis of the acetal and thus fastening the release of the initial aldehyde. The presence of surfactants plays also a prominent role in the kinetics of hydrolysis; Cordes and Bull proved that anionic surfactants catalyse the hydrolysis of acetals and hemiacetals and that cationic ones inhibit this reaction^[167]. This comes from the fact that anionic surfactants stabilise the cationic transition states that occur during acetal catalysis, thus promoting their hydrolysis. It is also noteworthy that non-ionic and zwitterionic surfactants tend to inhibit these reactions, perhaps reflecting the lower polarity at the micellar surface compared to the bulk phase.

Although acetal formation and hydrolysis are reversible phenomena, acetals usually do not spontaneously form in water requiring a synthetic step to get the profragrance before its incorporation into formulations. To overcome this issue, it would be interesting to study other

^[166] Gerke, T. (Henkel KGaA), DE 19718537 (1998)

^[167] Cordes, E. H.; Bull, H. G. Mechanism and catalysis for hydrolysis of acetals, ketals, and ortho esters, *Chem. Rev.* **74**, 581 – 603 (1974)

dynamic chemical functions that can form profragrances in solution at room temperature without catalysts, and which can then be hydrolysed from the same solution with a trivial trigger such as change of temperature, pH or concentration. An important class of compounds that have these properties correspond to the imine derivatives, arising from the condensation of amine derivatives and carbonyl compounds.

c) Dynamic profragrances

Unlike their non-dynamic counterparts, dynamic profragrances result from a thermodynamic equilibrium between the profragrance and its constituents (substrate and fragrance). The reversibility of the bond between the substrate and the volatile molecule make these systems well suited for the creation of dynamic mixtures for delivery systems, and any perturbation will result in a re-equilibration of the system. The dynamic link as well as the type and intensity of the perturbation are key parameters influencing the kinetics of release of the fragrance.

One of the first uses of hydrolytically labile fragrance precursors was realized by Kremers.^[168] His main aim was to protect aromas of food materials from volatilization, oxidation, and polymerization. The problem was solved by adding, during the product manufacture, a stable, substantially non-volatile, non-oxidable functional derivative formed by chemical interaction of a carbonyl group from one reactant with an amine group of another reactant, one being the fragrance to protect. The main constraints for choosing of the substrate were that it had to be compatible with food and in a reversible manner under the conditions of ultimate use. A more recent use of imines, based on previous work from Procter&Gamble,^{[169][170]} has been demonstrated by Luca for the stabilization and the controlled release of musks.^[171] The aim was to design a biodegradable and non-oxidable imine formed from the condensation of a musk carbonyl and an odourless amine. The strategy to make the odourless substrate was to use amines which also had an easily ionizable group like carboxylic acid or sulphate (**a**, Figure 38) or polyamines (**b**, Figure 38).

^[168] Kremers, R. E. (General Foods Corp.), US 2305620 (1942)

^[169] Bettiol, J.-L. P.; Busch, A.; Denutte, H.; Laudamiel, C.; Perneel, P. M. K.; Sanchez-Pena, M. M.; Smets, J. (The Procter&Gamble Company), WO 00/02991 (2000)

^[170] Busch, A.; Hombler, M.; Laudamiel, C.; Smets, J.; Trujillo, R.; Wevers, J. (The Procter&Gamble Company), EP 0971021 (2000)

^[171] Luca, T. (Flexitral Inc), WO2006012215 A1 (2006)

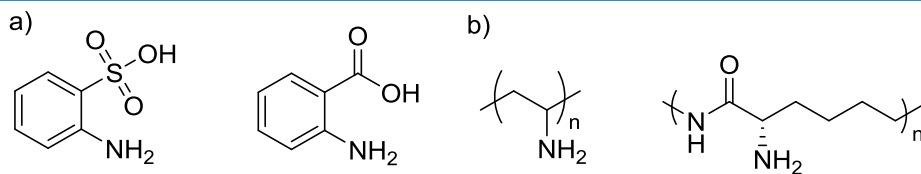


Figure 38 | Example of amines used for the formation of musk-releasing imines. a) Non-volatile aromatic amines b) Non-volatile polymeric amines. (Luca)^[171]

The proposed applications for these kinds of profragrances are broad: perfumes, soaps, bath or shower gels, shampoos *etc.* However, these applications required the use of the profragrance in important quantity (>30% in weight), probably because of the limited stability of imines in water. Indeed, imines usually hydrolyse rapidly in aqueous media, and sometimes more stable profragrances are needed. To achieve slower hydrolysis and releasing speed, A. Herrmann *et al.* prepared acylhydrazones from commercial hydrazides and volatile fragrance aldehydes^[172] (A, Figure 39).

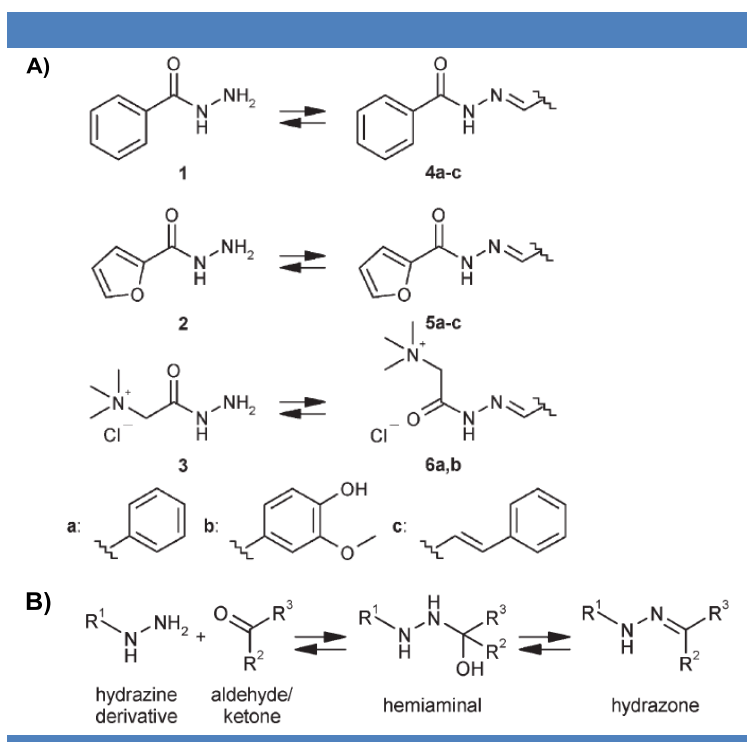


Figure 39 | A) Structures of acylhydrazones 4–6 obtained by reaction of hydrazides with different perfumery aldehydes B) Equilibrium for the reversible hydrazone formation. (A. Herrmann *et al.*)^[172]

^[172] Levrard, B.; Ruff, Y.; Lehn, J. M.; Herrmann, A., Controlled release of volatile aldehydes and ketones by reversible hydrazone formation - "classical" profragrances are getting dynamic. *Chem Commun*, (28), 2965-2967 (2006)

They found out that pH had a much stronger effect on the reaction rates than the structure of aldehydes or hydrazides. It was also found that at neutral pH, dehydration of the hemiaminal was the rate-determining step, whereas at lower pH hemiaminal formation was the slower step^{[173][174]} (B, Figure 39). Performance of delivery systems in fabric softeners were assessed by formation of a dynamic profragrance mixture composed of aldehydes, hydrazide and the resulting acylhydrazone in water in presence of a cationic surfactant at pH 4. Then, the profragrance mixture was diluted and deposited onto cotton and evaporation of aldehydes was followed by headspace analysis coupled to GC-MS.^[175] The fragrance concentration in the headspace above the sample was determined at constant time intervals and compared to a reference sample without hydrazide which was prepared and analysed under the same conditions. At the end of the experiment, due to the presence of the hydrazide precursor, the amount of released aldehyde was increased by a factor between 1.4 and 20 (Figure 40 for a typical plot of headspace concentrations). Once deposited onto cotton, fragrances evaporated from the mixture and shifted the equilibrium towards free hydrazine derivative.

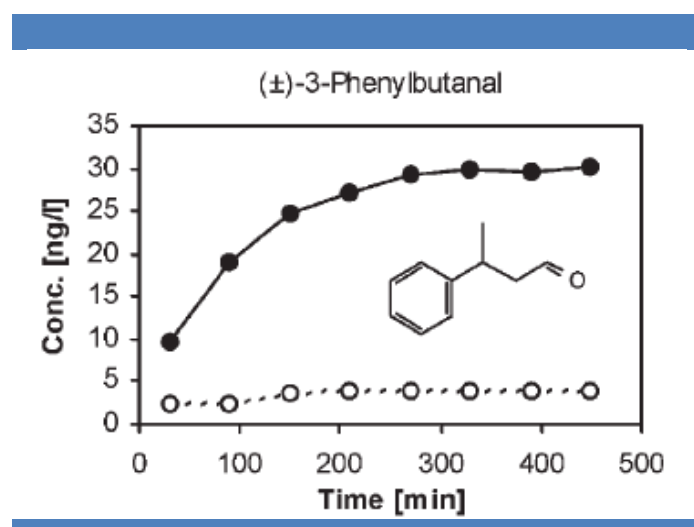


Figure 40 | Headspace concentrations measured for the evaporation of 3-phenylbutanal on a dry cotton sheet in the presence (—●—) or absence (—○—) of 2-hydrazinyl-N,N,N-trimethyl-2-oxoethanaminium chloride. (A. Herrmann *et al.*)^[172]

These results show clearly that dynamic mixtures prepared from sufficiently stable C=N bond derivatives (here acylhydrazone) can be efficient delivery systems for the controlled release of biologically active compounds.

^[173] Jencks, W. P. Mechanism and catalysis of simple carbonyl group reactions, *Prog. Phys. Org. Chem.* **2**, 63-128 (1964)

^[174] Nguyen, R.; Huc, I. Optimizing the reversibility of hydrazone formation for dynamic combinatorial chemistry, *Chem. Commun.* 942-943 (2003)

^[175] Jenner, K. The Chemistry of Fragrances (2nd ed.), Sell, S. C., Royal Society of Chemistry Publishing, Cambridge (2005)

This work was later extended by the study of amins made from the condensation of fragrance aldehydes and secondary diamines (**a**, Figure 41).^[176] The equilibration time was much slower for the formation of amins than it was for acylhydrazone (typically 2 weeks for amins at pH 8 and several hours for acylhydrazones at pH 4), and yielded at equilibrium a maximum of 80% of amina compared to free diamines.

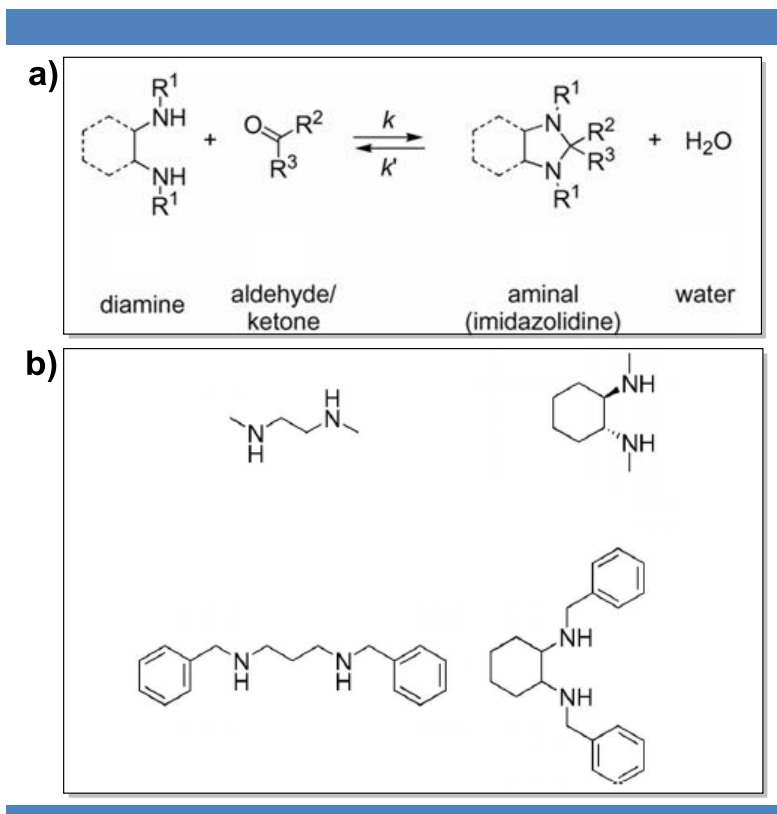


Figure 41 | a) Reversible formation of amins through reactions between diamines and carbonyl compounds. b) Secondary diamines used for the amina formation. (A. Herrmann *et al.*)^[176]

The amins were synthesized from various volatile aldehydes and ketones and several secondary diamines (**b**, Figure 41). Headspace measurements were performed on mixtures of secondary diamines and aldehydes and ketones in similar conditions than that used for acylhydrazones (See Figure 43 for example). It was found out diamines mainly affect the release of aldehydes, but have little to no influence on the release of ketones, as expected from the very low concentrations of amins measured at equilibrium in aqueous diamine/ketone mixtures. Nevertheless, some cyclic diamines showed stronger performance than hydrazides (Figure 42).

^[176] Buchs, B.; Godin, G.; Trachsel, A.; de Saint Laumer, J. Y.; Lehn, J. M.; Herrmann, A., Reversible Amina Formation: Controlling the Evaporation of Bioactive Volatiles by Dynamic Combinatorial/Covalent Chemistry. *Eur J Org Chem*, (4), 681-695 (2011)

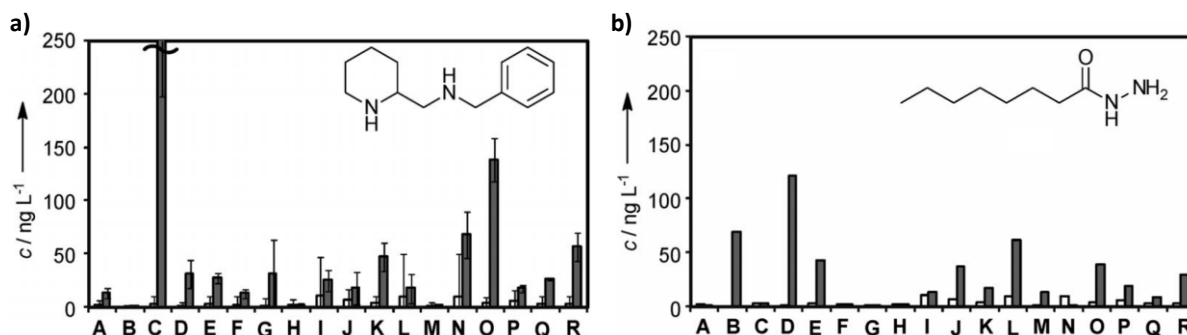


Figure 42 | Headspace concentrations measured for the evaporation of a mixture of volatile carbonyl compounds **A – R** (not shown) from dry cotton in the presence (grey bars) and in the absence (white bars) of **a)** a cyclic diamine and **b)** a hydrazide. (A. Herrmann *et al.*)^[176]

Aminals showed to be interesting chemical systems for the controlled release of aldehydes, and can efficiently be hydrolysed around pH 8. However, hydrazine and hydrazide derivatives are known carcinogens,^[177] and their use in cosmetic products is banned.^[178]

A higher level of stability can also be achieved by condensing volatile aldehydes and ketones with hydroxylamine derivatives, thus forming oximes. These oxime derivatives can either be formed from hydroxylamine and thiohydroxylamine (**a**, Figure 43), or acyl hydroxylamine derivatives (**b**, Figure 43).^[179]

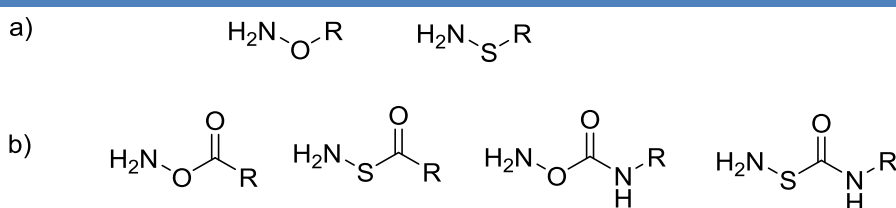


Figure 43 | **a)** Hydroxylamine derivatives used for the formation of oxime profragrances. **b)** Acylhydroxylamine derivatives used for the formation of acyloxime profragrances. (A. Herrmann *et al.*)^[179]

^[177] Gannett, P.M.; Powell, J.H. *J. Environ. Pathol. Toxicol. Oncol.* **21**(1), 1–31 (2002)

^[178] Regulation (EC) No 1223/2009 of the European parliament and of the council of 30 November 2009 on cosmetic products, Annex II list of substances prohibited in cosmetic products

^[179] Herrmann, A. ; Lehn, J.-M.; Godin G. (Firmenich SA, Université Louis Pasteur, CNRS), WO 2007085991 A2 (2007)

Headspace measurements were performed with mixtures of hydroxylamines and aldehydes and ketones in similar conditions than that used for acylhydrazones and amins, with an equilibration time for the dynamic mixture of five days. Except for 10-undecenal, headspace concentrations of aldehydes and ketones were found to be higher in the presence of the hydroxylamine derivative than in its absence (Figure 44). The presence of the hydroxylamine had thus a positive effect on the long-lastingness of the fragrance perception on dry fabric (only proved for the first 450 min), even if this positive effect might be too small to justify the cost of this delivery technology.

	90 min [ng/l]	210 min [ng/l]	330 min [ng/l]	450 min [ng/l]
Furfural	2.7 (1.0)	1.4 (0.3)	0.8 (0.0)	0.7 (0.2)
Citronellal	2.8 (1.5)	2.7 (1.1)	2.0 (1.0)	1.6 (1.2)
Trifernal	2.7 (1.0)	7.2 (6.7)	6.2 (5.9)	5.2 (5.1)
Delphone	1.1 (0.7)	0.5 (0.4)	0.3 (0.4)	0.5 (0.4)
10-Undecenal	4.4 (12.3)	6.7 (23.8)	5.9 (21.6)	4.7 (15.2)
Vertral [®]	2.1 (1.0)	2.5 (1.4)	2.1 (1.1)	1.9 (0.9)

Figure 44 | Amounts of different aldehydes and ketones detected from a sample containing the O-substituted hydroxylamine derivative as compared to the reference sample without the hydroxylamine derivative (in brackets). (A. Herrmann *et al.*)^[179]

d) Use of precursors in marketed products

Despite the broad variety of different precursors that have been developed, only a few of them have been commercialized, although the exact number of integrated precursors is difficult to count due to the industrial secret.^[3] This comes from the fact that a successful precursor must have an important number of secondary qualities:

- *It must be cost efficient:* consumer products are mass-produced and sold for relatively low prices, thus a delivery technology must either have a low impact on the price of the product or be so efficient that it can overcome the price.
- *It must be biocompatible:* strict regulations exist for cosmetic and fragrance products. Any new compound brought to the market has to be proved as safe for the consumer.

Chapter 1: Bibliography

- *It must be industrially feasible:* the synthesis has to be as easy as possible, with limited the number of steps and complicated purifications.
- *It should be versatile:* the precursor is industrially more interesting if it is able to release a broad variety of different fragrances.

All these elements have to be kept in mind when designing new profragrances. In the next chapter, I will present the synthesis and characterisation of dynablocks performed during my Ph.D.

Chapter 2: Synthesis and characterization of dynablocks

This Ph.D. relies on the simple design and the study of biocompatible responsive micelles, capable of releasing hydrophobic bioactive volatiles from an aqueous solution and that, depending on the modulation of external factors such as pH, temperature, and concentration. To reach this goal, we propose to take advantage of a new kind of micellar objects, recently described by the group of Professor Nicolas Giuseppone,^{[107][111][112][113]} and that are formed by the efficient self-assembly of biodegradable Dynamic Covalent Amphiphiles (DCAs), i.e. low cost surfactants that are made by the reversible molecular association of one hydrophilic and one hydrophobic block. This supplementary molecular thermodynamic equilibrium that takes place within the supramolecular micellar self-assembly offers unique opportunities for controlling the stability of the overall structure. Based on the knowledge that i) an amphiphilic aromatic imine could encapsulate up to three times its concentration of hydrophobic compound and that ii) the presence of an aromatic ring between the PEG chain and the imine moiety increased the stability of the imine in solution, the aims of the synthesis performed during my Ph.D. have been driven by two key applications:

- Encapsulation (Figure 45A) of a mixture of a DCA with a hydrophobic compound. The resulting self-assembly of the dynablocks into micellar self-assemblies will incorporate volatile molecules inside their micellar core, and their release will be triggered by a change of pH or concentration. The first goal of the synthesis was to isolate imines that were previously studied as mixtures in solution, and to tune their stability by the addition of additional reversible bonds within the micelles (hydrogen bonding) to get variations of the kinetics of hydrolysis. The influence of a linker between the hydrophilic and the hydrophobic blocks was investigated, and dynablocks with new reversible bonds were synthesised to modify the kinetics of hydrolysis and the pH of applications. From these new structures, semicarbazones and oximes were expected to be much more stable than their imine counterparts.
- Profragrances (Figure 45B) arising from a covalent reversible linkage between a hydrophilic block and a fragrance aldehyde. The resulting self-assembly of the dynablocks into micellar self-assemblies will incorporate volatile molecules inside the

molecular structure of the dynablocks, and the concentration or pH-triggered hydrolysis of the imine bond will lead to the release of volatile molecules. Families of fragrance-based dynablocks with different hydrophobic linkers were synthesised, in order to have kinetics of hydrolysis ranging from hours to weeks at different pH. The influence of several parameters such as viscosity, effect of CMC and presence of co-surfactant will be evaluated, as well as their incorporation into industrial formulations. However, due to patent applications concerns, we will not present the results obtained by Firmenich in applications.

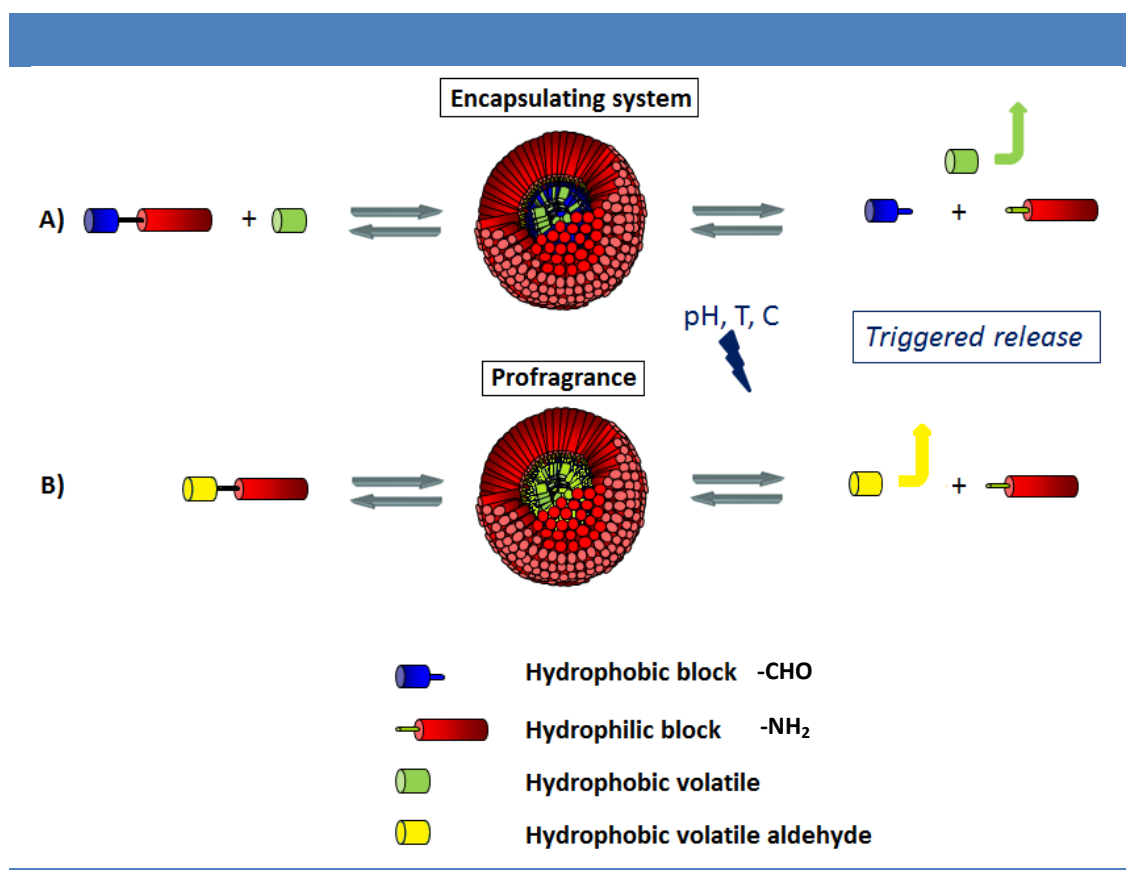


Figure 45 | General overview of the investigations planned on the DCA systems for the triggered release of flavor/fragrance. A) DCA for the controlled delivery of encapsulated molecules. B) DCA incorporating in its molecular structure the fragrance molecules to be released (Profragrances)

The literature described in chapter 1 has inspired our design of new dynamic encapsulating surfactants and profragrances. In particular, we have tried merging together the concepts of dynamic combinatorial chemistry and amphiphile micellisation. Previous work performed in our group regarding dynablocks have established that a library of amphiphiles with different

shapes (spherical and cylindrical micelles, vesicles), and imine links (aliphatic, benzylic, aromatic imines and oximes) can display different kinetics of formation and thermodynamic stability depending on the pH. Some molecules, notably imines made of aromatic amines, have also shown a higher stability in water and are even able to encapsulate some remaining hydrophobic aldehyde that can be further released upon hydrolysis of the imine bond by lowering the pH for instance.^{[107][111][112][113]} This type of amphiphilic molecules constitutes a very interesting starting point to develop a controlled release system that can stabilise hydrophobic volatile molecules in solution and release them upon stimulation. The large range of nucleophilicity available for amines, coupled to the different electrophilicities of aliphatic and aromatic aldehydes, makes possible to design imine derivatives with different kinetics of hydrolysis (and thus of release) at different pHs.

For further implementation in industrial applications, we have restricted our study to the simplest chemical structures of dynablocks, *i.e.* those accessible with few synthetic steps and in high yields, and starting from building blocks as cheap as possible.

1/ Chemistry of dynablocks

a) Choice of the reversible bond

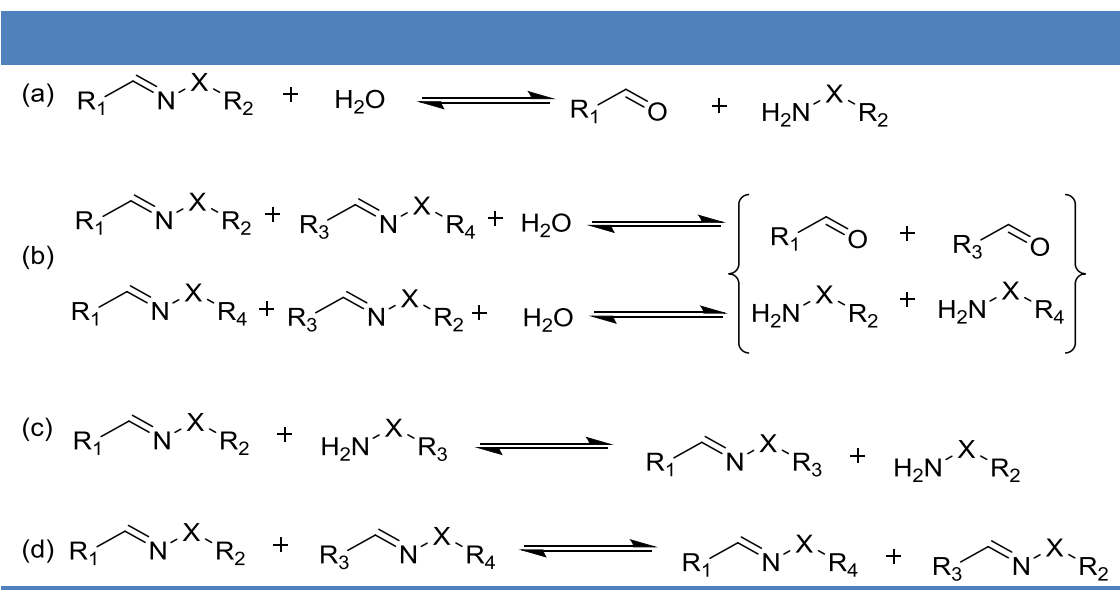
As previously mentioned, the reversible link between the hydrophilic and the hydrophobic block of the amphiphile will be constituted of an imine-type bond (C=N). This type of bond results from the reversible condensation of an aldehyde with an amine-type derivative which yields the C=N bond and a molecule of water.^[180] This chemical bond has been chosen for several reasons:

- Reversibility of the linkage and ease of synthesis starting from amine and aldehyde
- Sensitivity (and thus responsiveness) of imines to external parameters such as pH, concentration and temperature.
- Low toxicity of some amine, aldehyde and imine derivatives and thus their ability to be incorporated into consumer products.
- Ability of amines to form imines by condensation with fragrance aldehydes.

^[180] Sander, E. G.; Jencks, W. P. Equilibria for additions to the carbonyl group. *J. Am. Chem. Soc.* **90**, 6154-6162 (1968).

- Challenge of stabilizing imines in aqueous solutions thanks to micellar objects, thus providing new parameters to control the system.

If the imine condensation reaction between an amine and an aldehyde is performed in an organic solvent while eliminating water, it is possible to reach full conversion of the reactants. Then, if the imine is dissolved in water, it will hydrolyse to give back the starting aldehyde and the amine until a given thermodynamic equilibrium is reached (Scheme 1a); usually, the concentration of imine at equilibrium in water is very low.^[181]



Scheme 1 | Thermodynamic equilibria for imine condensation in water.

Imines are able to perform exchange reactions. In the case of a mixture of two or more imines, exchange of the amino fragment of the imine C=N double bond can occur according to three mechanisms:

- Partial hydrolysis of the two imines in the presence of water, and condensation of the free aldehydes and amines into new imines (Scheme 1b).^[182]
- Partial hydrolysis of an imine in the presence of water, and nucleophilic addition of a free amine to an imine carbon and concerted proton transfer from the amine NH bond to the imine nitrogen (Transimination, Scheme 1c).^{[183][184]}

^[181] Meguellati, K.; Fallah-Araghi, A.; Baret, J.-C.; El Harrak, A.; Mangeat, T.; Marques, C. M.; Griffiths, A. D.; Ladame, S., Enhanced imine synthesis in water: from surfactant-mediated catalysis to host-guest mechanisms. *Chem Commun*, **49** (96), 11332-11334 (2013)

^[182] Layer, R. W. Chemistry of imines. *Chem. Rev.* **63**, 489-510 (1963).

^[183] Giuseppone, N.; Schmitt, J.-L.; Schwartz, E.; Lehn, J.-M. Scandium(III) Catalysis of Transimination Reactions. Independent and Constitutionally Coupled Reversible Processes. *J. Am. Chem. Soc.* **127**, 5528-5539 (2005).

^[184] Ciaccia, M.; Cacciapaglia, R.; Mencarelli, P.; Mandolini, L.; Di Stefano, S., Fast transimination in organic solvents in the absence of proton and metal catalysts. A key to imine metathesis catalyzed by primary amines under mild conditions. *Chem Sci*, **4** (5), 2253-2261 (2013)

- Direct exchange of the amino fragments of the imines by imine metathesis (Scheme 1d).^[185]

One important property of the imine bond is its sensibility to external factors such as water concentration, pH or the presence of metal catalysts. The kinetics of hydrolysis of an imine derivative in water depends largely on the pH and the chemical nature of the imine, which means the atom or the group in α position of the amine (X in Scheme 1) plays a dominating role. Amine derivatives presenting an atom with a lone electron pair in α position like hydroxylamines and hydrazides form very stable C=N derivatives (oximes and hydrazones respectively), even at low pH. Some attempts to decrease the stability of oxime derivatives will be described later. Aromatic amines, thanks to their low pKa (~ 4.5), can still react with aldehydes in acidic conditions and yield moderately stable imines in water. Aliphatic amines, although very nucleophilic, get easily protonated at medium pHs (pKa ~ 9) and yield usually poorly stable imines in water.

This choice of amine derivatives with different pKas and groups in α position to the amine enables the formation of various imine derivatives with very different hydrolytic properties, in particular in the form of surfactants. One of the goals of our work was to control the rate of C=N hydrolysis in industrial formulations at different pHs (from pH 3 to pH 12) in order to selectively release fragrances. This should enable us to produce encapsulating systems and profragrances that get hydrolysed with suitable kinetic at a given pH. However, stabilising imines in aqueous solutions (in particular at low pH) is very challenging but it can also lead to too stable systems. In addition, the effect of co-surfactants present in formulations on the rate of hydrolysis had to be considered.

b) Choice of the hydrophilic block

To fine-tune the thermodynamics and kinetics of the C=N bond hydrolysis, we focused on both the hydrophilic and hydrophobic part of the amphiphile. As already said previously, an extensive work had already been performed in our group on dynamic covalent amphiphiles, and at the beginning of my work, the general structure of the previously studied molecules has

^[185] Zuckerman, R. L.; Krska, S. W.; Bergman, R. G. Zirconium-Mediated Metathesis of Imines: A Study of the Scope, Longevity, and Mechanism of a Complicated Catalytic System. *J. Am. Chem. Soc.* **122**, 751-761 (2000).

been preserved, especially regarding the hydrophilic part (Figure 46). The main characteristics of this hydrophilic block are thus as follows:

- PEG chain, that combines good solubility in aqueous and organic solvents, low cost, low toxicity and for which protocols for efficient large scale synthesis have been developed.
- Presence of a primary amine derivative for imine synthesis.
- Presence of a linker X, that can tune the thermodynamic properties of the amine.

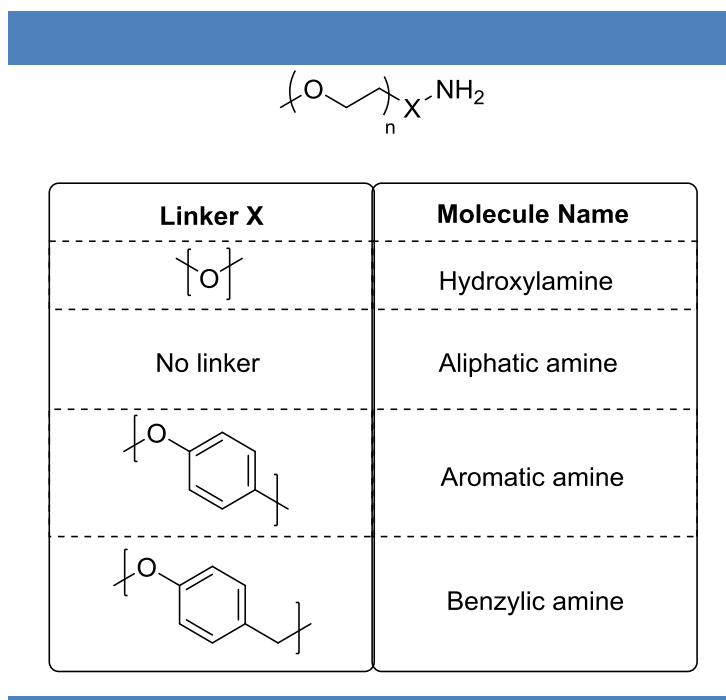


Figure 46 | Amine derivatives synthesised in previous work of the SAMS team ($n = 2$ to 112)).

From all the PEG chain sizes previously studied (2 to 112), a chain length of 11 PEG units has been chosen as hydrophilic block for most dynablocks. This choice is due to the good solubility of PEG₁₁ in water compared to smaller PEG, while at the same time being small enough to be cost efficient.

From the previous work (Figure 46),^[4] several PEG-amines have been resynthesised. The aromatic amine, has been synthesised as a reference for comparison with new systems. A few PEG-hydroxylamines have been synthesised, in an attempt to form oximes that would be less resistant to hydrolysis. Most of this work has been dedicated to the synthesis of aliphatic amines, most notably amines with hydrogen bonding properties (Figure 47A) and amines with hydrophobic linkers between the PEG chain and the primary amine (Figure 47B), as well as

some acyloximes derivatives. Several amines industrially available on large scales have also been used as hydrophilic block.

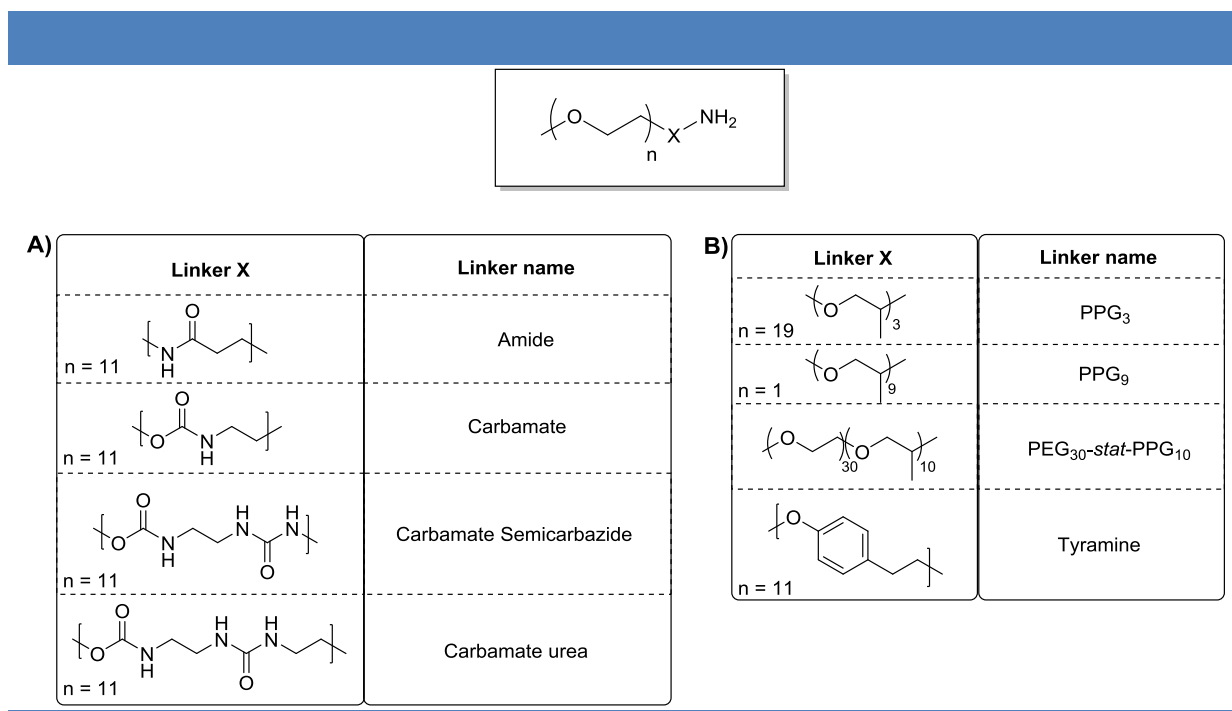


Figure 47 | Linkers used on the hydrophilic block between the PEG chain and the primary amine. A) Linkers with hydrogen bonding properties. B) Hydrophobic linkers.

c) Choice of the hydrophobic block

The hydrophobic block, containing the aldehyde moiety for most dynablocks, has been less modified than the hydrophilic block compared to previous studies. For encapsulation properties, imines have to be as stable as possible in water, so a benzaldehyde derivative (more electrophilic) has been used instead of an aliphatic aldehyde. 4-Octylbenzaldehyde has been mainly used, since it is commercially available and hydrophobic enough to give a low CMC ($\ll 10$ mM) to the imines to which it is condensed. Benzaldehydes with different size chains in *para* position were also used (**A**, Figure 48), to assess the influence of the hydrophobicity of the aldehyde on the micellisation properties of several imines. Concerning profragrances, the hydrophobic block (the aldehyde) is constituted of the volatile organic molecule that has to be released, so the choice was determined by the application. The two most utilised molecules were hexylcinnamal (very hydrophobic, containing an aromatic ring) (**B**, Figure 48) and citral (moderately hydrophobic) (**C**, Figure 48).

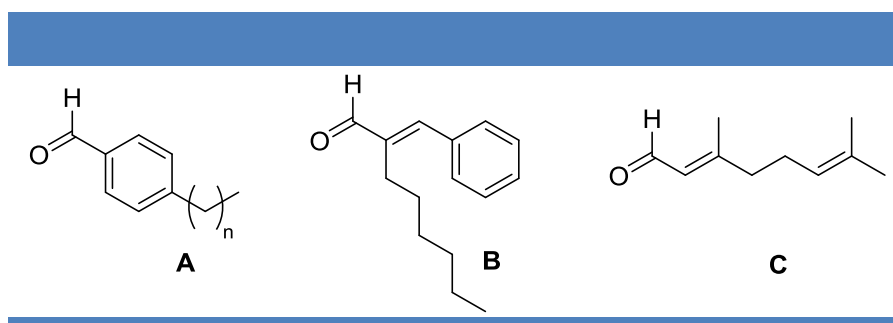


Figure 48 | Hydrophobic blocks. **A**: benzaldehyde derivatives, **B**: Hexylcinnamal, and **C**: Citral.

d) Design of dynablocks

From the molecular building blocks described above, dynablocks could readily be obtained by the condensation of hydrophobic aldehyde with a hydrophilic amine. Dynablocks for two kinds of application were developed (Figure 49):

- Dynablocks **D** designed for encapsulation. Since volatile molecules that need to be released are not a part of the dynablock itself, more freedom can be taken on the design of the molecule. Octylbenzaldehyde was chosen for the reasons given in **1c**) and modulations were performed on the hydrophilic part and the linker **X** to impact the stability of the self-assembly. The main advantage of this type of system is that it can release molecules with any kind of chemical function. A possible drawback is that the encapsulating properties will probably depend on the hydrophobicity of the volatiles (hydrophobicity can be estimated using chemdraw^[186] thanks to the calculation of Log P, the octanol/water partition coefficient).
- Dynablocks **E** and **F**: designed to be profragrances. Here, fragrance volatile aldehydes are a constituent of the dynablocks (hydrophobic part). Therefore, tuning the hydrolytic ability of the imine can only be achieved through modification of the hydrophilic part. The main advantage of this type of releasing system is that it can release any kind of molecule containing an aldehyde moiety. The main drawback is that it can only release one chemical function (carbonyl).

^[186] https://www.cambridgesoft.com/Ensemble_for_Chemistry/ChemDraw/

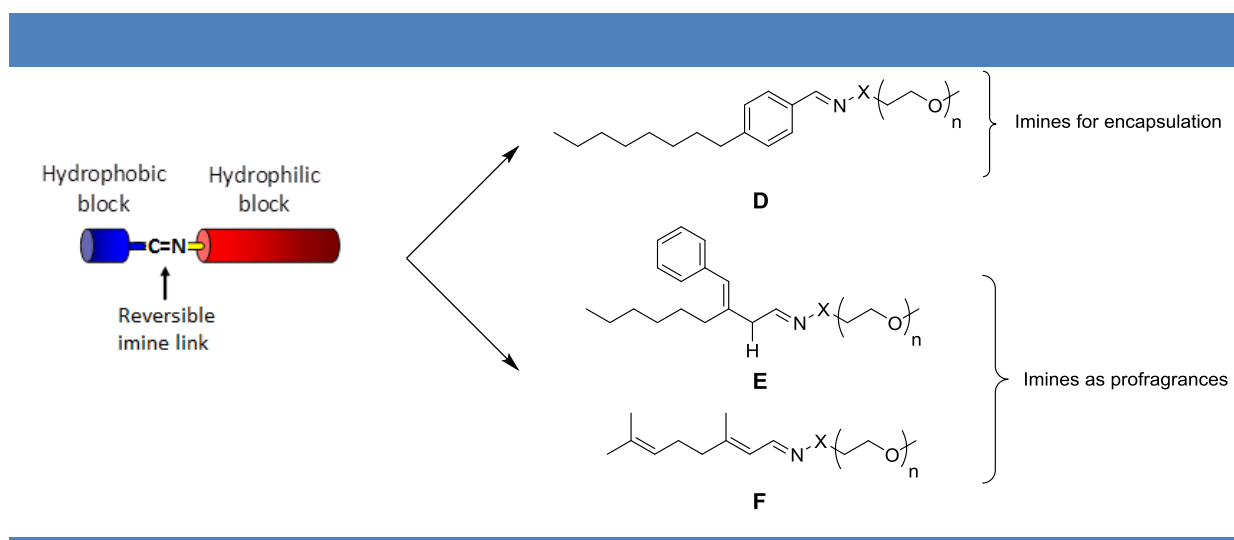


Figure 49 | Representation of **D**-type dynablock for encapsulation applications and of **E**-type and **F**-type dynablocks for their use as profragrances.

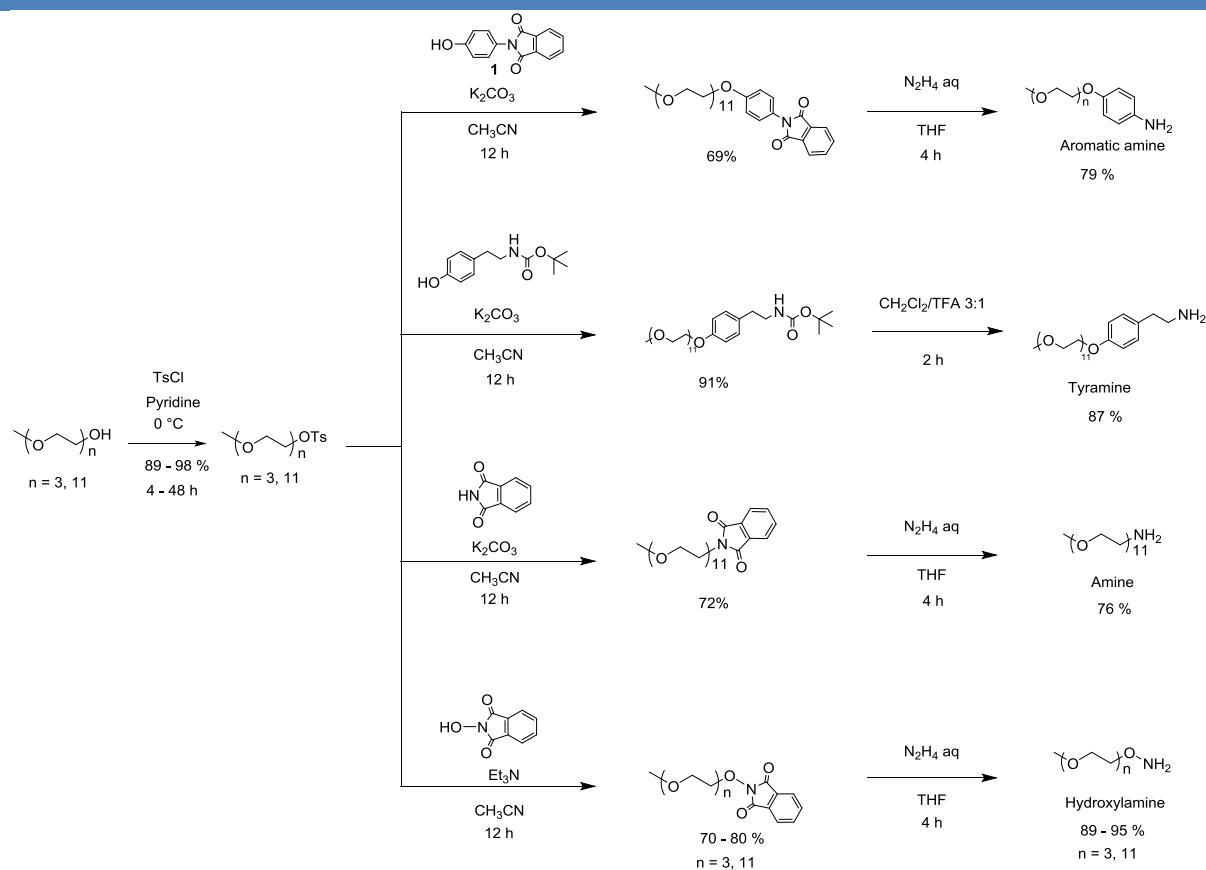
By combining the advantages of these two approaches, it might also become possible to use these systems to release a broad variety of fragrances.

2/ Synthesis of the hydrophilic amine derivatives

a) General synthetic scheme for PEG functionalisations.

The hydrophilic part of the dynablock is derived from commercially available mono-functional polyethylene glycol monomethylether (PEG). Although some early experiments were performed with PEG₃ hydroxylamines, all further synthesis involving PEG derivatives were made with polydisperse PEG₁₁ (with a size distribution going from PEG₆ to PEG₁₆ as measured by mass spectroscopy). One main problem associated with the derivatisation of PEG compounds is the extreme difficulty of purification of their mixtures, and therefore chemical reactions that do not produce side products have to be chosen. The systematic method that has been previously developed in our group to functionalise these polymers with good yields and easy extractions has been kept.^[4] The general synthetic pathway (Scheme 2) starts from the tosylation of the hydroxy group of the monomethylether PEG in order to get an efficient leaving group for the subsequent nucleophilic substitution. The resulting tosylate is then substituted by a phthalimide or phenol derivative in the presence of a base and in

acetonitrile at reflux. Depending on the nature of the desired amine, three different phthalimide groups and one type of phenol were used. After a deprotection reaction in THF using aqueous hydrazine (N_2H_4 aq) for the phthalimides, or in CH_2Cl_2 /TFA 3:1 for the boc-protected tyramine derivative, the corresponding amino-PEGs were obtained with suitable overall yields.



Scheme 2 | General scheme for the functionalization of PEG with amine groups.

b) Tosylation of PEGs

The first step to derivatise PEG-OH is to substitute the primary alcohol^[187] with a better leaving group for further reactions with nucleophiles. This chemical modification was achieved through a tosylation reaction. Monomethylether PEG₃ and PEG₁₁ were stirred in pyridine with *p*-toluenesulfonyl chloride at 0°C to yield compounds **1** and **2** (Scheme 3).

^[187] Biron, E.; Otis, F.; Meillon, J.-C.; Robitaille, M.; Lamothe, J.; Van Hove, P.; Cormier, M.-E.; Voyer, N. Design, synthesis, and characterization of peptide nanostructures having ion channel activity. *Bioorg. Med. Chem.* **12**, 1279-1290 (2004).



Scheme 3 | Synthesis of tosylated PEGs **1** and **2**.

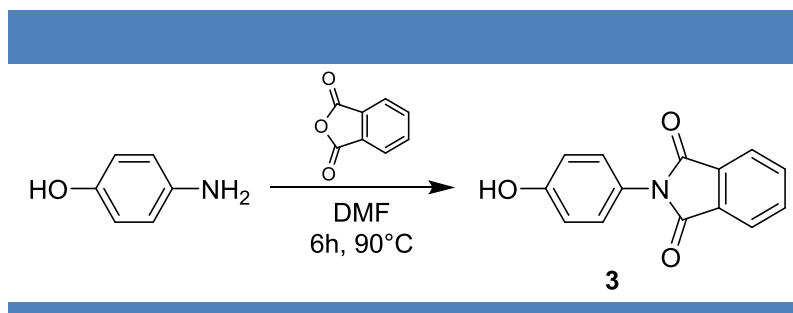
Reaction conditions used for Scheme 3: PEG_nOH (1.0 equiv.), TsCl (3*1.2 equiv.), pyridine, -5 °C, 4 – 48 h, **1**: 97%, **2**: 89%.

Reactions were performed as previously described,^[112] with a slow addition of tosyl chloride at a temperature below 0°C to avoid any displacement of the tosylate with a chlorine atom as a secondary reaction. However, in the case of the tosylation of PEG₁₁OH, the reaction rate was slower than reported (48h instead of 8h), and the quantity of tosyl chloride had to be increased to reach full conversion. A reason might be the enhanced trapping of the *p*-toluenesulfonyl pyridinium cation (resulting from the reaction of TsCl with pyridine) by the oxygen of the PEG chains that occurs more favourably at 5°C than at 0°C. Pure compounds were easily obtained after extraction and without further purification in good yields, thanks to the much higher affinity of PEGs for chlorinated solvents than for water.

c) Substitution of tosylated PEGs and deprotection

Nucleophilic substitution of the tosylate was achieved using either a phthalimide derivative or a phenol group in the presence of a base in acetonitrile at reflux. All substitutions were efficiently performed with a very similar protocol, even when the nature of the nucleophile was very different (phthalimide, *N*-hydroxyphthalimide, phenols). Isoindoline-1,3-dione (phthalimide), 2-hydroxyisoindoline-1,3-dione (*N*-hydroxyphthalimide) and Boc-protected tyramine are commercially available. 2-(4-Hydroxyphenyl)isoindoline-1,3-dione **3** (aromatic phthalimide) had already been synthesised by Dr. Rémi Nguyen by condensation of *p*-aminophenol and phthalic anhydride in DMF at 90°C in 90% yield (Scheme 4)^[188] and was thus readily available.^[4] For all reactions, protected PEG amines were isolated in good yields without specific purification except an extraction work-up.

^[188] Hoefle, M. L. Preparation of 4-(substituted-isoindol-2-yl)phenoxy-pentanoic and -heptanoic acids as antiarteriosclerotic agents. *U.S. Patent n° US 4737512* (1988).

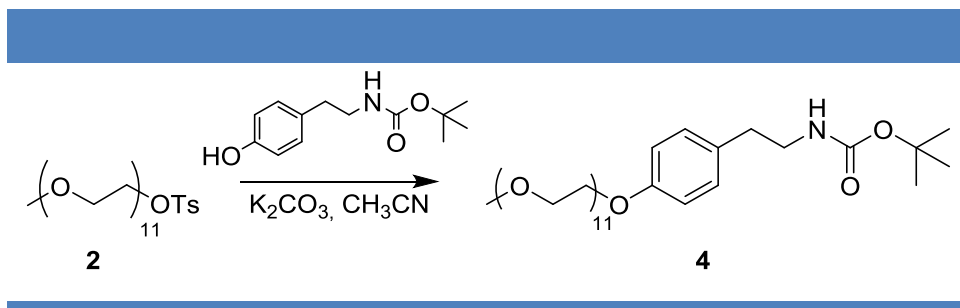


Scheme 4 | Synthesis of 2-(4-hydroxyphenyl)isoindoline-1,3-dione **3**.

Reaction conditions used for Scheme 4: *p*-aminophenol (1.0 equiv.), phthalic anhydride (1.0 equiv.), DMF, 90°C, 6 h, **3**: 90 %.

Formation of Boc-protected PEG Tyramine **4** (Scheme 5):

Commercially available Boc-protected tyramine and potassium carbonate were used for the formation of Boc-protected PEG Tyramine **4**. A low quantity of nucleophile (Boc-tyramine, 1 eq.) was used, in order to avoid wasting expensive Boc-tyramine. A saturated aqueous solution of NaHCO₃ was used for the extraction (degradation occurred when using Na₂CO₃).

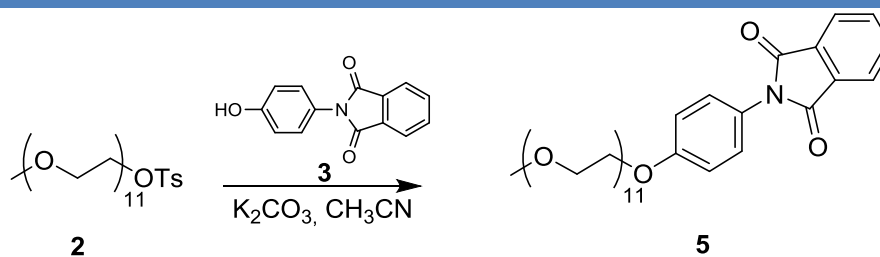


Scheme 5 | Substitution reaction of tosylated PEG **2** with Boc-tyramine.

Reaction conditions used for Scheme 5: PEG₁₁OTs (1.0 equiv.), Boc-protected tyramine (1.0 equiv.), K₂CO₃ (1.6 equiv.), CH₃CN, reflux, 12 h, **4**: 91 %.

Formation of PEG aromatic phthalimide **5** (Scheme 6):

Readily available 2-(4-hydroxyphenyl)isoindoline-1,3-dione **3** and potassium carbonate were used for the synthesis of PEG aromatic phthalimide **5**. A saturated aqueous solution of Na₂CO₃ was used for the extraction.

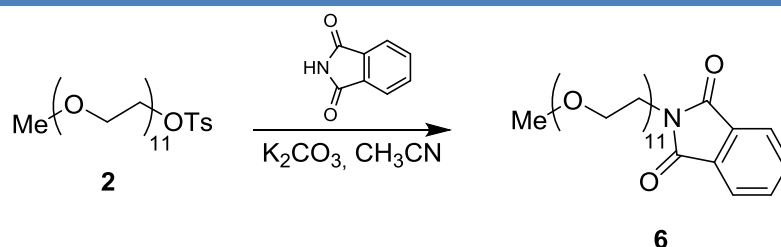


Scheme 6 | Substitution reaction of tosylated PEGs **2** with aromatic phthalimide **3**.

Reaction conditions used for Scheme 6: PEG₁₁OTs (1.0 equiv.), **1** (1.4 equiv.), K_2CO_3 (1.6 equiv.), CH_3CN , reflux, 12 h, **5**: 69 %.

Formation of PEG Phthalimide **6** (Scheme 7):

Commercially available phthalimide and potassium carbonate were used for the formation of PEG phthalimide **6**. A saturated aqueous solution of Na_2CO_3 was used for the extraction.

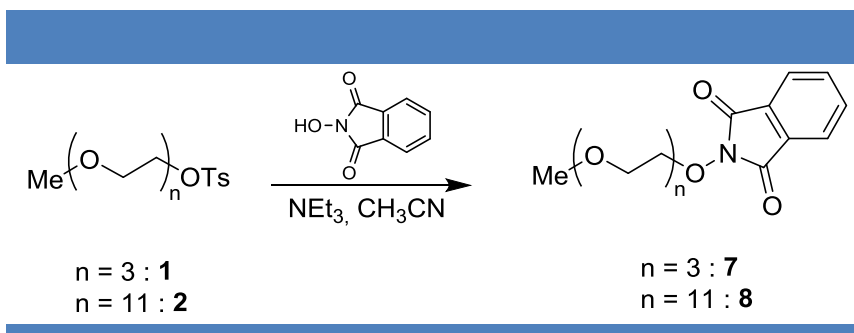


Scheme 7 | Substitution reaction of tosylated PEG **2** with phthalimide.

Reaction conditions used for Scheme 7: PEG₁₁OTs (1.0 equiv.), phthalimide (1.4 equiv.), K_2CO_3 (1.6 equiv.), CH_3CN , reflux, 12 h, **6**: 72 %.

Substitution with *N*-hydroxyphthalimide (Scheme 8):

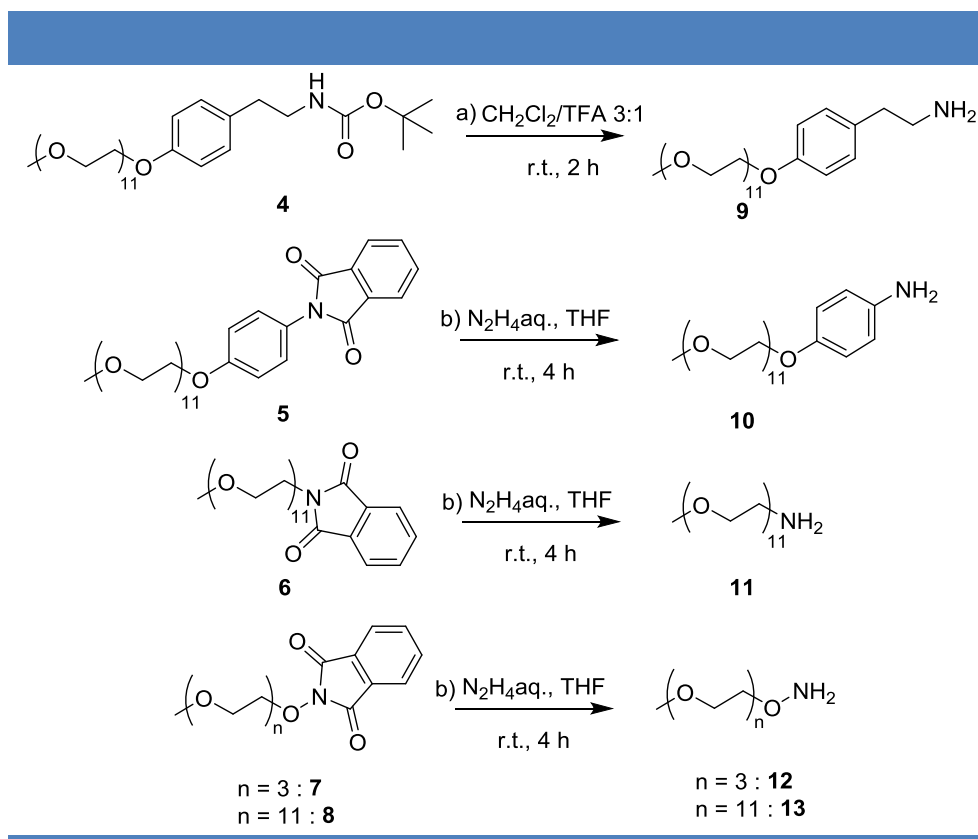
Commercially available *N*-hydroxyphthalimide and triethylamine were used for the formation of PEG hydroxyphthalimide **7** and **8**. A saturated aqueous solution of Na_2CO_3 was used for the extraction.



Scheme 8 | Substitution reaction of tosylated PEGs **1-2** with *N*-hydroxyphthalimide.

Reaction conditions used for Scheme 8: PEG_nOTs (1.0 equiv.), *N*-hydroxyphthalimide (1.2 equiv.), NEt₃ (1.2 equiv.), CH₃CN, reflux, 12 h, **7**: 80 % , **8**: 70 %.

The last step to achieve hydrophilic amine blocks was the deprotection of either the Boc group or the phthalimide moiety. This was performed at room temperature using a CH₂Cl₂/TFA 3:1 mixture to deprotect the Boc group and with aqueous hydrazine in THF to deprotect phthalimides (Scheme 9).^[189]



Scheme 9 | Deprotection reactions of compounds **4-8**.

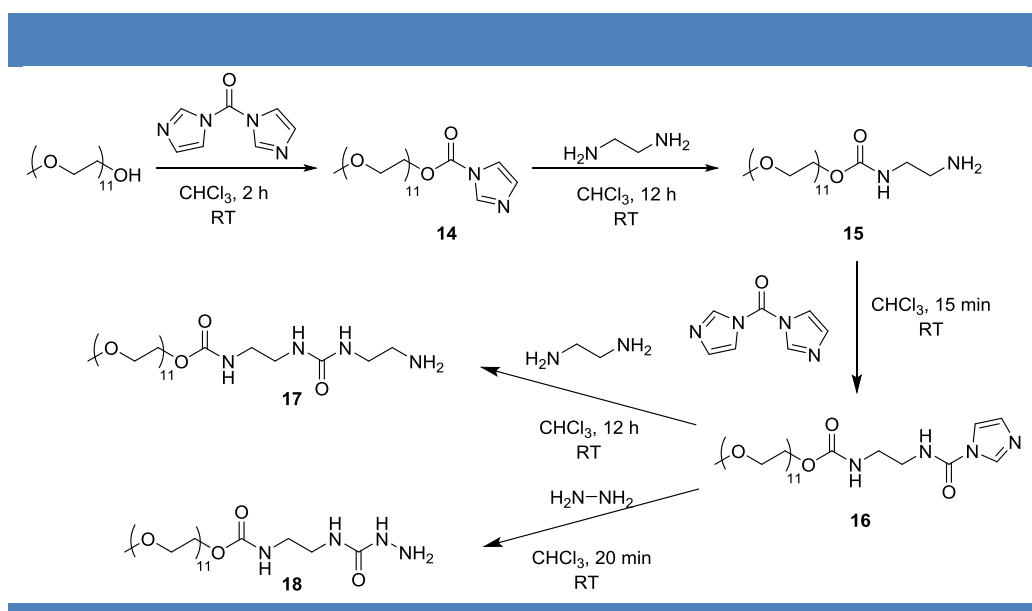
^[189] Jeong, K.-S.; Park, E.-J. Self-Assembly of Interlocked Supramolecular Dendrimers. *J. Org. Chem.* **69**, 2618-2621 (2004).

Reaction conditions used for Scheme 9: a) Compound **4** (1.0 equiv.), CH₂Cl₂/TFA 3:1, r.t., 2 h, 87 % b) Compounds **5-8** (1.0 equiv.), N₂H₄_{aq} (40 equiv.), THF, r.t., 4 h, 76% - 95%.

All deprotection reactions were quantitative, as analysed by ¹H NMR, but during the purification some PEGs were transferred from the organic to the aqueous phase, thus lowering the overall yield. All excess reactants could be removed with 2 to 5 extractions. All PEG-amines were stored under argon in their protected forms to avoid degradation. Aromatic amine **10** is especially sensitive to oxidation.

d) Synthesis of PEGs with hydrogen bonding abilities

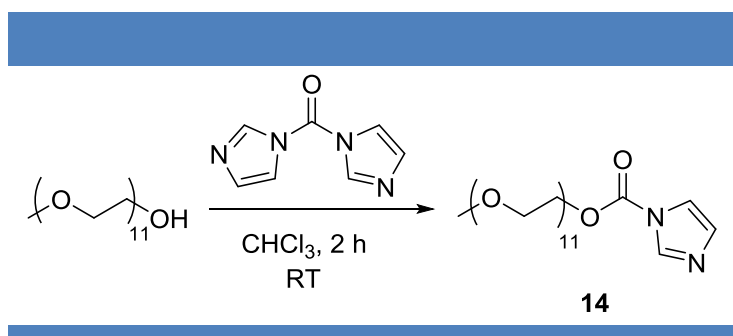
After the synthesis of several PEG amine derivatives with different functionalities, some PEGs with hydrogen-bonding abilities (**17-18**) were produced in 4 steps from commercially available monomethyl ether PEGs (Scheme 10). The synthesis was performed directly from PEG₁₁OH and involved fast and easy couplings with 1,1'-Carbonyldiimidazole (CDI), which was finally chosen for coupling reactions instead of the much slower reacting S,S'-Dimethyl dithiocarbonate.



Scheme 10 | General scheme for the functionalization of PEG with hydrogen-bonding abilities and amine derivative groups.

The general synthetic pathway (Scheme 10) starts from the reaction of the hydroxy group of the monomethylether PEG with CDI in order to get an efficient leaving group for the subsequent nucleophilic substitution. The resulting imidazole carboxylate **14** is then substituted by ethylene diamine present in very large excess in chloroform at room temperature. PEG carbamate amine **15** then reacts again with CDI to form the imidazole derivative intermediate **16**. PEG carbamate urea amine **17** and PEG carbamate semicarbazide **18** are then formed in chloroform at room temperature by reaction between the intermediate **16** with ethylene diamine and aqueous hydrazine respectively (a large excess of these reactants is needed to avoid the coupling between two PEG chains).

The first step to derivatise PEG-OH is to substitute the primary alcohol with a better leaving group for further reactions with nucleophiles. This chemical modification was achieved through a reaction with CDI. Monomethylether PEG₁₁ was stirred in chloroform with CDI at room temperature to yield the imidazole carboxylate intermediate **14** (Scheme 11).

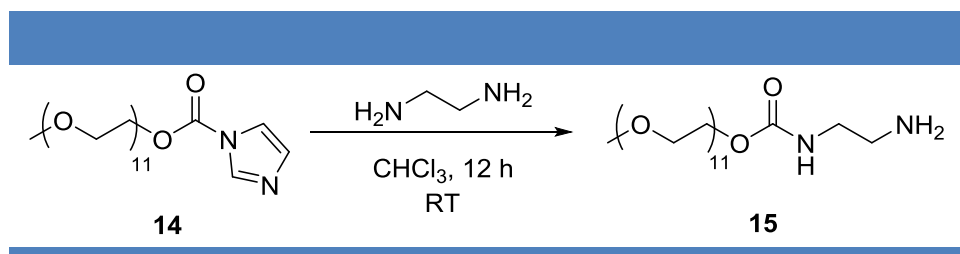


Scheme 11 | Synthesis of PEG imidazole carboxylate **14**.

Reaction conditions used for Scheme 11: PEG₁₁OH (1.0 equiv.), CDI (3 equiv.), CHCl₃, r. t., 2 h, **14**: quant.

The reaction was performed with a slow addition of CDI at room temperature. Three equivalents of CDI had to be used to overcome the presence of water among the PEG chains that could not be evaporated. The reaction was fast, as proved by CO₂ bubbles that could be observed immediately after the addition of CDI. Purification was achieved through addition of water to the reaction after 2 hours to hydrolyse the remaining CDI and extract imidazole to the aqueous phase. Elimination of imidazole from its mixture with **14** proved to increase the yield of the next reaction to form PEG₁₁ carbamate amine **15**.

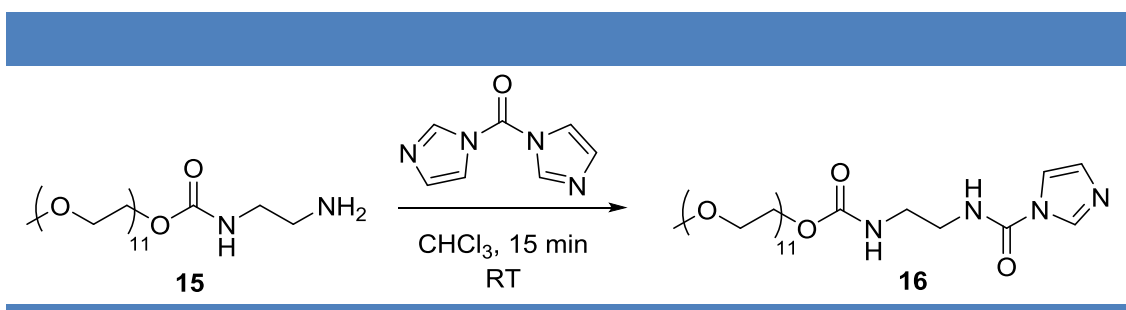
PEG₁₁ imidazole carboxylate **14** was then immediately used for the formation of PEG₁₁ carbamate amine **15** (Scheme 12), because **14** degraded rapidly after synthesis, mainly due to hydrolysis with water trapped in PEG chain and thermal degradation if heated at more than 40°C.



Scheme 12 | Synthesis of PEG carbamate amine **15**.

Reaction conditions used for Scheme 12: PEG₁₁ imidazole carboxylate **14** (1.0 equiv.), ethylene diamine (3 equiv.), CHCl₃, r. t., 12 h, **15**: 79%.

The reaction was performed by dissolving PEG₁₁ imidazole carboxylate **14** into a chloroform/ethylene diamine mixture, with 100 equivalents of ethylene diamine to minimise the coupling between PEG chains. The excess of ethylene diamine and imidazole could easily be removed by evaporation and extraction into the aqueous phase. This reaction yields an interesting hydrophilic block, with an amine moiety and the presence of a carbamate group for hydrogen bonding properties. In order to create more PEG derivatives with stronger hydrogen bonding abilities, PEG₁₁ carbamate amine **15** was reacted with CDI to form PEG carbamate imidazole carboxamide **16** (Scheme 13). The reaction was performed in similar conditions to that used for the formation of compound **14** from PEG₁₁OH.



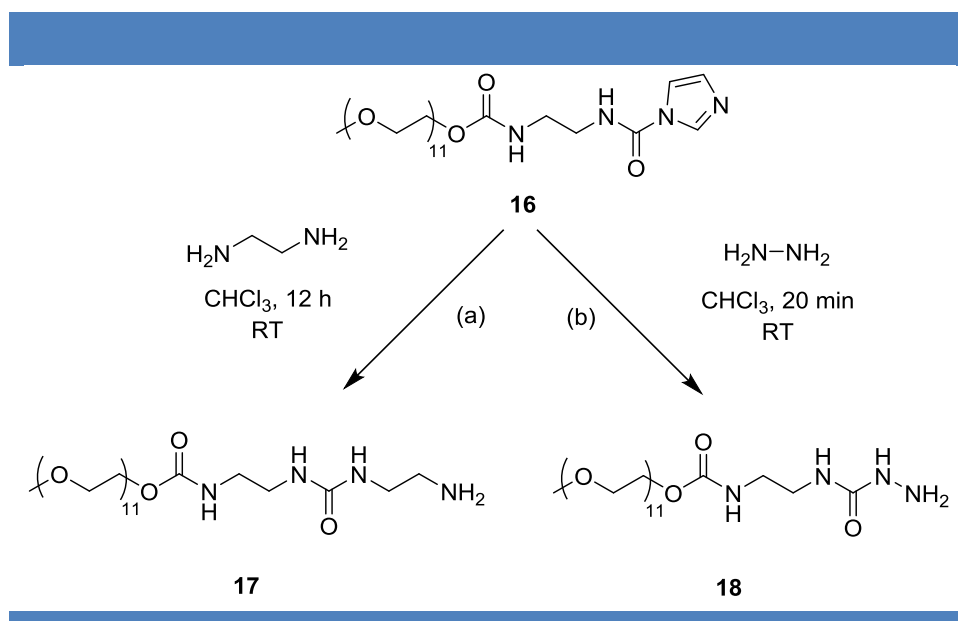
Scheme 13 | Synthesis of PEG imidazole carboxamide **16**.

Reaction conditions used for Scheme 13: PEG₁₁ carbamate amine **15** (1.0 equiv.), CDI (3 equiv.), CHCl₃, r. t., 2 h, **16**: 97%.

PEG carbamate imidazole carboxamide **16** was then dissolved in chloroform and was used for two reactions (Scheme 14):

- 1) Reaction with ethylene diamine at room temperature to form the aliphatic amine **17** that has strong hydrogen bonding properties thanks to its carbamate and urea groups.
- 2) Reaction with aqueous hydrazine at room temperature to form the semicarbazide **18** that also has strong hydrogen bonding properties thanks to the carbamate and the semicarbazide groups.

Pure compounds **17** and **18** were easily obtained by extraction and evaporation.

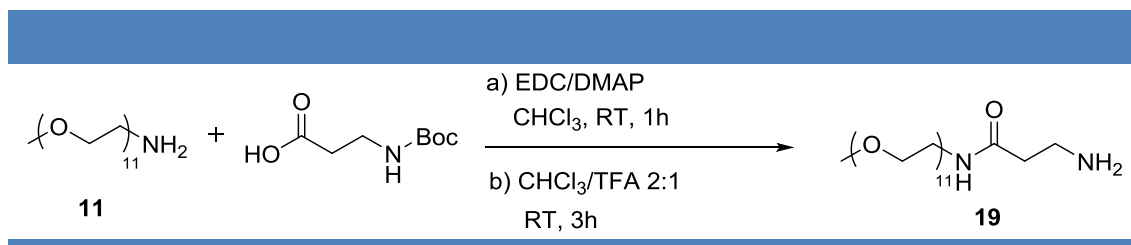


Scheme 14 | Synthesis of PEG carbamate urea amine **17** and PEG carbamate semicarbazide **18**.

Reaction conditions used for Scheme 14: a) PEG₁₁ imidazole carboxamide **16** (1.0 equiv.), ethylenediamine (100 equiv.), CHCl₃, r. t., 12 h, **17**: 77%. b) PEG₁₁ imidazole carboxamide **16** (1.0 equiv.), hydrazine (100 equiv.), CHCl₃, r. t., 20 min, **18**: 77%.

A last hydrophilic aliphatic amine with hydrogen bonding properties was obtained by chemical modification of PEG₁₁ amine **11** with β -Alanine. Boc- β -Ala-OH was dissolved in

chloroform, and EDC, DMAP and PEG₁₁NH₂ (**11**) were added in a sequential way (Scheme 15). After stirring at room temperature for 1h, the reaction was diluted with CHCl₃ and washed with saturated NH₄Cl_{aq} to eliminate all side products from the reaction. Then, the solution was mixed with a CHCl₃/TFA solution 2:1 for deprotection, yielding PEG₁₁ amide amine **19** after a rapid wash with Na₂CO₃.



Scheme 15 | Synthesis of PEG₁₁ amide amine **19**.

Reaction conditions used for Scheme 15: a) PEG₁₁ amine **11** (1.0 equiv.), Boc-β-Ala-OH (2 equiv.), EDC (2 equiv.), DMAP (0.2 equiv.), CHCl₃, r. t., 1 h b) CHCl₃/TFA 2:1, r. t., 3 h, **19**: 52%.

After the description of the synthesis of PEG amine derivatives with groups able to form hydrogen bonds, we now present the synthesis of several aldehydes.

3/ Synthesis of aldehydes

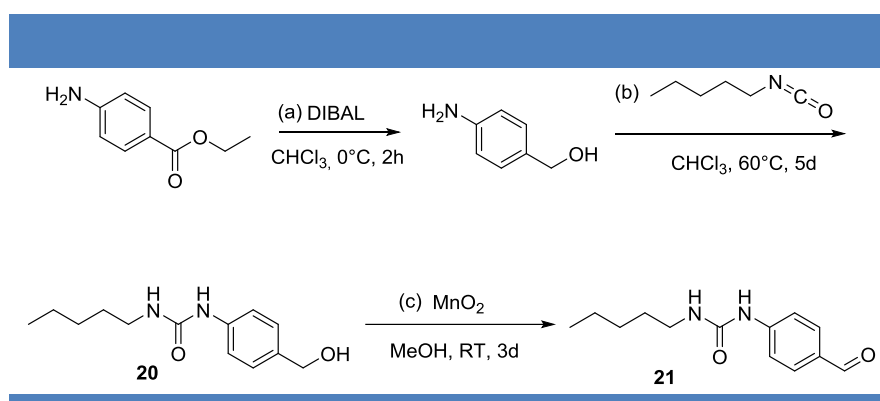
a) Hydrophobic benzaldehyde derivative

Although it had been decided to focus on the chemical modification of the hydrophilic block of the amphiphiles, a hydrophobic aldehyde with a urea group was synthesised to compare the influence of hydrogen bonding groups on both hydrophilic and hydrophobic blocks. 1-(4-formylphenyl)-3-pentylurea **21**, a hydrophobic aldehyde with a urea group, was formed in three steps (Scheme 16):

- a) Ethyl 4-aminobenzoate was reduced with diisobutylaluminium hydride (DIBAL-H) at room temperature to afford a mixture of 4-aminobenzyl alcohol (60%) and side products. The excess of DIBAL-H was quenched with ethyl acetate and aluminium salts were removed by a work-up with potassium sodium tartrate.

b) The mixture obtained from **a** was diluted in chloroform, pentyl isocyanate was added and the mixture was heated at 60°C. After 5 days, the reaction was allowed to reach room temperature, and a white solid precipitated in the solution. After filtration, this white solid proved unexpectedly to be pure 1-(4-(hydroxymethyl)phenyl)-3-pentylurea **20**.

c) 1-(4-(hydroxymethyl)phenyl)-3-pentylurea **20** was dissolved in methanol in presence of a large excess (15 equiv.) of manganese dioxide, that afforded a slow but total oxidation of **20** into 1-(4-formylphenyl)-3-pentylurea **21**.



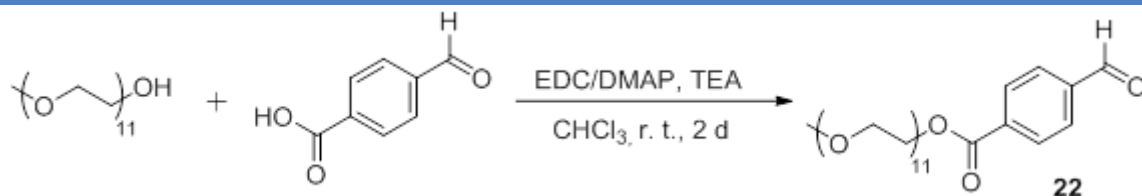
Scheme 16 | Synthesis of PEG₁₁ amide amine **19**.

Reaction conditions used for Scheme 16: a) Ethyl-4-aminobenzoate (1.0 equiv.), DIBAL-H in toluene (4 equiv.), CHCl₃, 0 °C, 2 h b) Pentyl isocyanate (0.6 equiv.), 60 °C, 5 d, **20**: 19%. c) 1-(4-(hydroxymethyl)phenyl)-3-pentylurea **20** (1 equiv.), Manganese dioxide (15 equiv.), MeOH, r. t., 3 d, **21**: 78%.

b) Hydrophilic benzaldehyde derivative

A hydrophilic benzaldehyde derivative has also been synthesised to see if the hydrolytic abilities of imines can be altered by transferring the aldehyde moiety from the hydrophobic to the hydrophilic part. PEG₁₁OH was coupled to 4-formylbenzoic acid with EDC/DMAP in a similar way it was used to synthesise PEG₁₁ Amide amine **19**, except that here triethylamine was used to neutralize the HCl from EDC/HCl. PEG₁₁ benzaldehyde **22** was purified by simple extractions in acidic conditions to eliminate the by-products of EDC and TEA and basic conditions to eliminate the excess of 4-formylbenzoic acid. Compound **22** was obtained with good yield following an easy one-step reaction from commercial products. This product

proved to be stable in aqueous solution for $3 < \text{pH} < 12$, with hydrolysis occurring above pH 12.



Scheme 17 | Synthesis of PEG₁₁ amide amine 19.

Reaction conditions used for Scheme 17: a) PEG₁₁OH (1.0 equiv.), 4-formylbenzoic acid (1.2 equiv.), EDC,HCl (1.1 equiv.), DMAP (1.1 equiv.), TEA (1.1 equiv.), CHCl₃, r. t., 12 h, **22**: 82%.

4/ Synthesis of imine derivatives

The various synthetic and commercial PEG amine derivatives, when coupled to aldehydes, have provided a large variety of amphiphilic blocks in sizes, functionalities, and hydrophilicities.^{[107][111][112][113]} According to previous studies on the structure of dynablocks, most of the imines which have been synthesised with a PEG₁₁ hydrophilic block are expected to self-assemble into micellar aggregates (Figure 50).

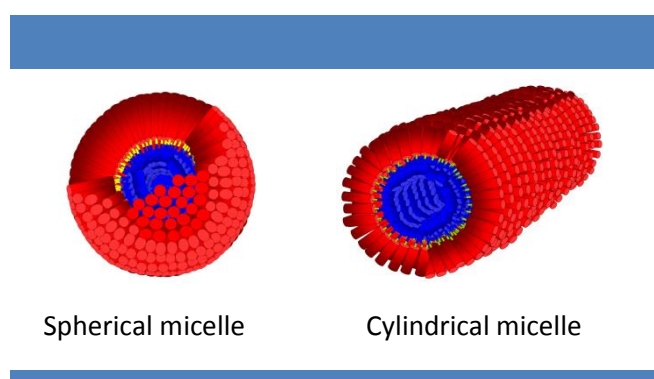


Figure 50 | Schematic representation of the expected micellar self-assemblies.

Micellar structures of dynablocks in water can considerably decrease the rate of the imine bond hydrolysis, and increase its concentration at equilibrium. What has started to be

understood previously by Rémi Nguyen^[4] and continued by me, is that the stability of a dynablock micellar system depends on three main parameters:

a) The chemical nature of the C=N bond, which partially determines the chemical stability of the dynablock, which also depends on the solvent, and on the reactivity of the corresponding amine and its concentration in solution. Oxime (resulting from the condensation of an aldehyde with a hydroxylamine) is the strongest imine bond. Benzylic imine and aromatic imine have comparable moderate stabilities. Finally, the weakest bond in water is the aliphatic imine (while more stable in organic solvents than the benzylic and the aromatic ones).

b) The imine bond stabilization by supramolecular structure formation can shift the equilibrium toward imine formation in water. Micellar systems that are formed provide a high stability to amphiphilic dynablocks. This stability directly depends on structural particularities of the micellar system, defined by the nature of the C=N bond, the presence of linkers between hydrophilic and hydrophobic blocks, and the geometry of the aggregates.

c) The solubilisation of non-reacting hydrophobic aldehyde by the micellar structure which avoids demixing process and keeps the system stable. However, if the quantity of hydrophobic material inside the micelle's core becomes too important, the system evolves toward the formation of micro-emulsions with a possible change in the stability of the imines.

Although properties vary a lot from one dynablock micellar system to another, the aim was always the same: to release volatile molecules by a change of pH or concentration, either from the hydrophobic core of micelles or from the amphiphile itself, with a controlled kinetics. To achieve this goal, imine derivatives with the following linkers were synthesised:

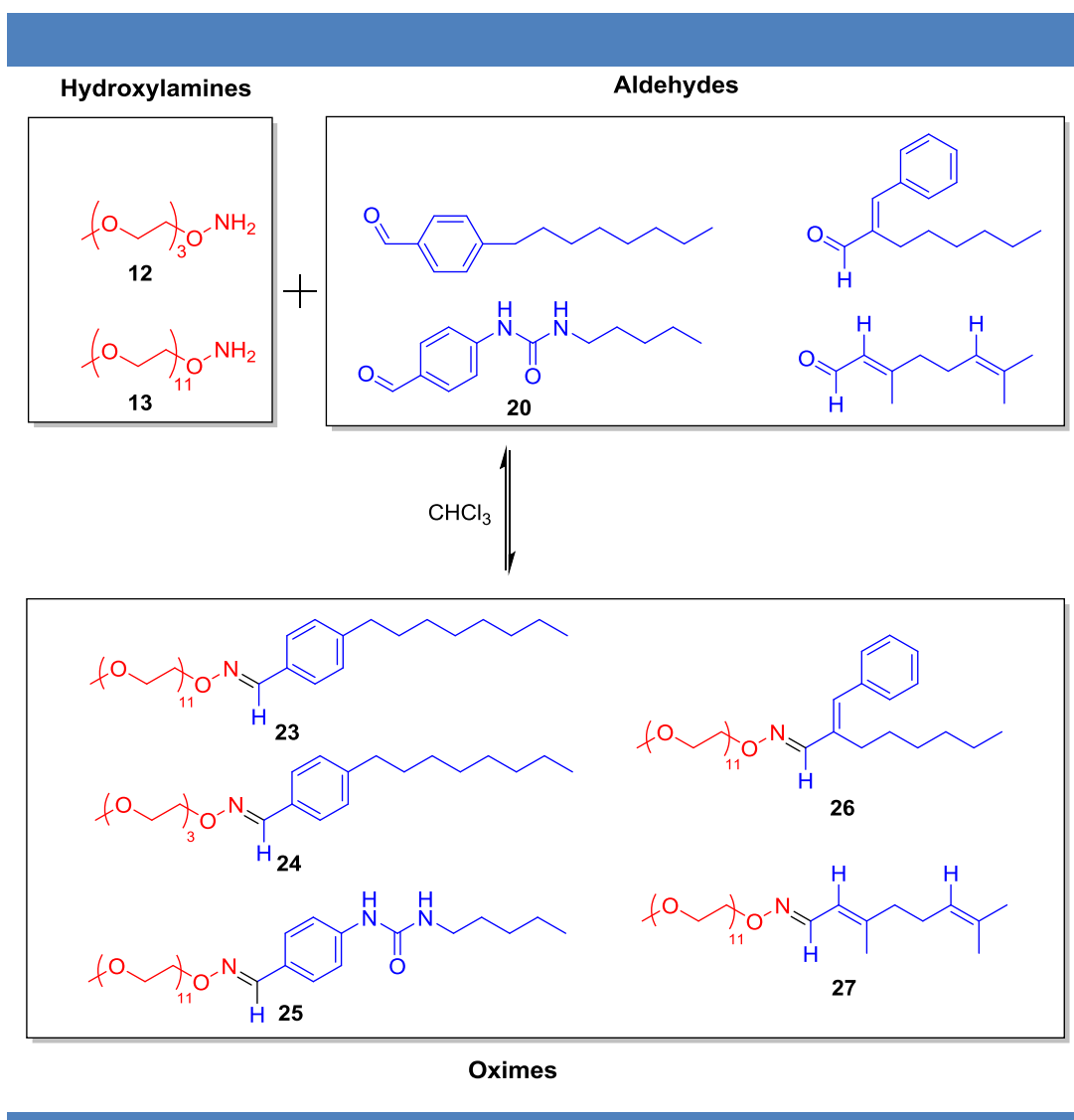
- Oximes; very stable, expected to hydrolyse at very low pH.
- Semicarbazones; stable, expected to hydrolyse under moderately acidic conditions.
- Aromatic and aliphatic imines; moderately stable, expected to hydrolyse at all pHs.
- Acyloximes; unknown stability, expected to hydrolyse under acidic and basic conditions.

The design of these molecules as well as their synthesis is presented in the next subchapters.

a) Oximes

One of the first couplings between an amine derivative and an aldehyde that I achieved was for the formation of oximes. Although known to be very stable, oximes could be interesting for the controlled release of fragrances in formulations at very low pH. The synthesis of oximes was performed by dissolving 1 equivalent of PEG_nONH₂ and 1 equivalent of aldehyde in chloroform at room temperature (Scheme 14). Removal of water was not necessary to reach full conversion. The following oximes have been synthesised:

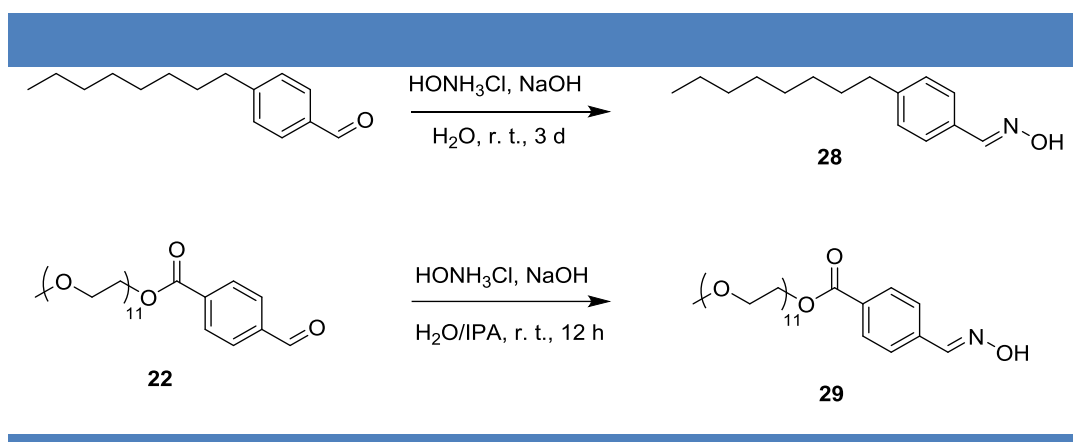
- PEG₁₁ONH₂ octylbenzaldehyde oxime **23** was resynthesised^[4] as a starting point to assess the ability of oximes to be hydrolysed in acidic media to be used for encapsulation.
- PEG₃ONH₂ octylbenzaldehyde oxime **24** was resynthesised^[4] to see if a decreased hydrophilicity of the PEG chain could destabilise the aggregates and ease the hydrolysis of the oxime bond.
- PEG₁₁ONH₂ 1-(4-formylphenyl)-3-pentylurea oxime **25** was synthesised to assess if the presence of hydrogen bonding groups in the hydrophobic block could destabilise the micellar structure and facilitate the hydrolysis of the oxime.
- PEG₁₁ONH₂ hexylcinnamal oxime **26** and PEG₁₁ONH₂ citral oxime **27** are profragrances and were synthesised to assess if volatile aldehyde can be released upon hydrolysis directly from the amphiphile.



Scheme 18 | Oxime coupling between PEG_nONH_2 and a set of aldehydes.

Reaction conditions used for Scheme 18: PEG_nONH_2 (1.0 equiv.), Aldehyde (1 equiv.), CHCl_3 , r. t., 1 – 3 d, 96 - 100%.

Some non-amphiphilic oximes were also formed, and used as reactants for the formation of acyloximes. Oximes **28** and **29** were obtained by the condensation of 4-octylbenzaldehyde and PEG_{11} benzaldehyde **22** with hydroxylamine hydrochloride in presence of sodium hydroxide as a base at room temperature (Scheme 19). The reaction was performed in water for compound **29** to dissolve the hydroxylamine salt, and in isopropyl alcohol/water mixture for compound **28** to dissolve both the aldehyde and the salt.



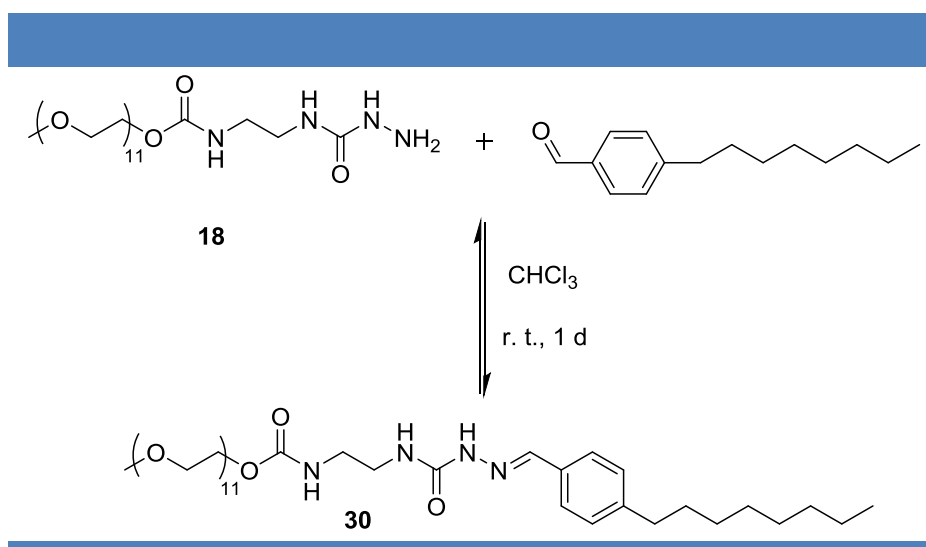
Scheme 19 | Oxime formation of **28** and **29** from 4-octylbenzaldehyde and PEG₁₁benzaldehyde.

Reaction conditions used for Scheme 19: a) Octylbenzaldehyde (1.0 equiv.), hydroxylamine hydrochloride (1.3 equiv.), sodium hydroxide (1.2 equiv.), water/isopropyl alcohol 1:1, r. t., 3 d, **28**: quant. b) PEG₁₁benzaldehyde **22** (1.0 equiv.), hydroxylamine hydrochloride (1.3 equiv.), sodium hydroxide (1.2 equiv.), water, r. t., 12 h, **29**: quant.

b) Semicarbazone

Acylhydrazone derivatives have already been largely used in the literature for encapsulation, and even for the formation of profragrances.^[172] Although they possess a very good stability in water at basic and neutral pHs, they have the drawback to hydrolyse at acidic pHs into a carbonyl and an hydrazine derivative, the latter being toxic or carcinogenic.^[190] However, a dynablock based on a semicarbazone bond has been synthesised, to compare its hydrolytic ability with other imine derivatives. The semicarbazone **29** was formed from the condensation of PEG₁₁carbamate semicarbazide **18** with 4-octylbenzaldehyde in chloroform at room temperature (Scheme 20). Like for the synthesis of the oximes, the condensation into semicarbazone was complete without removal of the water.

^[190] Malcamor, L.; Stark, A. A., Mutagenicity and Toxicity of Carcinogenic and Other Hydrazine Derivatives - Correlation between Toxic Potency in Animals and Toxic Potency in Salmonella-Typhimurium Ta1538. *Appl Environ Microb*, **44** (4), 801-808 (1982)



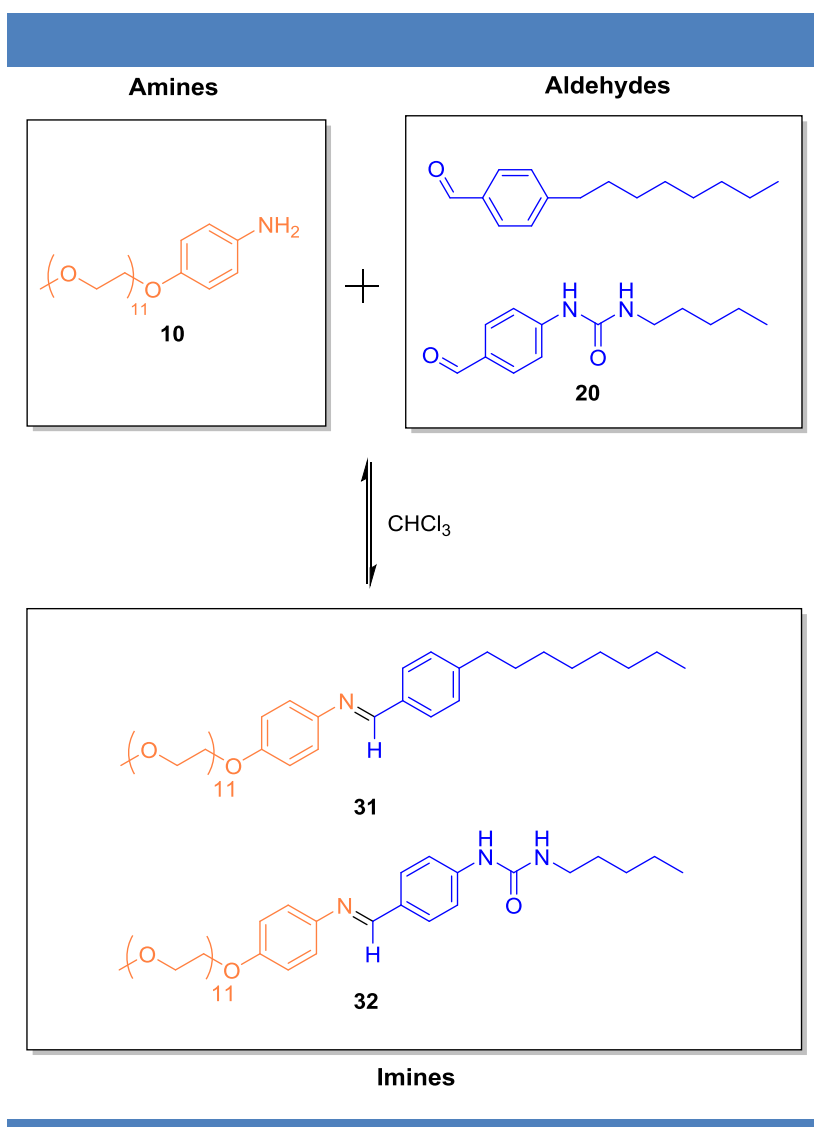
Scheme 20 | Imine coupling between 4-octylbenzaldehyde and a set of amines.

Reaction conditions used for Scheme 20: a) PEG₁₁carbamate semicarbazide (1.0 equiv.), 4-octylbenzaldehyde (1 equiv.), CHCl₃, r. t., 2 d, **30**: quant.

c) Imines designed for the encapsulation of hydrophobic volatiles

Imines were produced by the reversible coupling of a benzaldehyde derivative with a hydrophilic aromatic or aliphatic amine at room temperature in chloroform. To reach full conversion and avoid the residual presence of aldehydes, water was removed by evaporation when the equilibrium was reached, and a slight excess of amine was added. Total elimination of water from the system is extremely difficult to achieve, since water molecules are trapped by PEG chains. The first targeted application for these dynablocks is the encapsulation of hydrophobic fragrances. The first systems that have been synthesized are based on aromatic amines (Scheme 21), and are the following:

- PEG₁₁aromatic amine 4-octylbenzaldehyde imine **31**; the project was based on this system, since it was that initially able to encapsulate an excess of 4-octylbenzaldehyde.
- PEG₁₁aromatic amine 1-(4-formylphenyl)-3-pentylurea imine **32**; incorporation of an urea hydrogen bonding unit on the hydrophobic block was made to tune the stability of the micelle.



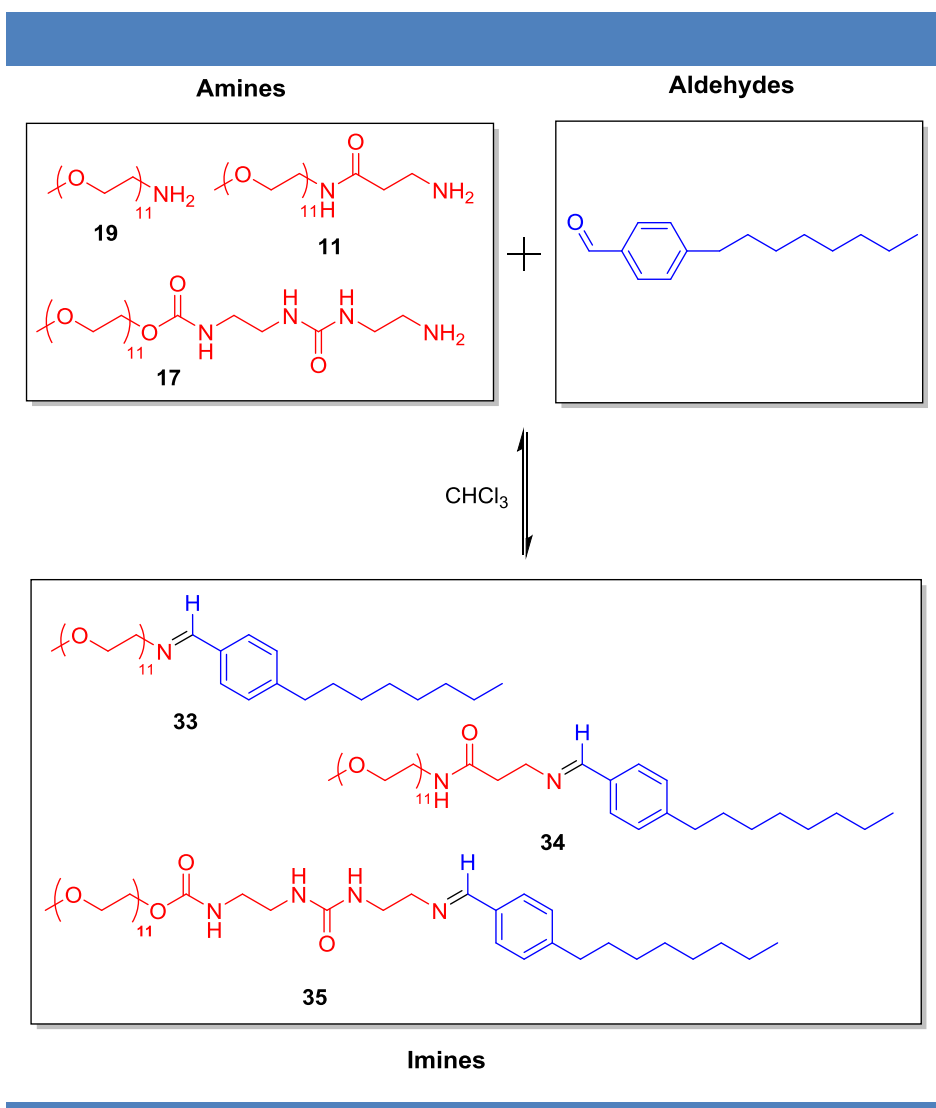
Scheme 21 | Imine coupling between PEG₁₁aromatic amine **10** and benzaldehyde derivatives.

Reaction conditions used for Scheme 21: a) PEG₁₁aromatic amine **10** (1.2 equiv.), benzaldehyde derivative (1 equiv.), CHCl₃, r. t., 1 - 2 d, 98 – 100%.

The study of aromatic imines was stopped after these two molecules, since using aromatic amines in cosmetic applications is complicated for regulation reasons. Benzylic imines were not studied for similar reasons. These systems were however a good start to assess the performance that can be possibly achieved with imines and were mainly used as reference compounds.

The next imines to be studied are based on the condensation of aliphatic amines with 4-octylbenzaldehyde (Scheme 22). The simple aliphatic imine **33** was synthesised as reference

compound for hydrolytic performance. Aliphatic imines **34** and **35** are derivatives of imine **33** and incorporate hydrogen bonding groups that can tune the stability of the micelles by creating hydrogen bonding between the hydrophilic blocks.

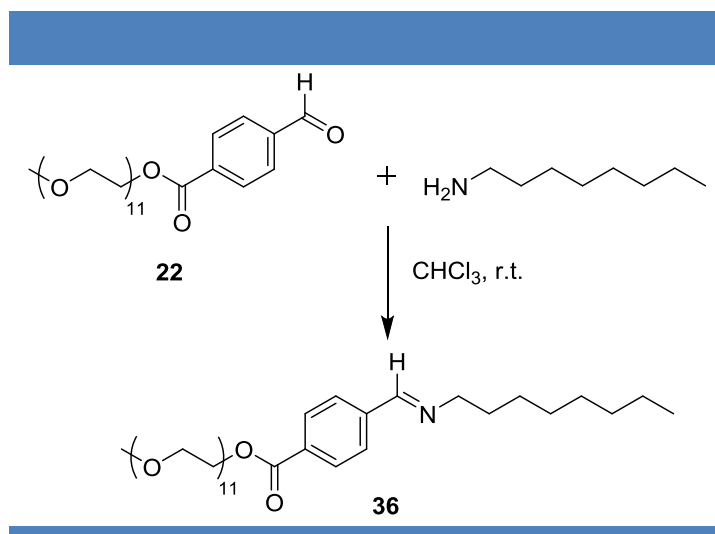


Scheme 22 | Imine coupling between 4-octylbenzaldehyde and a set of aliphatic amines.

Reaction conditions used for Scheme 22: a) PEG₁₁ aliphatic amine (1.2 equiv.), 4-octylbenzaldehyde (1 equiv.), CHCl₃, r. t., 1 - 2 d, 98 – 100%.

A last type of imine for encapsulation was synthesised by coupling PEG₁₁benzaldehyde **22** with octylamine to form imine **36** (Scheme 23). For this imine, the functionalities between the hydrophilic and the hydrophobic block were reversed, and the benzaldehyde moiety was put on the hydrophilic block. This molecule might give some useful information about how to

design dynablocks for encapsulation, by helping us to understand the importance of the localisation of the reacting chemical functions.



Scheme 23 | Imine coupling between PEG₁₁ benzaldehyde **22** and octylamine.

Reaction conditions used for Scheme 23: a) PEG₁₁ benzaldehyde **22** (1equiv.), octylamine (1.2 equiv.), CHCl₃, r. t., 1 d, **36**: 98%.

d) Imines for the study of hydrophobic chain length on micellisation

Imines were produced by the reversible coupling of benzaldehyde derivatives with a commercial aliphatic amine (Huntsman's Jeffamine M1000, **A** Scheme 24) at room temperature in chloroform (Scheme 24). Full conversion was achieved through the total evaporation of water under high vacuum. Jeffamine M1000 polyetheramine is a polyether monoamine with an average molecular weight of 1000 Da made of a diblock copolymer with a PO/EO ratio of about 3/19 and is a white waxy solid at room temperature. The motivation for the synthesis of these dynablocks was the determination of the influence of the hydrophobic chain length on the kinetics of hydrolysis of imines. Jeffamine M1000 was chosen for these experiments because it possesses several advantages:

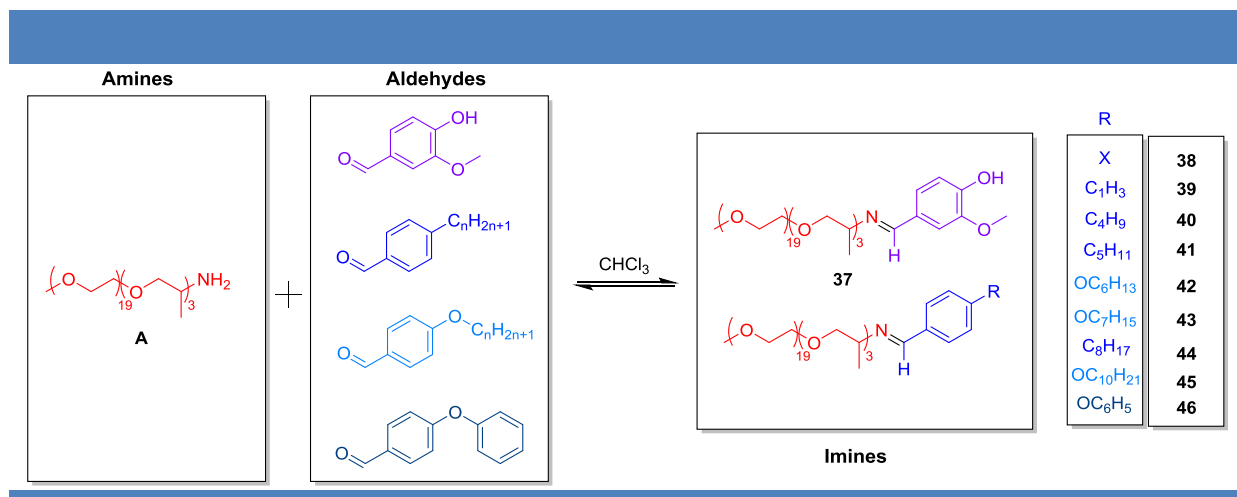
- Water solubility
- Presence of a hydrophobic linker between the PEG chain and the amine moiety (3 poly(propylene glycol) units), and thus a partial dissolution of the imine function inside the hydrophobic core might be possible after condensation with a hydrophobic aldehyde.

- Presence of an aliphatic amine moiety
- Not classified substance, not toxic.
- Cheap and commercially available in large scales.

According to Huntsman,^[191] the amines from the Jeffamine series have several applications, including: ore flotation agent, corrosion inhibitor, agricultural emulsifier, or for emulsification of epoxy resins. They also possess all the characteristics to be used as building block for dynablocks.

The synthesized dynablocks for the determination of the importance of the hydrophobic chain length on the micellisation process are the following:

- M1000 Vanillin imine **37**. This hydrophilic imine was used as a reference for the hydrolysis time of non-micellisable imines.
- M1000 alkyl(oxy)benzaldehyde derivatives imines **38-45** have been synthesised with different chain lengths. Since it was not possible to find commercially the whole series of benzaldehyde derivatives from benzaldehyde to decylbenzaldehyde, some alkyloxybenzaldehyde derivatives have been used.
- M1000 4-phenoxybenzaldehyde imine **46** has been synthesised to assess the influence of possible Π -stacking.



Scheme 24 | Imine coupling between Jeffamine M1000 **A** and benzaldehyde derivatives.

Reaction conditions used for Scheme 24: Jeffamine M1000 **A** (1.2 equiv.), benzaldehyde derivative (1 equiv.), CHCl₃, r. t., 1 - 2 d, 98 – 100%.

[191]

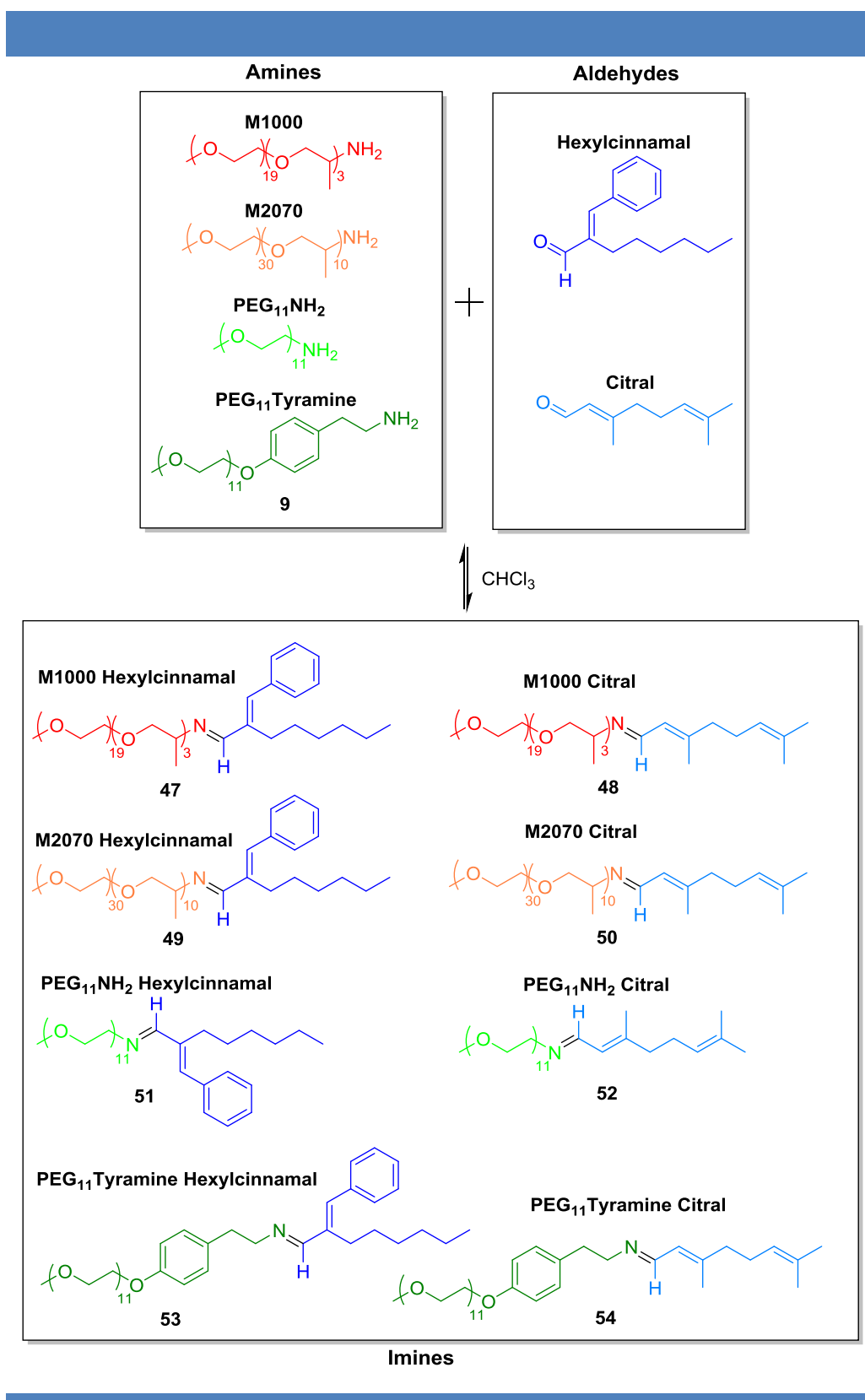
http://www.huntsman.com/performance_products/a/Products/Amines/Polyetheramines%20%20%20JEFFAMINE_R/Monoamine%20products

e) Aliphatic imines as profragrances

After the synthesis of imines for encapsulation and for the study of the influence of the hydrophobic tail on the micellisation, new imine profragrances have been synthesised to release fragrances directly from the dynablocks when hydrolysed in aqueous medium. Imines were produced by the reversible coupling of aldehyde fragrances with commercial and synthetic aliphatic amines at room temperature in chloroform (Scheme 25). Chosen aldehydes were citral and hexylcinnamal, two widely used aldehydes in the fragrance industry with different hydrophobicities (Hexylcinnamal: LogP = 4.10; Citral LogP = 2.18, calculated thanks to chemdraw^[186]). For each aldehyde, four different amines were chosen for the imine coupling, the first two being commercial and the last two synthetic:

- Jeffamine M1000, diblock copolymer with a PO/EO ratio of about 3/19, was chosen for the same reasons as that explained in the previous section **4d**). (M1000-based profragrances include imines **47** and **48**)
- Jeffamine M2070, statistical copolymer with a PO/EO ratio of about 10/30. Its properties are close to that of M1000 but the molecular mass is different (2000 g/mol) and the PO/EO ratio is different. It is also a statistical copolymer while M1000 is a diblock copolymer. Both M1000 and M2070 are water-soluble. (M2070-based profragrances include imines **49** and **50**)
- PEG₁₁NH₂ to assess the performance from “standard” PEG amine. (PEG₁₁NH₂-based profragrances include imines **51** and **52**)
- PEG₁₁Tyramine to have an aromatic hydrophobic linker between the PEG chain and the amine moiety, in order to potentially achieve the performance of aromatic or benzylic amines. (PEG₁₁Tyramine-based profragrances include imines **53** and **54**)

This set of amines with different chain lengths and hydrophobic linkers are expected to yield imines with very different stability in water and kinetics of hydrolysis, and thus to release fragrances with different rates.

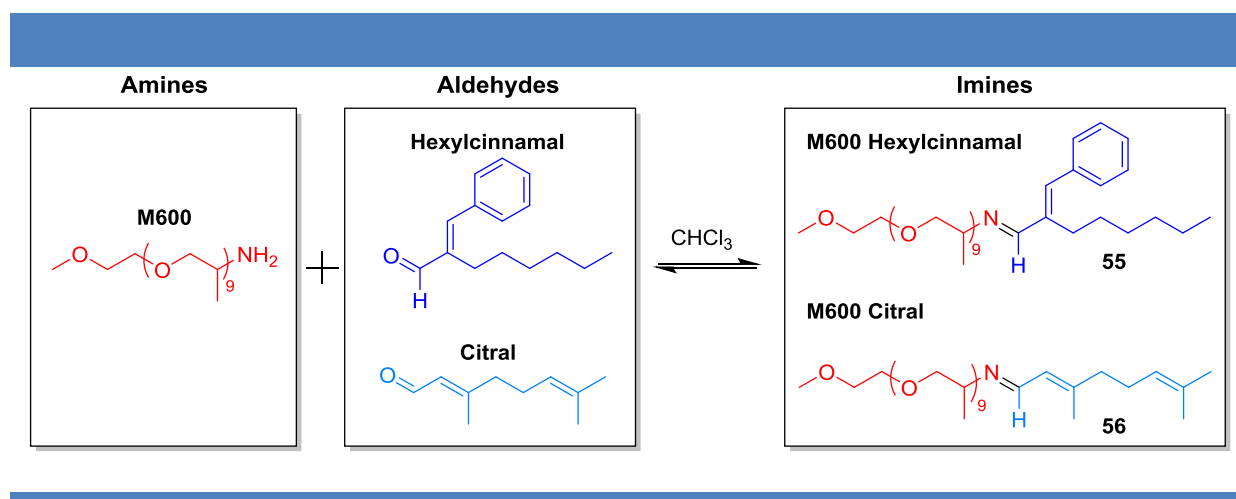


Scheme 25 | Imine coupling between a set of amines and aldehyde fragrances.

Reaction conditions used for Scheme 25: Amine (1.2 equiv.), fragrance aldehyde (1 equiv.), CHCl₃, r. t., 1 - 2 d, 95 - 98%.

Two more imines using citral and hexylcinnamal were formed. These aldehydes were condensed with Jeffamine M600 (Scheme 26), another commercial polyether amine from Huntsman. This poly(propylene glycol) amine is totally hydrophobic, and forms non-amphiphilic imines. These imines have to be used combined with either other dynablocks or industrial surfactants, in order to be inserted inside their micellar core. The goal of these imines is multiple:

- Dissolve in the micellar core of micelles aldehydes that would normally not go inside them.
- Stabilise aldehyde moieties by their conversion into an imine, and store them inside micelles.
- Slow down the hydrolysis of imines by hiding them inside hydrophobic mesophases.



Scheme 26 | Imine coupling between Jeffamine M600 and hexylcinnamal or citral.

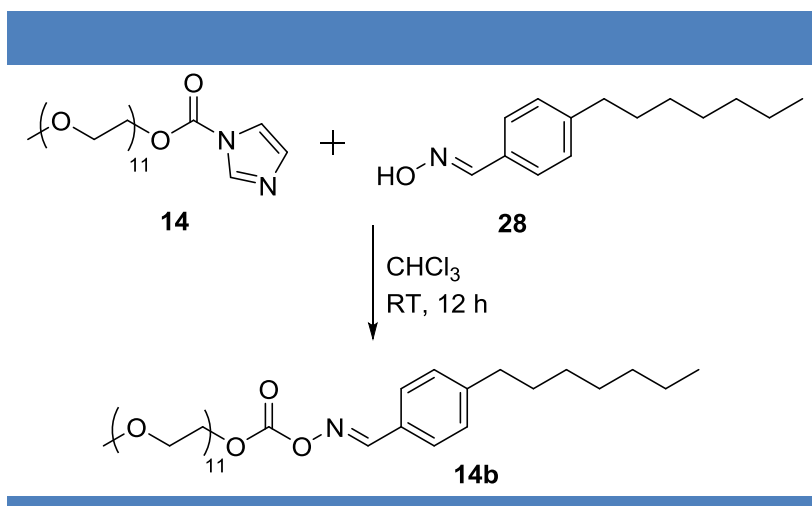
Reaction conditions used for Scheme 26: Jeffamine M600 (1.2 equiv.), aldehyde (1 equiv.), CHCl_3 , r. t., 1 - 2 d, **55**: quant., **56**: 98 %.

f) Acyloximes

After the study of some classical chemical links from DCC, less studied chemical functions like acyloximes were considered. The goal was to design an encapsulating system with a slow hydrolysis (half-hydrolysis time in days). The acyloximes could hydrolyse in dynamic or non-dynamic way. The first synthesised system was the carbonate oxime **14b**, resulting from the

coupling of PEG₁₁imidazole carboxylate **14** with octylbenzaloxime **28** (Scheme 27). The synthesis presented several difficulties:

- After 30% conversion into acyloxime **14b**, PEG₁₁Imidazole carboxylate **14** started to degrade faster than the reaction proceeded.
- Addition of excess of octylbenzaloxime **28** could increase the conversion only to a small extent.
- Addition of a base induced further degradation of **14**.

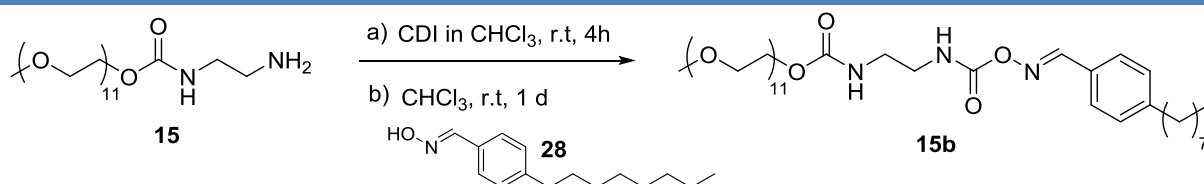


Scheme 27 | Coupling between PEG₁₁Imidazole carboxylate **14** and benzaldehyde oxime **28**.

Reaction conditions used for Scheme 27: PEG₁₁imidazole carboxylate **14** (1 equiv.), benzaldehyde oxime **28** (1 - 10 equiv.), CHCl₃, r. t., 12 h, not purified.

The molecule showed low stability, and could not be purified by extraction or by column chromatography. Some kinetics have been measured on the crude mixture but pure compound could not be obtained, since the excess of benzaldehyde oxime **28** and PEG₁₁OH resulting from the hydrolysis of **14** could not be removed quantitatively.

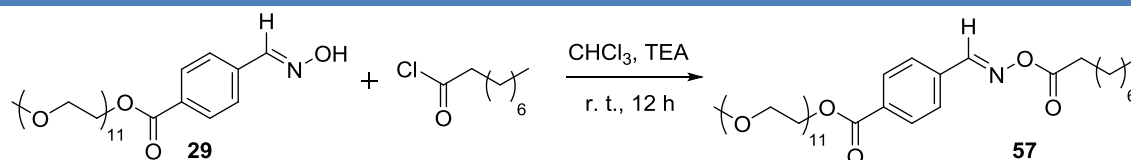
A potentially more stable carbamate oxime **15b** was envisioned from PEG₁₁ carbamate amine **15** and benzaldehyde oxime **28** thanks to a CDI coupling (Scheme 28). The reaction was also incomplete, but higher NMR yields (around 50%) were obtained compared to carbonate oxime **14b** (30%). **15b** proved also to be more stable than carbonate oxime **14b**, especially at low pH, but no attempt of purification worked.



Scheme 28 | Coupling between PEG₁₁ carbamate amine **15** and benzaldehyde oxime **28**.

Reaction conditions used for Scheme 28: a) PEG₁₁ carbamate amine **15** (1 equiv.), CDI (4 equiv.), CHCl₃, r. t., 4 h. b) benzaldehyde oxime (1 - 10 equiv.), CHCl₃, r. t., 1 d, not purified.

Finally we decided to synthesise acyloxime **57**, formed from the direct coupling of PEG₁₁benzaldehyde oxime **29** with nonanoyl chloride (Scheme 29). An excess of acyl chloride was necessary to overcome hydrolysis by water molecules trapped in the PEG chain. Acyloxime **57** has been purified by repetitive dissolution in water and ether, followed by filtrations to remove the precipitating nonanoic acid. This compound proved to be much more stable than acyloximes **14b** and **15b** and could be properly characterised.



Scheme 29 | Coupling between PEG₁₁benzaldehyde oxime **29** and nonanoyl chloride.

Reaction conditions used for Scheme 29: PEG₁₁benzaldehyde oxime **29** (1 equiv.), nonanoyl chloride (3 equiv.), CHCl₃, r. t., 30 min, **57**: 60%.

After having described in this chapter the synthetic work performed during my PhD thesis, the next chapter will be dedicated to the study of the kinetics of hydrolysis of imine derivatives and their encapsulation properties.

Chapter 3: Kinetics of hydrolysis and encapsulation properties of dynablocks

At the beginning of my Ph.D., the general properties of a basic set of non-ionic dynablocks made from PEG amine derivatives and 4-octylbenzaldehyde in water were known.^[4] These dynablocks were studied in water by ¹H NMR, DOSY NMR, and various scattering techniques to understand their behaviour, and most of their structural properties were elucidated. Two important facts were noticed during the formation of dynablocks:

- Self-assembly of the dynablocks in water was able to stabilise the imine bond, and a high concentration of imine at equilibrium was measured. The stabilisation properties of the structure were heavily dependent on the chemical nature of the imine bond, and dynablocks were able to catalyse the formation of their own constituent.
- Some dynablocks were able to encapsulate the non-condensed hydrophobic octylbenzaldehyde inside the hydrophobic core of the micelle, and thus increase its local concentration that favours the formation of more dynablocks with possible auto-catalysis effects.

From this previous work, it was obvious that dynablocks could be used for the encapsulation of hydrophobic compounds. Thermodynamic and kinetic parameters for the formation of these imines were also known. My initial goal was to synthesise the imines that were previously studied as mixtures in water, and then to measure their kinetics of hydrolysis by NMR. Then, derivatives were made to tune their stability. The ultimate goal of these studies was to have families of imines with different stabilities and kinetics of hydrolysis, and to choose the suitable imine depending on its time of hydrolysis and according to the pH necessary for application. Ultimately, the possibility to incorporate hydrophobic volatile molecules inside the micellar structure for release upon hydrolysis of the imine was assessed. A suitable delivery system should have the following characteristics:

- Easy synthesis, cheap reactants.
- Biocompatibility of the imines and their hydrolysis products.

- Slow speed of hydrolysis in water, to obtain a sustained release of the encapsulated hydrophobic fragrances over time. We first targeted that a typically suitable system would have a half-time of hydrolysis in the range of one day ($H_{1/2} = 24$ h).

1/ Hydrolysis of imine derivatives (for encapsulation applications)

Once the synthesis of imines was achieved, the study of their kinetics of hydrolysis was started immediately. Considering that the final application of these dynablocks would be in aqueous solution, the study of their hydrolysis by NMR was performed in deuterium oxide. A correction of the pH value was applied to take into account that the solvent is deuterated: $pD = pH_{\text{measured}} + 0.4$.^{[192][193]} The first system that was studied is PEG₁₁aromatic imine **31**, made from the condensation of PEG₁₁aromatic amine **10** and 4-octylbenzaldehyde. This imine was chosen for its high stability in aqueous solution and its ability to incorporate hydrophobic molecules in its micellar core.

a) Study of aromatic imines

Previous work on the formation of PEG₁₁aromatic imine **31** have been mainly performed at a concentration of 50 mM. For the hydrolysis of dynablocks, a smaller concentration of 10 mM was chosen, since it is closer to the standard concentration used in the industry for delivery systems (10 mM \approx 1% in weight of imine in the solution for most dynablocks). A plot of the concentration in imine in a deuterium oxide solution as a function of time is given in Figure 51. The concentration of imine in solution was determined by NMR by integrating the imine (\approx 8 ppm) and the aldehyde (\approx 9,5 – 10 ppm) peaks, according to the following formula:

$$C_{\text{imine}}(t) = C_0 * \frac{I_{\text{imine}}(t)}{I_{\text{aldehyde}}(t) + I_{\text{imine}}(t)}$$

^[192] Godoy-Alcántar, C., Yatsimirsky, A. K., Lehn, J. M. Structure-stability correlations for imine formation in aqueous solution. *J.Phys. Org. Chem.* **18**, 979–985 (2005).

^[193] Covington, A. K., Paabo, M., Robinson, R. A., Bates, R. G. Use of the Glass Electrode in Deuterium Oxide and the Relation between the Standardized pD (pa.) Scale and the Operational pH in Heavy Water. *Anal. Chem.* **40**, 700–706 (1968).

With $C_{\text{imine}}(t)$ being the concentration of imine at a given time t , C_0 the initial concentration of imine, and I_{aldehyde} and I_{imine} the respective integration by ^1H NMR of the aldehyde and the imine peaks. Time $t = 0$ corresponds to the time when the imine was dissolved in water.

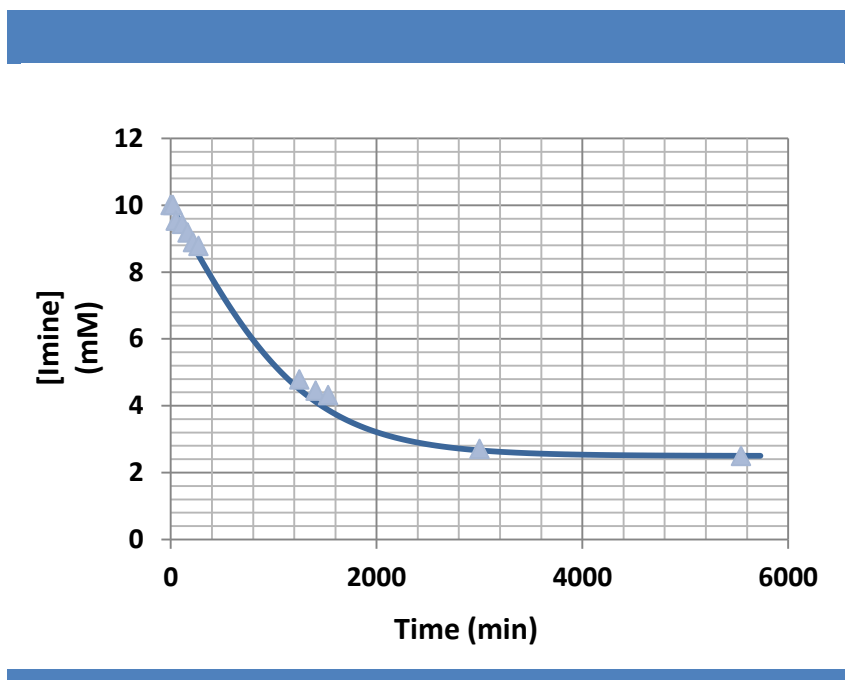


Figure 51 | Concentration of PEG₁₁aromatic imine **31** as a function of time ($C_0 = 10$ mM, pD 8.04, $C_{\text{eq}} = 2,5$ mM, $V_0 = 0,009$ mM/min).

A typical plot for the hydrolysis of PEG₁₁Aromatic imine **31** is displayed in Figure 51. It can be seen that the imine concentration at the beginning of the experiment is decreasing almost linearly for the first 400 minutes, and then the speed of hydrolysis decreases until it reaches equilibrium. The curve could not be fitted by a second-order kinetic plot, which proves a complex mechanism for the hydrolysis of this imine in water. This result is not surprising, since the imine is stabilised in water by the micellar structure (PEG₁₁aromatic imine **31** self-assemble into spherical micelles of 7 nm of hydrodynamic radius in water according to previous work).^[112] Several reasons can explain this complex hydrolytic process in water:

- Aromatic rings from both the aromatic amine and the benzaldehyde derivative create a hydrophobic area around the imine. The imine bond is “hidden” in the hydrophobic core, and thus partially protected from water.

- Amphiphilic imine molecules are dynamically located at several positions in solution; they can be i) constituents of the micelles, ii) partially dissolved inside the micellar core, or iii) free in solution (with a maximal concentration equal to the CMC). These different positions of imine molecules in the mixture are expected to give different individual hydrolysis time, and thus a complex overall kinetics of hydrolysis.

However, even if the hydrolysis does not follow a second-order kinetic, it is possible to measure the initial speed of hydrolysis V_0 from the kinetic plot, and from it to calculate the pseudo-first order kinetic constant k_h that the system would have if it would not have not been stabilised by the micelle formation ($k_h = V_0/C_0$, Table 1).

i) Influence of concentration on the kinetics of hydrolysis of PEG₁₁Aromatic imine **31**

To assess the influence of concentration on the kinetics of hydrolysis, three initial concentrations were chosen: 10, 25 and 50 mM. The plot corresponding to the hydrolysis of **31** at these three concentrations is displayed in Figure 52.

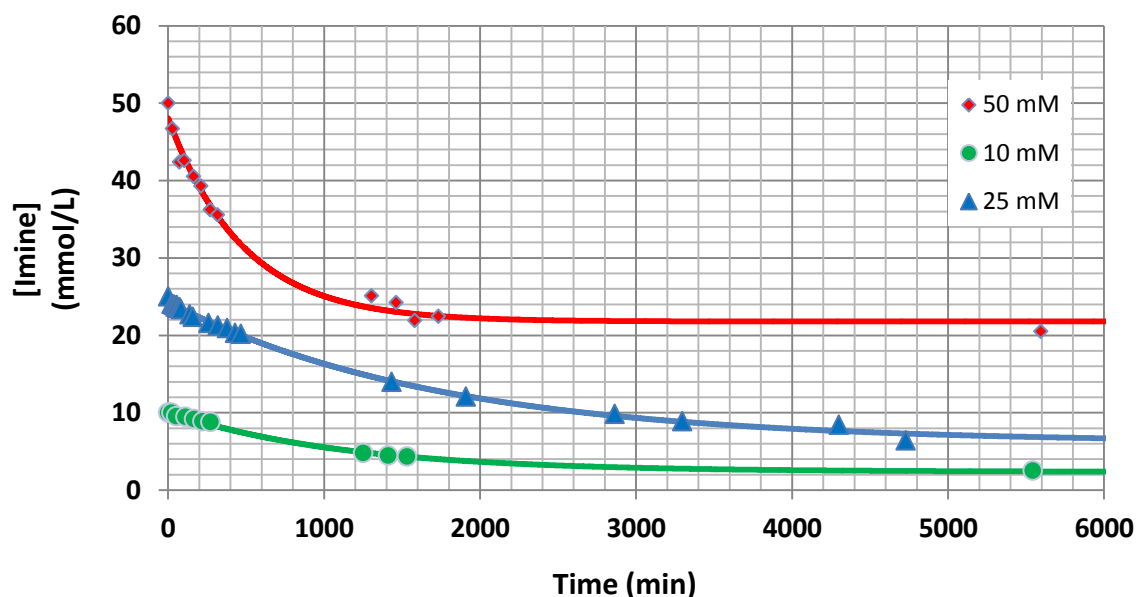


Figure 52 | Influence of concentration on the initial speed of hydrolysis of **31** at unmodified pD (7.4 < pD < 8.3)

The initial speed of hydrolysis of **31** at unmodified pD was plotted as a function of the concentration (Figure 53), and it was found that V_0 is increasing rapidly with concentration.

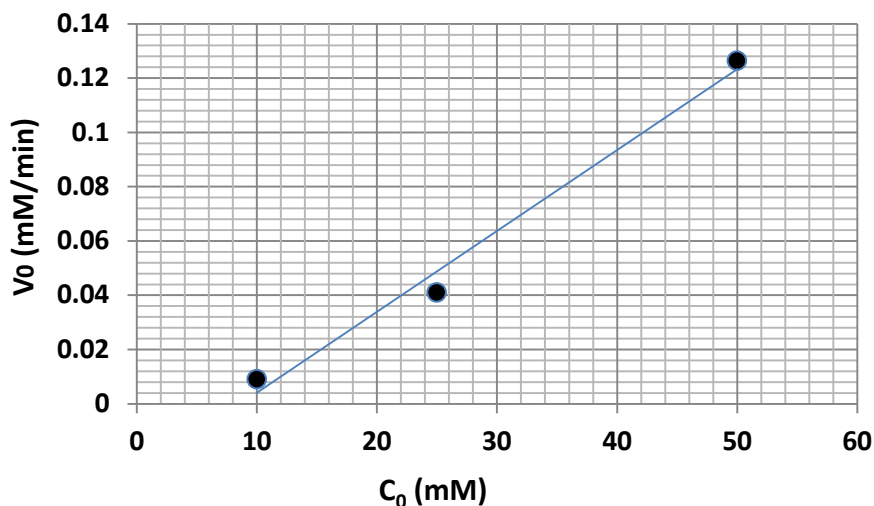


Figure 53 | Influence of initial concentration on the initial speed of hydrolysis of **31** at unmodified pD ($7.4 < \text{pD} < 8.3$)

The concentration at equilibrium as a function of the initial concentration of imine **31** was also plotted in Figure 54.

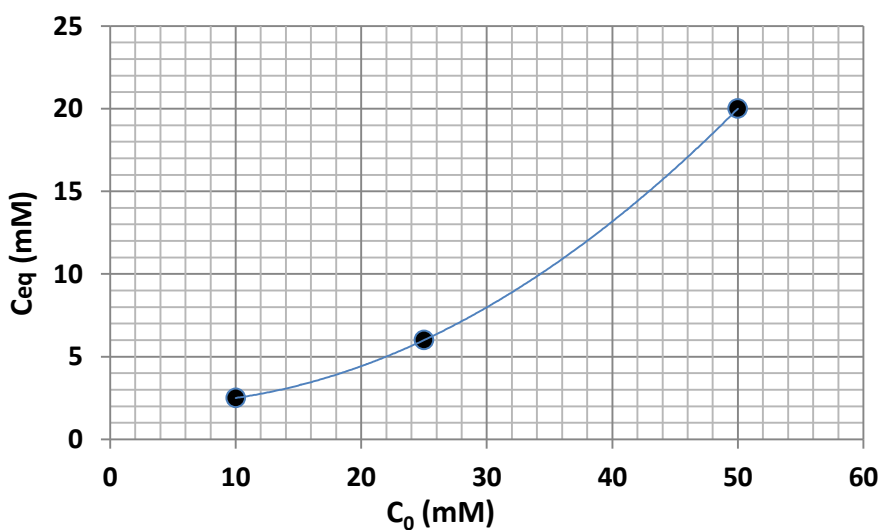


Figure 54 | Influence of the initial concentration on the concentration at equilibrium for the hydrolysis of **31** at unmodified pD ($7.4 < \text{pD} < 8.3$)

Amphiphilic imines are highly condensed compared to purely hydrophilic imines.^[192] The concentration at equilibrium increases when a larger initial quantity of imine is used. This result is not surprising, but has two implications:

- If the concentration C_0 is high, the concentration of imine at equilibrium will also be high and encapsulated hydrophobic compounds might not be released.

If the concentration C_0 is low enough, a near quantitative hydrolysis will occur, because the hydrophobic material will be removed by precipitation in the solution and will drive the thermodynamic equilibrium toward hydrolysis.

The kinetic data are summarised in Table 3.

Table 3 | Kinetic parameters (Initial rate of hydrolysis and pseudo-first order kinetic constant) of dynablock **31** for its hydrolysis in water.

C (mM)	V_0 (10^{-3} mM/min)	k_c (10^{-5} min $^{-1}$)
10	9.0	90
25	40.9	163.6
50	126.3	252.6

ii) Influence of pD on the kinetics of hydrolysis of PEG₁₁aromatic imine **31**

After having observed that the initial concentration has an important impact on the speed of hydrolysis and on the concentration at equilibrium, the influence of pD on the kinetics of hydrolysis of PEG₁₁aromatic imine **31** was assessed (Figure 55). The initial pD was modified at the launch of the kinetic by addition of a base or an acide (NaOD or CF₃COOD respectively). It should be noted that the pD was increased during the reaction by the release of free amine. The half-hydrolysis time is also displayed on the figure and corresponds to the time taken to reach half of the initial concentration (thus 5 mM for this experiment).

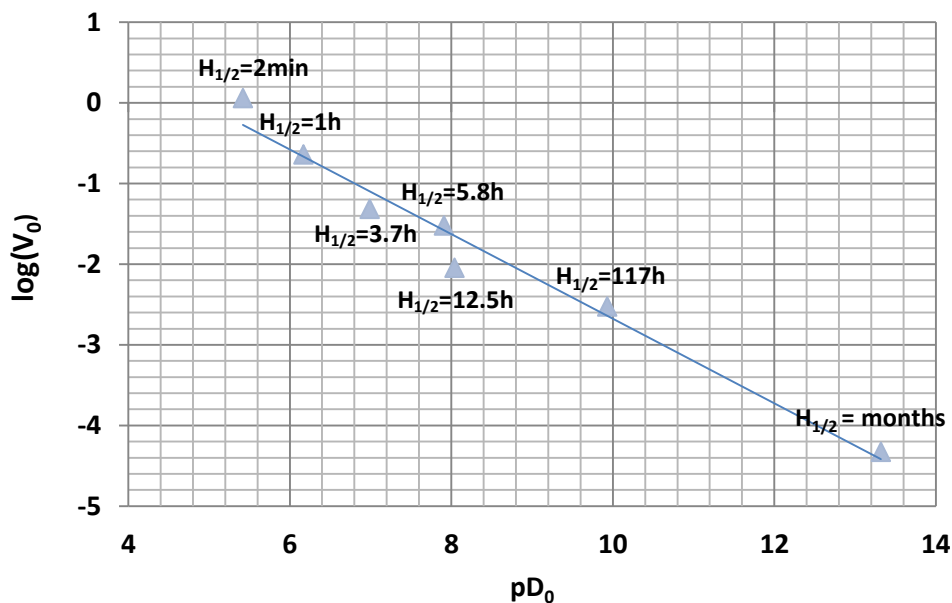


Figure 55 | Influence of the initial pD on the logarithm of the initial speed of hydrolysis V_0 of **31** at an initial concentration of 10 mM in D_2O .

It is striking to observe the importance of initial pD on the kinetics of hydrolysis. This modification allows to get a very broad range of hydrolysing times from dynablock **31**. However, it hydrolyses very rapidly at pD 5 (half-hydrolysis time of 2 minutes), but presents a suitable releasing time in the near neutral pD and the slightly basic zone ($H_{1/2} = 12.5$ h at pD 8.0 and $H_{1/2} = 117$ h at pD 9.9). A very interesting point of the system is its ability to be almost fully stable in aqueous solution at high pD (pD = 13), even with a concentration as low as 10 mM. This property could be used to store the imine in an aqueous solution at high pD before its use, and then trigger the release of the encapsulated volatile fragrance by adjusting the pD with the addition of acid or by dilution. This result also tends to show that, for this aromatic imine, the non-acid catalysed hydrolysis mechanisms are negligible.

iii) Hydrolysis of PEG₁₁Aromatic imine **31** followed by DLS

After the study of the kinetics of hydrolysis by NMR, we were interested in the evolution of the micelle size during the hydrolysis of PEG₁₁aromatic imine **31**. Since octylbenzaldehyde is released upon hydrolysis of the dynablock, we wanted to know if it stays encapsulated inside

the micelle and how the system evolves when hydrolysis proceeds. We expected to observe an increase of the size of the micelles until a constant average size of the micellar self-assembly is reached, due to the division of the thermodynamically unstable micelle above a critical size^[194]. Measurements of the hydrodynamic radius H_r as a function of time were performed by DLS on PEG₁₁aromatic imine **31** during its hydrolysis in deuterium oxide (Figure 56). A pD of 7.6 at 10 mM was chosen to enable a fast hydrolysis ($H_{1/2} \approx 6h$) with a relatively low concentration at equilibrium ($C_{eq} = 2.5$ mM).

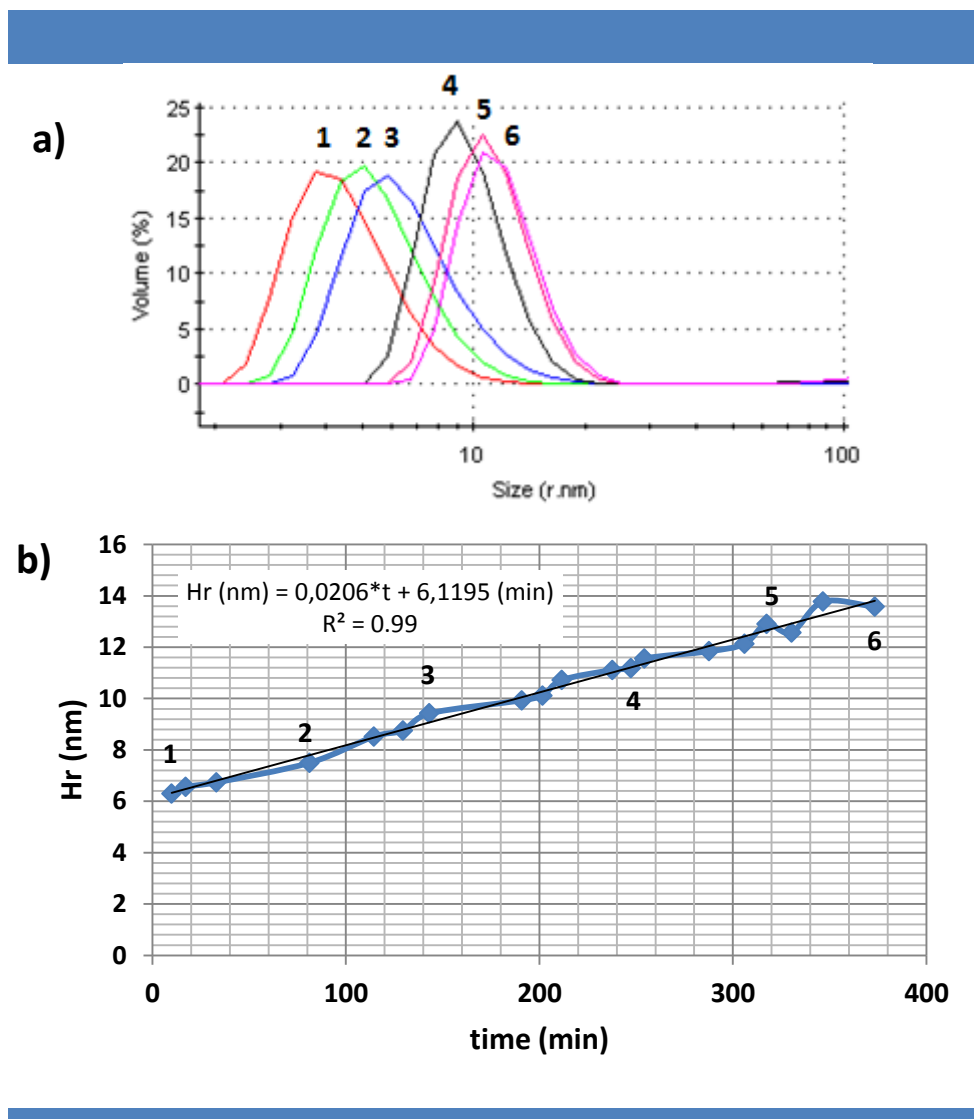


Figure 56 | DLS studies on micelles of PEG₁₁aromatic imine **31** during their hydrolysis in deuterium oxide (pD 8.0, 10 mM). a) DLS measurements of the hydrodynamic size of **31** aggregates and their evolution during its hydrolysis in D₂O. b) Hydrodynamic radius (H_r) as a function of time followed by DLS during the hydrolysis of **31** in water ($C = 10$ mM).

^[194] Pool, R.; Bolhuis, P. G. Prediction of an autocatalytic replication mechanism for micelle formation. *Phys. Rev. Lett.* **97**, 018302-1-4 (2006).

A typical DLS plot showing the size increase of the aggregates as a function of time and their polydispersity is shown in Figure 56. The polydispersity of the micellar system is quite broad, with sizes ranging from the half to the double of the average micellar size; this phenomenon is at least partially due to the polydispersity of PEG₁₁OH used for the synthesis of the amines (present from PEG₆ to PEG₁₆, as determined by ESI-MS, data not shown). From Figure 56b, it can be seen that the mean hydrodynamic radius of the micelles is growing lineary (growth of 0.02 nm/min) during the six first hours of hydrolysis (concentration in imine is at 5 mM at this moment), due to the encapsulation of the released 4-octylbenzalde upon hydrolysis. After 3 hours of hydrolysis, a microemulsion appears with its size increasing rapidly with time at 0.65 nm/min (Figure 57). The different steps of the hydrolysis are as follows:

- Hydrolysis of the micellar imine and increase of the micelle size.
- Apparition of a micro-emulsion, probably due to the fusion of micelles overcharged in aldehyde.
- Disappearance of the micellar structure. Micro-emulsion continues to grow.
- Macroscopic phase separation. The solution becomes milky at the top of the sample and DLS cannot detect objects that have become too big (size in the μm range).

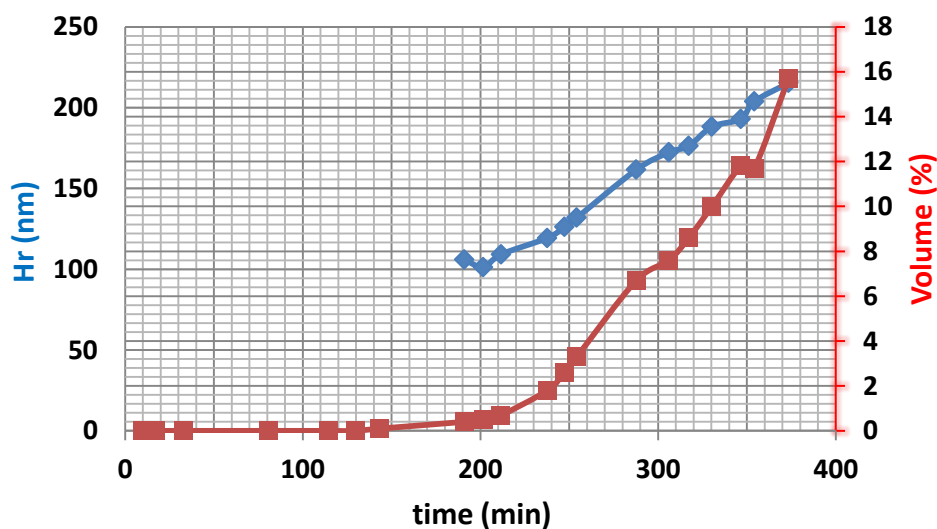


Figure 57 | Hydrodynamic radius Hr (blue) and volume percentage (red) of octylbenzaldehyde emulsion as a function of time followed by DLS (PEG₁₁aromatic imine **31** hydrolysis in D₂O, C = 10 mM).

Now that we have understood the influence of some key parameters such as pD, the concentration or the release of hydrophobic aldehyde on the kinetics of hydrolysis, it is possible to try to tune the kinetics of hydrolysis of the imines by stabilising or destabilising the micellar structure.

iv) Influence of the presence of a hydrogen bonding group on the hydrophobic block

One way to change the stability of the micellar structure is to create new interactions between blocks of the amphiphiles. We have tried to achieve this stabilisation by adding of a urea moiety on the hydrophobic block, and therefore by creating (strong) hydrogen bonds between all the hydrophobic blocks of the amphiphiles. To determine the effect of the addition of this urea moiety, a kinetics of hydrolysis of PEG₁₁aromatic amine 1-(4-formylphenyl)-3-pentylurea Imine **32** at 10 mM was measured in deuterium oxide (Figure 58).

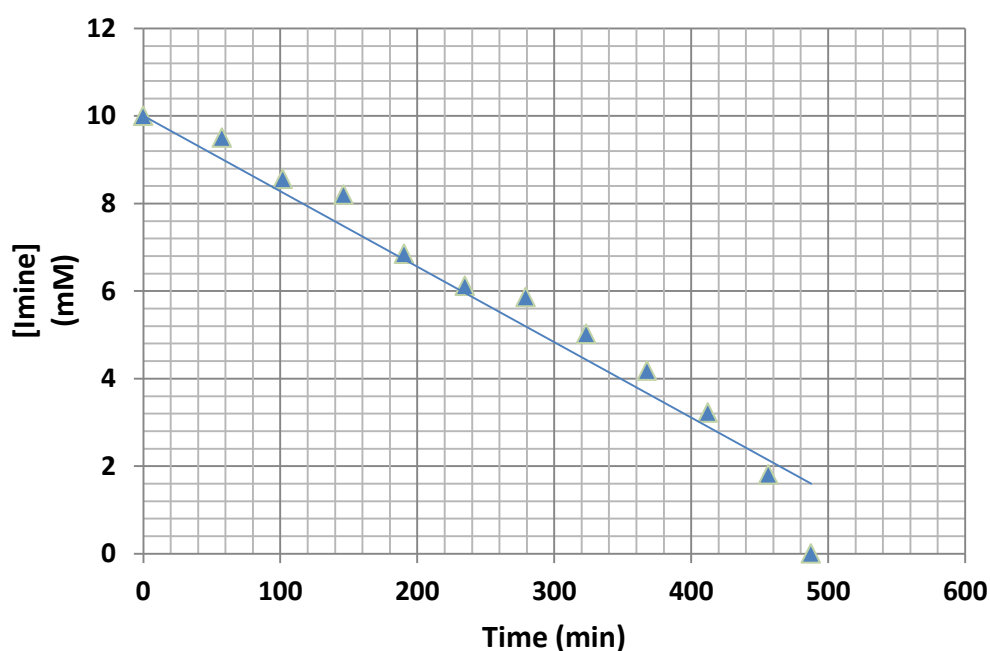


Figure 58 | Evolution of the concentration of imine **32** as a function of time (D_2O , $C_0 = 10$ mM, pD 8.9, pseudo-zero order constant $k = 0.017$ Mm/min).

This plot shows that the hydrolysis is surprisingly fast: a half-hydrolysis time of 291 min is observed and in less than 500 min, hydrolysis is complete. This fast hydrolysis is also correlated with a rapid increase of the hydrodynamic radius measured by DLS, going from 6 to 14 nm in less than 25 minutes (Figure 59).

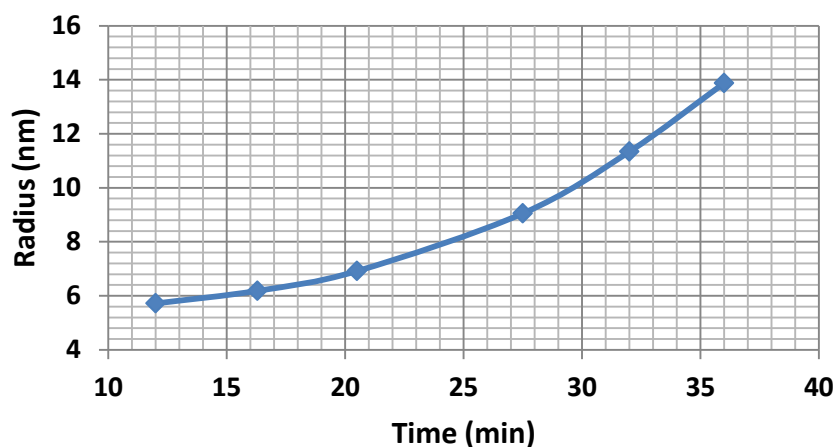


Figure 59 | Hydrodynamic radius of imine **32** as a function of time followed by DLS during its hydrolysis in water ($pD_0 = 8.9$, $C = 10$ mM).

During hydrolysis, the formation of a white suspension can be observed, which comes from the fact that 1-(4-formylphenyl)-3-pentylurea **21** is a solid in its pure form and is not soluble in water, and thus precipitates when released from the imine. Precipitation inside the micelle causes a strong perturbation of the micellar structure, and potentially exposes the imine group to water, fastening its hydrolysis. The phase separation caused by the precipitation also prevents PEG₁₁aromatic amine **10** to react with the aldehyde, thus increasing even more the overall hydrolysis rate and shifting the thermodynamic equilibrium toward quantitative hydrolysis .

This experiment demonstrates that the stability of imines and micelles can easily be tuned by chemical modification of the blocks, and that the speed of hydrolysis is strongly influenced by phase separation (here precipitation of the aldehyde). The half-hydrolysis time went from almost 5 days with PEG₁₁aromatic imine **31** to 14 hours with PEG₁₁aromatic amine 1-(4-formylphenyl)-3-pentylurea imine **32** under similar conditions (10 mM in D₂O, $pD = 10$). This demonstrates the versatility of dynablocks for the development of encapsulating systems

with different rate of hydrolysis at different pDs. This is clearly evidenced on Table 4 and Figure 60 for a direct comparison between dynablock **31** and **32**.

Table 4 | Kinetic parameters of dynablocks **31** and **32** for their hydrolysis in water.

$H_{1/2}$ (h)	V_0 (mM/min)	pD
4.8	0.0141	8.94
14.2	0.0072	10.43

$H_{1/2}$ (h)	V_0 (mM/min)	pD
18.1	0.009	8.04
116.9	0.00297	9.93

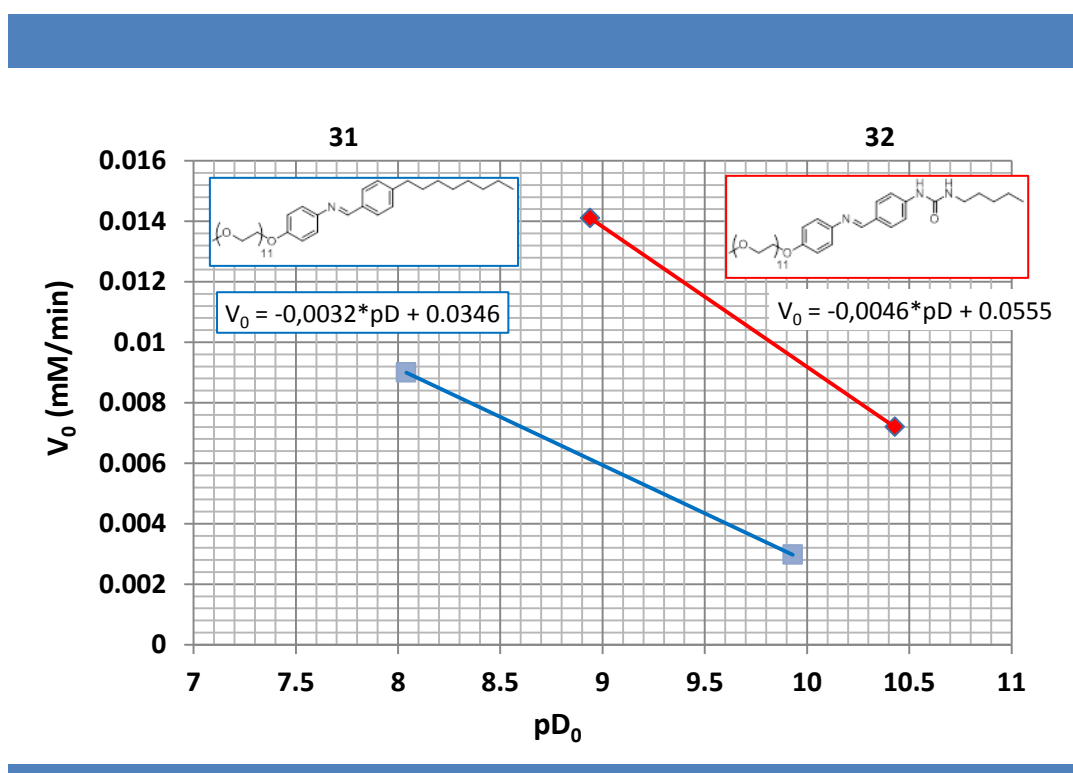


Figure 60 | Initial rate of hydrolysis of imine **31** and **32** as a function of initial pD ($C_0 = 10$ mM,)

Imines made of aromatic amine proved to be interesting and tunable systems. However, they present a main drawback: aromatic amines are toxic, and their use in cosmetic applications is banned. For this reason, new dynablocks based on the much less toxic aliphatic amines have been synthesised, and their properties have been investigated depending on the chemical modifications of their hydrophilic block.

b) Study of aliphatic imines

In this section, the hydrolysis of several closely related imines is studied. The general idea was to measure the kinetics of hydrolysis of PEG₁₁NH₂ 4-octylbenzaldehyde imine **33**, and to try to tune its hydrolysis rate by adding groups able to make hydrogen bonding between the hydrophilic blocks. Hydrolyses were performed in deuterium oxide at a concentration of 10 mM (typical concentration used in applications), for an easier comparison with the results obtained from aromatic imines.

i) Hydrolysis of PEG₁₁Aliphatic imine **33**

The first imine we studied was PEG₁₁NH₂ 4-octylbenzaldehyde imine **33**. The plot of its concentration as a function of time at unmodified pD (10.25) and at 10 mM is given in Figure 61.

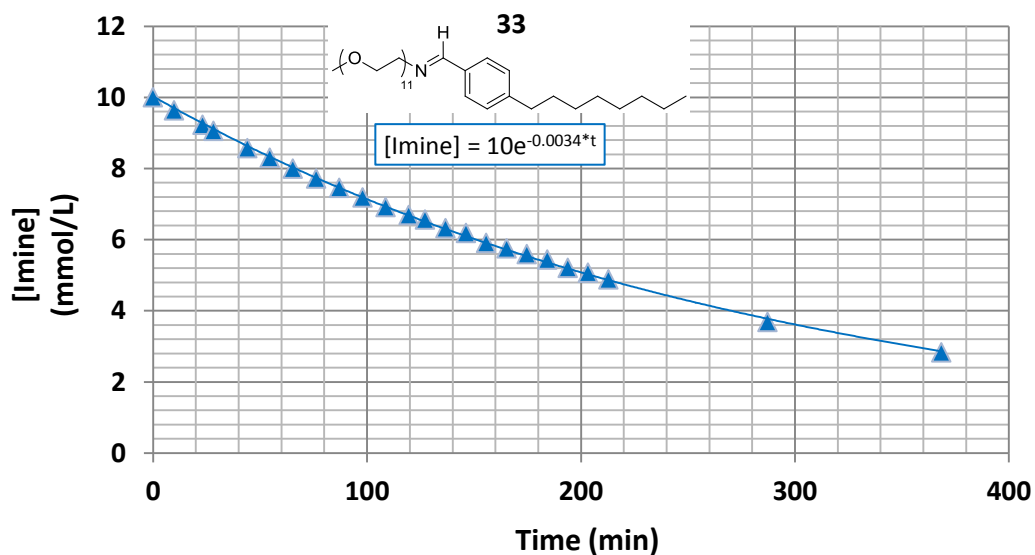


Figure 61 | Concentration of PEG₁₁Aliphatic imine **33** as a function of time at unmodified pD ($C_0 = 10$ mM, pD 10.25, $k = 0.0034 \text{ min}^{-1}$).

Several aspects can be noted:

- The hydrolysis of this aliphatic imine is much faster than that of aromatic imine **31**, even at high pD. ($H_{1/2} = 205$ min compared to several days or weeks for **31** at the same pD)
- Hydrolysis is almost complete after 24 h (only a very small quantity of imine is detected by NMR)
- The curve can be fitted by a pseudo-first order kinetic, which shows that the imine group is not well protected from water by the structure, thus explaining the fast hydrolysis. This is not surprising, considering that the imine linkage is directly connected to the PEG chain, and it is supposed to be located at the interface between the hydrophobic core and the water-solubilised shell.

This system, if used for encapsulation, could only be efficient to release volatiles on an hour time scale, and it would also be difficult to prevent hydrolysis for storage. The possibility to tune the stability of the aliphatic imine was then explored by modifying the hydrophilic block with hydrogen bonding units, to assess if the creation of supramolecular interactions between the PEG chains can influence the hydrolysis time of the imine.

ii) Influence of the presence of a hydrogen bonding group on the hydrophilic block

We first studied PEG₁₁amide imine **34**. The influence of pD on its kinetics of hydrolysis was explored (Figure 62), and two pD zones can be observed:

- $9 < \text{pD} < 13$: Low influence of the pD on the kinetics of hydrolysis: $H_{1/2}(\text{pD } 9) = 2.2\text{h}$, $H_{1/2}(\text{pD } 12) = 3.2\text{h}$
- $\text{pD} < 8.3$: Very fast initial hydrolysis (from 10 to 6.6 mM in 17 min), and then relatively fast hydrolysis until complete hydrolysis.

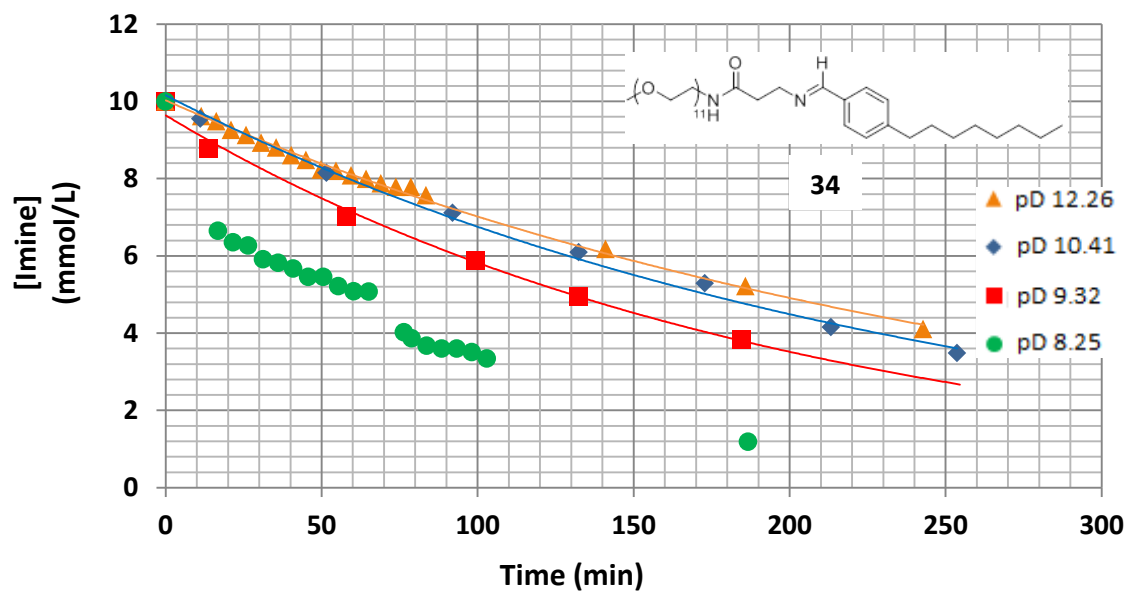


Figure 62 | Concentration of PEG₁₁amide imine **34** as a function of time at several pDs ($C_0 = 10$ mM).

This kinetics of hydrolysis revealed to be slightly faster than that obtained from PEG₁₁aliphatic imine **33**. After a few hours of hydrolysis, a white compound was found to precipitate inside the NMR tube. To understand its origin, the hydrolysis of **34** was followed by DLS (Figure 63). The first point measured at 14 minutes by DLS indicates a particle size of 3.8 nm (Figure 63a), and the presence of an emulsion of 110 nm (Figure 63b). Both are rapidly increasing over time, until no micellar aggregate is detected after 550 minutes. However, the micro-emulsion continues to grow, ultimately leading to a slow phase separation between the hydrophobic octylbenzaldehyde emulsion stabilised by the rest of imine surfactants, and water. This phase separation takes weeks.

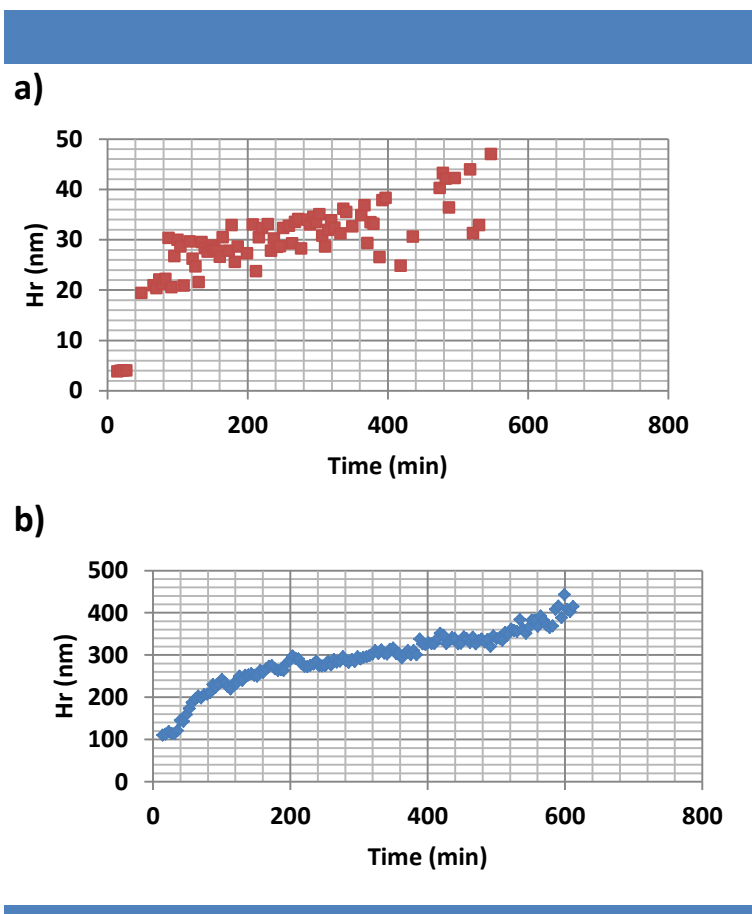


Figure 63 | Hydrolysis of PEG₁₁amide imine **34** followed by DLS at unmodified pDs ($C_0 = 10$ mM, $pD_0 = 10$). a) Hydrodynamic radius of the micelles as a function of time. b) Hydrodynamic radius of the micro-emulsion as a function of time.

A second aliphatic imine with stronger hydrogen bonding abilities (PEG₁₁carbamate urea imine **35**) was hydrolysed and results were compared to the other imines (Figure 64). Since the presence of an amide moiety had a small destabilizing effect, it was expected that the presence of a carbamate and a urea moiety would destabilise even more the micelle.

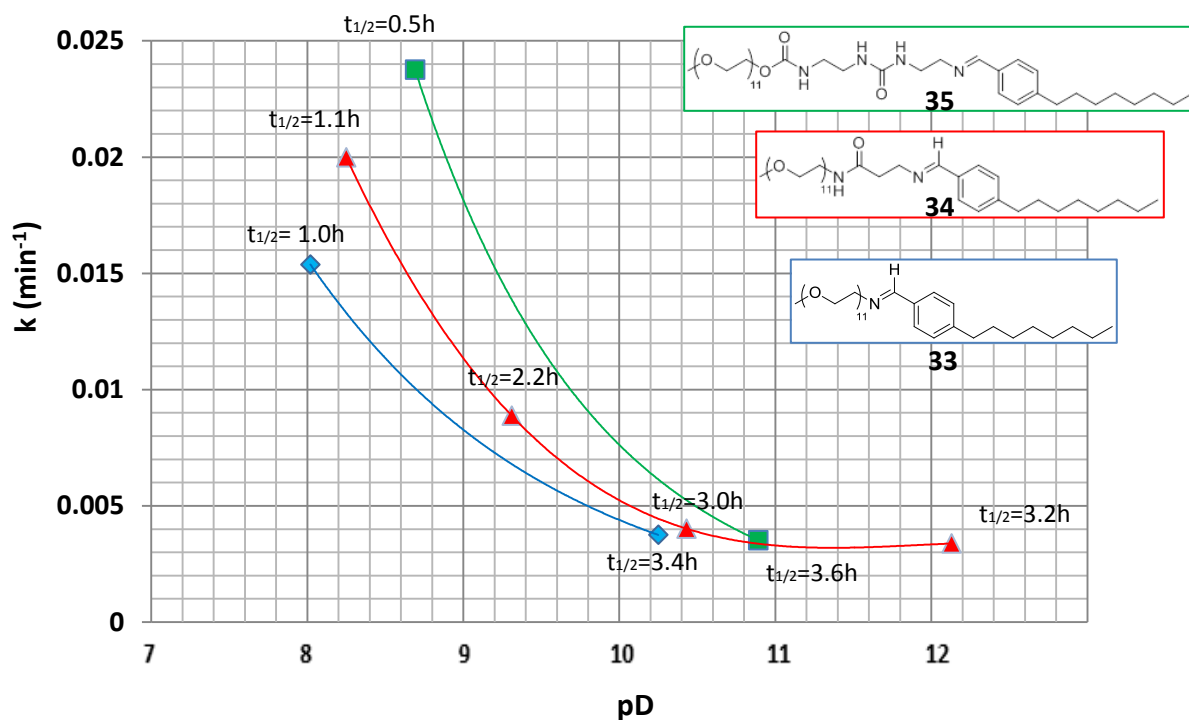


Figure 64 | Pseudo-first order kinetic constants of aliphatic imines **33** (blue), **34** (red) and **35** (green) as a function of pD. For each kinetic, the half-hydrolysis time is given ($C_0 = 10$ mM).

The effect of these hydrogen bonding moieties can be observed on Figure 64, with for example a half-hydrolysis time of 30 minutes for imine **35** compared to the 1 hour need to hydrolyse **33**. These aliphatic imines present two main differences compared to the aromatic imine **31**:

- Their hydrolysis is much faster (Half-hydrolysis time of 2 – 3 hours at pD 10 compared to 117 hours for imine **31**)
- They are not stabilised in very basic conditions (Half-hydrolysis time of 3 – 4 hours at pD below 12 compared to months for imine **31**)

These imines are particularly interesting compared to previously studied aromatic amines as they expand the ability to have a releasing system that gets hydrolysed in the hour time scale

under basic conditions. However, systems that would have slow hydrolysis (time scale in days) at neutral pD were still needed.

iii) Influence of pD on the kinetics of hydrolysis of octylamine PEG₁₁benzaldehyde imine **36**

The development of a more stable imine was initiated with the study of octylamine PEG₁₁benzaldehyde imine **36**. This molecule was designed to possess a hydrophobic linker (aromatic ring) between the imine bond and the hydrophilic block, in order to partially protect the imine bond from water. This strategy proved successful with the aromatic imine. To adapt it to aliphatic amines, the aldehyde moiety was switched from the hydrophobic to the hydrophilic block and commercial octylamine was used as hydrophobic part (an example of this strategy with a PEG aliphatic amine will also be discussed in chapter 4). The hydrolysis of **36** was performed at different pH in the near neutral – basic zone (Figure 65). For that, the pD was modified just after addition of the imine in deuterium oxide by addition of an acid (CF₃COOD) or a base (NaOD). The pD was then allowed to increase upon release of free amine.

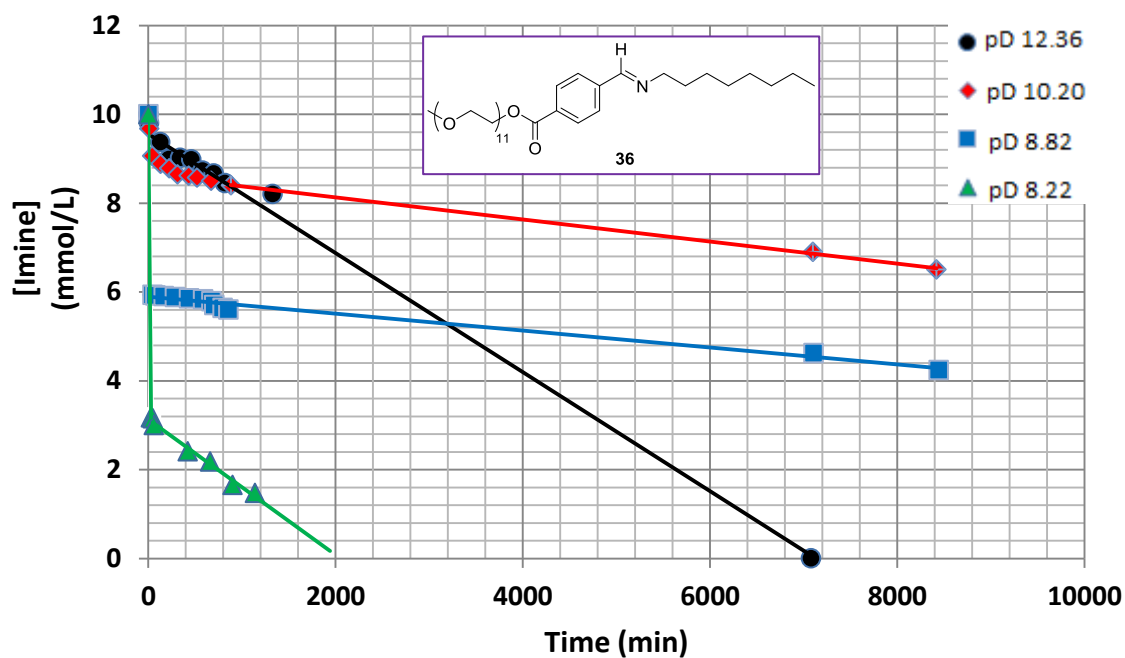


Figure 65 | Evolution of the concentration of octylamine PEG₁₁benzaldehyde **36** concentration as a function of time in D₂O at different pD₀ (C₀ = 10 mM, unmodified pD₀ = 10.2).

From Figure 65 and other unrepresented data, it is possible to describe the behaviour of octylamine PEG₁₁benzaldehyde imine **36** according to the initial pD:

- pD₀ < 7,4 : Quantitative hydrolysis in less than 1 hour
- 7.4 < pD₀ < 9.9 : Very fast initial hydrolysis followed by very slow hydrolysis until near complete hydrolysis
- 9.9 < pD₀ < 11.4 : Very slow hydrolysis until near complete hydrolysis
- pD₀ > 11.4 : Moderate speed of hydrolysis due to the ester link hydrolysis.

Octylamine PEG₁₁benzaldehyde imine **36** is a very versatile imine, with a half-hydrolysis time that can be tuned by the addition of an acid or a base: from 10 days at unmodified pD₀ 10.2 to 30 minutes at pD₀ 8.8. However, if a base (NaOD in our case) is added and the pD raises to values above 11.4, the rate of hydrolysis of the imine will increase again, due to the non-reversible hydrolysis of the ester linkage between the PEG chain and the benzaldehyde moiety, thus destroying the micelle (Figure 66). This reaction could be used to release benzoic acid derivatives and alcohols in a non-reversible way (H_{1/2} ≈ 1 day at pD 12.4). This possibly unwanted reaction could be avoided by replacing the ester linkage by an ether one.

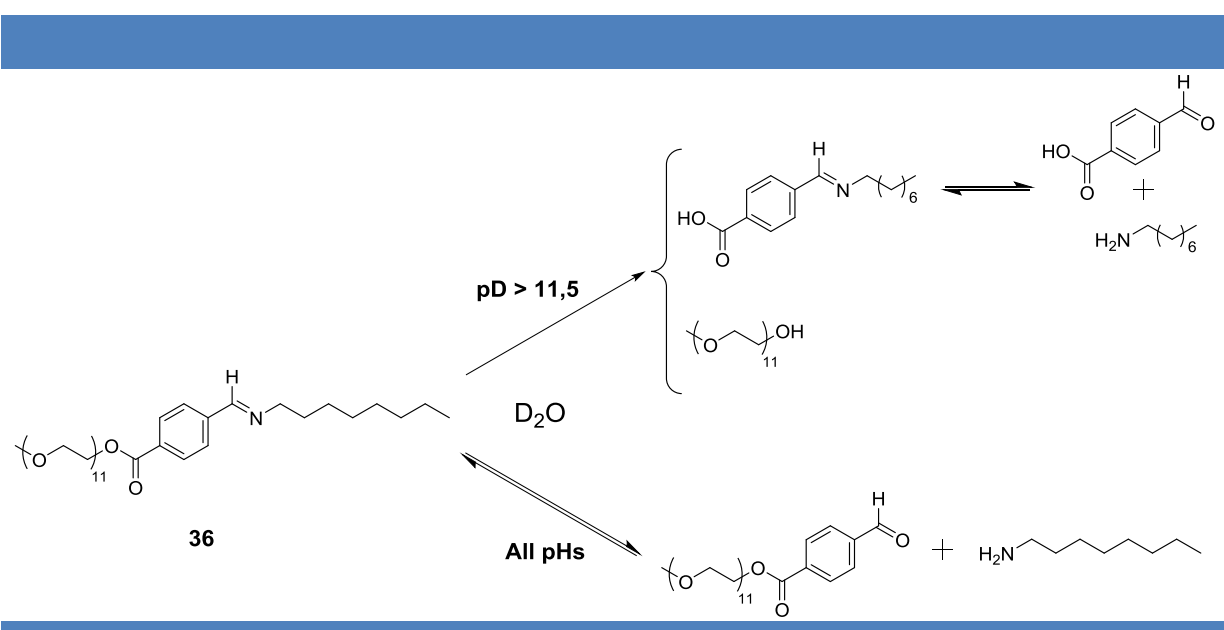


Figure 66 | General scheme for the hydrolysis of octylamine PEG₁₁benzaldehyde imine **36** in deuterium oxide at various pHs.

A direct comparison can be established between octylamine PEG₁₁benzaldehyde imine **36** and PEG₁₁aromatic imine **33** (Table 5), since they almost possess the same hydrophobic linker between the hydrophilic chain and the imine moiety (that of **36** is one carbon longer though) and even if this comparison is complicated by the high pD dependence of $H_{1/2}$ for both systems. However, it can be said that both imines have similar half-time of hydrolysis, with a $H_{1/2}$ in hours in the pD 8 range and a $H_{1/2}$ in days in the pD 10 range, showing a similar high stability provided by the hydrophobic linker that protects the imine bond from hydrolysis in the micellar structure. Nevertheless, PEG₁₁aromatic imine **33** performs better at lower pDs ($H_{1/2} = 5.8$ h at pD 8.0 compared to $H_{1/2} = 0.5$ h at pD 8.2 for **36**) and octylamine PEG₁₁benzaldehyde imine **36** performs better at the higher pDs ($H_{1/2} = 242$ h at pD 10.2 compared to $H_{1/2} = 117$ h at pD 9.9 for **33**). This fact can be explained by the differences of reactivity between PEG₁₁aromatic amine **10** (pKa 4.5) and octylamine (pKa 10.6), PEG₁₁aromatic amine **10** being more reactive than octylamine at lower pDs and octylamine being more reactive at higher pDs. These results confirm the effects of both the hydrophobic linker on imine stabilisation in water and the nature of the amine used to make dynablocks on pD dependence.

Table 5 | Kinetics parameters (half-hydrolysis time and pseudo-zero order kinetic constant k_c) of dynablocks **33** and **36** for its hydrolysis in water.

Imine	pD	$H_{1/2}$ (h)
PEG ₁₁ aromatic imine 33	7.9	5.8
PEG ₁₁ aromatic imine 33	8.0	12.5
PEG ₁₁ aromatic imine 33	9.9	117
Octylamine PEG ₁₁ benzaldehyde imine 36	8.2	0.5
Octylamine PEG ₁₁ benzaldehyde imine 36	8.8	78
Octylamine PEG ₁₁ benzaldehyde imine 36	10.2	242

iv) Influence of concentration on the kinetics of hydrolysis of octylamine PEG₁₁benzaldehyde imine **36**

After having tested the influence of pH on the kinetics of hydrolysis of imine **36**, the influence of the initial concentration was also assessed (Figure 67). Kinetics were measured after addition of acid, to decrease the pD from 10 to 8.3 and to evaluate the performance of the system at near neutral pD.

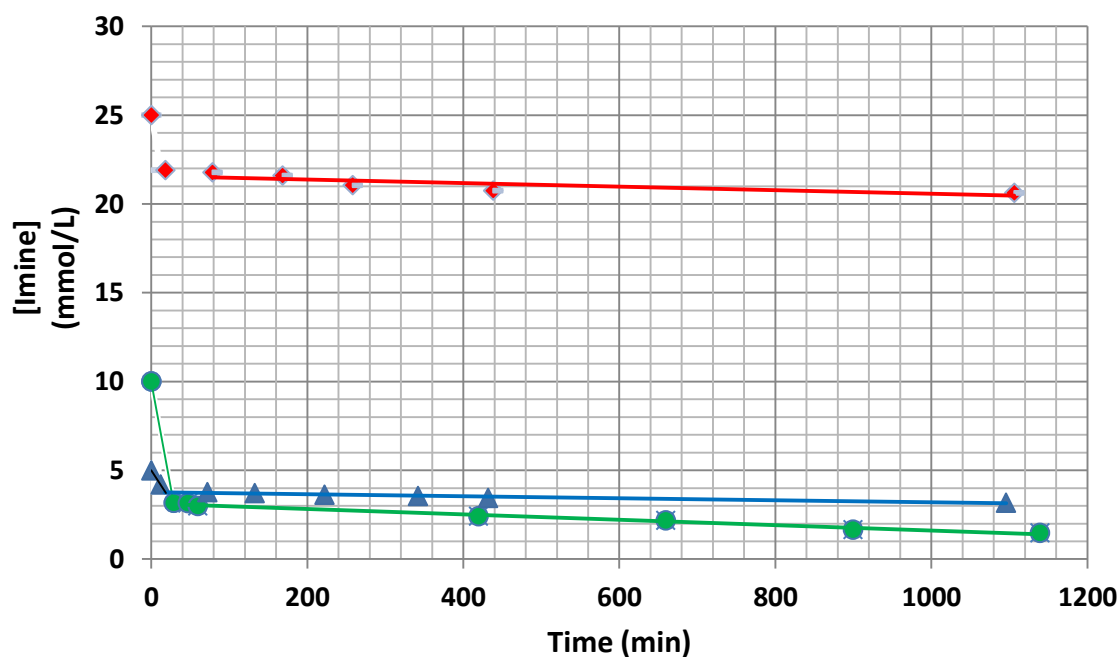


Figure 67 | Evolution of the concentration of octylamine PEG₁₁benzaldehyde imine **36** with time at different initial concentrations and at pD₀ 8.3 ($C_0 = 5, 10$ and 25 mM).

As previously observed (Figure 65), a very fast initial hydrolysis can be seen, followed by a slow hydrolysis until near complete hydrolysis when initial concentration is below 10 mM. **36** is surprisingly more rapidly hydrolysed at 10 mM than at 5 mM, but this result is probably due to the smaller pD used for the hydrolysis at 10 mM than for that at 5 mM, even if the difference is small (in Figure 65 it can be seen that the sensitivity of the imine to pD in this pD range is very important). It can also be seen that at 25 mM, imine **36** is considerably stabilised with a very slow hydrolysis of $0.57 \cdot 10^{-3}$ mM/min. All the kinetic data on octylamine PEG₁₁benzaldehyde imine **36** are compiled in Table 6.

Octylamine PEG₁₁benzaldehyde imine **36** proved to be a versatile imine able to very slowly hydrolyse in basic conditions (from pD 8 to 11), with a half-hydrolysis time of 10 days at a concentration as low as 10 mM, and performance could even be improved by increasing the initial concentration of imine. The strategy to protect the imine bond in the hydrophobic micellar core proved to be efficient to slow down its hydrolysis. This system also demonstrated a pseudo-zero order kinetic constant, which is the sign of a complex hydrolytic behaviour resulting from the structure stabilisation of the imine bond. This system is a valuable for the aliphatic imine family, which now possess members with half-hydrolysis time ranging from minutes to weeks in the near neutral to basic range.

Table 6 | Kinetics parameters (half-hydrolysis time and pseudo-zero order kinetic constant k_c of dynablock **36** for its hydrolysis in water.

C (mM)	pD	k_c (10^{-3} mM/min)	$H_{1/2}$ (h)
5	8.26	0.57	8.80
10	8.22	1.53	0.55
10	8.82	0.19	78.2
10	10.20	0.25	242
10	12.36	1.34	63.4
25	8.30	1.00	151

v) Influence of reactive encapsulated compounds on the kinetics of hydrolysis of octylamine PEG₁₁benzaldehyde imine **36**

Now that the hydrolytic stability of octylamine PEG₁₁benzaldehyde imine **36** alone in solution has been determined, we attempted to tune its kinetics of hydrolysis by incorporating reactive hydrophobic compounds inside the micellar core. Two classes of compounds were envisaged: amines and aldehydes. The first experiment was performed by hydrolysing a mixture of octylamine PEG₁₁benzaldehyde imine **36** with octylamine, both at a concentration of 10 Mm (Figure 68).

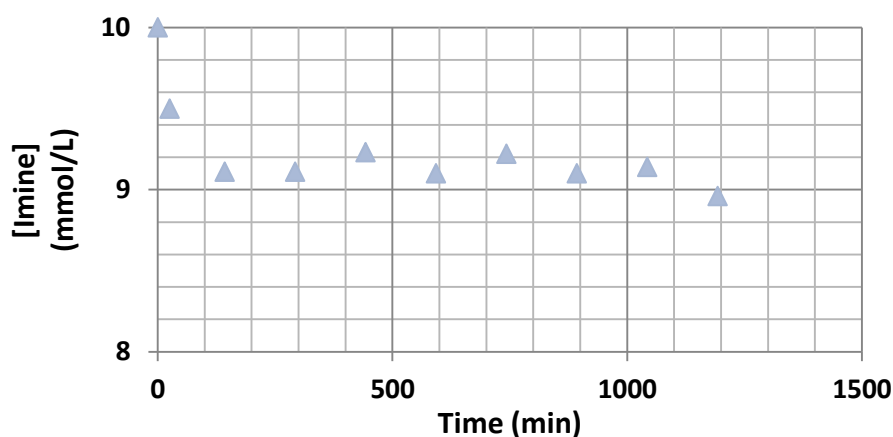


Figure 68 | Concentration of octylamine PEG₁₁benzaldehyde imine **36** followed by ¹H NMR as a function of time, in presence of 10 mM of octylamine (C₀ = 10 mM, pD 9.16).

The excess of octylamine proved to have two important effects:

- The initial hydrolysis was lower compared to that without addition of octylamine (Figure 65, concentration going from 10 to 9.1 mM in 142 minutes at pD 9.1 when octylamine is added, and concentration going from 10 to 5.9 mM in 44 minutes at pD 8.8 without added octylamine).
- The hydrolysis occurring after the initial hydrolysis is also much slower. Hydrolysis was followed only for one day, but during this time concentration was constant, which was not the case under the same conditions but without addition of octylamine.

This effect was predictable, because any addition of reactant (octylamine or PEG₁₁benzaldehyde **22**) is shifting the equilibrium toward imine formation. However, it was not expected that the addition of such a small amount of amine would yield an imine concentration at equilibrium as high as 9.0 mM, if the equilibrium is reached (it could also be an extremely slow hydrolysis). It comes probably from the incorporation of the extra amine inside the micellar core, thus creating a high local concentration in reacting species that considerably shift the equilibrium toward imine formation.

A second experiment was performed by incorporating octylbenzaldehyde inside the micellar core under the same conditions as previously described (Figure 69).

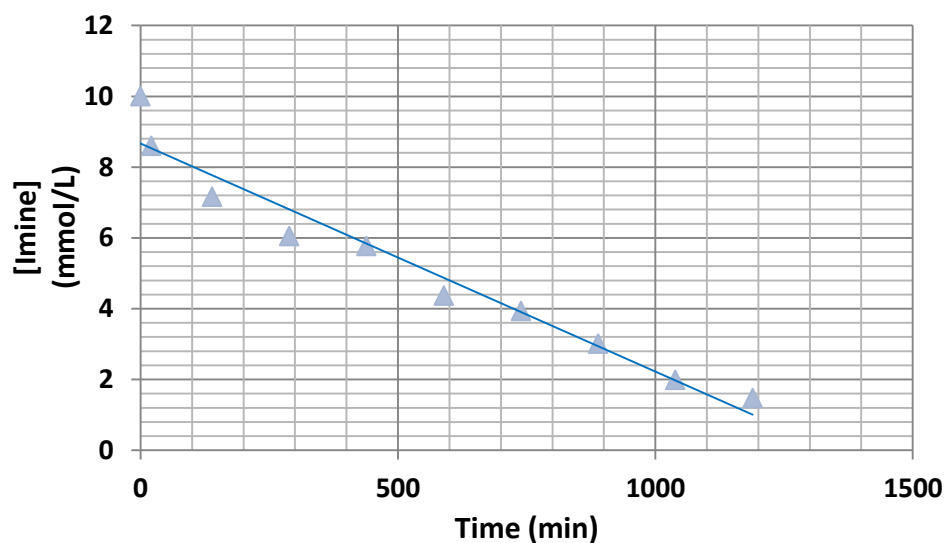


Figure 69 | Concentration of octylamine PEG₁₁benzaldehyde imine **36** concentration followed by NMR as a function of time, in presence of 10 mM of octylbenzaldehyde ($C_0 = 10$ mM, pD 9.15).

In that case, the opposite behaviour was observed compared to the addition of octylamine: after a small initial hydrolysis from 10 to 8.6 mM, concentration of **36** decreased very rapidly until reaching quantitative hydrolysis with a half-hydrolysis time of 8.8 h. When octylamine PEG₁₁benzaldehyde imine **36** is hydrolysed, the released octylamine is dissolved in the hydrophobic core, where octylbenzaldehyde is encapsulated. There two competing reactions are taking place at the same time:

- A first one, slow, occurs between octylamine and PEG₁₁benzaldehyde **22** at the interface between the hydrophobic core and the hydrophilic part.
- A second one, much faster, takes place inside the micellar hydrophobic core where both concentrations of octylamine and octylbenzaldehyde are very high.

This latter reaction, by forming a hydrophobic imine inside the micellar core, consumes octylamine and thus shifts the equilibrium toward the quantitative hydrolysis of imine **36**. This phenomenon can easily be seen by comparing two NMRs, one at the beginning of the reaction and the when imine **36** is almost completely hydrolysed after 20 hours (Figure 70).

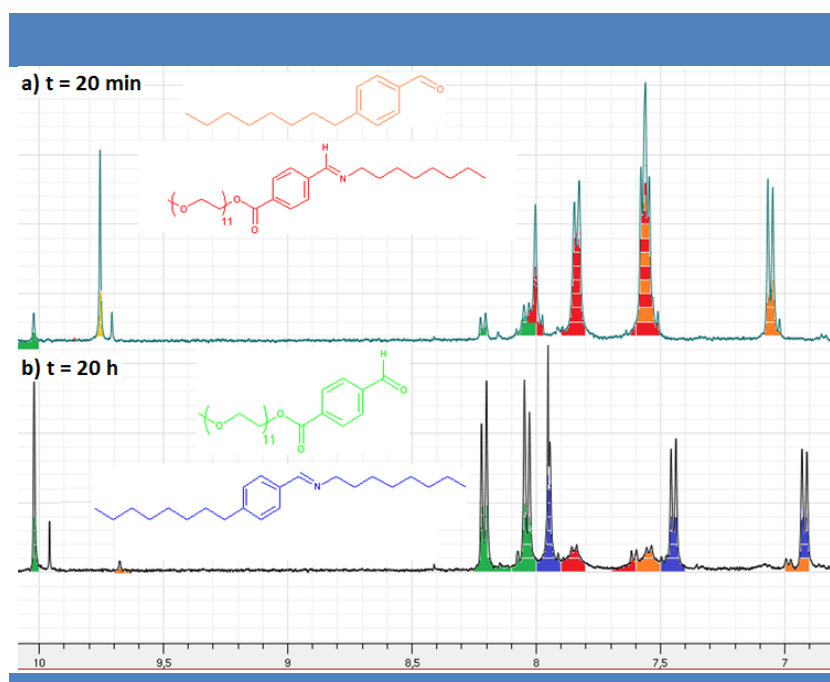


Figure 70 | ^1H NMR of octylamine PEG₁₁benzaldehyde imine **36** as a function of time of hydrolysis in water ($C_0 = 10$ mM, unmodified pD). a) $t = 20$ min. b) $t = 20$ h.

All the kinetic parameters available for the different hydrolysis of octylamine PEG₁₁benzaldehyde imine **36** are summarised in Table 7.

Table 7 | Kinetics parameters (pseudo-zero order) of dynablock **36** for its hydrolysis in water

Concentration Dynablock 36 (mM)	Encapsulated compound	Encapsulated compound Concentration (mM)	pD	k_c (10^{-3} Mm/min)	$H_{1/2}$ (h)
Influence of encapsulated compounds on the kinetics of hydrolysis					
10	None	None	8.82	0.19	78.2
10	<chem>CCCCCCCCN</chem>	10mM	9.16	Not determined	Not determined (weeks)
10	<chem>CCCCCCCCc1ccc(C=O)cc1</chem>	10 mM	9.15	6.4	8.8
Influence of initial concentration on the kinetics of hydrolysis					
5	None	None	8.26	0.57	8.80
10	None	None	8.22	1.53	0.55
25	None	None	8.30	1.00	151
Influence of initial pD on the kinetics of hydrolysis					
10	None	None	8.22	1.53	0.55
10	None	None	8.82	0.19	78.2
10	None	None	10.20	0.25	242
10	None	None	12.36	1.34	63.4

This system, although efficient and tuneable, can only be at pDs above 8, and designing another dynablock was necessary to achieve hydrolytic stability at low pDs (from 3 to 7). For this reason, new imine derivatives (namely oximes), known for their hydrolysis at low pH,^[195] were studied.

c) Hydrolysis of oximes

The first oxime we studied was PEG₁₁ONH₂ 4-octylbenzaldehyde oxime **23**, which is structurally similar to aromatic imine **31** and aliphatic imine **33**. Its hydrolytic stability was first assessed at pD 5.4 and for a concentration of 10 mM, but when no aldehyde was detected after 12 hours, the pD was drastically decreased to 1.4. This change of pH had no impact on the hydrolysis of the oxime, and after 12 hours still no aldehyde was detected. DLS was showing that the oxime was present in solution in a micellar form, with a radius of 5.1 nm (Figure 71).

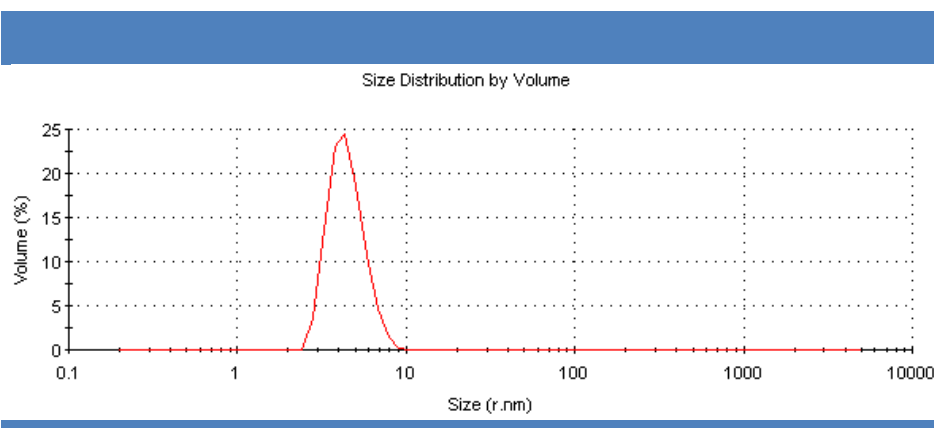


Figure 71 | Hydrodynamic radius distribution of PEG₁₁ oxime **23** determined by DLS in water (C = 10 mM, pD = 1.4).

After this experiment, our goal was to decrease the stability of oxime derivatives. However, this stability is a result of both the oxime linkage and the structure stabilisation provided by the micelle, so an attempt to destabilise the micellar structure by shortening the PEG chain was envisioned. However the hydrolysis of PEG₃ONH₂ 4-octylbenzaldehyde oxime **24** was not easier than that of oxime **23**, with no aldehyde detected by NMR at pD 1.4 for 12 hours at

^[195] Kalia, J.; Raines, R. T., Hydrolytic Stability of Hydrazones and Oximes. *Angew. Chem. Int. Ed.*, **47** (39), 7523-7526 (2008)

10 mM. Additionally, compound **24** revealed to be poorly soluble in water, and a very polydisperse micro-emulsion was detected by DLS. Another attempt to destabilise the micellar structure was performed by condensing PEG₁₁hydroxylamine **13** with 1-(4-formylphenyl)-3-pentylurea **21**, a strategy that worked to destabilise PEG₁₁aromatic imine **31**. In the case of the oxime, this strategy did not work and no hydrolysis occurred at pD 1.4, which suggests that the hydrolytic stability is rather resulting from the oxime linkage than from structure stabilisation. Two last attempts to weaken the oxime linkage were tried by replacing the aromatic benzaldehyde by two aliphatic aldehyde, but neither oxime **26** nor oxime **27** could be hydrolysed, whatever the pD (pD 1.4 and pD 13.4 were tried).

After having seen that oximes were too stable under acidic condition, a new class of imine derivative was studied, semicarbazones, that are known to be less stable in acidic conditions than oximes.^[195]

d) Hydrolysis of semicarbazone 30

PEG₁₁carbamate semicarbazide 4-octylbenzaldehyde semicarbazone **30** was the only semicarbazone studied. Although this class of compound and its derivatives (hydrazones, acylhydrazones) would be interesting to develop encapsulating systems that could release hydrophobic compounds from mixtures under acidic conditions, it was decided to not go deeply into their study, since upon hydrolysis their release hydrazine derivatives, banned from cosmetic applications. The hydrolysis of **30** was performed as a reference for comparison with other imine derivatives. It revealed to be relatively stable under acidic conditions with a V_0 of $1.4 \cdot 10^{-3}$ mM/min and a complex kinetic behaviour (neither pseudo-first order nor pseudo-zero order, which is a sign of complex hydrolytic mechanism or structure stabilisation, Figure 72). At pD 1.84, a rate of hydrolysis similar that obtained with PEG₁₁Aromatic imine **31** at pD 11 was observed.

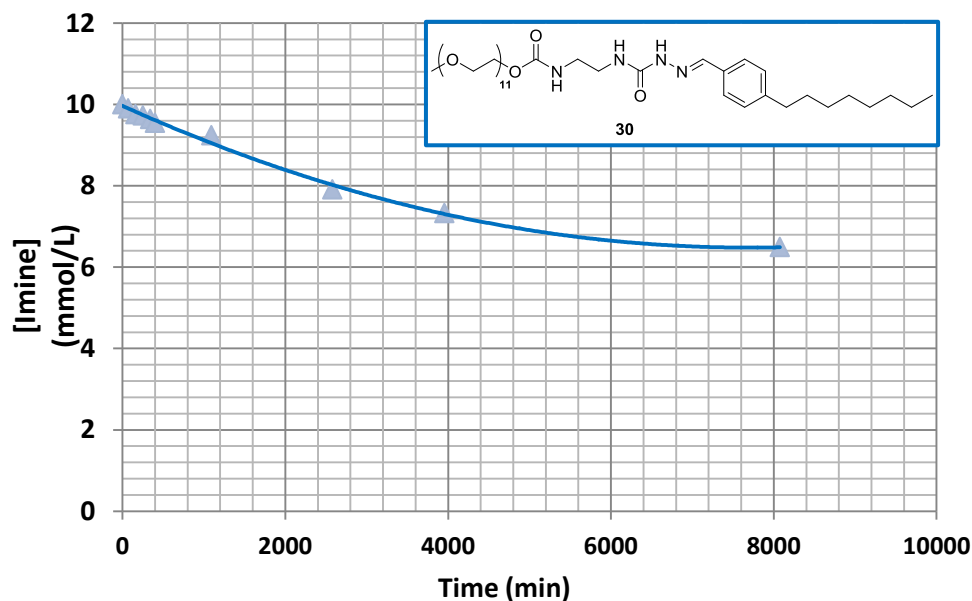


Figure 72 | Concentration of semicarbazone **30** as a function of time ($C_0 = 10$ mM, pD 1.8, $V_0 = 1.4 \cdot 10^{-3}$ mM/min)

e) Hydrolysis of acyloximes

The last class of molecules to be studied were acyloximes. These imine derivatives, depending on the pH, were thought of being hydrolysed according to two different mechanisms:

- Under acidic conditions: reversible hydrolysis of the oxime bond, yielding a hydroxylamine-type molecule and an aldehyde.
- Under basic conditions: hydrolysis of the ester bond, yielding an oxime and an acid.

The main aim of this study was to see if the ester link of acyloximes was stable enough to resist to the hydrolysis of the oxime bond. Unfortunately, carbonate oxime **14b** (Figure 73) was too unstable, and degraded over time at room temperature. As previously mentioned, this compound could not be isolated, since the excess reactant could not be removed by extractions and any attempt of purification through silica gel column chromatography failed for stability reasons. A single hydrolysis experiment on an impure fraction at unmodified pH

gave a half-hydrolysis time of 2.2 days with carbonate oxime **14b** yielding PEG₁₁OH and 4-octylbenzaloxime **28** upon hydrolysis and with no trace of aldehyde. A carbamate oxime, known to be more stable than carbonate oxime,^[196] was also synthesised (compound **15b**), but it was not stable enough to be used as encapsulating system.

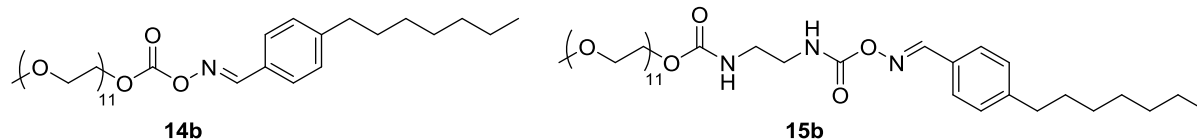
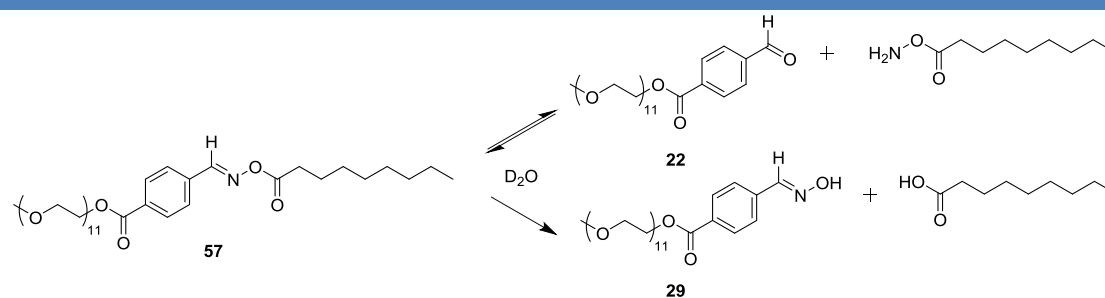


Figure 73 | Chemical structure of carbonate oxime **14b** and carbamate oxime **15b**. Both compounds could not be isolated and were thermosensitive and unstable.

However, compound **57** proved to be much more stable and could be purified by extractions. Its hydrolysis was performed at pD 1.4, to avoid the irreversible ester hydrolysis while favouring oxime hydrolysis. This strategy worked only partially, since both hydrolyses potentially occurred (Scheme 30). After several hours of hydrolysis, a benzaldehyde derivative was detected by NMR, which indicates that the reversible reaction depicted in Scheme 30 possibly happened. However, a more detailed study of this compound should be done, preferably using mass spectroscopy to identify properly all products from the reaction.



Scheme 30 | Chemical structure of carbonate oxime **14b** and carbamate oxime **15b**. Both compounds were not isolated and were both thermosensitive and unstable.

^[196] Bachovchin, D. A.; Wolfe, M. R.; Masuda, K.; Brown, S. J.; Spicer, T. P.; Fernandez-Vega, V.; Chase, P.; Hodder, P. S.; Rosen, H.; Cravatt, B. F., Oxime esters as selective, covalent inhibitors of the serine hydrolase retinoblastoma-binding protein 9 (RBBP9). *Bioorg & Med Chem Letters*, **20** (7), 2254-2258 (2010)

The total concentration of oxime derivatives (**57** + **29**) was plotted over time (Figure 25), showing a very slow hydrolysis. However, we could not determine if the detected benzaldehyde resulted from the hydrolysis of acyloxime **57** or from oxime **29**.

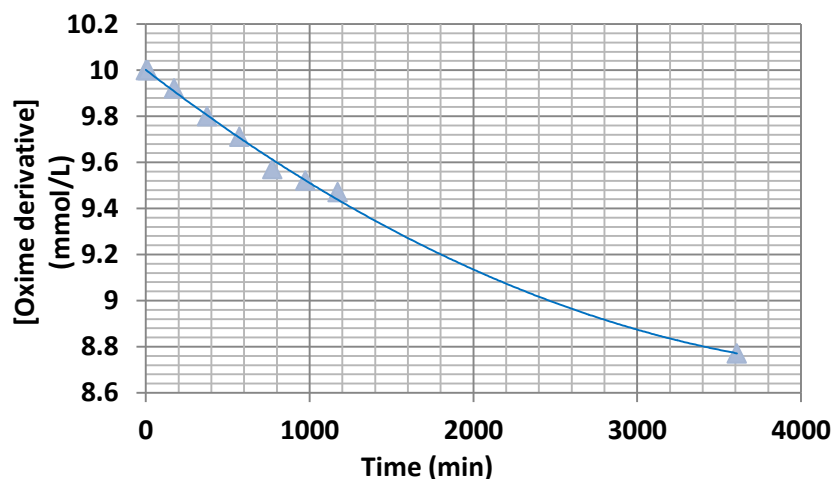


Figure 74 | Total concentration of oxime derivatives (**57** + **29**) as a function of time ($C_0 = 10$ mM, pD 1.4, $V_0 = 4.65 \cdot 10^{-3}$ mM/min)

Acyloximes were not sufficiently stable to perform reversible hydrolysis, but they could easily be envisioned for the future development of oxime releasing systems, notably to release fragrance oximes^[197] or drugs, like milbemycin oxime.^[198]

After the description of the hydrolytic abilities of several families of imine derivatives, I will present in the next part the encapsulating properties of several of these imines.

^[197] Zhukovskaya, N. A.; Dikumar, E. A.; Potkin, V. I.; Vyglazov, O. G., Synthesis and structure-aroama correlation of anisaldehyde oxime esters. *Chem Nat Compd*, **45** (2), 148-151 (2009)

^[198] Xu, X. J.; Lai, S. H.; Ji, M. H.; Zhu, G. N.; Zhao, J. H., Synthesis, Characterization and Insecticidal Activity of Milbemycin Analogues. *Chinese J Org Chem*, **32** (6), 1084-1092 (2012)

2/ Characterisation of micelles and of their encapsulation properties

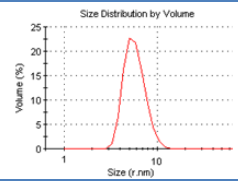
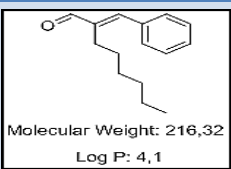
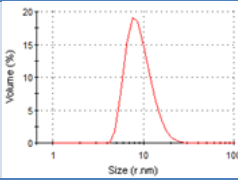
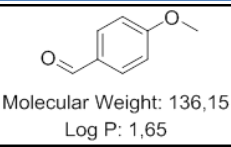
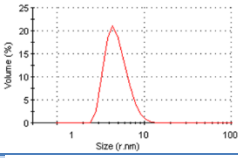
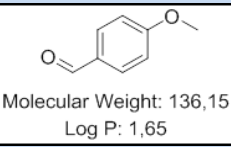
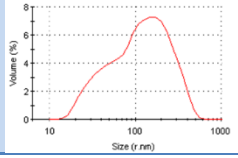
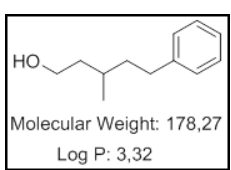
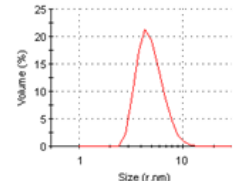
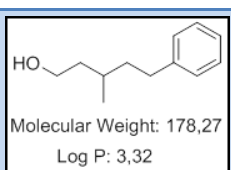
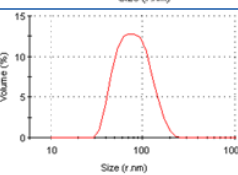
a) Encapsulation followed by DLS

Dynamic light scattering is a convenient technique to characterise the encapsulating properties of the previously developed systems, since it can detect any size modification of the micelles due to encapsulation, or detect the presence of micro-emulsion coming from the presence of hydrophobic molecules in solution.

i) PEG₁₁aromatic imine **31**

The first DLS experiments were performed to assess the encapsulation properties of PEG₁₁aromatic imine **31**. Imine **31** was mixed with several aldehydes (hexylcinnamal, anisaldehyde and 3-methyl-5-phenylpentan-1-ol) at different concentration to check if any micelle size increase can be detected. Aldehydes were chosen to have different hydrophobicity, measured by the logarithm of their octanol/water partition coefficient, LogP. It is expected that molecules with high LogP will be encapsulated, and those with lower LogP not. Results are displayed in Table 8.

Table 8 | Hydrodynamic radius measured by DLS for aromatic imine **31** in the presence of several aldehydes at different concentrations. DLS plots displaying the polydispersity of the system are also shown (LogP values were calculated with chemdraw software)^[186].

Concentration Dynablock 31 (mM)	Encapsulated Fragrance	Fragrance Concentration (mM)	Radius (nm)	Plot
10	None	None	6.3	
10	 Molecular Weight: 216,32 Log P: 4,1	10mM	7.0	
10	 Molecular Weight: 136,15 Log P: 1,65	15 mM	6.2	
10	 Molecular Weight: 136,15 Log P: 1,65	35 mM	142	
10	 Molecular Weight: 178,27 Log P: 3,32	10 mM	6.3	
10	 Molecular Weight: 178,27 Log P: 3,32	25 mM	90.1	

Two main results can be extracted from this table:

- The system encapsulates only molecules that are hydrophobic enough, as shown by the increase of the micelle size from 6.3 to 7 nm in the presence of hexylcinnamal (LogP 4.1). When the more hydrophilic 3-methyl-5-phenylpentan-1-ol was added (LogP 3.32), no size increase occurred with a concentration of 10 mM.
- The concentration of fragrance to be encapsulated greatly affects the size of the aggregates. When the concentration of fragrance was more than 2.5 the concentration of imine, a stabilised micro-emulsion was formed. This micro-emulsion, which could

easily be seen with the naked eyes (milky solution), was very polydisperse and stabilised by the presence of amphiphilic imines. Phase separation only occurred after several weeks.

ii) PEG₁₁Amide imine **34**

A second system constituted of PEG₁₁amide imine **34** at 10 mM in the presence of 10 mM of hexylcinnamal was studied. The size of the particles detected by DLS was followed over time, and compared to PEG₁₁amide imine **34** alone in solution at 10 mM (Figure 75).

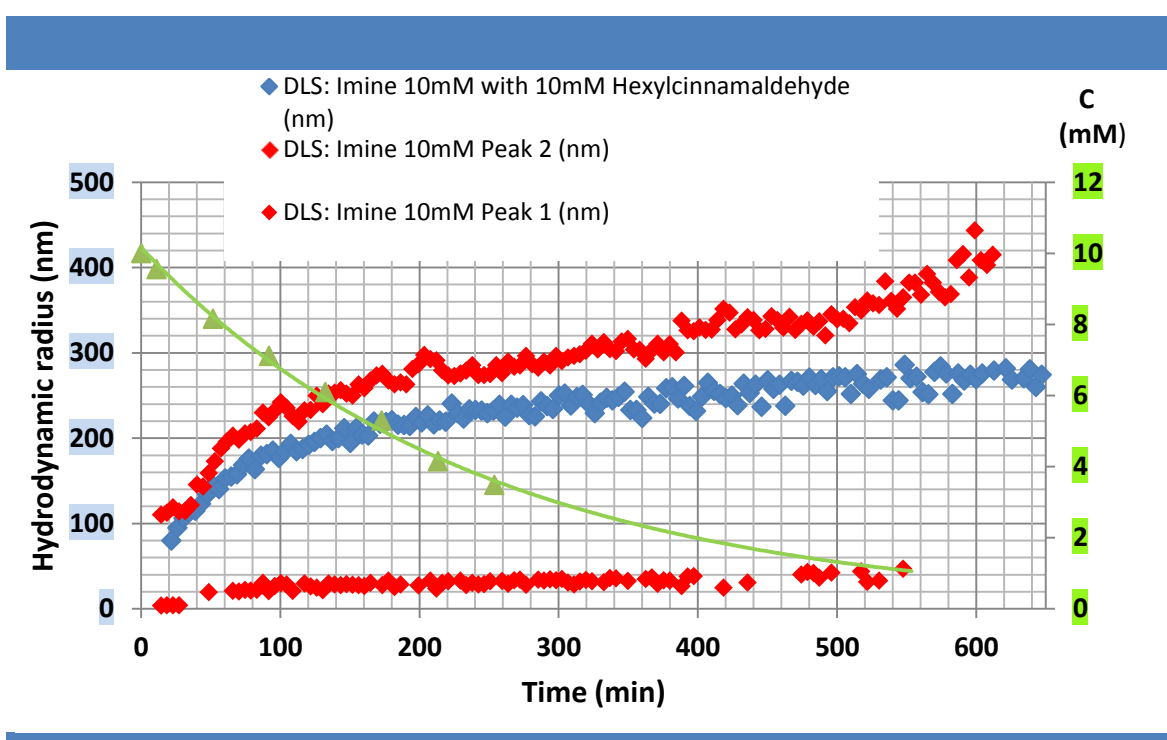


Figure 75 | Evolution of concentration and hydrodynamic radius of PEG₁₁Amide imine **34** as a function of time followed by DLS during its hydrolysis in deuterium oxide. **In red:** DLS of **34** (C₀ = 10 mM), unmodified pD. **In blue:** DLS of **34** (C₀ = 10 mM), hexylcinnamal (10 mM), unmodified pD. **In green:** Concentration of **34** followed by NMR (C₀ = 10 mM), unmodified pD.

Surprisingly, two populations exist in solution when PEG₁₁amide imine **34** is dissolved in deuterium oxide at 10 mM. The presence of micelles was expected due to the similarity of the structure of this imine with aromatic imine **31**, but the presence of a micro-emulsion of more than 100 nm was surprising. This flocculation of micelles is possibly enhanced by the presence of hydrogen bonding between the PEG chains, favouring the aggregation of these

imines, or at least of the hydrolysed PEG amines. The addition of hydrophobic hexylcinnamal at a concentration of 10 mM led to the disappearance of the micellar structure, but not to an emulsion with larger droplets: upon addition of hexylcinnamal, the hydrodynamic radius drops from 110 to 80 nm at the beginning of the hydrolysis.

This result tends to show that great care must be taken when choosing the quantity of hydrophobic compound to incorporate inside the micellar core, since a drastic change of the morphology of the system can occur, with a transition of structure from micelles to a micro-emulsion.

b) Encapsulation followed by DOSY NMR

Investigations on the structure of the dynablocks were then continued with their study by DOSY NMR, since this characterisation technique enables a clear distinction between encapsulated and non-encapsulated compounds. In the case of a hydrophobic compound encapsulated inside the core of the micelle, both the encapsulated compound and the micelle should have the same diffusion coefficient, and thus the same hydrodynamic radius. A typical measurement performed by DOSY NMR is displayed in Figure 76. In this experiment, PEG₁₁aromatic imine **31** at a concentration of 50 mM is mixed with 35 mM of hex-3-en-1-ol. It can easily be seen that hex-3-en-1-ol is not encapsulated (hydrodynamic radius of 0.35 nm), conversely to the released 4-octylbenzaldehyde that stays within the micelle (hydrodynamic radius of 9.65 nm, the same as for imine **31**).

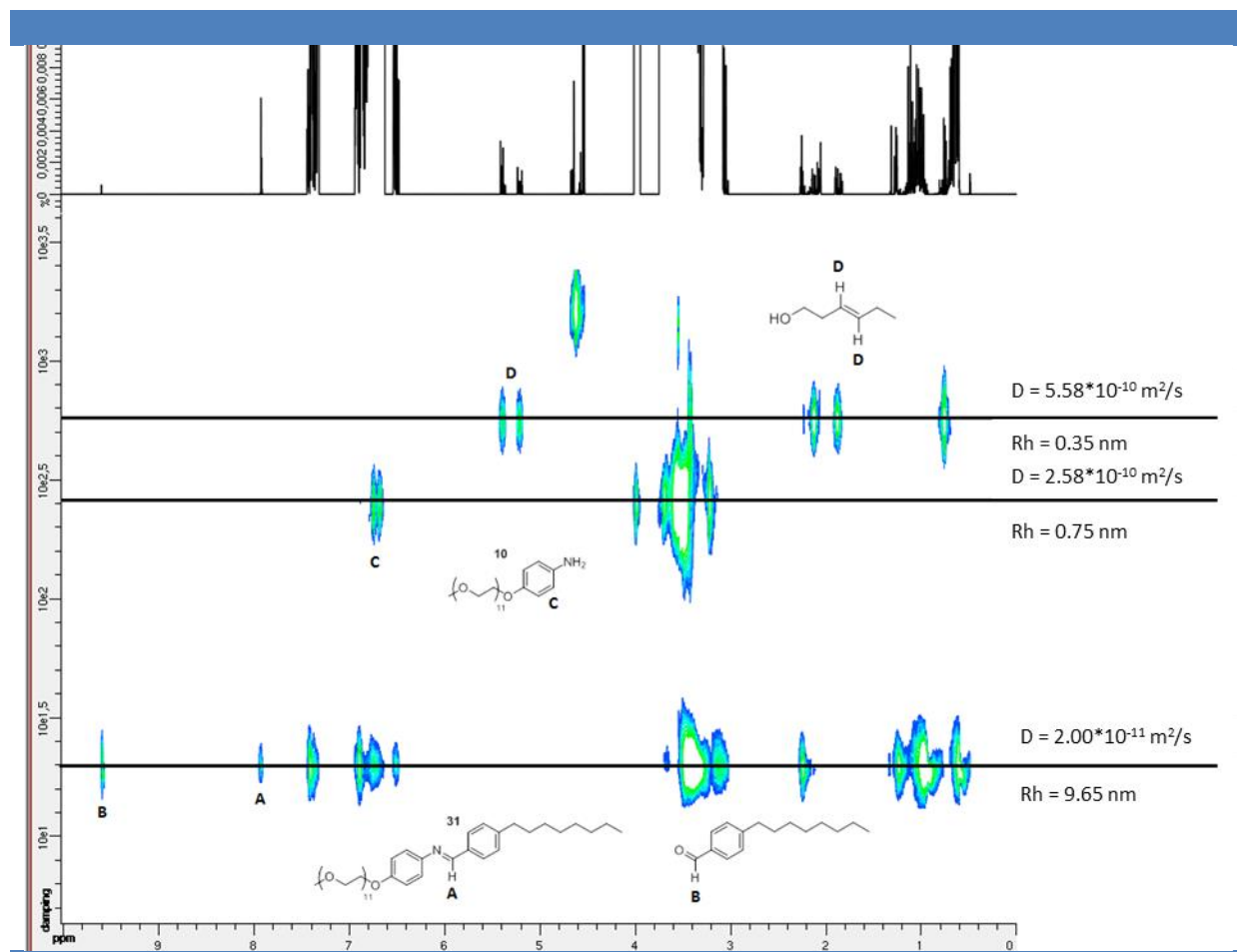
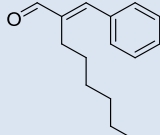
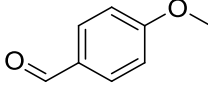
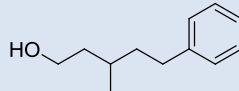
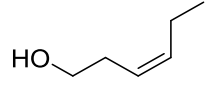


Figure 76 | DOSY NMR spectra of PEG₁₁Aromatic imine **31** 50 mM + hex-3-en-1-ol 35 mM in solution in deuterium oxide (t = 2 d).

A direct comparison between the results obtained by DLS and that obtained by DOSY can be found in Table 9. For all these encapsulation experiments performed by DLS or DOSY, pD was kept around 13 to avoid the effect of the hydrolysis on the size of the aggregates.

Table 9 | Hydrodynamic radius of aggregates obtained from dynablock **31**/fragrance mixtures measured by DLS and DOSY NMR. “I” corresponds to the imine, “V” to the volatile fragrance.

Exp.	Molecules		Conditions		Encapsulation?		Aggregate
	Imine (I)	Volatile (V)	C (mM)	pD	Hydrodynamic radius (nm)	Diffusion Coefficient ($\mu\text{m}^2/\text{s}$)	Molecules in solution
1	31	 LogP = 4.10	I: 10 V: 10	13.6	DLS : 6.9 nm DOSY : 7.45 nm 0.63 nm Yes	DOSY 25.9 306	I + V 11
2	31	 LogP = 1.65	I: 10 V: 10	13.2	DLS : 6.2 nm DOSY : 6.11 nm 0.68 nm 0.32 nm No	DOSY 31.6 6.09 6.31	I 11 V
3	31	 LogP = 3.32	I: 10 V: 30	13.3	DLS : 6.3 nm DOSY : 198 nm 7.55 nm 1.45 nm 0.65 nm No	DOSY 0.975 25.6 1.41 2.82	V I V 11
4	31	 LogP = 1.48	I: 50 V: 35	12.5	DOSY : 9.65 nm 0.75 nm 0.35 nm No	DOSY 20.0 258 558	I 11 V

It can be observed that the hydrodynamic radius obtained by DLS and DOSY NMR are very close, and that in all cases the growth of micelles detected by DLS are indeed corresponding to encapsulation phenomena as proved by DOSY NMR. The combination of these two techniques indicates that to be encapsulated, a hydrophobic compound has to be sufficiently hydrophobic, *i.e.* with a LogP above 3.3.

c) TEM

As said previously, when too many hydrophobic compounds are added to an imine solution, or when the hydrolysis is already well advanced, a micro-emulsion is forming, leading to a

macroscopic phase separation. This behaviour was even emphasised by the presence of hydrogen bonds between the hydrophilic blocks, like in the case of PEG₁₁amide imine **34**. To have an idea about what this emulsion looks like, TEM pictures of a solution of **34** were taken after one week of hydrolysis, when the concentration of imine is far below 1 mM (Figure 77).

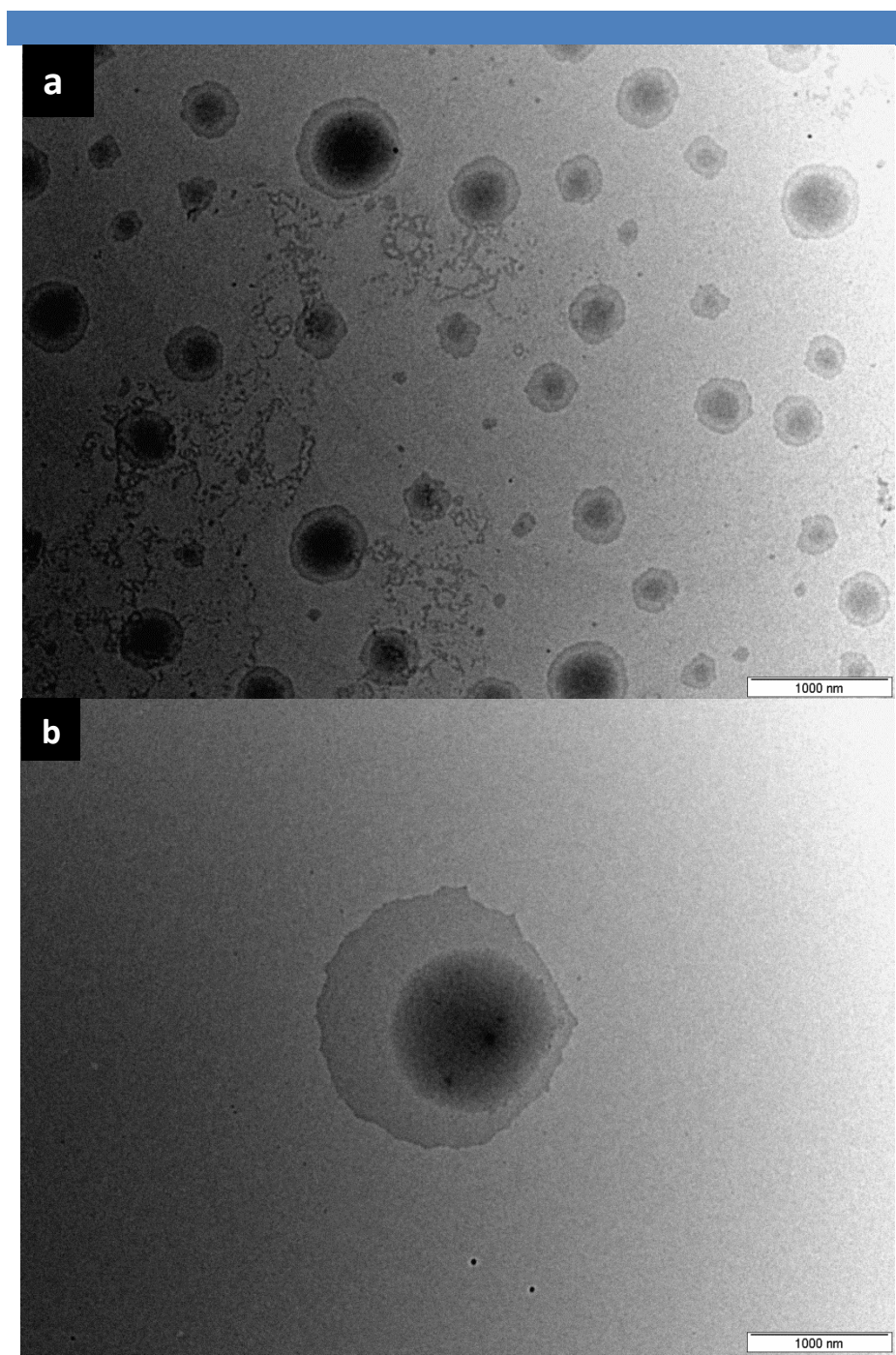


Figure 77 | TEM pictures of the emulsion of PEG₁₁Amide imine **34** after one week of hydrolysis (near complete hydrolysis).

The TEM pictures show the formation of spherical aggregates with a maximal size of 1 μm . On Figure 77b, aggregates constituted of 2 distinct parts can be seen. The very dark part could consist of the hydrophobic octylbenzaldehyde that is largely present in the emulsion, and the more transparent one could be composed from aggregated PEGamide amine **19**, but also of imines that are present outside the emulsion, and that stabilise it.

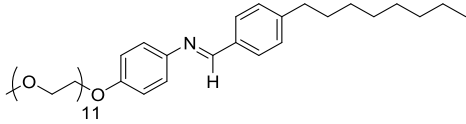
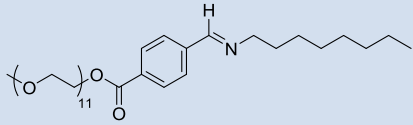
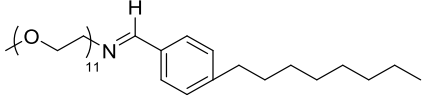
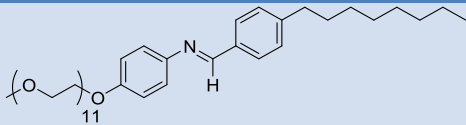
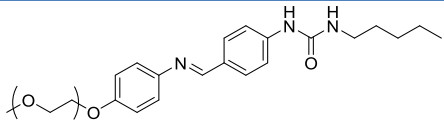
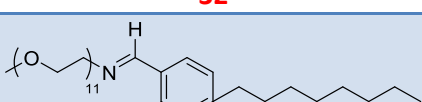
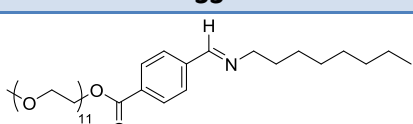
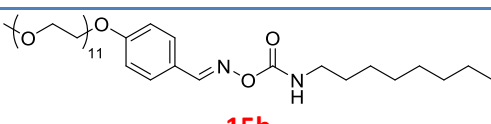
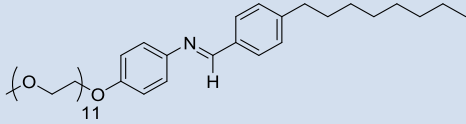
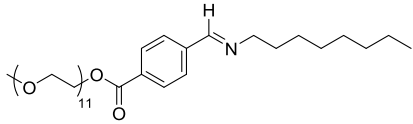
3/ Conclusion

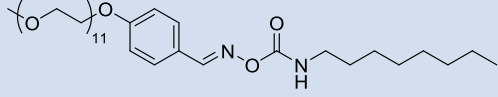
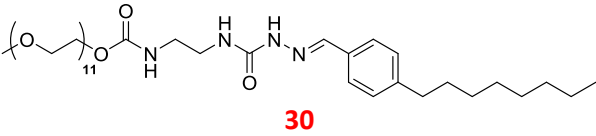
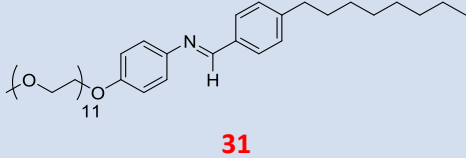
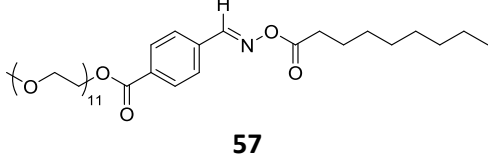
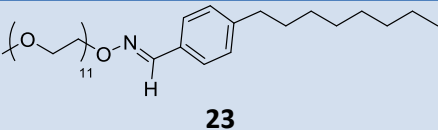
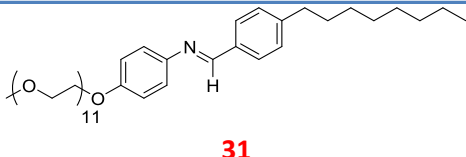
The kinetics of hydrolysis of imine derivatives of several types (aliphatic and aromatic imines, oximes, semicarbazone and acyloximes) have been measured and compared. The ability of these systems to encapsulate volatile hydrophobic compounds has been assessed for two key imines **31** and **34**, and DLS and DOSY NMR measurements proved that volatiles can be encapsulated inside the micelles if they are hydrophobic enough ($\text{LogP} > 3.3$). All tested imines were able to form stabilised micro-emulsion with aldehydes, possibly leading to a slower release of the volatiles into the air, even for the more hydrophilic fragrances. The different families of imines exhibited different kinetics of hydrolysis, but some general observations can be made:

- Decreasing the pD at initial time was always increasing the speed of hydrolysis, except for acyloximes which were hydrolysed through another mechanism (mainly hydrolysis of the ester bond).
- Increasing the concentration was (usually) leading to a longer half-hydrolysis time and a faster initial rate of hydrolysis.
- The presence of hydrogen bonding units on the hydrophilic or the hydrophilic block can efficiently destabilise the micellar structure and lead to faster hydrolysis.
- Any process that will affect the equilibrium constant (phase separation of a reactant from the reacting medium, addition of encapsulated reacting molecules...) can potentially impacts the kinetics of hydrolysis.

From an application point of view, it is possible to choose between several releasing systems according to the desired half-hydrolysis time and the pH of the application. A list of the molecules performing the best according to pD and expected hydrolysis time scale is available in Table 10.

Table 10 | Guide to choose the dynablock-based encapsulating system according to the expected half-hydrolysis time. The pD proposed corresponds to an initial concentration of imine at 10 mM. A red color indicates an unsuitable imine for cosmetic applications (for toxicity or stability reasons).

Half-Hydrolysis time scale	Domain of pD	Imines
Minutes	5.5 < pD < 7	 <p>31</p>
	pD = 7.5	 <p>36</p>
	pD < 8	 <p>33</p>
Hours	7 < pD < 8.7	 <p>31</p>
	8 < pD < 10.5	 <p>32</p>
	8 < pD < 12.5	 <p>33</p>
	pD = 8.5	 <p>36</p>
	pD > 13	 <p>15b</p>
Days	8,7 < pD < 10.5	 <p>31</p>
	9 < pD < 11	 <p>36</p>

	9.5 < pD < 13	 <p style="text-align: center;">15b</p>
Weeks	pD < 2	 <p style="text-align: center;">30</p>
	10 < pD < 11.5	 <p style="text-align: center;">31</p>
	pD < 2	 <p style="text-align: center;">57</p>
Months or even more	pD < 1	 <p style="text-align: center;">23</p>
	11.5 < pD < 13.5	 <p style="text-align: center;">31</p>

In the next chapter, we will use the knowledge established in this chapter to develop new aliphatic amine-based profragrances that can slowly hydrolyse to release hydrophobic fragrance aldehydes into their environment. These systems were evaluated both alone in solution and in the presence of other co-surfactants, like in application formulations.

Chapter 4: Study of dynamic profragrances and their kinetics of hydrolysis

After having studied the kinetics of hydrolysis of dynablocks with various imine-type linkers for encapsulation applications, we focused on the development of new amphiphilic profragrances that could be easily incorporated into already marketed applications. We chose to develop these profragrances with an imine bond made from the condensation of a hydrophilic aliphatic amine with fragrance aldehydes (that are usually hydrophobic). Imines made from aliphatic amines, although not the most stable kind of imine-type derivative, present the advantage to be compatible with cosmetic applications and can nevertheless have slow kinetics of hydrolysis in water (see chapter 3). One important parameter to stabilise the imine bond in solution is the presence of a hydrophobic linker between the hydrophilic PEG chain and the imine bond, thus enabling its partial dissolution in the hydrophobic core of the micelle, and therefore avoiding contact with water. This strategy, that proved to be efficient for octylamine PEG₁₁benzaldehyde imine **36**, was extended in this work to other types of hydrophobic linkers, notably poly(propylene glycol) and tyramine linkers (Figure 78A to see the amines that were used for dynamique profragrances). The new PEG₁₁Tyramine amine **9** was synthesised to combine the hydrophobic character of aromatic and benzylic amines to the low toxicity of aliphatic amines. The hydrophobic block of the profragrances consists of the volatile organic molecule that has to be released, so the aldehydes were chosen to have different hydrophobicities and to be industrially widely used (Figure 78B). The first objective of this work was to develop several profragrances that can efficiently release fragrance aldehydes in a water-based solution with a half-time of hydrolysis of around one day, and this for the largest possible pH range. The second goal was to keep the same level of performance in industrial formulations. Profragrances can be used in either one or two-component systems:

- One-component system: If the imine is stable enough in solution at a given pH, it can be incorporated inside a formulation during its manufacturing. A trigger (pH or concentration change) is then needed for the release of aldehydes.
- Two-component system: If the imine is not stable enough in solution, it needs to be incorporated inside the formulation at the moment the customer utilises the product. The hydrolysis of the imine will then start at this moment with known kinetics.

Since we have decided to choose the applications of the profragrances according to their properties, no system in particular (one- or two-component) has been targeted.

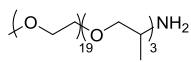
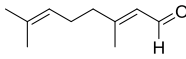
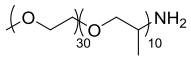
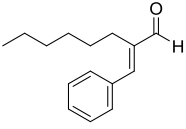
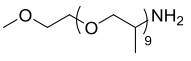
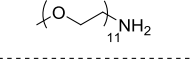
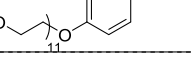
A)		B)	
Name	Name	Aldehyde	Name
	Jeffamine M1000		Citral
	Jeffamine M2070		Hexylcinnamal
	Jeffamine M600		
	PEG ₁₁ Amine 11		
	PEG ₁₁ Tyramine 9		

Figure 78 | Hydrophilic and hydrophobic blocks used for the synthesis of the profragrances. A) Amines used to synthesise profragrances. It can be noted that Jeffamine M2070 is a PEG-PPG statistical copolymer, and that Jeffamine M600 is a hydrophobic amine (non-water soluble). B) Fragrance aldehydes used to synthesise profragrances.

This chapter will be divided into several parts, starting from the study of the kinetics of hydrolysis of profragrances, first with hexylcinnamal-based systems and then with the citral derivatives. Then, non-amphiphilic imines will be studied, followed by the determination of the influence of the hydrophobic chain length on the kinetics of hydrolysis. Finally, profragrances will be incorporated into formulations and the influence of several parameters such as the presence of co-surfactants will be investigated.

1/ Hydrolysis of amphiphilic hexylcinnamal-based profragrances

a) Hydrolysis at 10 mM

First, hydrolyses of hexylcinnamal-based profragrances were investigated at 10 mM, a typical concentration for such systems which corresponds to a mass concentration of approximately 1 percent for most dynablocks (10 mM \approx 1WT%). A direct comparison of M1000 hexylcinnamal imine **47**, PEG₁₁amine hexylcinnamal imine **51** and PEG₁₁tyramine hexylcinnamal imine **53** is displayed in Figure 79.

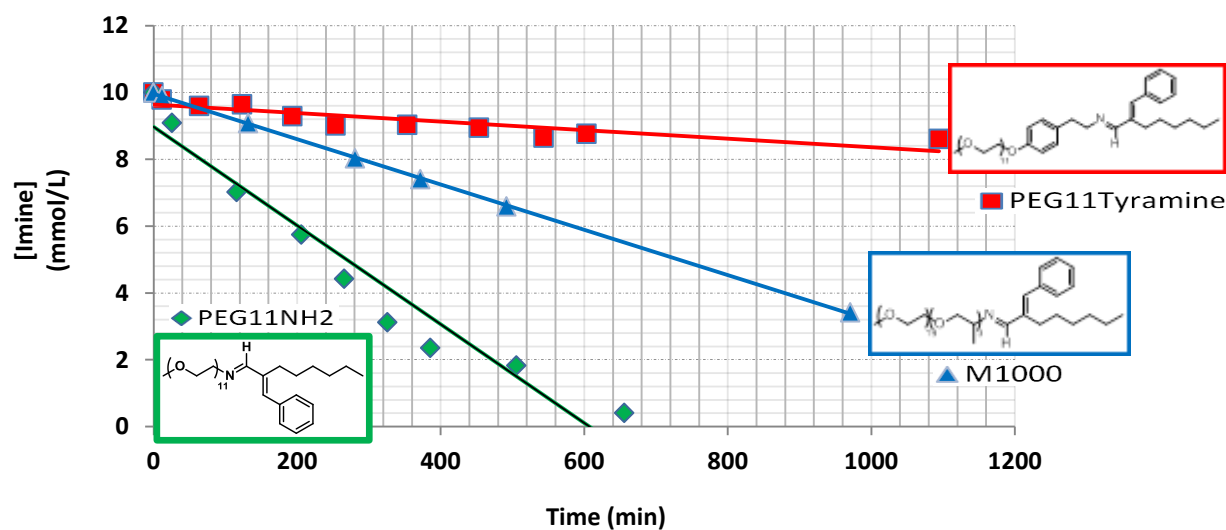


Figure 79 | Evolution of the concentration of M1000 hexylcinnamal imine **47**, PEG₁₁NH₂ hexylcinnamal imine **51** and PEG₁₁Tyramine hexylcinnamal imine **53** concentration as a function of time at 10 mM for an unmodified pD (10.1 < pD < 10.5).

The kinetics of hydrolysis of these three imines is significantly different, even if all of them seem to have, for an initial concentration of 10 mM, a relatively linear relationship of imine concentration against time. PEG₁₁amine hexylcinnamal imine **51** is unsurprisingly the fastest imine to be hydrolysed, with a half-time of hydrolysis of 4.5 hours, and has a performance very similar to that obtained with PEG₁₁amine octylbenzaldehyde **33** (see chapter 3). M1000 hexylcinnamal imine **47**, with its moderately hydrophobic PPG₃ linker, already performs much better with a H_{1/2} of 12 hours, which starts to be an interesting release time for applications. Finally, PEG₁₁tyramine hexylcinnamal imine **53**, with its more hydrophobic tyramine linker, exhibited the highest resistance to hydrolysis with an estimated H_{1/2} of about 2.5 days. M2070 hexylcinnamal imine **49** had the same rate of hydrolysis as M1000 hexylcinnamal imine **47**. This high resistance to hydrolysis can be explained by two phenomena:

- The presence of the linker creates a hydrophobic environment around the imine link, thus preventing water from approaching, and ultimately leading to a local decrease of

the concentration of water around the imine that shifts the equilibrium toward imine formation.

- The presence of the hydrophobic linker decreases the CMC of the amphiphile, and thus decreases the concentration of free easily-hydrolysed dynablock unimers in solution.

Kinetic data is summarized in Table 11.

Table 11 | Kinetic parameters (Initial rate of hydrolysis and half-time of hydrolysis) of dynablocks **47**, **51** and **53** in deuterium oxide at 10 mM (unmodified pD).

Imine	C (mM)	pD (Unmodified)	V ₀ (10 ⁻³ mM/min)	H _{1/2} (days)
M1000 hexylcinnamal 47	10	10.5	6.8	0.51
PEG ₁₁ NH ₂ hexylcinnamal 51	10	10.5	14.8	0.19
PEG ₁₁ Tyramine hexylcinnamal 53	10	10.1	1.3	2.48

In Chapter 3, we have shown that when all dynablocks are dissolved in deuterium oxide, they form micellar structures which then evolved toward a micro-emulsion as hydrolysis proceeded. However, the new M1000 hexylcinnamal imine **47** possess a different chemical structure than the formerly studied dynablocks (longer PEG chain, PPG₃ linker), and could exhibit a different behaviour in solution. To verify this hypothesis, the hydrolysis of **47** was followed by DLS (Figure 80, concentration starting at 10 mM and reaching 6 mM after 10 hours). Two peaks were detected by DLS:

- One corresponding to a micelle, with a radius starting at 12 nm and reaching a maximum at 14.5 nm between 200 and 300 min, which then decreases slowly to 12 nm.
- One corresponding to a micro-emulsion, probably emerging from micellar aggregation. Even if this peak could be detected before 300 min, the inconsistency of its detected size evidences its presence only in very low quantity. After 300 min, it grows over time until phase separation occurs after several weeks.

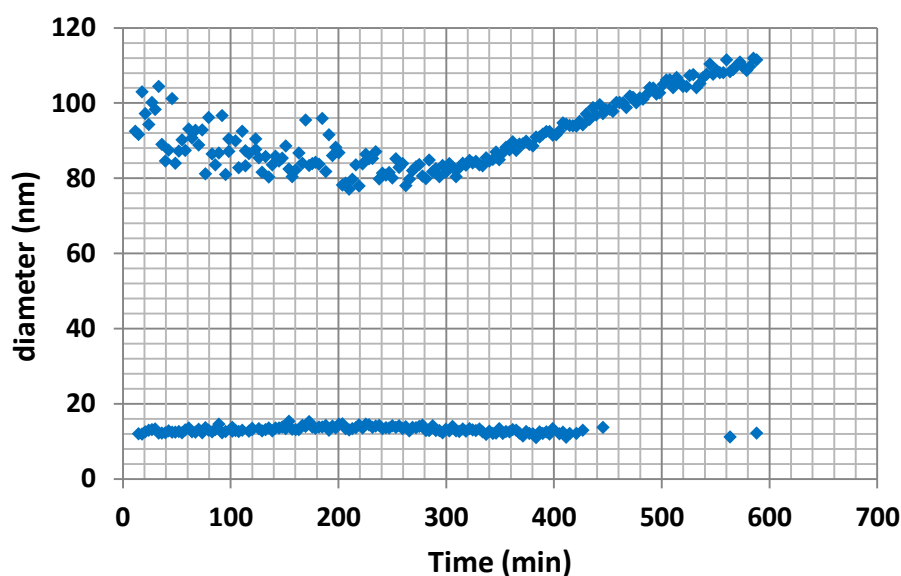


Figure 80 | Hydrodynamic radius of M1000 hexylcinnamal imine **47** as a function of time followed by DLS during its hydrolysis in deuterium oxide ($C_0 = 10$ mM, unmodified pD 10.4).

The fact that the micelle's size decrease at the moment the micro-emulsion starts to grow is a sign that a possible transfer of hydrophobic material from the micellar core to the micro-emulsion is taking place, probably through the fusion of micelles overcharged of hydrophobic material with the emulsion. DOSY NMR confirms the presence of encapsulated hexylcinnamal inside the micelle's core (hydrodynamic diameter of micelles: 11.0 nm). Although the analysis of the SANS data is currently under investigation, some preliminary information can be extracted from the curves. The behaviour of M1000 hexylcinnamal imine **47** in deuterium oxide (Figure 81) is characterized by the following sequence: (i) a Guinier regime in the low- q range, associated with the finite size of the supramolecular self-assemblies; (ii) one intermediate regime, in which the q -dependence of the scattered intensity can be described by a power law with an exponent close to -4; (iii) and a q^{-1} -regime in the high- q range. The data obtained at low- q can be fitted by a Guinier expression ($\ln(I(q)) = \ln(I(0)) - (1/2)R_g^2 q^2$) giving the radius of gyration (Figure 82): $R_g = 18.8$ Å, which is a typical value for this kind of dynablock.^[113] The q^{-4} regime is the signature of a three-dimensional object with a relatively smooth surface, probably a spherical micelle. At very large q , the q dependence of the SANS scattered intensity can be described by a power law with an

exponent close to 1 characteristic of the rod-like behaviour of the polymer chains (i.e., free blocks and blocks within the micellar structures).^[112]

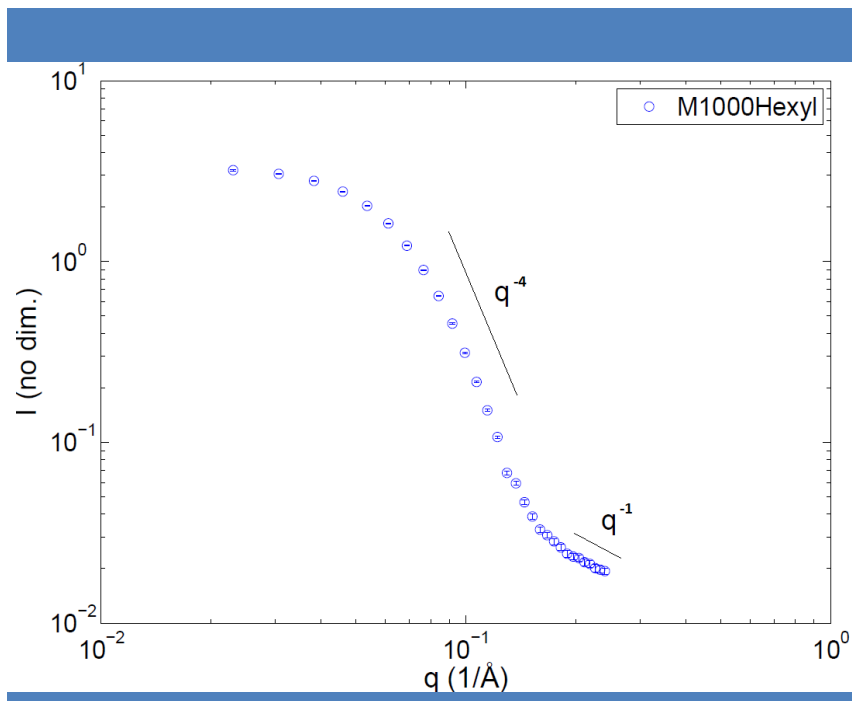


Figure 81 | SANS scattering pattern of M1000 hexylcinnamal imine 47.

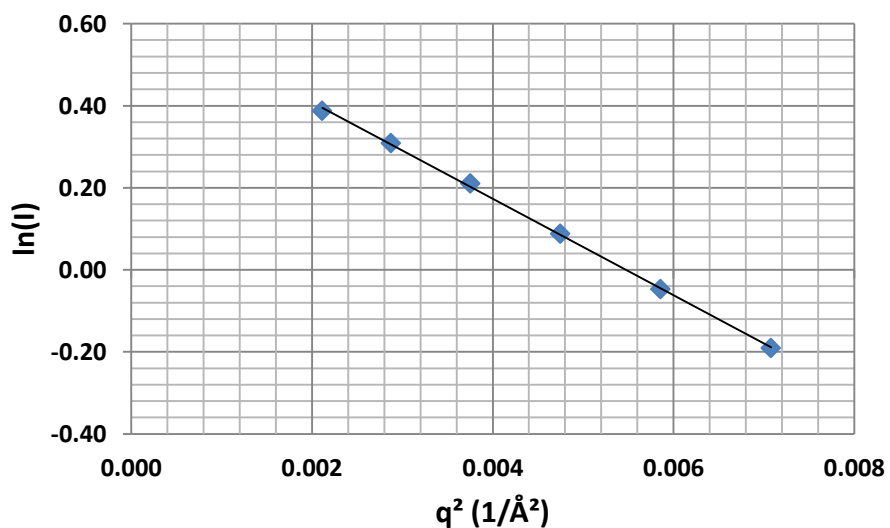


Figure 82 | Guinier plot of M1000 hexylcinnamal imine 47 at low q.

b) Influence of concentration

After having studied the kinetics of hydrolysis of the hexylcinnamal-based profragrances at 10 mM, the effect of the initial concentration on the half-time of hydrolysis was investigated for imines made of M1000, M2070 and PEG₁₁NH₂ (Figure 83). The influence of the initial concentration on PEG₁₁tyramine hexylcinnamal imine **53** was not studied, since the compound is already sufficiently stable in solution at 10 mM, and its half-time of hydrolysis at higher concentration could reach several weeks.

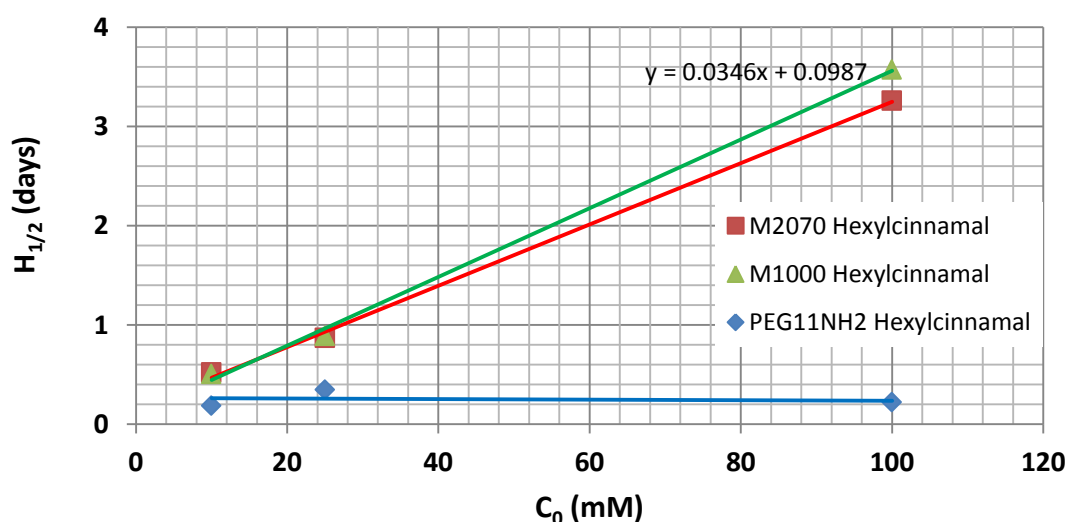


Figure 83 | Influence of concentration on the half-time of hydrolysis of M1000 hexylcinnamal imine **47**, M2070 hexylcinnamal imine **49** and PEG₁₁NH₂ hexylcinnamal imine **51** at unmodified pD (10.5 < pD < 11.3).

The half-time of hydrolysis of PEG₁₁NH₂ hexylcinnamal imine **51** is around 5 hours at all concentrations, which is consistent with a pseudo-first order kinetic due to a very weak stabilization of the imine bond by the micellar structure (Figure 84 for the hydrolysis of **51** at 25 and 100 mM with time). M1000 hexylcinnamal imine **47** and M2070 hexylcinnamal imine **49**, which form more stabilised imines in solution thanks to hydrophobic linkers between the PEG chain and the imine moiety, display an apparent linear relationship between their half-

time of hydrolysis and their initial concentration, a feature usually attributed to pseudo-zero order kinetic. This result has two implications:

- It is possible to slow down the release of volatile aldehyde by increasing the initial concentration of M1000 and M2070-based profragrances. This enables to tune the hydrolysis time and thus the release of the fragrances by modifying the initial concentration.
- It is possible to considerably increase the speed of hydrolysis by diluting the system. This feature can be useful to store profragrances in concentrated solution after manufacturing, and to complete the hydrolysis by dilution while using the product by the end-users.

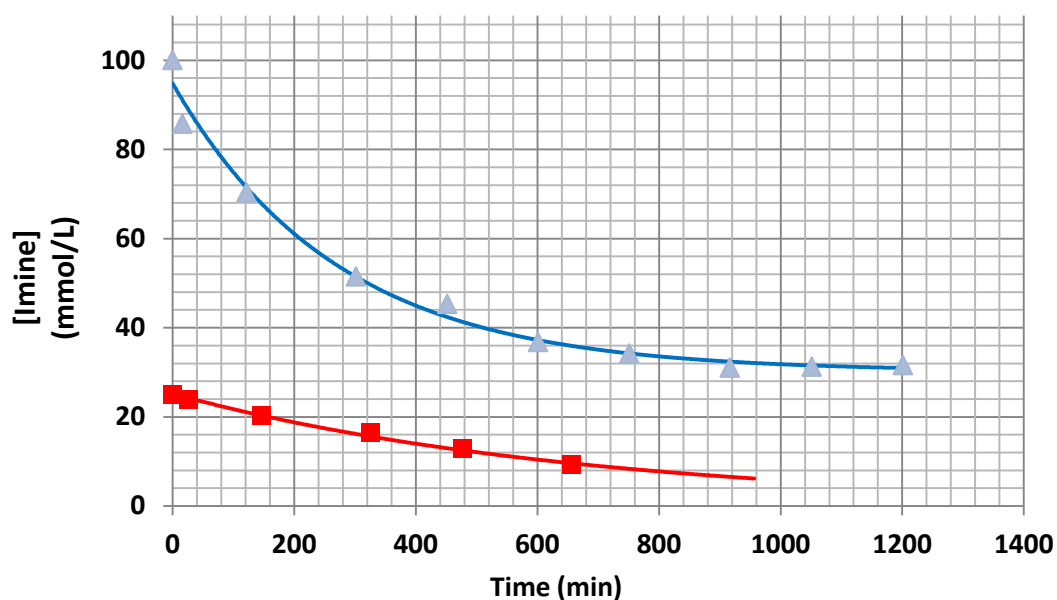


Figure 84 | Concentration of PEG₁₁NH₂ hexylcinnamal imine **51** as a function of time at C₀ = 25 and 100 mM and at unmodified pD (10.4)

Kinetic data are summarised in Table 12.

Table 12 | Kinetic parameters (Initial rate of hydrolysis and half-time of hydrolysis) of dynablocks **47**, **51** and **53** in deuterium oxide at different initial concentrations (unmodified pD).

Imine	C (mM)	pD (Unmodified)	V ₀ (10 ⁻³ mM/min)	H _{1/2} (days)
M1000 hexylcinnamal 47	10	10.5	6.8	0.50
M1000 hexylcinnamal 47	25	10.6	9.7	0.90
M1000 hexylcinnamal 47	50	10.7	8.0	2.36
M1000 hexylcinnamal 47	100	11.1	9.3	3.60
M1000 hexylcinnamal 47	500	11.2	36.1	5.00
PEG ₁₁ NH ₂ hexylcinnamal 51	10	10.5	14.8	0.19
PEG ₁₁ NH ₂ hexylcinnamal 51	25	10.5	23.7	0.35
PEG ₁₁ NH ₂ hexylcinnamal 51	100	10.4	856	0.22
M2070 hexylcinnamal 49	10	10.7	6.3	0.52
M2070 hexylcinnamal 49	25	9.8	9.5	0.87
M2070 hexylcinnamal 49	100	9.4	9.9	3.26

c) Influence of pH

An important piece of information that is still needed before incorporating our profragrances into industrial formulations is the effect of pD on the kinetics of hydrolysis. Modifications of pD can be performed by two methods:

- Addition of an acid or a base at the beginning of the experiment. The initial pH can be measured and will slowly increase while hydrolysis proceeds (usually until it reaches the pD it had before the addition of a base or an acid).
- Addition of the profragrance into a buffer solution, which will guarantee a constant pD during the reaction.

This latter method was used to investigate the kinetics of hydrolysis of M1000 hexylcinnamal imine **47** (Figure 85A) and PEG₁₁tyramine hexylcinnamal imine **53** (Figure 85B) under slightly acidic conditions (HEPES Buffer, pD 6,6). M2070 hexylcinnamal imine **49** was not studied since its kinetics of hydrolysis proved to be very close to that obtained for imine **47**. PEG₁₁NH₂ hexylcinnamal imine **51** was not studied either because its hydrolysis is already very fast at unmodified pD.

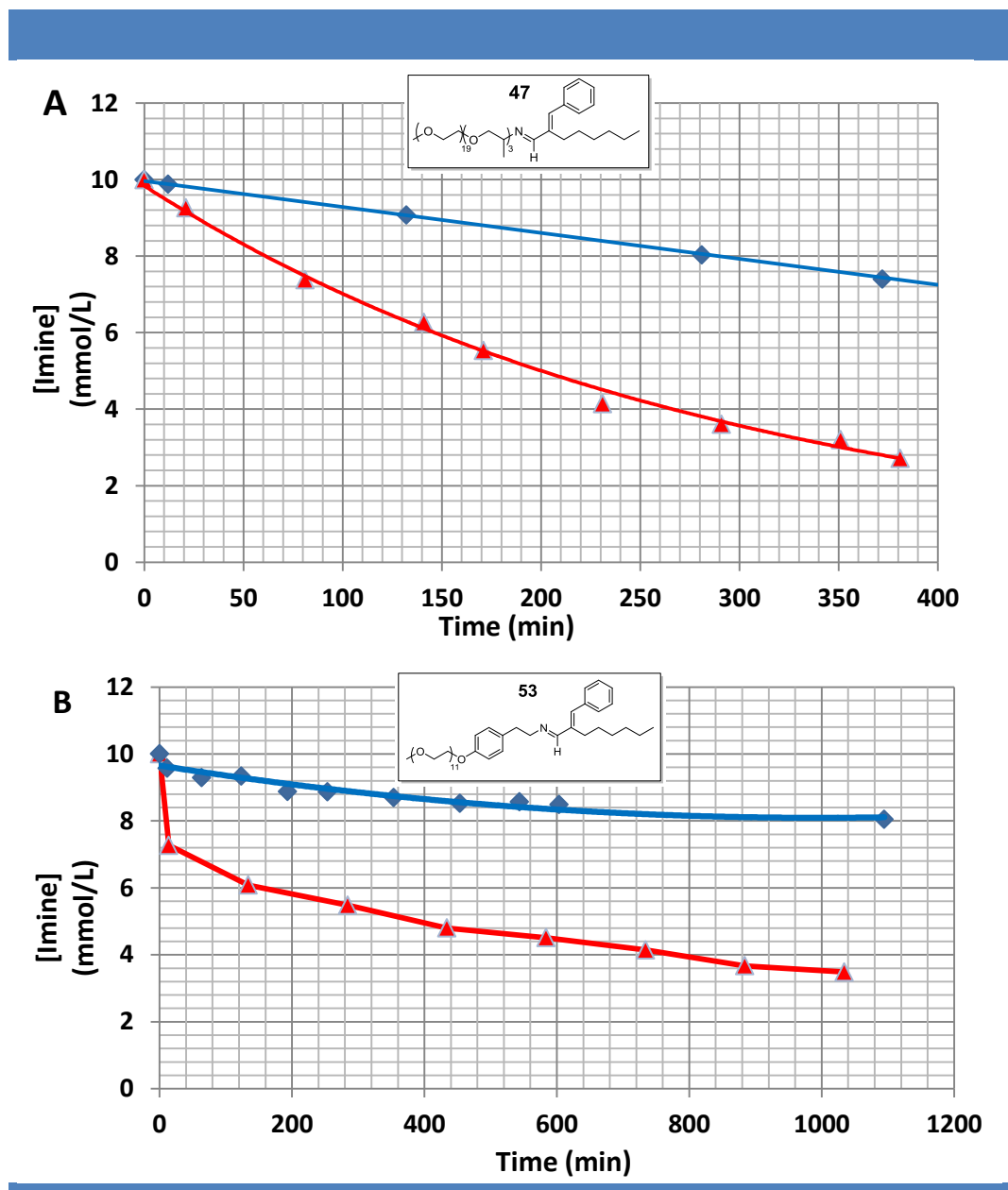


Figure 85 | Evolution of the concentration of M1000 hexylcinnamal imine **47** (A) and PEG₁₁Tyramine hexylcinnamal imine **53** (B) concentrations as a function of time at 10 mM in the presence (red) or absence (blue) of 100 mM HEPES buffer (pD 6.6).

The presence of a pD 6.6 buffer considerably increased the speed of hydrolysis of M1000 hexylcinnamal imine **47** and PEG₁₁tyramine hexylcinnamal imine **53**. The half-time of hydrolysis of M1000 hexylcinnamal imine **47** dropped from 12 hours at unmodified pD to a little more than 3 hours, while that of PEG₁₁tyramine hexylcinnamal imine **53** changed from 2.5 days to 6 hours. These results show the difficulty to sufficiently slow down the hydrolysis of imine bonds in an acidic medium, but also demonstrate that it is probably possible with

imine **53** to have a half-time of hydrolysis close to that needed for applications at neutral or slightly basic pD ($0.5 < H_{1/2} < 1$ day).

The speed of hydrolysis of M1000 hexylcinnamal imine **47** in an acidic medium, that proved to be fast in the presence of a buffer, was assessed by tuning the initial pD with the addition of deuterated trifluoroacetic acid at $t = 0$ (Figure 86).

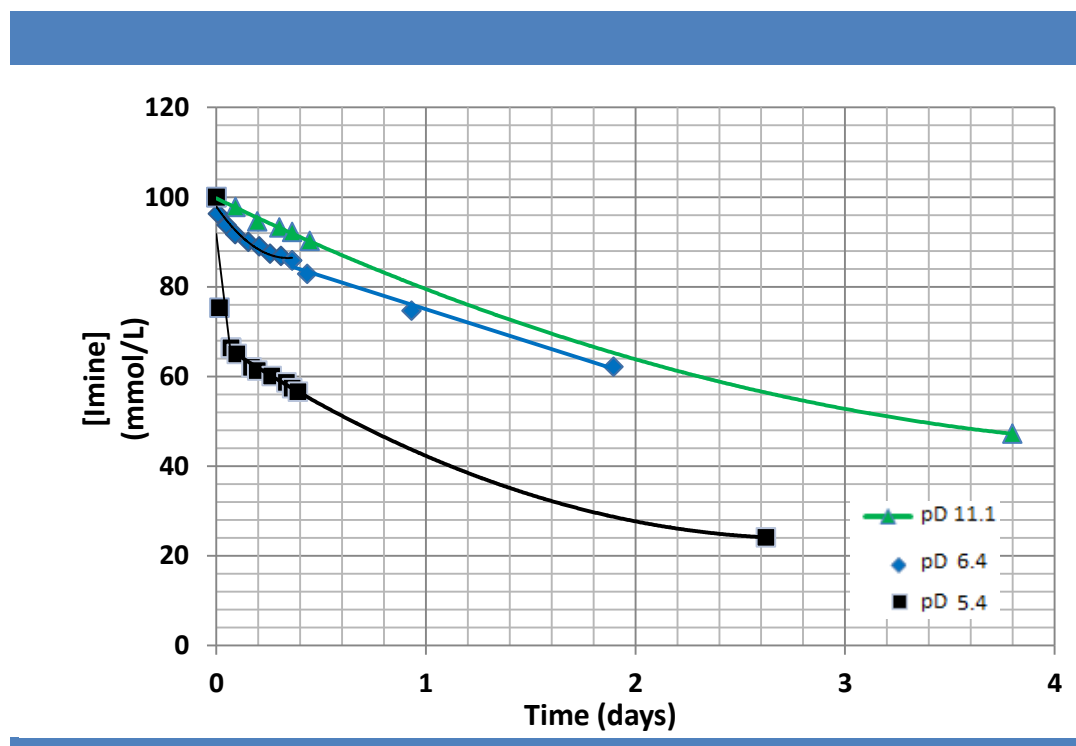


Figure 86 | Concentration of M1000 hexylcinnamal imine **47** as a function of time for $C_0 = 100$ mM at different initial pD (Addition of deuterated trifluoroacetic acid at $t = 0$).

For an addition of acid until reaching pD₀ 6.4, the influence on the half-time of hydrolysis is low ($H_{1/2} = 2.8$ instead of 3.6 days at unmodified pD), with the pD of the system increasing rapidly during hydrolysis. However, if the pD is further decreased (pD 5.4 for instance), the initial hydrolysis is very fast (33mM hydrolysed in less than 2 hours), and the effect on the half-time of hydrolysis is more noticeable (decrease to 16 hours). This result shows that a pH trigger can be used efficiently to tune the half-time of hydrolysis of our system.

Kinetic data are given in Table 13.

Table 13 | Kinetic parameters (initial rate of hydrolysis and half-time of hydrolysis time) of dynablock **47** and **53** in acidic deuterium oxide. Reactions with constant pD during the reaction were either performed at unmodified pD (basic) or in a HEPES buffer (acidic).

Imine	C (mM)	pD ₀	pD _{final}	V ₀ (10 ⁻³ mM/min)	H _{1/2} (days)
M1000 hexylcinnamal 47	10	10.4	10.5	6.8	0.51
M1000 hexylcinnamal 47	10	6.6	6.9	24.9	0.13
M1000 hexylcinnamal 47	100	5.1	10.2	19.7	0.65
M1000 hexylcinnamal 47	100	6.1	10.8	17.6	2.84
M1000 hexylcinnamal 47	100	10.7	10.7	14.9	3.57
PEG ₁₁ Tyramine hexylcinnamal 53	10	10.4	10.5	1.3	2.48
PEG ₁₁ Tyramine hexylcinnamal 53	10	6.6	6.9	195.0	0.27

d) Kinetic considerations

According to previous observations, we hypothesised that imines that are not stabilised in solution will exhibit pseudo-first order kinetics, while that stabilised by hydrophobic groups around the imine moiety will rather exhibit pseudo-zero order kinetics. In order to check this, several kinetics of hydrolysis at 10 mM were fitted with the sum of both kinetics, using the following equation:

$$C_{fit}(t) = C_{0th\ order}(t) + C_{1st\ order}(t)$$

$$\text{Thus: } C_{fit}(t) = C_{eq} - k_0 * t + A * e^{-k_1 t}$$

The plots are displayed in Figure 87 and the kinetic constants in Table 14.

Table 14 | Kinetic parameters (initial rate of hydrolysis and half-time of hydrolysis) of dynablock **47**, **51** and **53** in deuterium oxide at 10 mM (unmodified pD).

Imine	C ₀ (mM)	C _{eq} (mM)	k ₀ (10 ⁻³ mM/min)	A (mM)	k ₁ (10 ⁻³ min ⁻¹)
PEG ₁₁ NH ₂ Hexylcinnamal 51	10	0	1.9	9.96	2.7
M1000 Hexylcinnamal 47	10	4.11	5.1	5.87	0.33
PEG ₁₁ Tyramine Hexylcinnamal 53	10	7.38	0.17	2.21	1.1

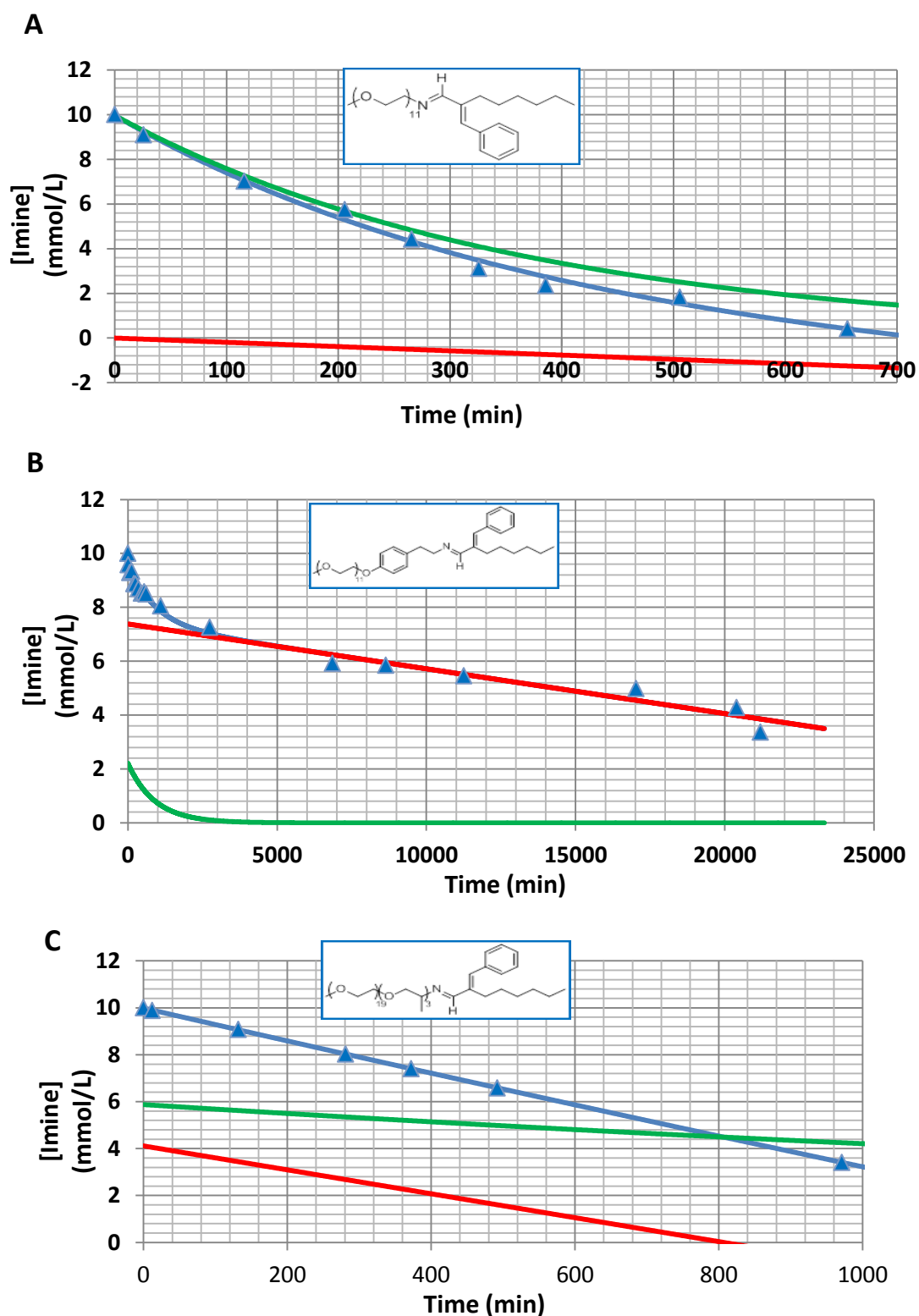


Figure 87 | Concentration as a function of time of several hexylcinnamal-based profragrances ($C_0 = 10$ mM, unmodified pD). Plots were fitted with a sum of 0 + 1 order kinetic (blue) with the contribution

of the 0th order in red, and that of 1st order in green. A) PEG₁₁NH₂ hexylcinnamal imine **51** B) PEG₁₁tyramine hexylcinnamal imine **53** C) M1000 hexylcinnamal imine **47**.

All kinetic plots could be fitted to this model, which means that two different mechanisms are involved in the hydrolysis of the dynablocks, one leading to a pseudo-first-order reaction rate and another one to a pseudo-zero-order reaction rate. A proposed explanation of the origin of these reaction rates follows:

- Pseudo-first-order reaction rate: for molecules without hydrophobic linker, this results from the hydrolysis of the imine bond with an excess of water (“fast” hydrolysis). For molecules with a hydrophobic linker, it may result from the hydrolysis of the imine bond inside the hydrophobic core of the micelle, where the imine is in excess and water only present in small quantity (“slow” hydrolysis).
- Pseudo-zero-order reaction rate: this usually occurs when a small fraction of reactant molecules are in a location or state in which they are able to react, and this fraction is continually refilled from the larger pool.^[199] This is exactly the case for the dynablock unimers in solution, which are at a constant concentration (CMC) and are rapidly hydrolysed (not protected any more by the hydrophobic linker).

In Figure 87, it is possible to see that PEG₁₁NH₂ hexylcinnamal imine **51** is mainly hydrolysed with a pseudo-first-order rate, as expected by the absence of hydrophobic linkers, and that PEG₁₁tyramine hexylcinnamal **53** is mostly hydrolysed with a pseudo-zero-order rate. M1000 hexylcinnamal imine **47** is hydrolysed almost equally by the two mechanisms. This demonstrates that the addition of a hydrophobic linker between the imine bond and the hydrophilic chain can, by protecting the imine bond and decreasing the CMC, be an efficient strategy to decrease the speed of hydrolysis of imines in solution.

^[199] Petrucci, R. H.; Harwood, H. S.; Herring, G.; Madura, J. D. General Chemistry: Principles & Modern Applications. Ninth ed. Upper Saddle River, N.J.: Pearson Education (2007)

2/ Hydrolysis of amphiphilic citral-based profragrances

a) Hydrolysis at 10 mM

The hydrolysis of citral-based profragrances was investigated at 10 mM, the same concentration previously used for hexylcinnamal-based profragrances. M1000 citral imine **48**, M2070 citral imine **50** and PEG₁₁imine citral imine **52** concentrations against time are displayed in Figure 88. PEG₁₁tyramine citral **54** was not studied, since it was surprisingly difficult to isolate and its fast decomposition was observed in water for unknown reasons.

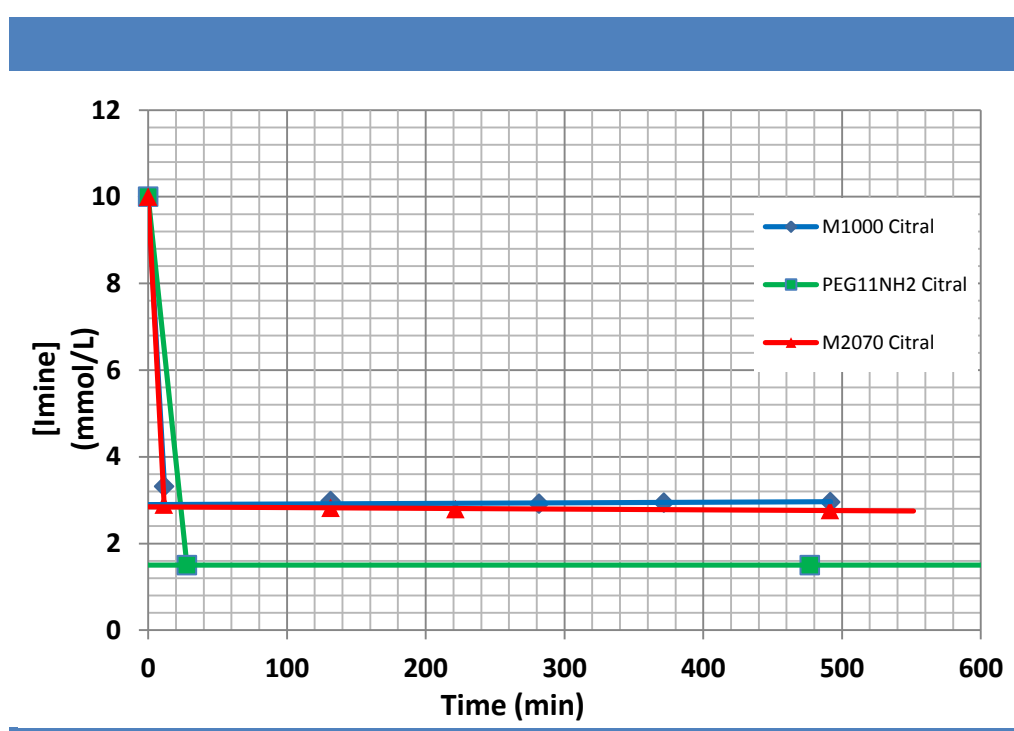


Figure 88 | Concentration of M1000 citral imine **48**, PEG₁₁NH₂ citral imine **52** and M2070 citral imine **50** as a function of time at C₀ = 10 mM for an unmodified pD (9.3 < pD < 11.0).

The kinetics of hydrolysis of these three imines is very peculiar. After a very fast initial hydrolysis, an equilibrium with still an important amount of condensed product was rapidly reached. Like in the case of the hexylcinnamal-based profragrances, the hydrolysis of M1000 citral imine **48** and M2070 citral imine **50** gives very similar results, with a concentration at equilibrium of 2.8 mM. The concentration of PEG₁₁NH₂ citral imine **52** is noticeably smaller, with a concentration at equilibrium of 1.5 mM. DOSY NMR showed that M1000 citral imine **48** is present in solution in its micellar form (Hr 4.7 nm) and as unimers (Hr 1.2 nm), while

citral is present mainly within the micelle. All these results tend to show a complex behaviour of the citral-based profragrances in solution. The imine bond between the different PEG amines and citral seems to be weak, thus explaining the very fast hydrolysis of the system. Moreover, citral is rather poorly hydrophobic and partially soluble in water (0.6 mg/mL), and a CMC much higher than for hexylcinnamal-based profragrances is expected, thus explaining again the fast hydrolysis and the presence of unimers detected by DOSY in solution. This could also explain the better performance of M1000 and M2070-based profragrances that, thanks to their hydrophobic linkers, decrease the CMC of the amphiphiles and favour the interactions with citral, thus leading to a higher concentration at equilibrium. However, the imine concentration at equilibrium is rather high (Table 15), which is a sign that even if M1000 citral imine **48** is rapidly hydrolysed, the high concentration of reacting species in the micelle is able to significantly shift the equilibrium toward imine formation.

Table 15 | Concentration at equilibrium of dynablocks **48**, **50** and **52** in deuterium oxide at 10 mM (unmodified pD).

Imine	C ₀ (mM)	pD (Unmodified)	C _{eq} (mM)
M1000 citral 48	10	9.3	2.9
M2070 citral 50	10	9.8	2.8
PEG ₁₁ NH ₂ citral 52	10	11.1	1.5

Although the analysis of the SANS data is currently under investigation, some preliminary information can be extracted from Figure 89 for M1000 citral imine **48**. The SANS data of M1000 citral imine **48** curve exhibits the same overall behaviour as M1000 hexylcinnamal imine **47** (Figure 81), characterized by the following sequence: (i) a Guinier regime in the low- q range, associated with the finite size of the supramolecular self-assemblies; (ii) one intermediate regime, in which the q -dependence of the scattered intensity can be described by a power law with an exponent close to -4; (iii) and a q^{-1} -regime in the high- q range. The data obtained at low- q can be fitted by a Guinier expression ($\ln(I(q)) = \ln(I(0)) - (1/2)R_g^2 q^2$) giving the radius of gyration: $R_g = 21.6 \text{ \AA}$, which is a typical value for this kind of dynablock.^[113] The q^{-4} regime is the signature of a three-dimensional object with a relatively smooth surface, probably a spherical micelle.

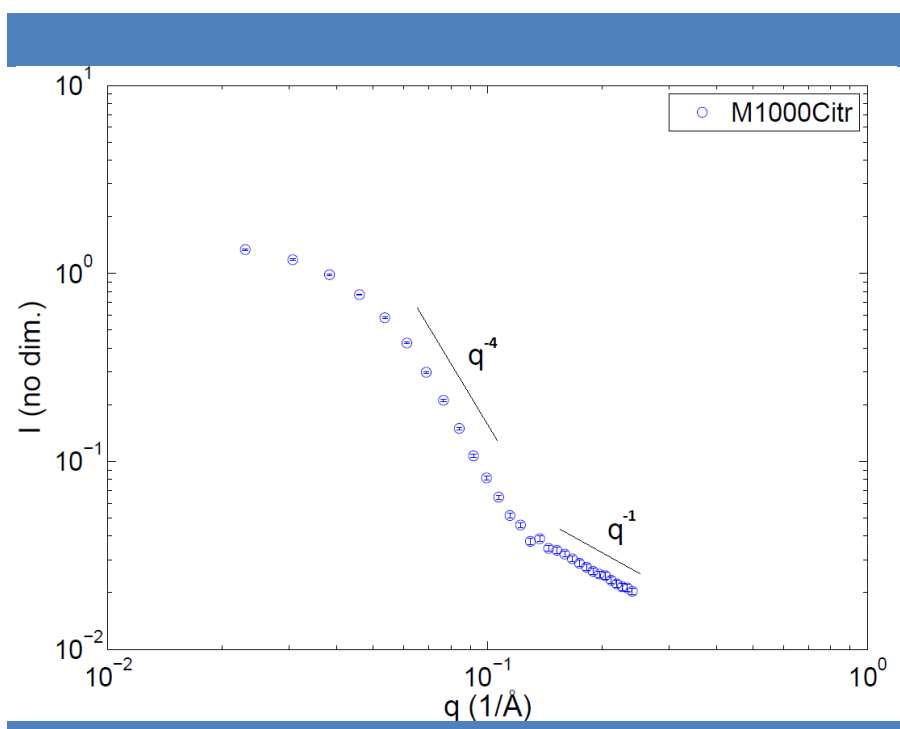


Figure 89 | SANS scattering pattern of M1000 citral imine **48**.

b) Influence of concentration

After having studied of the kinetics of hydrolysis of citral-based profragrances at 10 mM, the effect of the initial concentration on the percentage of imine at equilibrium was investigated for imines made of M1000, M2070 and PEG₁₁NH₂ (Figure 90). It can be seen that an increase in initial concentration leads to a higher percentage of imine at equilibrium. All imines give relatively similar results, except PEG₁₁NH₂ citral imine **52** that seems to be much less stable at lower concentration. These results are interesting from the application point of view, since it is possible to store these profragrances in a concentrated solution for a long time, where only a small fraction of the citral would be in its free aldehyde form. When incorporated in a sealed packaging, the imine concentration should be stable over time. Upon opening of the small quantity of free citral will evaporate, slowly shifting the equilibrium toward total imine hydrolysis. Moreover, citral is known to be poorly stable in aqueous solution due to the presence of an aliphatic aldehyde moiety, and the storage of this aldehyde under a stable imine form could be a solution to this problem of stability.

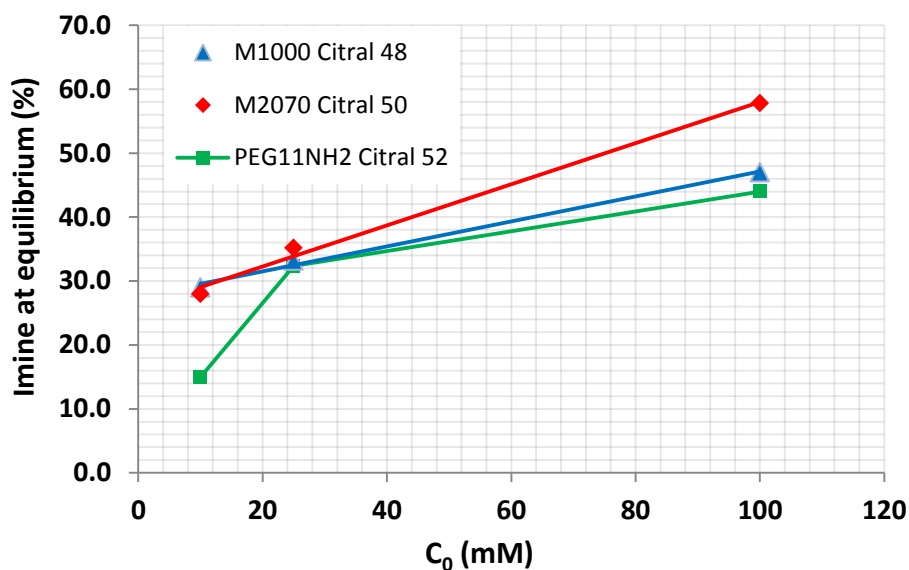


Figure 90 | Influence of initial concentration on the percentage of imine at equilibrium for **M1000 citral imine 48**, **PEG₁₁NH₂ citral imine 52** and **M2070 citral imine 50** at unmodified pD (9.25 < pD < 11.65).

Kinetic data is given in Table 16.

Table 16 | Concentration at equilibrium of dynablocks **48**, **50** and **52** in deuterium oxide at unmodified pD (10 < C_{eq} < 500).

Imine	C ₀ (mM)	pD (Unmodified)	C _{eq} (mM)	Imine at equilibrium (%)
M1000 citral 48	10	9.3	2.9	29.0
M1000 citral 48	25	11.4	8.3	33.2
M1000 citral 48	50	11.5	23.1	46.2
M1000 citral 48	100	11.7	47	47.0
M1000 citral 48	500	11.2	416	83.2
M2070 citral 50	10	9.8	2.8	28.0
M2070 citral 50	25	11.0	8.8	35.2
M2070 citral 50	100	11.0	57.8	57.8
PEG ₁₁ NH ₂ citral 52	10	11.1	1.5	15.0
PEG ₁₁ NH ₂ citral 52	25	11.2	8.1	32.4
PEG ₁₁ NH ₂ citral 52	100	11.3	44	44.0

c) Influence of pH

The influence of pD on the concentration at equilibrium was studied for M1000 citral imine **48** (Figure 91). It was decided not to study it for M2070 citral imine **50** and PEG₁₁NH₂ Citral **52**, since the results are expected to be very close to that obtained with **48**.

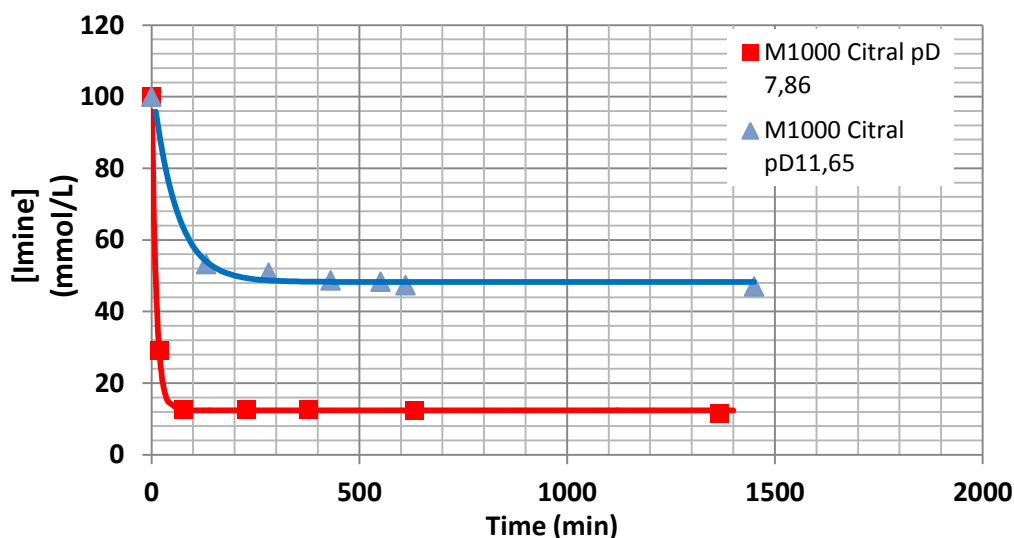


Figure 91 | Evolution of the concentration of M1000 citral imine **48** with time at pD 11.7 and 7.9 (initial concentration of 100 mM).

A decrease of pD from basic to neutral conditions had an important impact on the concentration at equilibrium by shifting this concentration from 47 to 12 mM. Citral-based profragrances appear highly sensitive to pD change, and thus could be better used in applications requiring basic conditions.

Kinetic data is given in Table 17.

Table 17 | Concentration at equilibrium of dynablock **48** for its hydrolysis in deuterium oxide at 100 mM (pD 11.7 and 7.9).

Imine	C ₀ (mM)	pD ₀	pD _{final}	C _{eq} (mM)	Imine at equilibrium (%)
M1000 citral 48	100	11.65	11.7	47	47.0
M1000 citral 48	100	7.86	7.9	12	12.0

3/ Hydrolysis of non-amphiphilic profragrances

a) Hydrolysis of M1000 Vanillin

After having studied the kinetics of hydrolysis of several amphiphiles, it has been decided to make a direct comparison between them and a fully hydrophilic imine, M1000 vanillin imine **37**, to show more clearly the benefits of the micellisation on the kinetics of hydrolysis. The kinetics of hydrolysis of M1000 vanillin imine **37** was compared to that of two M1000-based amphiphiles, M1000 citral imine **48** and M1000 hexylcinnamal imine **47** (Figure 92).

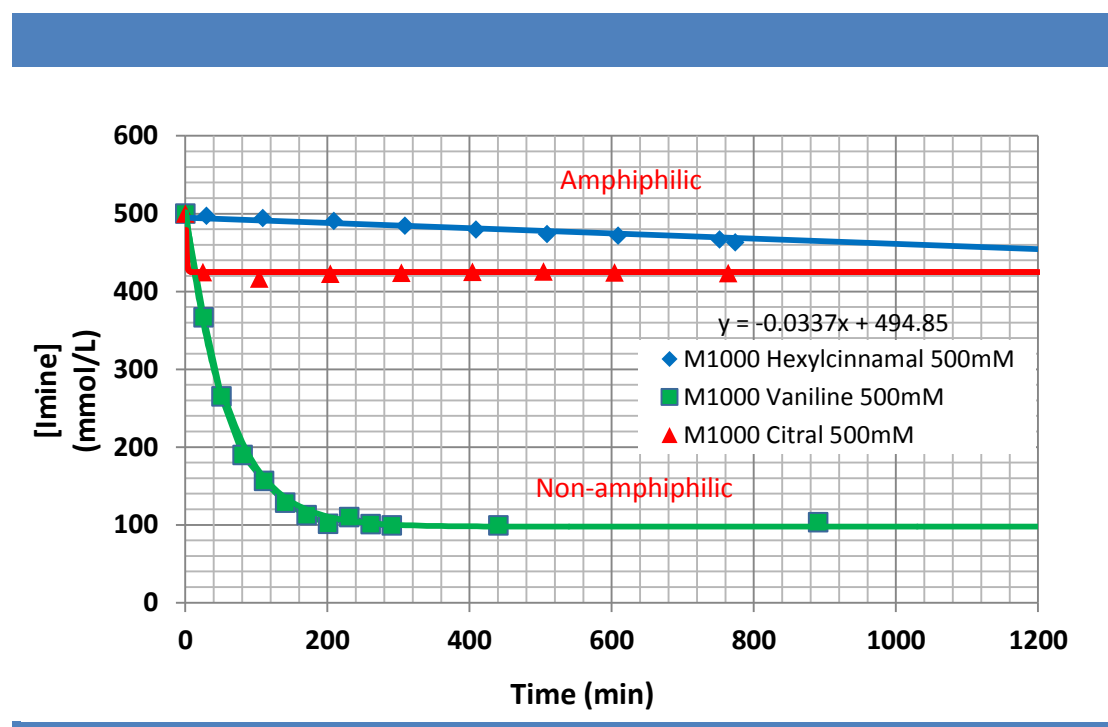


Figure 92 | Concentrations of M1000 hexylcinnamal imine **47**, M1000 citral imine **48**, and M1000 vanillin imine **37** as a function of time at $C_0 = 500$ mM (Unmodified pD).

At such high initial concentration (500 mM), the half-time of hydrolysis of M1000 hexylcinnamal **47** was not measured but can be estimated to be more than 5 days, whereas that of M1000 vanillin imine **37** is 1 hour. The concentration at equilibrium of M1000 citral **48** is of 424 mM, whereas that of M1000 vanillin imine **37** is 103 mM.

These results prove once more the strong effect of the imine micellar stabilisation. M1000 vanillin imine **37** was hydrolysed at several initial concentrations, and the results are displayed in Table 18.

Table 18 | Concentration at equilibrium of dynablock **37** at different initial concentrations (Unmodified pD).

Imine	C ₀ (mM)	pD (Unmodified)	C _{eq} (mM)	Imine at equilibrium (%)
M1000 Vanillin 37	10	10.1	0	0.0
M1000 Vanillin 37	100	10.1	6	6.0
M1000 Vanillin 37	500	10.1	97	19.4

b) Hydrolysis of M600-based profragrances

Thanks to the previous studies on amphiphilic imines, it is now known that hydrophobic linkers can partially protect the imine bond from water in solution. But would a hydrophobic imine encapsulated inside a micelle present the same stability as the amphiphilic imines? To answer this question, hydrophobic M600 hexylcinnamal imine **55** and M600 citral imine **56** were encapsulated into Texapon® (sodium laureth sulphate) micelles, a widely used anionic surfactant for liquid soaps [CH₃(CH₂)₁₀CH₂(OCH₂CH₂)₂OSO₃Na]. A concentration of Texapon® of four percents in weight (4wt%) was chosen, which corresponds to a similar concentration as that used for body wash applications. The kinetics of hydrolysis of encapsulated M600 citral imine **56** was compared to that M1000 citral imine **48** with or without the addition of Texapon® (Figure 93).

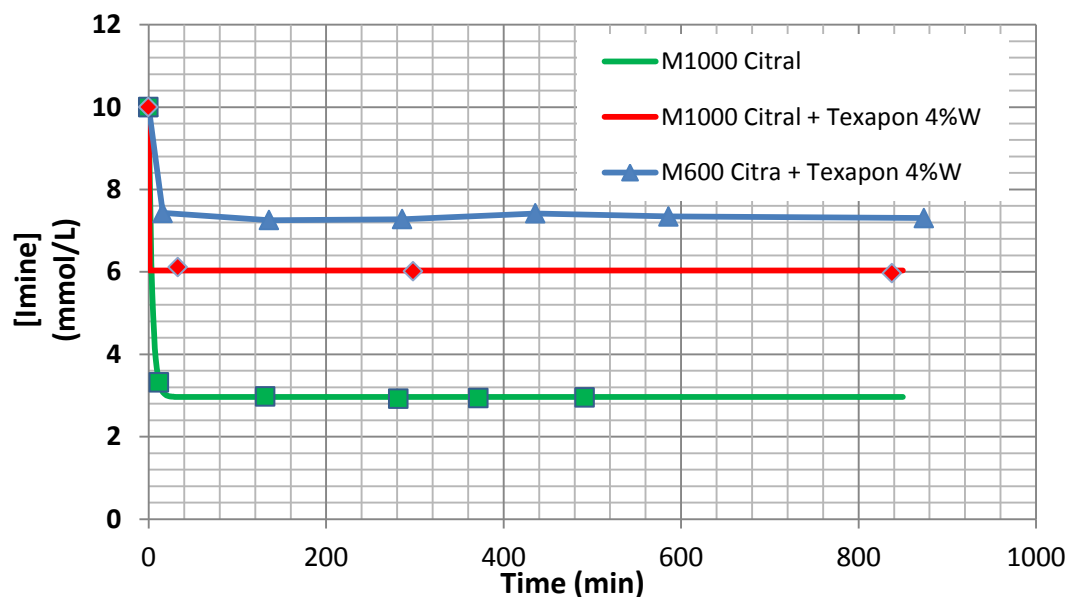


Figure 93 | Comparison of the kinetics of hydrolysis and the concentration at equilibrium of imines in the following formulations: M600 citral imine **56** + Texapon® 4 wt%, M1000 citral imine **48** + Texapon® 4 wt%, M1000 citral imine **48**. (Unmodified pD)

Encapsulated M600 citral imine **56** presents a behaviour very close to that of M1000 citral **48**, with a very fast initial hydrolysis. However, its concentration at equilibrium is much higher, reaching 7.3 mM when the mixed micelles of M1000 citral **48** and Texapon® only reach 6.0 mM, and M1000 citral **48** reaches 3.0 mM (Table 19). However, M1000 citral imine **48** with (pD 11.4) and without Texapon® (pD 9.3) cannot be directly compared, since their unmodified pDs differ by 2 units. These results prove that hydrophobic imine-based profragrances can efficiently stabilise imine bonds in water, when encapsulated inside a suitable non-dynamic imine. It also proves that the presence of non-dynamic surfactants can enhance the stability of the dynablocks, probably by keeping the aldehyde inside the micelles, thus shifting the equilibrium toward imine formation.

Unfortunately, M600 hexylcinnamal imine **55** could not be efficiently dissolved in the Texapon® solution at unmodified pD, and its kinetics of hydrolysis was not measured. M600 hexylcinnamal imine **55** and M600 citral imine **56** were also hydrolysed in the presence of a

HEPES pD 6.6 buffer, but had a half-hydrolysis time of less than 90 minutes, showing the same pD sensitivity as the other citral-based profragrances.

Table 19 | Concentration at equilibrium of dynablock **37** at different initial concentrations (Unmodified pD).

Imine	Added surfactant? (Texapon® 4wt%)	C ₀ (mM)	C _{eq}	pD
M600 citral 56	YES	10	7.3	11.3
M1000 citral 48	YES	10	6	11.4
M1000 citral 48	NO	10	3	9.3

4/ Mixture of several imines/aldehydes

The study of the hydrolysis of single types of imine in water being completed, our attention was focused on the interaction between imines incorporating different aldehydes, and on the effects of the presence of a reactive aldehyde at the initial stage of imine hydrolysis. These considerations are important, since the dynablocks have been designed to be incorporated into industrial formulations, possibly composed of complex mixtures of fragrances, some of them being reactive aldehydes. However, the mixing possibilities being virtually endless, we have limited our study to M1000-based profragrances, and to the use of citral and hexylcinnamal. M1000-based profragrances have been chosen for their relatively slow hydrolysis and/or their high concentration at equilibrium, coupled with a large scale industrial availability, low prices, non-toxicity and ease of synthesis.

a) Mixture of imines

M1000 hexylcinnamal imine **47** and M1000 citral imine **48** were hydrolysed simultaneously in deuterium oxide at unmodified pD (Figure 94). The initial concentration was chosen to be of 50 mM for both imines, since the concentration of M1000 citral imine **48** at equilibrium at 10 mM is too low to study precisely its variations (a limitation due to the use of ¹H NMR). The concentration of M1000 citral imine **48** at equilibrium (23.1 mM) was not modified by the presence of M1000 hexylcinnamal imine **47**. The half-time of hydrolysis of **47** increased from 2.09 to 2.36 days, thanks to the fast release from **48** at 28.9 mM of M1000 into the

solution, shifting the equilibrium of **47** toward imine formation. However, this effect is rather weak and the molecules in the mixture largely behave like if they were alone in solution.

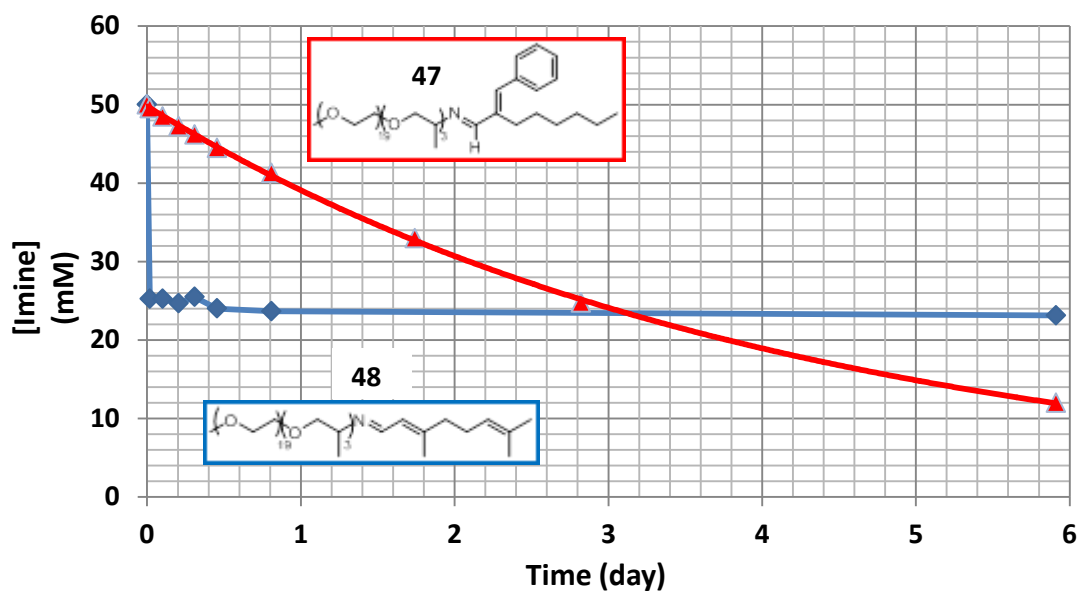


Figure 94 | Evolution of the concentration of M1000 hexylcinnamal imine **47** ($C_0 = 50$ mM) and M1000 citral imine **48** ($C_0 = 50$ mM) with time (Unmodified pD 11.56).

b) Mixture of imine and aldehyde

We then studied the influence of the presence of free aldehyde in a mixture with imines.

i) M1000 hexylcinnamal imine **47** and citral

The influence of the presence of citral during the hydrolysis of M1000 hexylcinnamal imine **47** was determined (Figure 95).

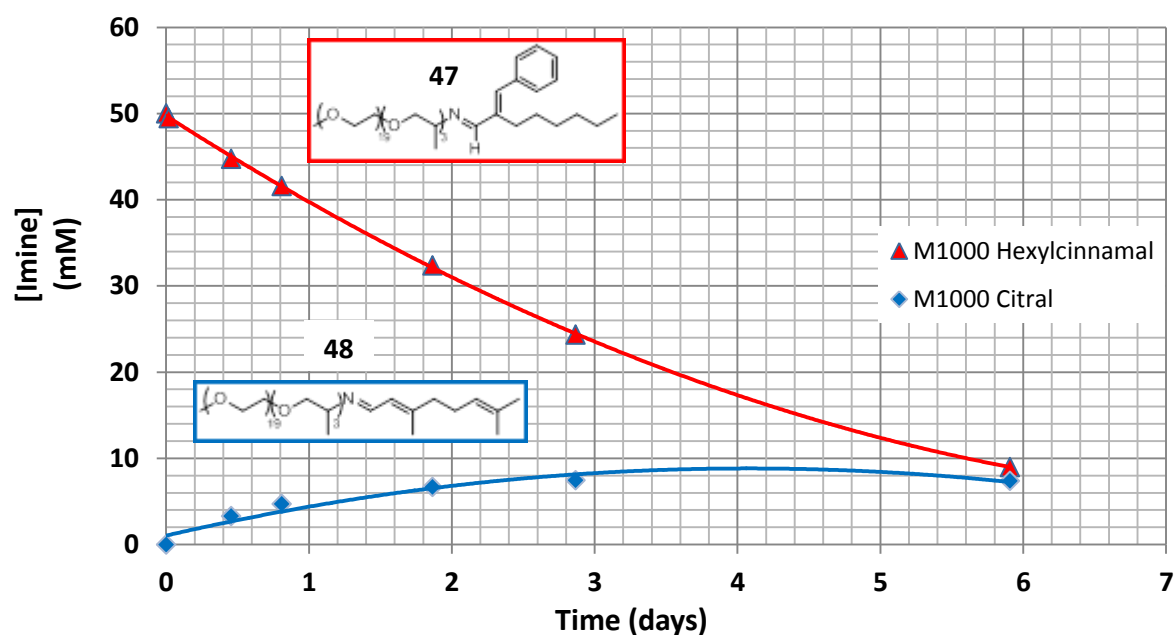


Figure 95 | Concentrations of M1000 hexylcinnamal imine **47** ($C_0 = 50$ mM) and M1000 citral imine **48** ($C_0 = 0$ mM) as a function of time in the presence of 50 mM of citral at $t = 0$ (Unmodified pD 11.57).

The kinetics of hydrolysis of M1000 hexylcinnamal imine **47** was almost unmodified by the presence of citral, but some M1000 citral imine **48** was formed during the hydrolysis of **47**. The reaction was not continued until reaching thermodynamic equilibrium, but the concentration of **48** at equilibrium seems not to exceed 10 mM, that is lower than that obtained by the direct hydrolysis of M1000 citral imine **48** at a concentration of 50 mM (23 mM). This result might be due to a non-encapsulation of citral inside the micelle made of M1000 hexylcinnamal imine **47**, and its precipitation in the solution thus decreases the quantity of reacting citral in solution.

ii) M1000 citral imine **48** and hexylcinnamal

Here, the influence of the presence of hexylcinnamal during the hydrolysis of M1000 citral imine **48** was determined (Figure 96).

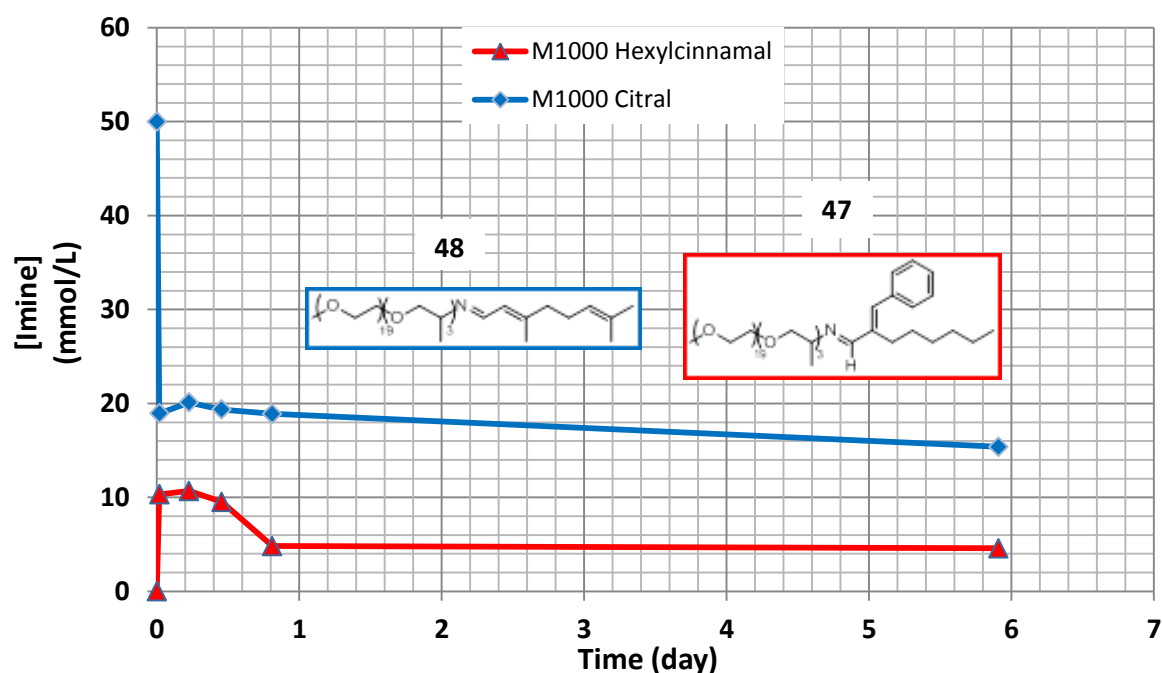


Figure 96 | Concentrations of M1000 hexylcinnamal imine **47** ($C_0 = 0$ mM) and M1000 citral imine **48** ($C_0 = 0$ mM) as a function of time in the presence of 50 mM of hexylcinnamal at $t = 0$ (Unmodified pD 11.56).

The concentration at equilibrium of M1000 citral imine **48** in the presence of hexylcinnamal is smaller than if **48** is alone in solution (15 instead of 23 mM). This result was expected since a part of the free M1000 is consumed by the formation of M1000 hexylcinnamal imine **47**, thus shifting the equilibrium toward the hydrolysis of **48**. The concentration of M1000 hexylcinnamal imine **47** is low at equilibrium, as expected from its near quantitative hydrolysis during the experiments to measure of its kinetics of hydrolysis.

The differences between the kinetics of exchange when starting from a mixture of citral + M1000 hexylcinnamal imine **47** (Figure 95) or from hexylcinnamal + M1000 citral imine **48** (Figure 96) are important. For the exchange from a citral + M1000 hexylcinnamal imine **47** mixture (Figure 95), the hydrolysis of **47** is very slow, and thus the concentration of M1000 will increase slowly over time, and the kinetics of formation M1000 citral imine **48** will do the same. For the hydrolysis of a mixture of hexylcinnamal + M1000 citral imine **48** (Figure

15), the fast hydrolysis of **48** increases very rapidly the concentration of M1000 in solution, and the formation of M1000 hexylcinnamal imine **47** is thus favoured since it is catalysed by the micelles of **48**.

From the thermodynamic point of view, it would be expected that the concentrations of M1000 hexylcinnamal imine **47** and M1000 citral imine **48** at equilibrium in both experiments are the same. This would be true if the solutions were agitated, however, in the absence of agitation, the concentrations at equilibrium are higher with the mixture starting from M1000 citral imine **48** since this imine can more easily dissolve the very hydrophobic hexylcinnamal ($\text{LogP} = 4.1$), than for the mixture starting from M1000 hexylcinnamal imine **47**, which possibly cannot encapsulate the more hydrophilic citral ($\text{LogP} = 2.2$) that precipitates from the beginning.

Overall, the presence of another imine or an aldehyde during the hydrolysis of a given imine had a small effect on the kinetics of hydrolysis or the concentration at equilibrium. However, in our case we have chosen an equimolar quantity of imine and aldehyde, but in the presence of a larger quantity of several aldehydes (like in some formulations), the concentration at equilibrium could be potentially decreased and the kinetics of hydrolysis fastened.

5/ Influence of hydrophobic chain length, co-surfactants and viscosity

a) Influence of the hydrophobic chain length

Having understood the effect of hydrophobic linkers, the effect of the variation of the CMC on the kinetics of hydrolysis has been assessed by the modification of the hydrophobic chain length at the para position of benzaldehyde derivatives (Figure 97). For this experiment, M1000 was chosen as hydrophilic block for its ability to stabilise imine bonds in solution thanks to its PPG₃ linker, and for its commercial availability. Chosen aldehydes were notably a mix of 4-alkylbenzaldehydes and 4-alkyloxybenzaldehydes, the full family of aldehydes from benzaldehyde to 4-decylbenzaldehyde being not commercially available. The initial concentration was set at 10 mM.

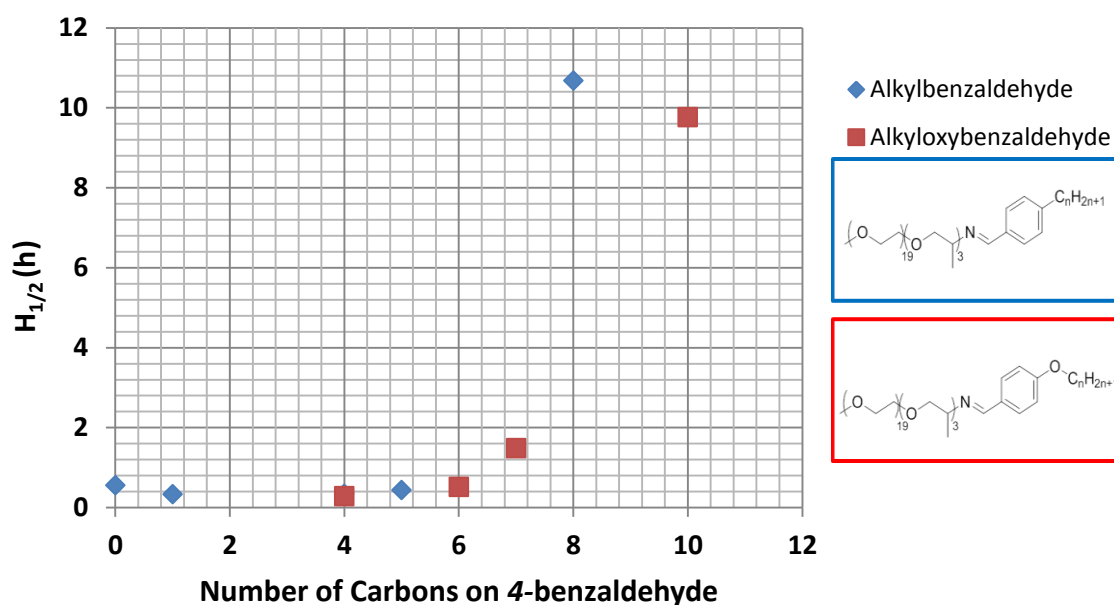


Figure 97 | Influence of the hydrophobic chain length at the *para* position of alkyl- and alkyloxybenzaldehydes on the half-time of hydrolysis of M1000-based dynablocks ($C_0 = 10$ mM, unmodified pD 10.9). Blue: **alkylbenzaldehydes**. Red: **alkyloxybenzaldehydes**.

It can be seen that the first noticeable slowdown of the imine hydrolysis only starts with the use of 4-heptyloxybenzaldehyde as hydrophobic block (half-time of hydrolysis of 1.5 hours compared to the 0.5 hour of 4-hexyloxybenzaldehyde), and the effect really becomes important with 4-octylbenzaldehyde (half-time of hydrolysis of 10.7 hours). These results can be well visualised using a plot of the concentration versus time (Figure 98).

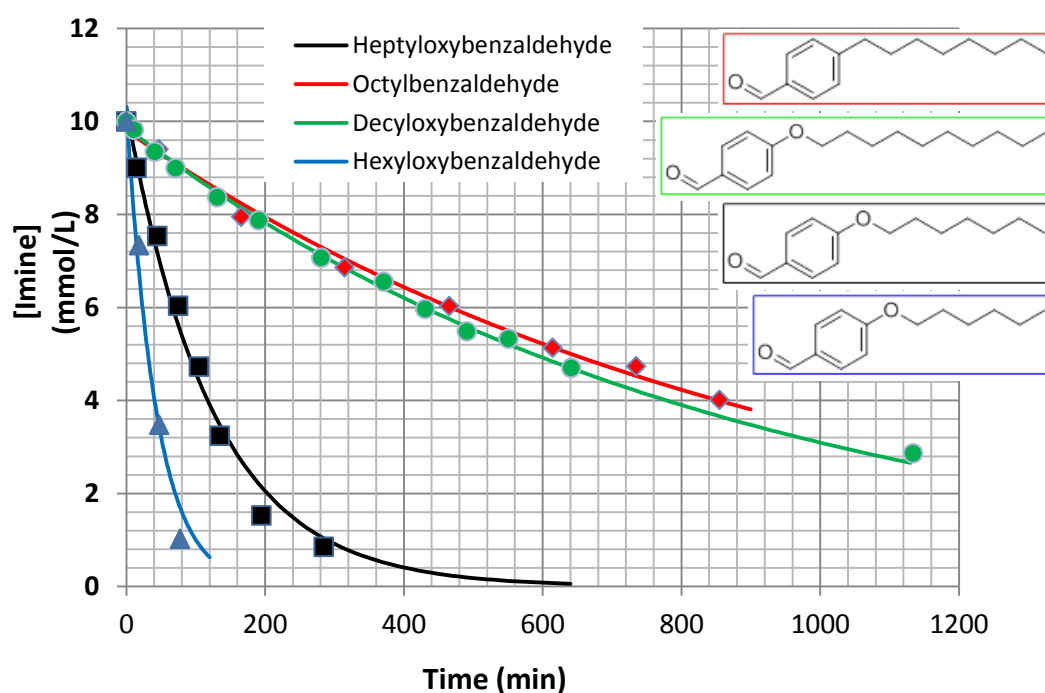


Figure 98 | Concentration as a function of time of several M1000 based dynablocks. **Red:** M1000 octylbenzaldehyde imine **44**, **Green:** M1000 decyloxybenzaldehyde imine **45**, **Black:** M1000 heptyloxybenzaldehyde imine **43**, **blue:** M1000 hexyloxybenzaldehyde imine **42**.

These results teach us that the CMC is a very important parameter to consider when designing a dynablock, and even if it was not directly measured, its effects on the kinetics of hydrolysis are very important. If used alone in solution, a dynablock profragrance should have a hydrophobic block long enough in order to slow down its hydrolysis. Since it is not possible to modify the hydrophobicity of the fragrance aldehyde, the linker between the hydrophilic chain and the imine moiety has to be the entity that will be chemically modified. It might even be possible to tune the linker size to get the hydrolysis time needed for the controlled release of a given aldehyde. Kinetic data are given in Table 20. From the kinetic plots, pseudo-first order kinetic constants k_1 were calculated. For dynablocks with micellar structure that do not follow a purely pseudo-first order kinetic constants (from heptyloxybenzaldehyde), k_1 was obtained with the best fit available for a first order kinetic.

Table 20 | Kinetics of hydrolysis and concentration at equilibrium of various dynablocks (**37 - 46**) with different hydrophobic chain size (Unmodified pD). **M1000 4-alkyloxybenzaldehyde** imines are in red, and **M1000 4-alkylbenzaldehydes** are in blue.

Imine	Number of Carbons in <i>para</i>	C ₀ (mM)	C _{eq} (mM)	pD	k ₁ (10 ⁻³ min ⁻¹)	H _{1/2} (h)
M1000 vanillin 37	0	10	< 1,0	10.2	26.7	0.44
M1000 benzaldehyde 38	0	10	4.68	10.9	84.4	0.56
M1000 tolualdehyde 39	1	10	3.67	10.8	78.6	0.33
M1000 butylbenzaldehyde 40	4	10	< 1.0	11.0	34.1	0.34
M1000 pentylbenzaldehyde 41	5	10	< 1.0	10.7	26.8	0.44
M1000 hexyloxybenzaldehyde 42	6	10	< 1.0	10.9	23.3	0.52
M1000 phenoxybenzaldehyde 46	6	10	< 1.0	11.0	24.3	0.48
M1000 heptyloxybenzaldehyde 43	7	10	< 1.0	10.9	8.1	1.49
M1000 octylbenzaldehyde 44	8	10	< 1.0	11.1	11	1,68
M1000 decyloxybenzaldehyde 45	10	10	< 1.0	10.9	12	9.77

b) Influence of the presence of co-surfactants

The influence of the presence of non-dynamic co-surfactants on the kinetics of hydrolysis of profragrances was investigated for two reasons:

- It is expected that co-surfactants might decrease the rate of hydrolysis and increase the concentration at equilibrium of the dynablocks, by lowering their CMC value and by providing micellar structures even when the imine concentration is low.^{[200][201][202]}
- The profragrances will *in fine* be incorporated into industrial formulations (body-wash, detergent...), already containing one or several non-dynamic surfactants.

Chosen surfactants and reactants are all of industrial importance and of four types (Table 21):

- Anionic surfactant: sodium dodecyl sulphate (SDS) and sodium laureth sulphate (Texapon®). This latter one will be the most studied surfactant in this chapter, due to its wide use in cleaning products and for liquid body-wash, an application we are particularly interested in.

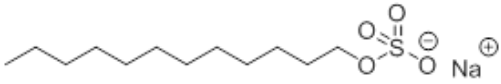
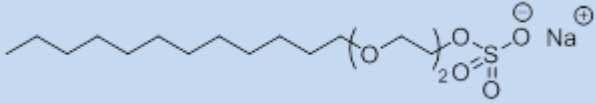
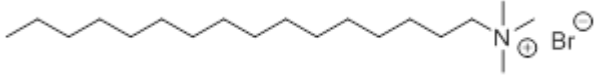
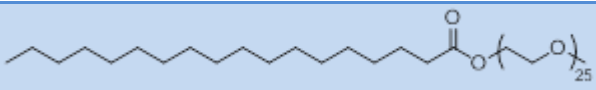
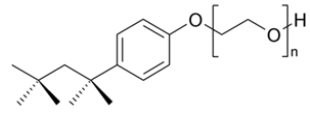
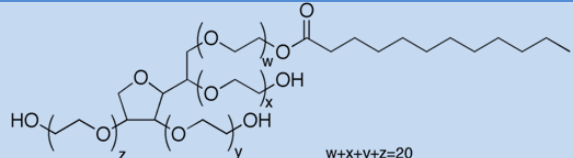
^[200] Hua, X. Y.; Rosen, M. J., Calculation of the Coefficient in the Gibbs Equation for the Adsorption of Ionic Surfactants from Aqueous Binary-Mixtures with Non-Ionic Surfactants. *J Colloid Interf Sci*, **87** (2), 469-477 (1982)

^[201] Rosen, M. J.; Hua, X. Y., Synergism in Binary-Mixtures of Surfactants. *J Am Oil Chem Soc*, **59** (4), A274-A274 (1982)

^[202] Rosen, M. J., Synergism in Mixtures Containing Zwitterionic Surfactants. *Langmuir*, **7** (5), 885-888 (1991)

- Cationic surfactant: cetrimonium bromide; used as antiseptic agent and in hair conditioning products.
- Non-ionic surfactant: PEG₂₅ monostearate, Triton® X-100 and Tween® 80; widely used as detergents, and incorporated in food, drug and cosmetic applications.
- Reacting imines: Jeffamine M1000 and M2070.

Table 21 | Chemical structure of common co-surfactants used to tune the stability of dynablocks in solution.

Surfactant Name	Surfactant type	Chemical structure
Sodium dodecyl sulfate (SDS)	Anionic	
Sodium laureth sulphate (Texapon® NSO IS)	Anionic	
Cetrimonium bromide (hexadecyl-trimethyl-ammonium bromide)	Cationic	
PEG ₂₅ Monostearate	Non-ionic	
Triton® X-100 polyethylene glycol p-(1,1,3,3-tetramethylbutyl)-phenyl ether (n = 9, 10)	Non-ionic	
Tween® 80 (Polyoxyethylene 20 sorbitan monooleate)	Non-ionic	

i) Influence of co-surfactants on the kinetics of hydrolysis of M1000 Hexylcinnamal imine **47**

The influence of the presence of non-dynamic co-surfactants on the kinetics of hydrolysis of M1000 hexylcinnamal imine **47** was investigated under the following conditions:

- Initial imine concentration: 10 mM (= 1.03 wt%)
- pD unmodified (usually 10.5)
- Surfactant concentration: 4wt%
- Solvent: D₂O

The results can be classified into three categories:

- Surfactants that slow down the M1000 hexylcinnamal **47** imine hydrolysis (Figure 99).
- Surfactants that accelerate the M1000 hexylcinnamal **47** imine hydrolysis.
- Surfactants that modify the M1000 hexylcinnamal **47** imine hydrolysis with a more complex behaviour (Figure 100).

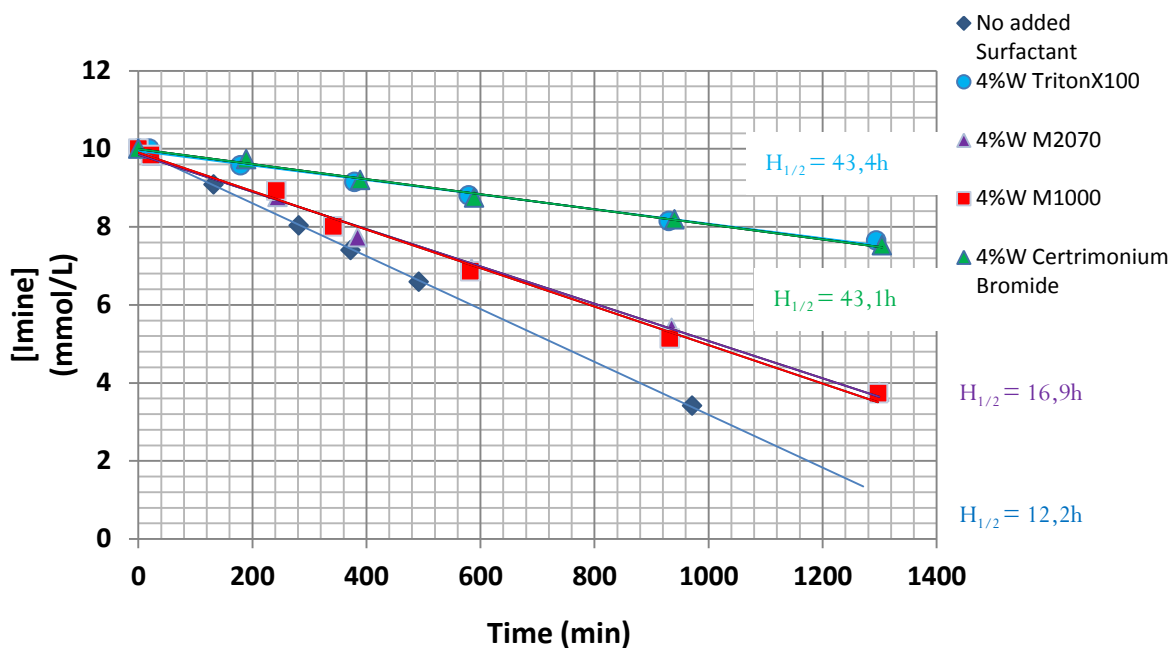


Figure 99 | Concentration as a function of time of M1000 Hexylcinnamal imine **47** in the presence of various surfactants and reacting amines in solution. ($C_0 = 10$ mM, unmodified pD 10.5, surfactant concentration = 4wt%).

Figure 99 represents the surfactants and reactants that slow down the hydrolysis of M1000 hexylcinnamal imine **47** which can be regrouped in two categories:

- 1) Amines that moderately decrease the speed of hydrolysis. The presence of an excess of M1000 and M2070 shifts the equilibrium toward imine formation and slows down slightly its hydrolysis (half-time of hydrolysis time increased from 12.2 to almost 17 hours).
- 2) Cationic surfactant certrimonium bromide and Triton® X-100, that considerably slow down the hydrolysis of M1000 hexylcinnamal imine **47** from 12.2 to 43 hours.

All plots show a linear relationship between concentration and time, a sign of pseudo-zero order hydrolysis attributed to the hydrolysis of free unimers in solution. A proposed explanation for this slowdown of hydrolysis is that by adding a co-surfactant, the CMC of the system decreases^{[200][201][202]} and less dynablocks are present as unimers in solution. A second phenomenon that can lead to a slowdown of the hydrolysis is that the addition of a surfactant into the solution would increase the viscosity of the micellar core,^[203] thus slowing down the dynamic exchange between the dynablocks in the micelles and in solution. In this case, the concentration of unimers in solution would not be equal to the CMC anymore, but would be limited by the exchange kinetic. The influence of viscosity will be studied in part 5d of this chapter.

From all the tested surfactants, only the presence of SDS drastically decreased the half-time of hydrolysis of M1000 hexylcinnamal imine **47** from 12.2 to 4.9 hours. This result is due to the partial precipitation of SDS in solution, possibly trapping the imine inside solid aggregates. Surfactants that modify the M1000 Hexylcinnamal imine **47** hydrolysis with a complex behaviour are displayed in Figure 100. In particular, the hydrolysis rate in the presence of Texapon® was almost not affected until the concentration 5.5 mM, where it starts to slow down. This result might be the effect of an increase of viscosity due the free M1000 in solution. Another complex hydrolysis is that observed in the presence of PEG₂₅stearate, which provokes a very fast initial hydrolysis followed by an equilibrium rapidly reached at 4.4 mM. A possible explanation is that the rate of formation of the aggregates is slow (thus leading to a fast hydrolysis of the imine at the beginning of the experiment), but that afterwards the formed aggregates are very efficient to stabilise the imine bond in solution.

^[203] Kwon, G. S.; Forrest, M. L. Micelle composition of polymer and passenger drug. WO 2006110862 A2 (2006)

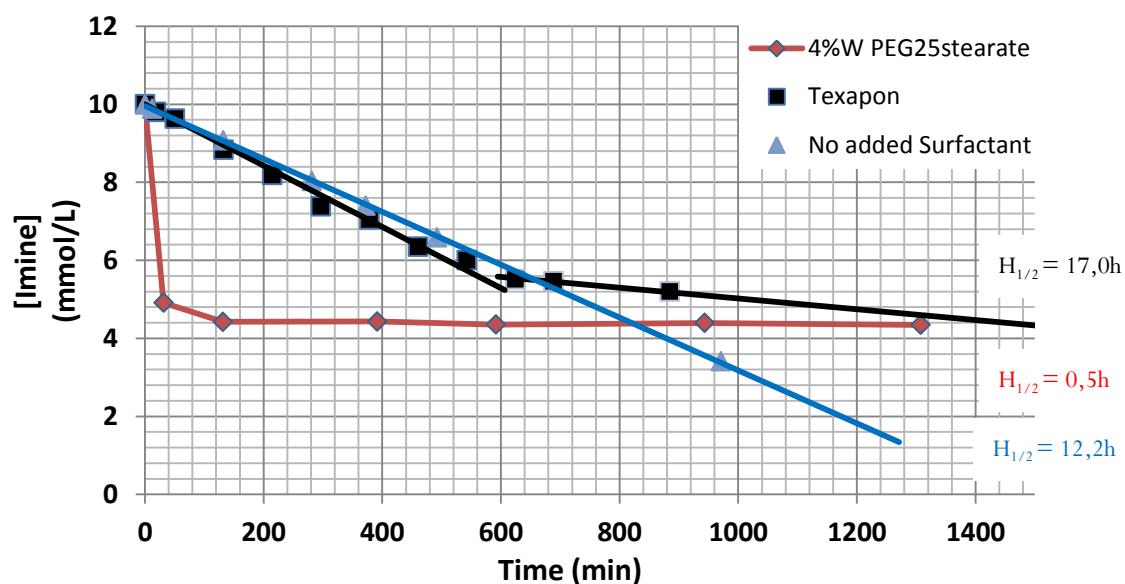


Figure 100 | Concentration as a function of time of M1000 hexylcinnamal **47** in the presence of various surfactants. ($C_0 = 10 \text{ mM}$, unmodified pD 10.5, surfactant concentration = 4wt%).

All the kinetic data is presented in Table 22.

Table 22 | Kinetic parameters (half-time of hydrolysis, pseudo-zero order kinetic constant) of M1000 hexylcinnamal **47** hydrolysis in the presence of various surfactants at 10 mM (Unmodified pD).

Surfactants that **slow down hydrolysis** are in green. That that **accelerates** is in red.

Imine	Surfactant type	Surfactant (4wt%)	$k_0 (10^{-3} \text{ mM/min})$	$H_{1/2} (\text{h})$
M1000 Hexylcinnamal	Non-ionic	Triton®	1.9	43.4
M1000 Hexylcinnamal	Cationic	Certrimonium Bromide	1.9	43.1
M1000 Hexylcinnamal	Anionic	Texapon®	7.8 and 1.4	17.0
M1000 Hexylcinnamal	Reactive amine	M2070	4.9	16.9
M1000 Hexylcinnamal	Reactive amine	M1000	4.9	16.6
M1000 Hexylcinnamal	No added surfactant	No added surfactant	6.8	12.2
M1000 Hexylcinnamal	Anionic	SDS	Not determined	4.9
M1000 Hexylcinnamal	Non-ionic	Peg ₂₅ Stearate	Not determined	0.5

ii) Influence of co-surfactants on the concentration at equilibrium of M1000 citral imine **48**

The influence of the presence of non-dynamic co-surfactants on the concentration at equilibrium of M1000 citral imine **48** was investigated under the following conditions:

- Initial imine concentration: 10 mM (= 0.97 wt%)
- pD: unmodified (usually around 10.5)
- Surfactant concentration: 4wt%
- Solvent: D₂O

The results can be classified in two categories:

- Surfactants that increase the M1000 citral imine **48** concentration at equilibrium (Figure 101).
- Surfactants that have no effect on the M1000 citral imine **48** imine concentration at equilibrium (Figure 102).

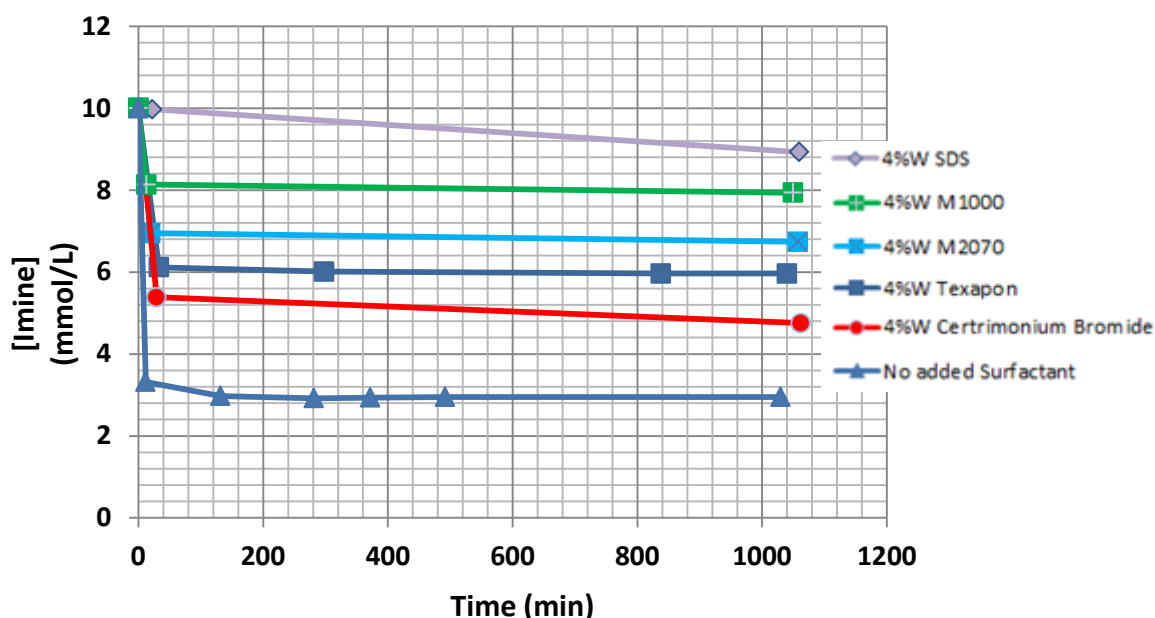


Figure 101 | Concentration as a function of time of M1000 citral **48** in the presence of various surfactants. ($C_0 = 10$ mM, unmodified pD 10.5, surfactant concentration = 4wt%).

Figure 101 shows the surfactants and reactants that increase the concentration of M1000 citral imine **48** at equilibrium. It can be remarked that the addition of reactive M1000 and M2070 has an important effect on the concentration at equilibrium, increasing from 3 mM in their absence to 6.7 mM for the addition of M2070, and 7.9 mM for the addition of M1000. This result clearly proves that the high concentration at equilibrium in this system is due to a high local concentration of the reacting species in the micelle or at its interface, since adding a

large quantity of reactive amines can convert most of the free aldehyde to imines. This effect is logically more important for M1000 than for M2070, since a same molar quantity of M1000 is twice that for M2070 for the added quantity (4wt%). Another important observation is that the concentration at equilibrium is better increased by anionic surfactants (8.9 mM for SDS, 5.9 mM for Texapon®) and not at all by non-ionic surfactants (Figure 102). This means that the formation of mixed micelles M1000 citral imine **48**/non-ionic surfactants does not confine the reactants (citral and M1000) in the micelle better than the micelles of M1000 citral imine **48** alone in solution. Anionic surfactants, however, can stabilise the transition state of the imine (its protonated form) and possibly increase the sequestration of protonated M1000 in micelles by favourable electrostatic interactions with its sulphate head, thus increasing its local concentration.^[204] It can be noted that PEG₂₅ monostearate, although having no influence on the concentration at equilibrium, seems to decrease the rate of hydrolysis of M1000 citral imine **48** (Although not enough points have been taken to measure its kinetic).

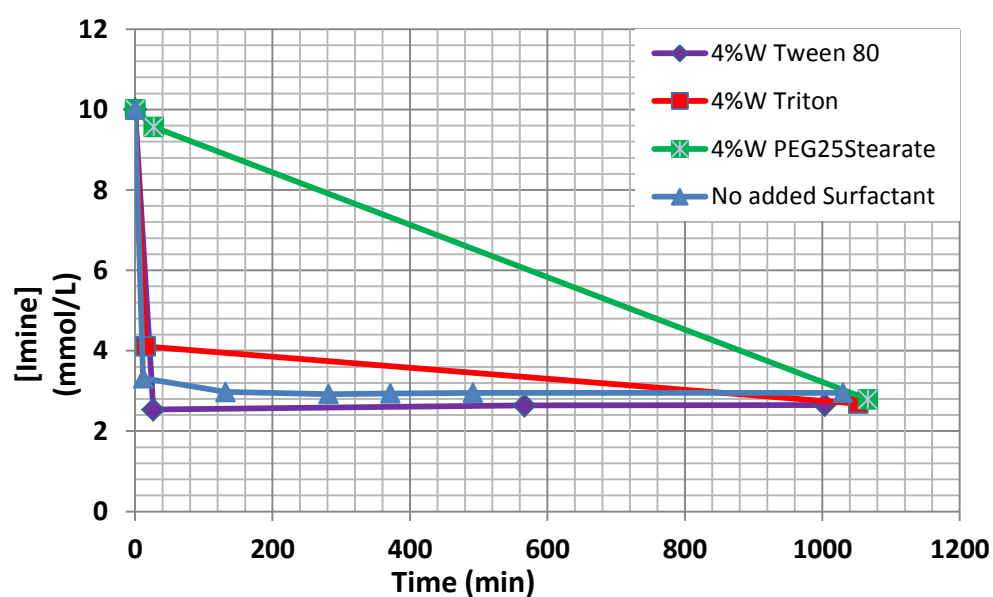


Figure 102 | Concentration as a function of time of M1000 citral **48** in the presence of various surfactants. ($C_0 = 10$ mM, unmodified pD 10.5, surfactant concentration = 4wt%).

^[204] Meguellati, K.; Fallah-Araghi, A.; Baret, J. C.; El Harrak, A.; Mangeat, T.; Marques, C. M.; Griffiths, A. D.; Ladame, S., Enhanced imine synthesis in water: from surfactant-mediated catalysis to host-guest mechanisms. *Chem Commun*, **49** (96), 11332-11334 (2013)

Concentrations at equilibrium for each added surfactant are presented in Table 23.

Table 23 | Concentration at equilibrium of M1000 citral **48** in the presence of various surfactants at 10 mM (Unmodified pD). Surfactants that **increase the concentration at equilibrium** are in green. Those **without effect** are in blue.

Imine	Surfactant type	Surfactant (4wt%)	C _{eq} (mM)
M1000 Citral	Anionic	SDS	8.93
M1000 Citral	Reactive amine	M1000	7.94
M1000 Citral	Reactive amine	M2070	6.74
M1000 Citral	Anionic	Texapon®	5.96
M1000 Citral	Cationic	Certrimonium Bromide	4.75
M1000 Citral	No added surfactant	No added surfactant	2.95
M1000 Citral	Non-ionic	Peg ₂₅ Stearate	2.79
M1000 Citral	Non-ionic	Triton®	2.68
M1000 Citral	Non-ionic	Tween® 80	2.64

iii) Influence of co-surfactants on the concentration at equilibrium of M2070 citral imine **50**

The influence of the presence of non-dynamic co-surfactants on the concentration at equilibrium of M2070 citral imine **50** was investigated under the following conditions:

- Initial imine concentration: 10 mM (= 1.93 wt%)
- pD unmodified (10.4)
- Surfactant concentration: 4wt%
- Solvent: D₂O

The concentrations at equilibrium of M2070 citral imine **50** in the presence of surfactants are expected to be the same as that obtained for M1000 citral imine **48**. However, the slowdown of the speed of hydrolysis in the presence of PEG₂₅ monostearate in the case of **48** is intriguing and for this reason, M2070 citral imine **50** was hydrolysed under the same conditions, as well as with the whole series of all non-ionic surfactants (Figure 103).

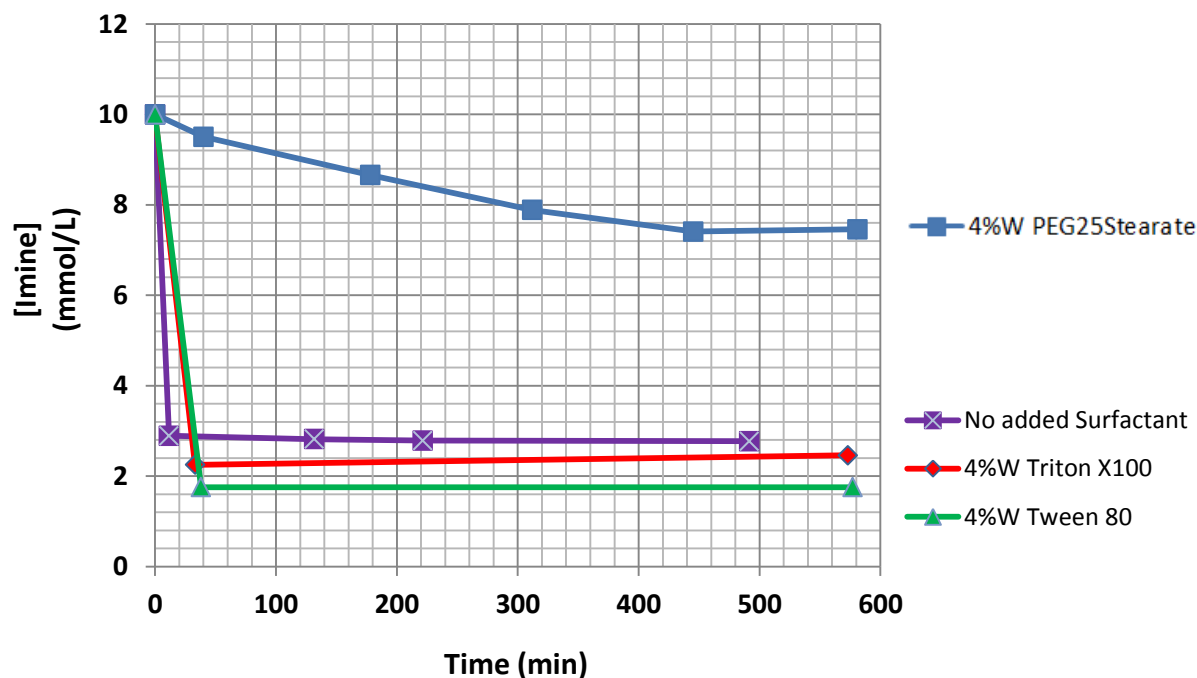


Figure 103 | Concentration as a function of time of M2070 citral **50** in the presence of various non-ionic surfactants. ($C_0 = 10$ mM, unmodified pD 10.4, surfactant concentration = 4wt%).

Similarly to M1000 citral imine **48**, Triton® X-100 and Tween® 80 did not improve the concentration at equilibrium of imine **50**. The rate of hydrolysis of M2070 citral **50** in the presence of PEG₂₅ monostearate, however, was surprisingly slow and reached a high concentration of 7.5 mM at equilibrium. This result, difficult to explain at first sight, can be partially understood in the light of an example found in the literature.^[205] In this example, Ochiai and Danjo managed to protect from hydrolysis an ester bond situated on the hydrophobic part of latanoprost (a molecule of pharmaceutical interest), and proposed as a mechanism that the hydrolysis was inhibited by interaction between the ester group and complex micelles made of PEG₂₅ monostearate associated with benzalkonium chloride (Figure 104).

^[205] Ochiai, A.; Danjo, K., The stabilization mechanism of latanoprost. *Int j pharm*, **410** (1-2), 23-30 (2011)

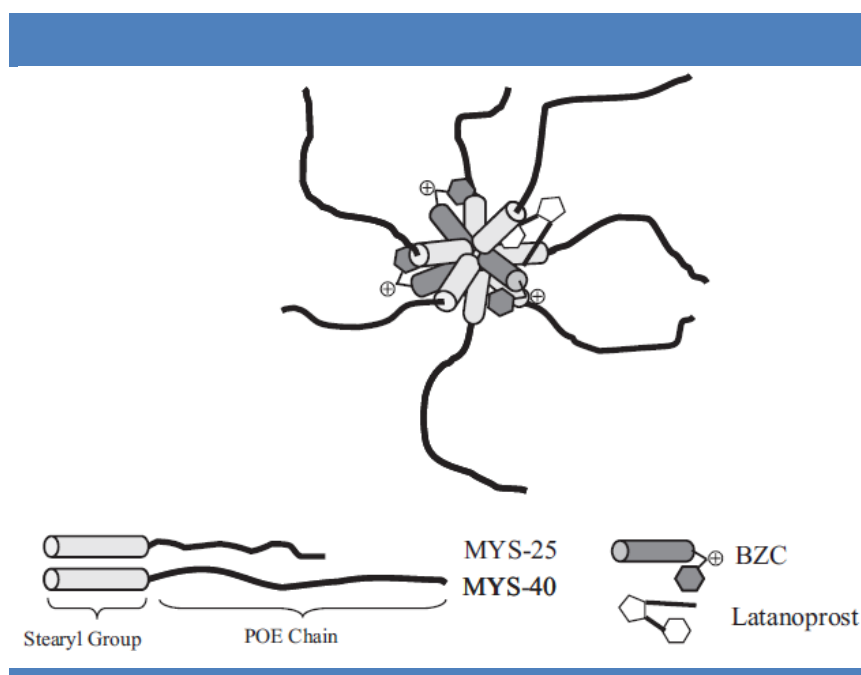


Figure 104 | Proposed schematic representation of complex micelles with latanoprost.^[205]

This system looks similar to ours, with the use of the same surfactant (PEG₂₅ monostearate), the presence of an ammonium group that can be incorporated into micelles (M2070 protonated) and a hydrolysable function to protect (imine in our case). The kinetics of hydrolysis of M2070 citral **50** with PEG₂₅ monostearate could be explained by the following mechanism:

- At the beginning of the hydrolysis, the concentration of M2070 is low and protonated M2070 amines are not present in sufficient quantity to form enough complex micelles with PEG₂₅ monostearate. All imines cannot be protected by interaction with complex micelles and some of the imines get hydrolysed.
- The hydrolysis stops when enough M2070 has been released and enough complex micelles are present to stabilise the remaining imines.

This interaction between the imine and the complex micelles must be very dependent on the hydrophobicity of the imine. M2070 could be a good compromise as its structure incorporates hydrophilic PEG units and hydrophobic PPG units. This theory should of course be validated by supporting measurements; SAXS and SANS could be powerful techniques to investigate the structure of these self-assemblies.

Now that the stability of M2070 citral **50** with PEG₂₅ monostearate under basic conditions has been elucidated, we verified whether the imine could be stabilised under acidic conditions. A hydrolysis experiment was performed under the same conditions but in the presence of a phosphate buffer at pD 4.4 (Figure 105).

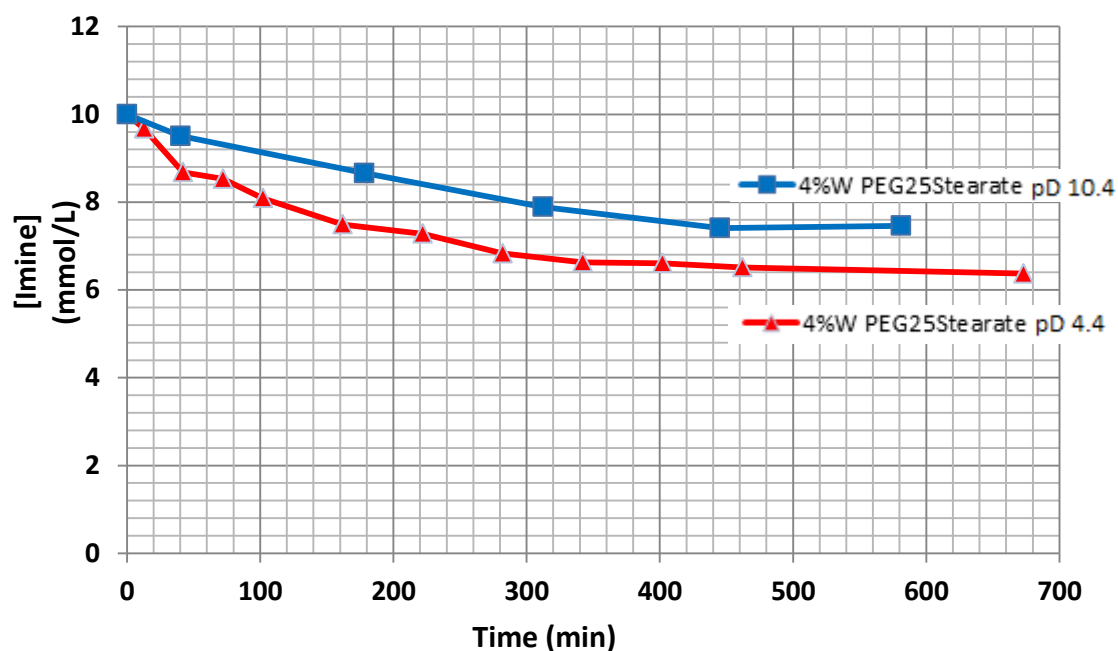


Figure 105 | Concentration as a function of time of M2070 citral **50** in the presence of PEG₂₅ monostearate at unmodified pD (10.4) and in monobasic phosphate buffer (pD 4.4). ($C_0 = 10\text{mM}$, , $[\text{PEG}_{25} \text{ Monostearate}] = 4\text{wt}\%$).

Very interestingly, M2070 citral **50** proved to be very stable under these conditions. The initial rate of hydrolysis is just slightly increased, and the concentration at equilibrium slightly reduced from 7.5 to 6.4 mM. This example is the first in our study, for which the kinetics of hydrolysis of a citral-based profragrance could be measured, and the first for which the imine was stable and not fully hydrolysed in acidic conditions.

These results open the door to various applications for the controlled release of citral, ranging from basic to acidic media. It could also be a way to efficiently stabilise citral in solution, by avoiding its (acid-promoted) oxidative degradation.^[206]

Concentrations at equilibrium are summarised in Table 24.

Table 24 | Concentration at equilibrium of M2070 citral **50** in the presence of various non-ionic surfactants at 10 mM (Unmodified pD and phosphate buffer pD 4.4). Surfactants that **increase the concentration at equilibrium** are in green. Thats **that decrease it** are in red.

Imine	pD (Buffered)	Surfactant (4wt%)	C _{eq} (mM)	k ₁ (10 ⁻³ min ⁻¹)
M2070 citral	10.4	Peg ₂₅ Stearate	7.5	12.4
M2070 citral	4.4	Peg ₂₅ Stearate	6.4	31.9
M2070 citral	10.4	No added surfactant	2.8	Immediate hydrolysis
M2070 citral	10.4	Triton®	2.5	Immediate hydrolysis
M2070 citral	10.4	Tween® 80	1.8	Immediate hydrolysis

iv) Influence of co-surfactants on the concentration at equilibrium of M600 citral imine **56**

The influence of the presence of non-dynamic co-surfactants on the concentration at equilibrium of M600 citral imine **56** was investigated under the following conditions:

- Initial imine concentration: 10 mM (= 0.66 wt%)
- pD unmodified (10.4)
- Surfactant concentration: 4wt%
- Solvent: D₂O

The concentrations of M600 citral imine **56** in presence of various surfactants at equilibrium are expected to be slightly higher to that measured for M2070 citral imine **50** and M1000 citral imine **48**, thanks to the enhanced stabilisation of the imine bond in the hydrophobic environment of the micelle core. M600 citral imine **56** was hydrolysed in the presence of the same non-ionic surfactants as for M2070 citral imine **50**. We then verified, if the presence of

^[206] Djordjevic, D.; Cercaci, L.; Alamed, J.; McClements, D. J.; Decker, E. A., Stability of citral in protein- and gum arabic-stabilized oil-in-water emulsions. *Food Chemistry*, **106** (2), 698-705 (2008)

Texapon® can stabilise **56** in the same way as M1000 citral imine **48** was stabilised with anionic surfactants (Figure 106). M600 citral **56** was not studied alone in solution, since it is non-soluble.

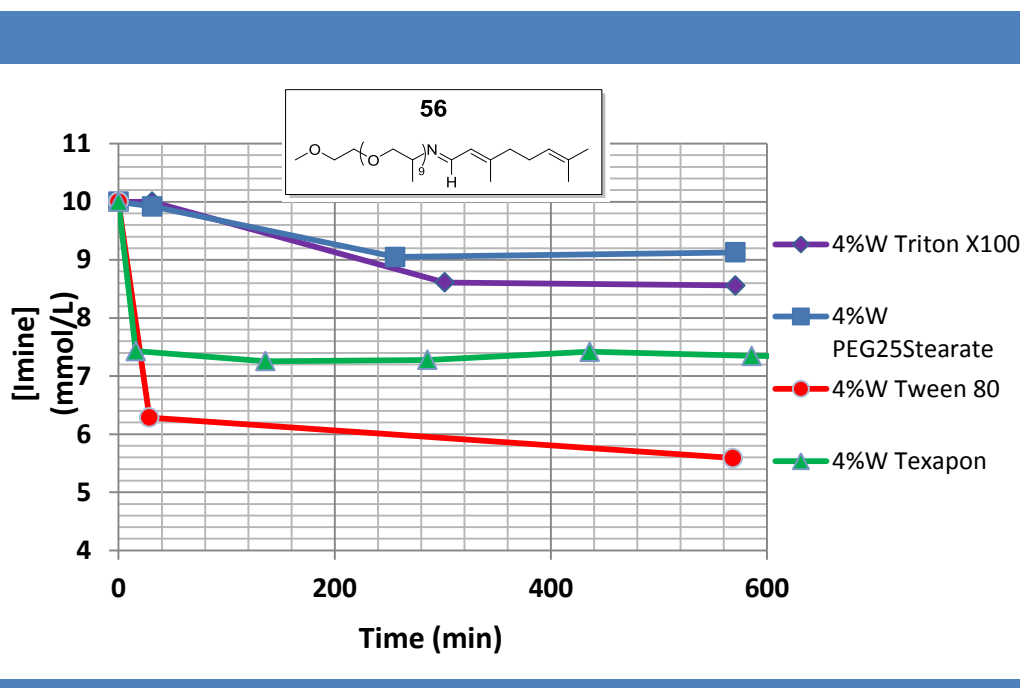


Figure 106 | Concentration as a function of time of M600 citral **56** in the presence of various non-ionic surfactants. ($C_0 = 10\text{mM}$, unmodified pD 10.4, surfactant concentration = 4wt%).

M600 citral imine **56** has a (very) high concentration at equilibrium with all the tested surfactants, showing that a wide range of micellar systems can efficiently encapsulate it as well as citral and M600. The high concentration of reactants inside the micelle core, coupled to the hydrophobic environment around the micelle (thus decreasing the local concentration in water), explains the high stability of these imines. Moreover, it can be noted that the higher the hydrophobicity of the chains of the surfactant, the higher the concentration of M600 citral imine **56** at equilibrium. The most hydrophobic tail, that of PEG₂₅ monostearate (18 carbons), yields a concentration at equilibrium of 9.1 mM whereas the smallest tail (Tween® 80, 12 carbons) yields a concentration of 5.6 mM. This result is probably due to the fact that larger tails produce a better solubilising environment for the hydrophobic imines, and are more efficient for preventing water from entering the micelle's core. The hydrolysis of M600 citral imine **56** at acidic pD was also performed under similar conditions than those used for M2070 imine **50**, in phosphate buffer at pD 5.8 (Figure 107).

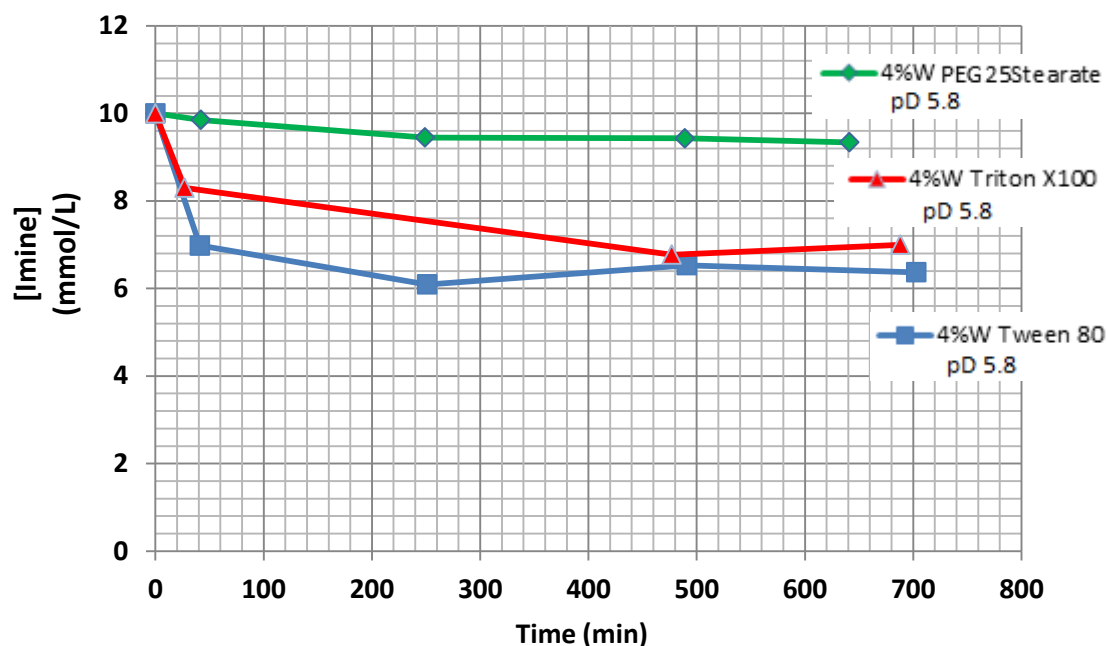


Figure 107 | Concentration as a function of time of M600 citral **56** in the presence of various non-ionic surfactants. ($C_0 = 10$ mM, phosphate buffer pD 5.8, surfactant concentration = 4wt%).

The stability of M600 citral **56** at pD 5.8 with the various surfactants is approximately the same as at pH 10.4, with even a higher concentrations of imine as in previous experiments in some cases (Table 25 for the concentration at equilibrium), proving that the phase separation of the imine into the hydrophobic micelle core is an efficient approach to avoid almost any contact between imine and water, thus stabilising the imine bond (and notably citral) until evaporation of the solvent or destruction of the micelles by dilution.

Table 25 | Concentration at equilibrium of M600 citral **56** in the presence of various surfactants at 10 mM (Unmodified pD and phosphate buffer pD 4.4).

Imine	pD (buffered)	Surfactant (4wt%)	C_{eq} (mM)
M600 citral	10.4	Peg ₂₅ Stearate	9.1
M600 citral	10.4	Triton®	8.6
M600 citral	10.4	Tween® 80	5.6
M600 citral	10.4	Texapon®	7.3

M600 citral	5.8	Peg ₂₅ Stearate	9.3
M600 citral	5.8	Triton®	7.0
M600 citral	5.8	Tween® 80	6.4
M600 citral	6.6	Texapon®	< 2

c) Influence of the concentration of co-surfactants

Although the effect on the kinetics of hydrolysis of the complex interactions of surfactants with the dynablocks has been understood for some key systems, the effect of the concentration of these surfactants has not been studied (all experiments were performed with a concentration of 4wt%). For this reason, it has been decided to vary the concentration of a surfactant of industrial interest, namely Texapon® (sodium laureth sulphate), that is usually used in liquid soaps. Its concentration has been varied from 2 to 10% by weight, the typical concentrations found in liquid soaps (Figure 108). These concentrations are all well above the CMC (2wt% \approx 6*CMC). The chosen dynablock for this experiment is M1000 hexylcinnamal **47**, for its slow hydrolysis and its cheap cost for mass production and introduction into consumer products.

No noticeable effect of the kinetics of hydrolysis was detected for all the concentrations of Texapon® tested, and M1000 hexylcinnamal **47** could be incorporated into formulations containing Texapon® (like body-wash formulations) whatever the concentration in sodium laureth sulphate.

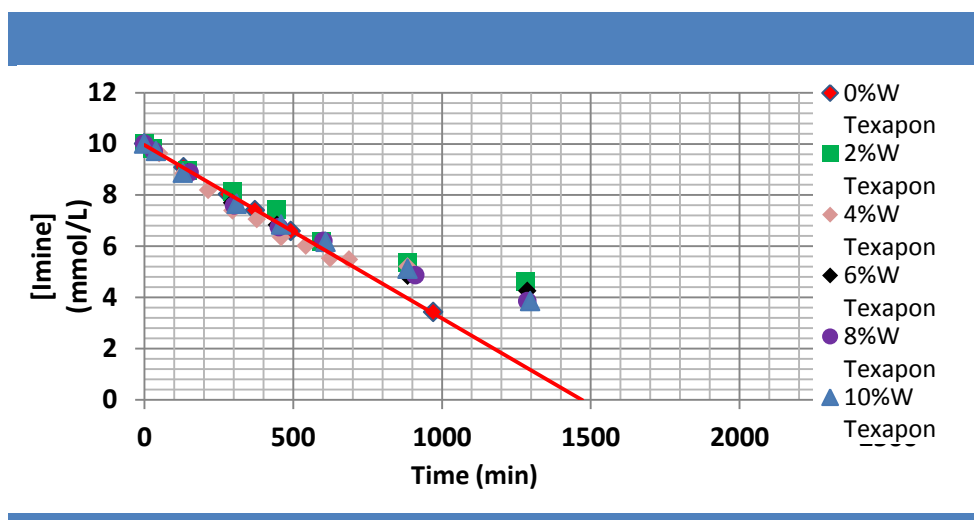


Figure 108 | Concentration as a function of time of M1000 Hexylcinnamal **47** in the presence of Texapon®. ($C_0 = 10$ mM, unmodified pD 10.5, Texapon® concentration = 2...10wt%).

d) Influence of the concentration of salt in liquid body wash

In section 4b, the slowdown of the hydrolysis of M1000 hexylcinnamal **47** was partially attributed to an increase of the viscosity that decreases the rate of dynamic exchange between the dynablocks in micelles and in solution. To understand the effect of viscosity, M1000 hexylcinnamal **47** was hydrolysed at 10 mM in the presence of Texapon® (4wt%) with different salt concentrations ranging from 0 to 10% by weight (Figure 109). The speed of hydrolysis was greatly reduced when the concentration of salt was increased, which proves that viscosity plays an important role in the kinetics of hydrolysis of M1000 hexylcinnamal **47**. The half-time of hydrolysis was increased from 0.71 days without salt to 1.74 days at a salt concentration of 5wt%. The salt concentration could not exceed 10wt%, due to the broadening of the imine and aldehyde peaks by NMR that was preventing their precise integration. The same phenomenon occurred at 10wt% after 900 minutes. We believe that it is possible to considerably slow down the hydrolysis with a high viscosity of the medium, but this has to be proven either by changing the thickener (use high molecular weight polymers for example) or by using other characterisation techniques (for instance UV spectroscopy). This result is important from an application point of view, since liquid body-wash formulations do not only contain surfactants (usually sodium laureth sulphate), but also thickening agents to increase the viscosity. These thickening agents are often acrylic acid polymers or salts, that increase the viscosity of anionic surfactant solutions.

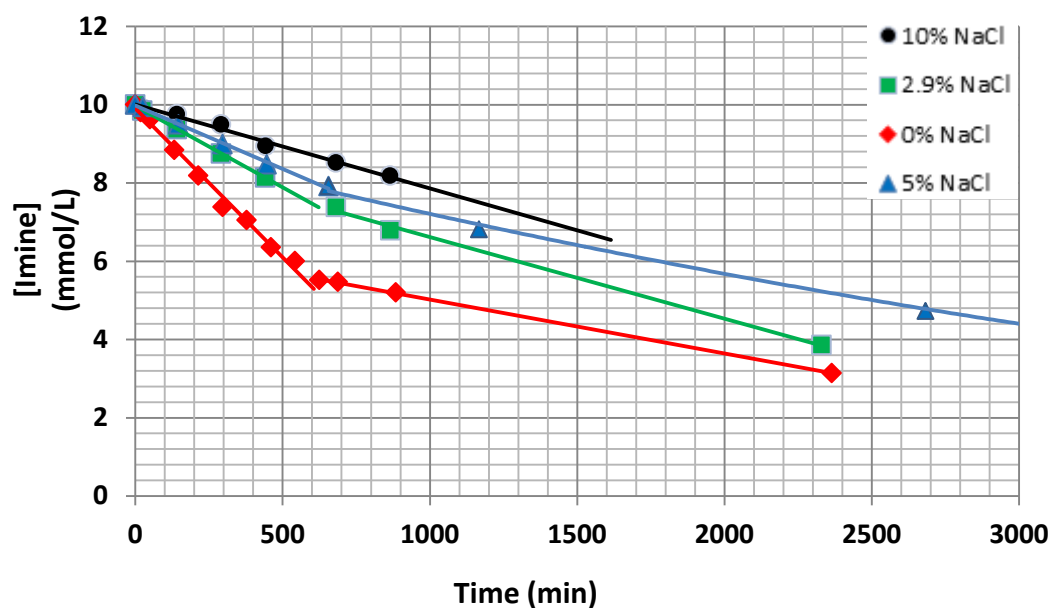


Figure 109 | Concentration as a function of time of M1000 Hexylcinnamal **47** in the presence of Texapon® with various salt concentrations. ($C_0 = 10$ mM, unmodified $9.6 < \text{pD} < 9.9$, salt concentration = 0...10 wt%).

The effect of salt concentration on the initial rate of hydrolysis and the half-time of hydrolysis of M1000 hexylcinnamal **47** is displayed in Figure 110 and Table 26.

Table 26 | Half-time of hydrolysis and initial rate of hydrolysis of M1000 hexylcinnamal **47** at 10 mM in the presence of Texapon® 4wt% and at various salt concentrations (unmodified pD, $0 < C_{\text{salt}} (\text{wt}\%) < 10$).

%NaCl	pD	$V_0 (10^{-3} \text{ min}^{-1})$	$H_{1/2} (\text{days})$
0	9.7	7.6	0,71
2,9	9.6	4.2	1,23
5	9.5	3.3	1,74
10	9.2	2.1	Not determined

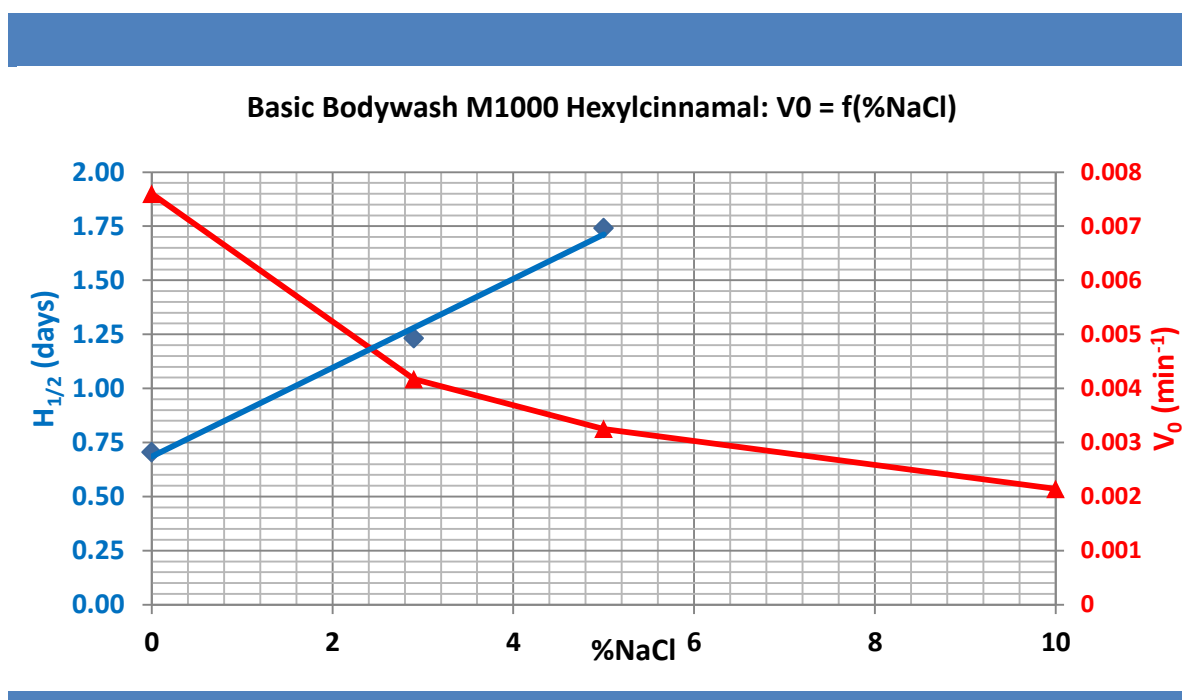


Figure 110 | Half-time of hydrolysis and initial rate of hydrolysis as a function of the mass percentage of NaCl in a 10 mM solution of M1000 hexylcinnamal **47** containing Texapon® at 4wt%. (unmodified pD).

The effect of the concentration of salt (0...20wt%) on the concentration at equilibrium of M1000 citral imine **48** at unmodified pD was also assessed, but no influence on the change of viscosity could be detected. This result was expected, since the high concentration at equilibrium of **48** comes from the high local concentration of the reactants in or at the interface of micelles, which are not influenced by viscosity. The kinetics of hydrolysis was also not influenced.

6/ Hydrolysis of profragrances in formulations

The key effects of several parameters such as viscosity or the presence of surfactants being understood, the integration of profragrances into formulation prototypes was investigated. Only the first three applications tested will be discussed in the thesis, but more applications incorporating these systems are under investigation and will not be discussed here in further detail for intellectual property reasons.

The kinetics of hydrolysis of profragrances were investigated in the following formulations:

- Basic body-wash. This could take advantage of a slower release of volatile fragrances triggered by dilution during its use. It also presents the advantage of being basic (pH \approx 10), the best pH range for imine stabilisation.
- Liquid detergent. This difficult application requires the discovery of new profragrances and releasing technologies.
- Solid soap. This application possesses the advantage of being both basic and solid (a state possibly stabilising the imine bond).

All systems were evaluated according to their stability in the formulation (a slow rate of hydrolysis or a high concentration at equilibrium will be seen as “better”, since they are more likely to provoke a slower release over time).

a) *Liquid body-wash*

A simple model of liquid body-wash was proposed by the formulators of Firmenich, and further adapted for ^1H NMR analysis (Table 27). The key ingredient is sodium laureth sulphate (Texapon®), already partially studied in Section 5b.

Table 27 | Proposed and adapted body-wash formulation.

Proposed body-wash formulation (pH \approx 10)		→	^1H NMR Adapted body-wash formulation (pD 10.5)	
Product	wt%		Product	wt%
KOH	6			
Texapon® solution (28% of surfactant)	14		Texapon® (dry) 4	
H ₂ O	79		D ₂ O 96	
Profragrance	1		Profragrance 10mM (= 1 wt%)	

i) Hexylcinnamal-based body-wash formulation

In Figure 111, the comparative hydrolysis rates between M1000 hexylcinnamal **47** and PEG₁₁NH₂ hexylcinnamal **51** in solution and in a basic body-wash formulation are displayed.

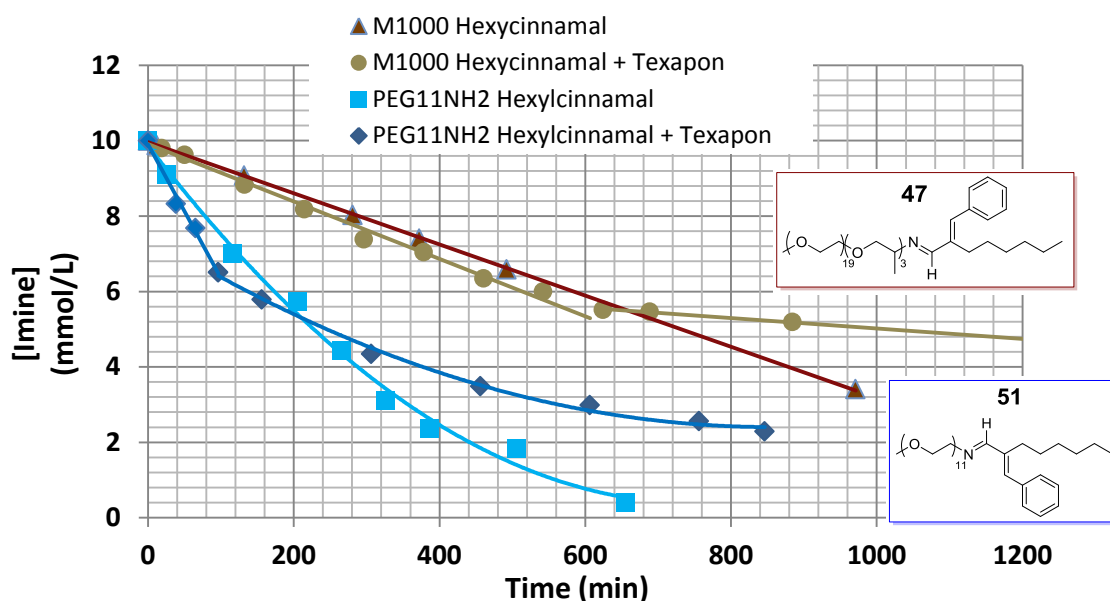


Figure 111 | Concentration as a function of time of M1000 hexylcinnamal **47** and PEG₁₁NH₂ hexylcinnamal **51** in solution and in a basic body-wash formulation. ($C_0 = 10$ mM, unmodified pD 10.5).

Both M1000 hexylcinnamal **47** and PEG₁₁NH₂ hexylcinnamal **51** are affected by the body-wash formulation in the same way: compared to these profragrances alone in solution, the initial hydrolysis rate is almost the same, but a stabilising effect appears during the hydrolysis, managing to increase slightly their half-time of hydrolysis and possibly an increase of the concentration at equilibrium (which is usually close to quantitative hydrolysis for hexylcinnamal-based profragrances at 10 mM). PEG₁₁NH₂ hexylcinnamal **51** is useful for this application if a releasing speed in hours is needed ($H_{1/2} = 4.3$ h), and M1000 hexylcinnamal **47** for releasing speed in the half-day range ($H_{1/2} = 17.0$ h).

M2070 hexylcinnamal **49**, which presents the same hydrolysis rate as M1000 hexylcinnamal **47** when hydrolysed alone in solution, keeps the same tendency in the body-wash, and even performs slightly better ($H_{1/2} = 17.5$ h, Figure 112).

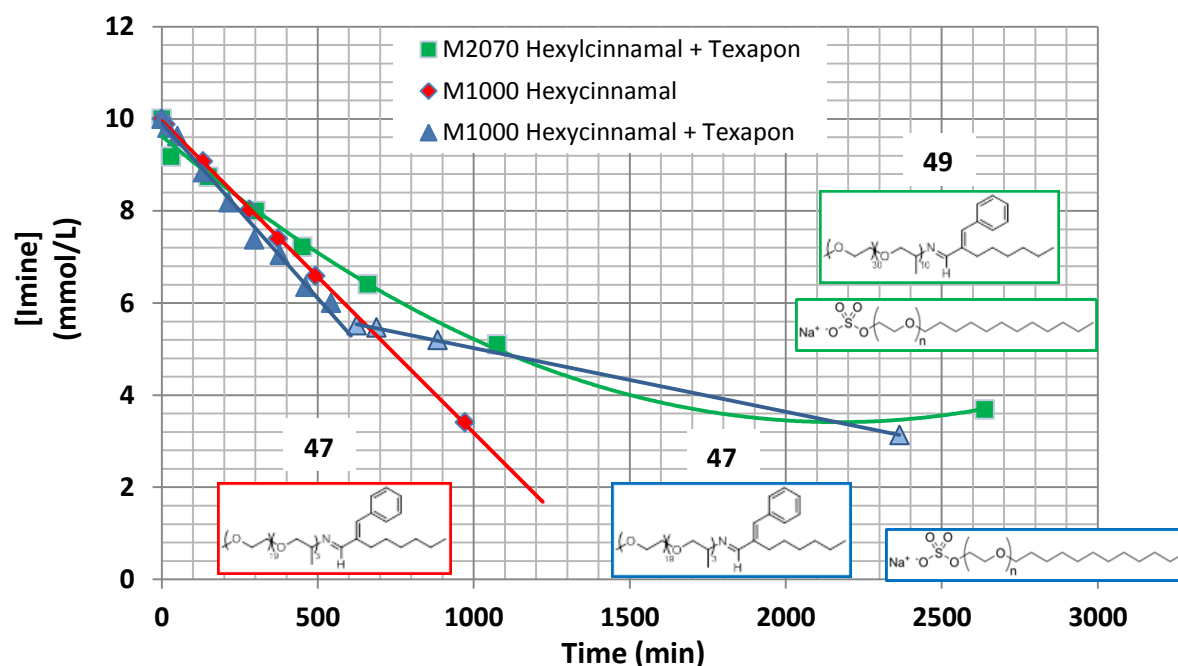


Figure 112 | Concentration as a function of time of M1000 hexylcinnamal **47** and M2070 hexylcinnamal **49** in solution and in a basic body-wash formulation. ($C_0 = 10$ mM, unmodified pD 10.5).

PEG₁₁tyramine hexylcinnamal **53**, which had a long half-time of hydrolysis when used alone in deuterium oxide ($H_{1/2} = 2.5$ days), is surprisingly much faster hydrolysed in the basic body-wash formulation ($H_{1/2} = 9.2$ hours) than when used alone, which makes it less efficient to use M1000 hexylcinnamal **47** in this formulation (Figure 113). These results can be partially explained by DOSY NMR:

- When used alone in solution, PEG₁₁tyramine hexylcinnamal **53** forms aggregates of 96 nm in solution, containing both the imine and the hydrolysed hexylcinnamal
- In the body-wash formulation, PEG₁₁Tyramine hexylcinnamal **53** forms 3 kinds of aggregates: one of 6.9 nm, containing notably PEG₁₁tyramine **9**, one of 1.1 nm containing almost all the imine and one at 0.6 nm containing all the aldehyde.

Even if the complicated DOSY NMR spectrum could not be fully understood, the fast rate of hydrolysis of PEG₁₁tyramine hexylcinnamal **53** in the body-wash formulation might be

explained by the presence of several types of aggregates, with a phase transfer of the aldehyde from the imine phase to another one, thus shifting the equilibrium toward imine hydrolysis by eliminating the aldehyde from the reactive medium.

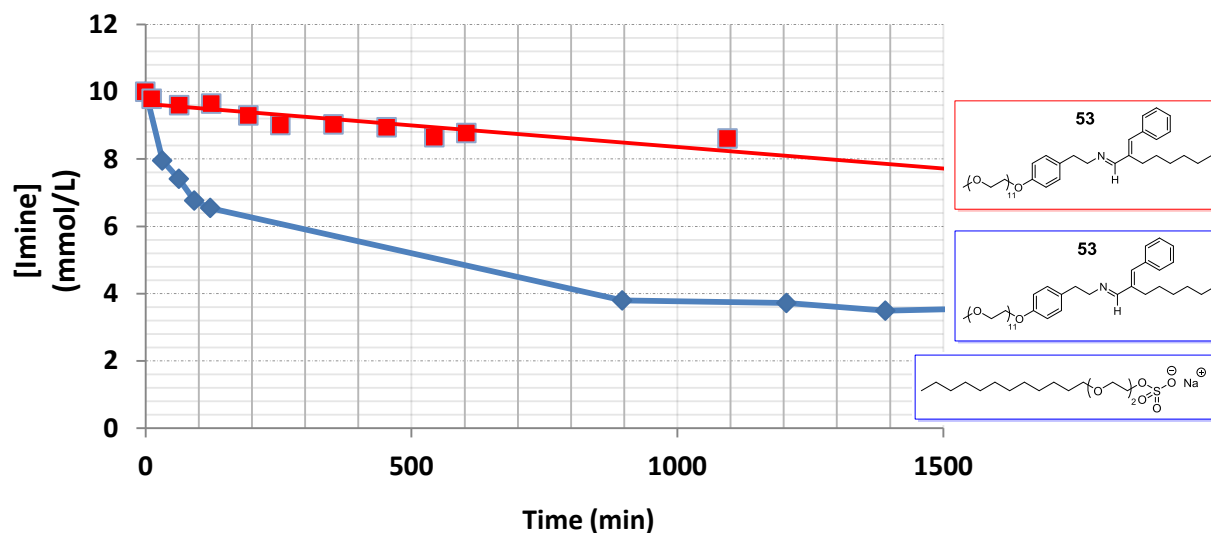


Figure 113 | Concentration as a function of time of PEG₁₁ tyramine hexylcinnamal **53** in solution and in a basic body-wash formulation. ($C_0 = 10$ mM, unmodified pD 10.5).

The difference when bring in the presence of Texapon® can also be detected by SANS: the radius of gyration is reduced from 2.2 to 1.3 nm, and the q -dependency in the middle q range is decreased from q^{-4} to q^{-3} (i.e. from a three-dimensional object with a relatively smooth surface to an object with a fractal surface), which is a sign of a change of geometry of the aggregates, possibly exposing more of the imine moiety to hydrolysis and thus increasing its speed of hydrolysis. Kinetic data is summarised in Table 28.

Table 28 | Half-time of hydrolysis and initial speed of hydrolysis for several profragrances in basic body-wash applications.

BASIC BODY-WASH				
Imine	C ₀ (mM)	pD (Unmodified)	V ₀ (10 ⁻³ mM/min)	H _{1/2} (hours)
PEG ₁₁ NH ₂ hexylcinnamal 51	10	10.5	35.4	4.3
M1000 hexylcinnamal 47	10	10.5	7.8	17.0
M2070 hexylcinnamal 49	10	10.5	Not determined	17.5
PEG ₁₁ tyramine Hexylcinnamal 53	10	10.6	Not determined	9.2

ii) Citral-based body-wash formulation

M1000 citral imine **48** and M2070 citral imine **50** were studied in the body-wash formulation (Figure 114). Their concentrations at equilibrium were considerably increased compared to that of M1000 citral imine **48** and M2070 citral imine **50** alone in solution at unmodified pD, and **50** proved to be that performing the best. The M1000 citral imine **48** concentration at equilibrium was increased from 2.9 to 6 mM, and M2070 citral imine **50** concentration at equilibrium was increased from 2.8 to 6.7 mM. This higher concentration of imine can be either due to the higher pD of the body-wash formulation, or to a stabilisation by the surfactants. Measurements of M1000 citral imine **48** alone in solution with a pD around 10 – 11 are necessary to reach a final conclusion.

Concentrations at equilibrium are summarised in Table 29.

Table 29 | Concentrations at equilibrium of several profragrances in basic body-wash applications and alone in solution.

Imine	Formulation	C ₀ (mM)	pD (Unmodified)	C _{eq} (mM)
M1000 Citral 48	Body-wash	10	11.9	6.0
M2070 Citral 50	Body-wash	10	10.7	6.7
M1000 Citral 48	Alone in solution	10	9.3	3.0
M2070 Citral 50	Alone in solution	10	9.7	2.8

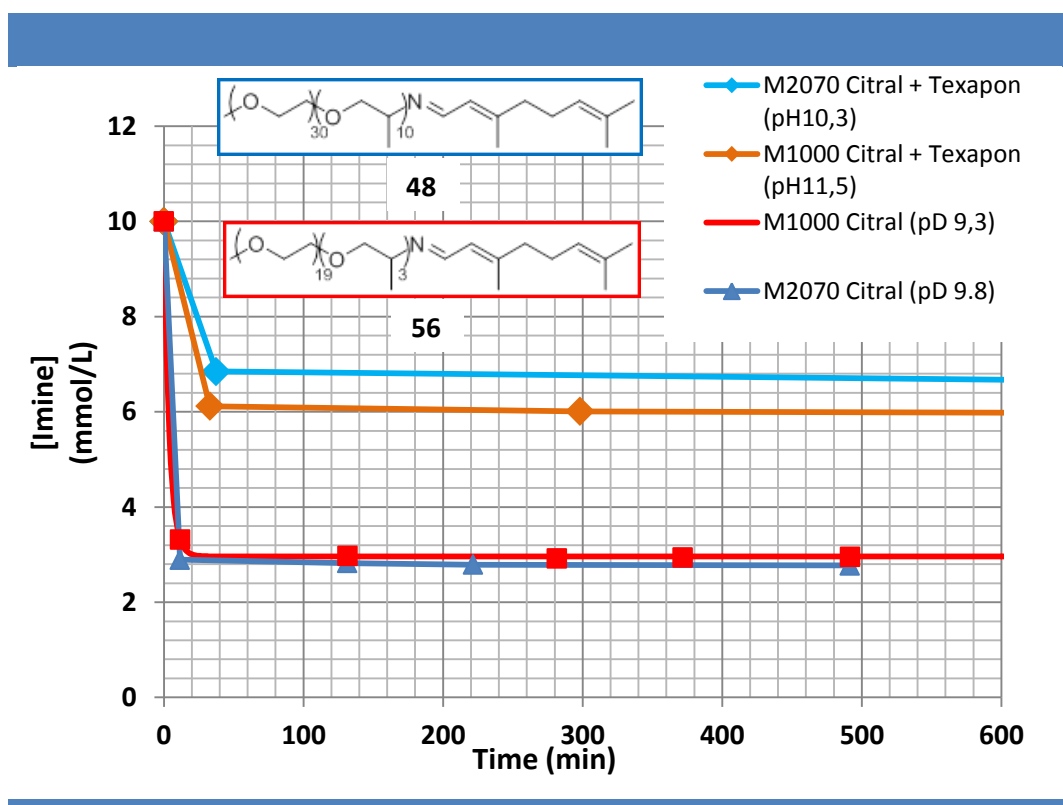


Figure 114 | Concentration as a function of time of M1000 citral **48** and M2070 citral **50** in solution and in a basic body-wash formulation. ($C_0 = 10$ mM, unmodified $10.7 < pD < 11.9$ for body-wash solutions, unmodified $9.3 < pD < 9.7$ for body-wash solutions).

b) Liquid Detergent

A simple model of a liquid detergent was proposed by the formulators of Firmenich, and further adapted for ^1H NMR analysis (Table 30). The key ingredients are Hostapur® SAS 30 (Sodium C14-17 sec-Alkyl sulphonate) and Genapol® LA70 (Ethoxylated C12-16 Alcohols). Unfortunately, no precise chemical structure for these compounds is available, but they are made of a mixture of anionic and non-ionic surfactants.

Table 30 | Adapted body-wash formulation

Product	wt%eight
Hostapur® SAS 30 (28% H_2O)	5.4
Genapol® LA70	17
D_2O	76.6
Profragrance	1

i) Hexylcinnamal-based detergent formulation

PEG₁₁tyramine hexylcinnamal imine **53**, although poorly stabilised by the presence of Texapon® in body-wash formulations, is hydrolysed only slightly faster in liquid detergent than alone in solution (Figure 115), with a half-time of hydrolysis reduced from 2.5 days to 1.8 day. However, it was not very resistant to the decrease of pD toward the near neutral zone (pD 8.2) with a decrease half-time of hydrolysis of 15 hours.

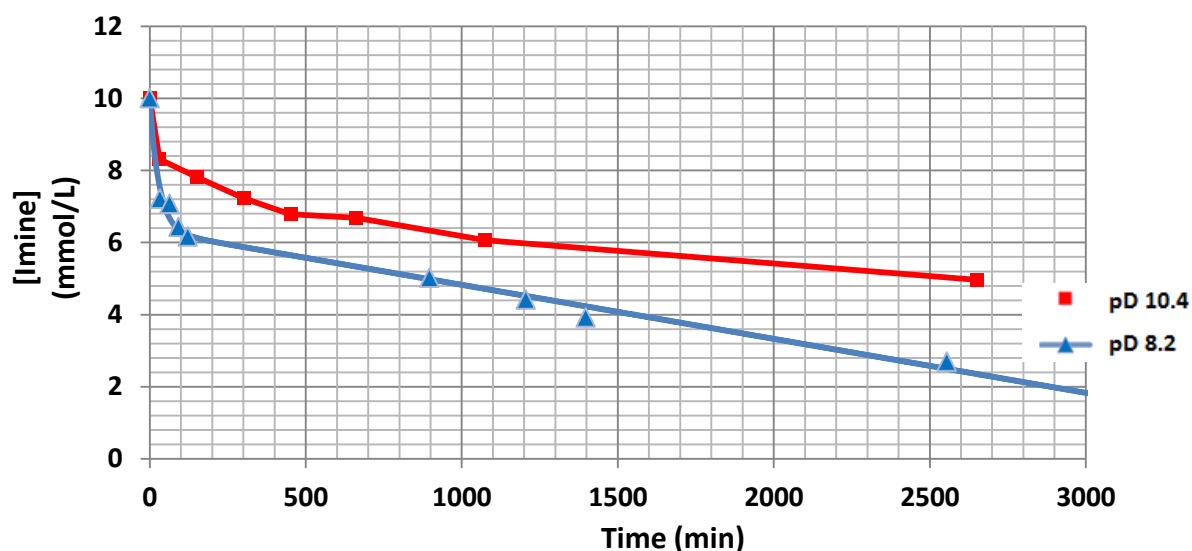


Figure 115 | Concentration as a function of time of PEG₁₁tyramine hexylcinnamal imine **53** in solution and in a liquide detergent formulation at basic and near neutral pD. ($C_0 = 10$ mM, pD 8.2 and 10.4).

M1000 hexylcinnamal imine **47** performed very similarly as PEG₁₁tyramine hexylcinnamal imine **53** under basic conditions (**47**: $H_{1/2} = 41$ hours, **53**: $H_{1/2} = 42.5$ hours), but was performing much better than **47** under nearly neutral conditions with a half-time of hydrolysis of 35 hours (Figure 116).

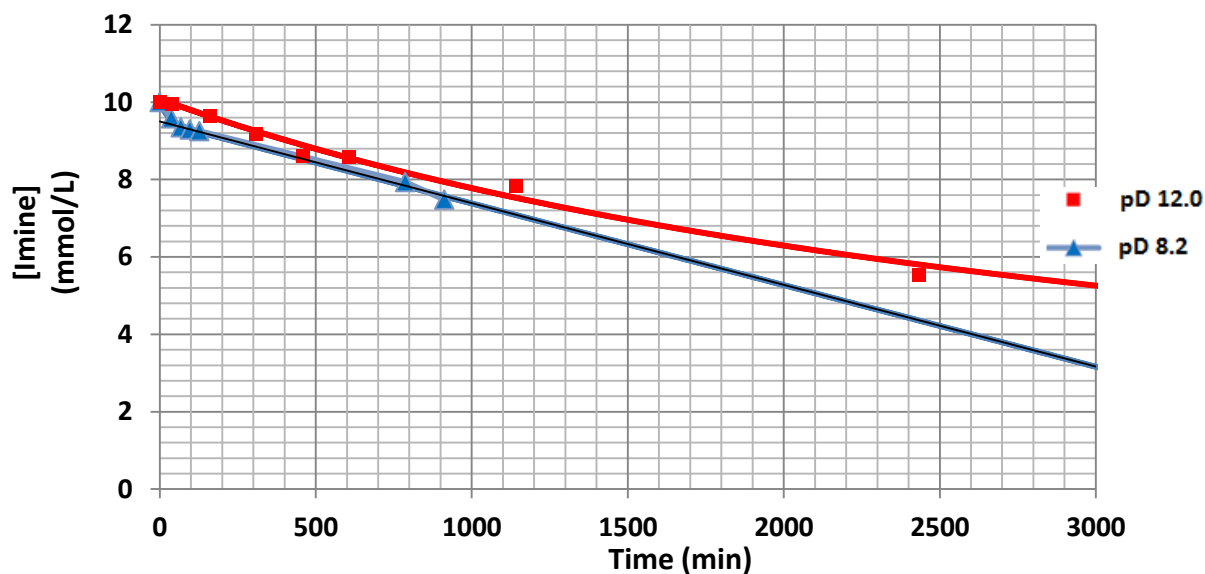


Figure 116 | Concentration as a function of time of M1000 hexylcinnamal imine **47** in solution and in a liquid detergent formulation at basic and near neutral pD. ($C_0 = 10$ mM, pD 8.2 and 12.0).

Overall both systems were performing quite well in this liquid detergent formulation. Kinetic data are summarized in Table 31.

Table 31 | Half-time of hydrolysis and initial speed of hydrolysis for several profragrances in liquid detergent applications.

LIQUID DETERGENT				
Imine	C_0 (mM)	pD (Unmodified)	V_0 (10^{-3} mM/min)	$H_{1/2}$ estimated (hours)
M1000 hexylcinnamal 47	10	12.0	2.2	41
M1000 hexylcinnamal 47	10	8.2	2.2	35.0
PEG ₁₁ tyramine Hexylcinnamal 53	10	10.4	Not determined	42.5
PEG ₁₁ tyramine Hexylcinnamal 53	10	8.2	Not determined	15

ii) Citral-based detergent formulation

In Figure 117, one can see that in this formulation, M1000 citral imine **48** was poorly stabilised in comparison to its behaviour alone in solution (concentration at equilibrium increased from 3.0 to 3.5 mM), and the concentration at equilibrium of M600 citral imine **56** was lower than when it is used with Texapon® (concentration at equilibrium of 6.0 mM in the liquid detergent formulation, and of 7.3 mM in the body-wash formulation).

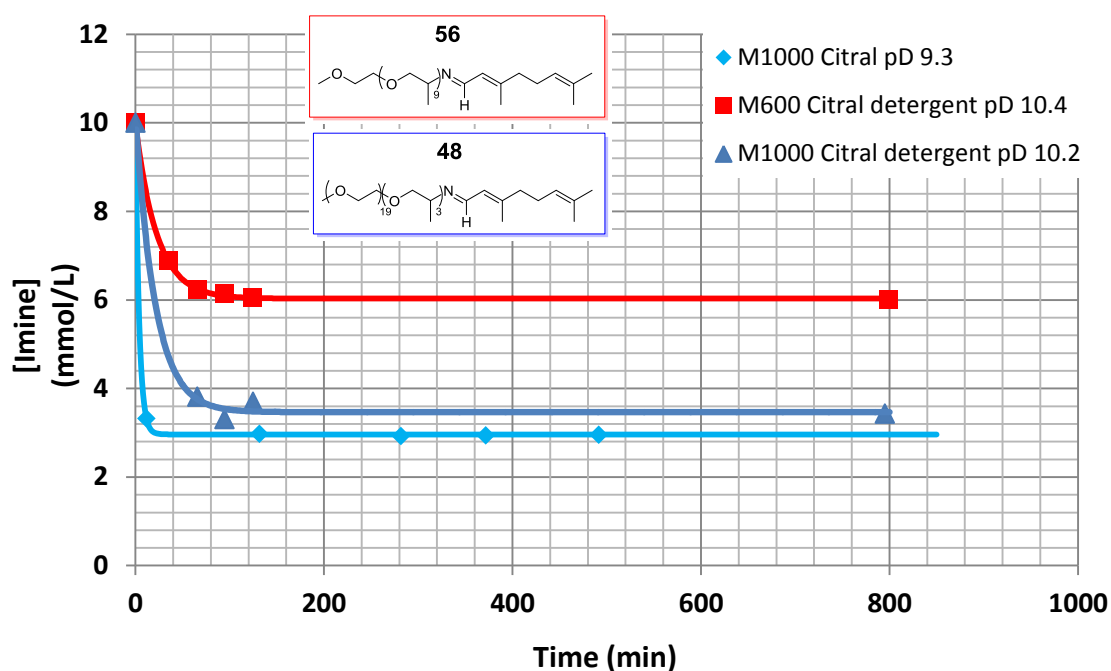


Figure 117 | Concentration as a function of time of M1000 citral imine **48** and M600 citral imine **56** in a liquid detergent formulation at basic and near neutral pD. ($C_0 = 10\text{mM}$).

This liquid detergent formulation does not seem to enhance or to decrease the stability of M1000 citral imine **48**. However, the concentration at equilibrium of M600 citral imine **56** in this formulation is lower ($C_{\text{eq}} = 6.0\text{ mM}$) than in the body-wash ($C_{\text{eq}} = 7.3\text{ mM}$).

Concentrations at equilibrium are summarised in Table 32.

Table 32 | Concentrations at equilibrium of several profragrances in liquid detergent, body-wash and alone in solution.

Imine	Formulation	C ₀ (mM)	pD (Unmodified)	C _{eq} (mM)
M1000 Citral 48	Liquid detergent	10	10.2	3.5
M600 Citral 56	Liquid detergent	10	10.4	6.0
M1000 Citral 48	Alone in solution	10	9.3	3.0
M600 Citral 56	Body-wash	10	10.4	7.3

c) Solid Soap

A simple recipe of solid soap was proposed by the formulators of Firmenich, and further adapted for ¹H NMR analysis (Table 33). The key ingredients are Texapon® and three fatty acids (lauric acid, myristic acid and stearic acid) plus a base.

Table 33 | Proposed and adapted body-wash formulation

Product	wt%eight	Product	wt%eight
Texapon® solution (28%Surfactant)	14	Texapon® (dry)	3.92
H ₂ O	58.7	D ₂ O	63.75
Lauric acid	14.5	Lauric acid	14.5
Myristic acid	4.8	Myristic acid	4.8
Stearic acid	1	Stearic acid	1
KOH	6	NaOD 40% in D ₂ O	11
Profragrance	1	Profragrance	1

The kinetics of hydrolysis of M1000 hexylcinnamal **47** in the solid soap formulation was measured by taking at several moments 100 mg of the soap and by diluting it 10 times to follow the imine concentration inside the soap (Figure 118). The kinetics of hydrolysis of M1000 hexylcinnamal **47** in the diluted soap solution was measured twice at t = 5 hours and at t = 15 days. It results in a relatively high concentration at equilibrium (5.3 mM) for a hexylcinnamal-based profragrance. This imine at equilibrium enables both a “blooming” effect when dissolved into water (by the rapid evaporation of the hexylcinnamal), and a long-lasting effect due to slow hydrolysis of the remaining imine.

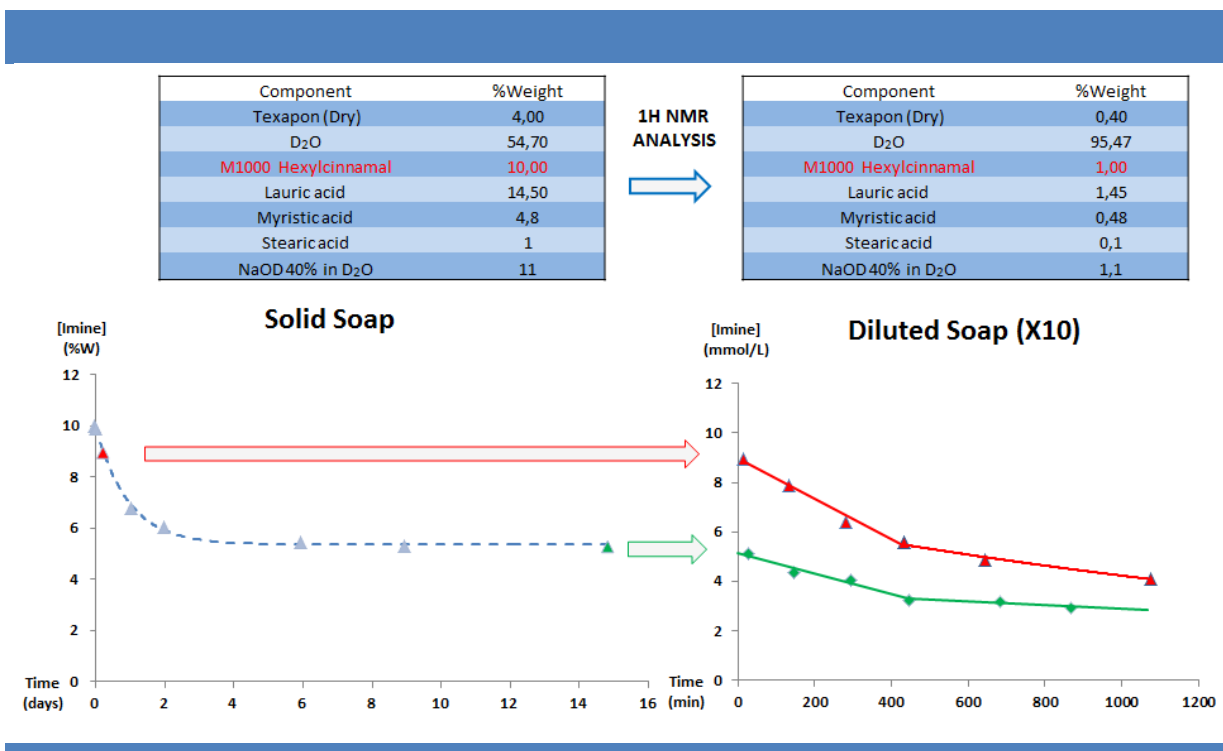


Figure 118 | Kinetics of hydrolysis of M1000 Hexylcinnamal **47** in a solid soap formulation. Kinetic was followed by ¹H NMR by taking a sample of the soap containing the profragrance (100 mg) and by diluting it ten times. The kinetics of hydrolysis of M1000 Hexylcinnamal **47** was also performed twice on the diluted soap sample. Curve **red** is after 5 hours of hydrolysis in the soap and **green** is after 15 days in the soap.

The same experiment was performed with M1000 citral imine **48** (Figure 119). When diluted 10 times, the soap solution containing **48** always had a concentration of 7.2 mM at equilibrium. Since this imine is sensitive to dilution, it means that the imine concentration inside the soap is probably much higher than the 7.2 mM measured.

Component	%Weight	Component	%Weight
Texapon (Dry)	4,00	Texapon (Dry)	0,40
D ₂ O	54,70	D ₂ O	95,47
M1000 Citral	10,00	M1000 Citral	1,00
Lauric acid	14,50	Lauric acid	1,45
Myristic acid	4,8	Myristic acid	0,48
Stearic acid	1	Stearic acid	0,1
NaOD 40% in D ₂ O	11	NaOD 40% in D ₂ O	1,1

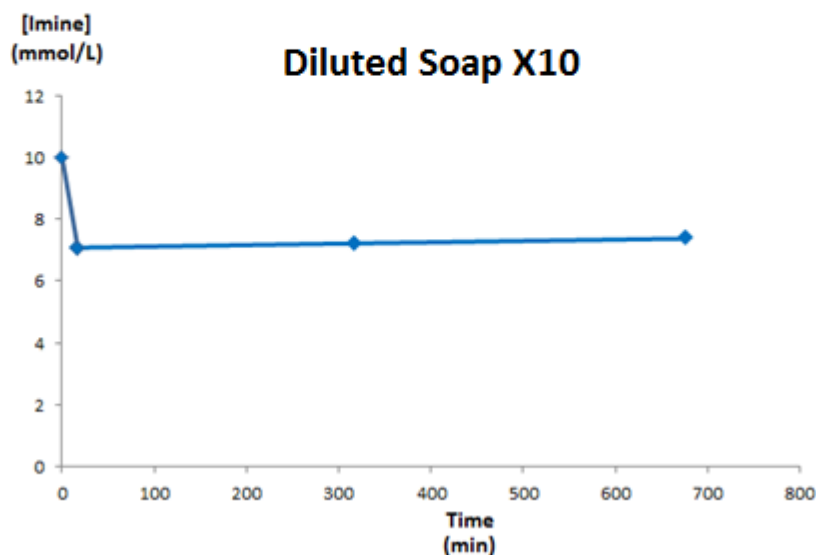


Figure 119 | Kinetics of hydrolysis of M1000 citral **48** in a solid soap formulation. Kinetic was followed by ¹H NMR by taking a sample of the soap containing the profragrance (100 mg) and by diluting it ten times.

As a conclusion, solid soaps enable to keep a high concentration of imine at equilibrium, which then get hydrolysed with a known rate when diluted. Dynablocks are a promising technology to develop new systems for the controlled release of fragrance aldehydes from solid soap, but also probably from any solid compound stored at low humidity that can keep a very high imine concentration until its use.

7/ Conclusion

A guide to choose the “best” dynablock (lower hydrolysis rate or high concentration at equilibrium) according to the aldehyde to release and according to the targeted application is available in Table 34. Since most fragrances evaporate rapidly when in contact with air, the aim of controlled delivery technologies is to increase the retention time of fragrances inside formulations. For this reason, a dynablock will be considered as a more efficient releasing system if it can keep aldehydes under non-volatile imine forms as long as possible (it still has to be hydrolysable though).

Table 34 | Guide to choose the “best” dynablock according to the aldehyde to release and to the targeted application.

Application	Aldehyde to release	Best Dynablock
Basic Body-wash	Hexylcinnamal ($H_{1/2}$ in hours)	M2070 Hexylcinnamal imine 49 (17.5)
	Citral (C_{eq} in mM)	M2070 Citral imine 50 (6.7)
Basic Detergent	Hexylcinnamal ($H_{1/2}$ in hours)	PEG ₁₁ Tyramine Hexylcinnamal imine 53 (42.5)
	Citral (C_{eq} in mM)	M600 Citral imine 56 (6.0)
Basic Solid soap	Hexylcinnamal (C_{eq} in mM)	M1000 Hexylcinnamal imine 47 (5.3 mM after 4 days)
	Citral (C_{eq} in mM)	Not Tested
		M1000 Citral imine 48 (7.2 mM)
Neutral Detergent	Hexylcinnamal ($H_{1/2}$ in hours)	M1000 Hexylcinnamal imine 47 (35.0)
	Citral (C_{eq} in mM)	Not Tested

A guide to choose the “best” dynablock to release citral (that leading to the higher concentration at equilibrium) according to the chosen surfactant family and the pD is available in Table 35. Some surfactant families were not tested for some profragrances for the following reasons:

- Its stability was expected to be low due to its similarity with a closely related profragrance.
- It was not very stable under basic conditions, so it was not tested under acid condition.

Table 35 | Guide to choose the “best” dynablock to release citral according to the chosen surfactant family and the pD.

Condi- tions	pD	Dynablock used for release		Anionic surfactants	Cationic surfactants	Non-ionic surfactants
Basic	10.5	M1000 Citral 48	Tested?	YES	YES	YES
			Best surfactant? (C _{eq} in mM)	SDS (8.9)	Certrimonium bromide (4.8)	Not efficient (2.8)
		M2070 Citral 50	Tested?	YES	NO	YES
			Best surfactant? (C _{eq} in mM)	Texapon® (6.9)	X	PEG ₂₅ Steara te (7.5)
	M600 Citral 56	Tested?	YES	NO	YES	
		Best surfactant? (C _{eq} in mM)	Texapon® (7.3)	X	PEG ₂₅ Steara te (9.1)	
Acidic	4.4	M1000 Citral 48	Tested?	NO	NO	NO
			Best surfactant? (C _{eq} in mM)	X	X	X
	4.4	M2070 Citral 50	Tested?	NO	NO	YES
			Best surfactant? (C _{eq} in mM)	X	X	PEG ₂₅ Steara te (6.4)
	5.8	M600 Citral 56	Tested?	YES	NO	YES
			Best surfactant? (C _{eq} in mM)	Not efficient (<2)	X	PEG ₂₅ Steara te (9.3)

A guide to choose the “best” dynablock to release hexylcinnamal (that leading to slow hydrolysis rate) according to the chosen surfactant family and the pD is available in Table 36. The table needs to be completed by additional experiments.

Table 36 | Guide to choose the “best” dynablock to release hexylcinnamal according to the chosen surfactant family and the pD.

Conditions	pD	Dynablock used for release		Anionic surfactants	Cationic surfactants	Non-ionic surfactants
Basic (pD 10.5)	10.5	M1000 Hexylcinnamal 47	Tested?	YES	YES	YES
			Best surfactant? (H _{1/2} in hours)	Texapon® (17.0)	Certrimonium bromide (43.1)	Triton® X-100 (43.4)
		PEG ₁₁ NH ₂ Hexylcinnamal 51	Tested?	YES	NO	NO
			Best surfactant? (H _{1/2} in hours)	Texapon® (4.3)	X	X
		M2070 Hexylcinnamal 49	Tested?	YES	NO	NO
			Best surfactant? (H _{1/2} in hours)	Texapon® (17.5)	X	X
		PEG ₁₁ Tyramine Hexylcinnamal 53	Tested?	YES	NO	NO
			Best surfactant? (H _{1/2} in hours)	Texapon® (9.2)	X	X

Conclusions and Perspectives

Dynablocks, involving dynamic covalent molecular associations between a hydrophilic and a hydrophobic block, can form biocompatible responsive micelles in aqueous solution. During my Ph.D. I have developed further these new systems and extended their implementation in the field of the controlled release of fragrance volatiles.

Two approaches were used to achieve a slower releasing time of the volatiles from aqueous solution: i) the encapsulation of hydrophobic volatiles into the core of a micelle and ii) their incorporation into profragrances. The change of the hydrolysis rate of the imines in micelles when decreasing the pH or the concentration was determined for numerous imines, helping us to understand the intensity of the triggers that has to be applied to provoke the controlled release according to the imine used.

The stability of a dynablock in solution results from two parameters: its supramolecular structure and the type of imine bond used. The structural stabilisation of easily hydrolysable imine bonds in water was achieved, thanks to the addition of different hydrophobic linkers between the hydrophilic block and the imine moiety. When increasing the hydrophobicity of the linkers, the kinetics of hydrolysis shifted from pseudo-first order kinetic to a pseudo-zero order relationship. This result was interpreted as a transition from the “classical” hydrolysis of all the imine molecules in the presence of an excess of water to the hydrolysis of only a small part of imines that are free in solution (at a concentration equal to CMC, the rest of the molecules being protected in the self-assembly). The size of the hydrophobic block was also a key parameter, since it controls the CMC and thus the speed of hydrolysis of the unimers.

The hydrolytic ability of several imine-type bonds was also investigated, furnishing a wide range of hydrolysis rates from a hour time scale in basic conditions with aliphatic amines (not structurally stabilised), to days for amines with aromatic linkers or weeks with the semicarbazone.

The hydrolysis rate of imine profragrances under various conditions (pH, concentration, presence of co-surfactants...) was also investigated, and they were incorporated into industrial formulations. The information extracted from this work (half-time of hydrolysis, concentration at equilibrium, compatibility with surfactants) is important to predict the compability of the profragrances with a given application. The fact that some of them can be

synthesised in one step from cheap commercial sources is a great asset for its incorporation into consumer products. Moreover, the stabilisation of citral in acidic solution was achieved, which is an important result considering the industrial importance of this widely used aldehyde very challenging to stabilise. These results could extend the use of this fragrance to new applications and dynablocks are currently extensively studied by Firmenich under real conditions of applications.

The possible extensions of this work are multiple. First, the study of the interactions between dynablocks and co-surfactants should be extended to more kinds of surfactants, since only one cationic surfactant and two anionic surfactants have been tested. The structure of these mixed micelles should also be understood by an in-depth interpretation of the SANS measurements. This is currently under investigation in our laboratory.

It is also possible to try to further improve the stability of the imines made of aliphatic amines in solution. I believe that an ideal structure to reach this goal would be an imine made of the condensation of a hydrophobic aldehyde (a fragrance for example) with an amphiphilic amine, the amine moiety being located at the end of the hydrophobic chain. A proposed amine would be a PEG_nStearate-NH₂. Since the aldehyde would be hydrophobic and the amine an amphiphile, both would stay in the micellar structure thus shifting the equilibrium strongly toward imine formation, while protecting the imine by a strongly hydrophobic environment (plus a low CMC). This kind of system might also be able to store poorly hydrophobic molecules inside the micelle, or stabilise in aqueous solution molecules that are prone to hydrolysis.

Another project that could emerge from this work is related to the design of a new (non-dynamic) pro-drug for the controlled release of oximes thanks to the aqueous hydrolysis of acyloximes. Since these molecules are very tunable, it might be possible to get a wide range of hydrolysis times.

EXPERIMENTAL PART

Experimental part

Syntheses and characterization of organic compounds

1/ Background on the experimental methods for the analyses of dynablocks

In order to understand and design new dynablocks, it is necessary to characterise in details their self-assemblies in water. Dynablocks can be analysed at two length scales (Figure 120):

- At the molecular scale: the chemical structure and the condensation of the blocks can be followed by ^1H NMR.
- At the supramolecular scale: the size and the geometry of the structures can be measured by scattering techniques.

A suitable technique for the correlation between the molecular and the supramolecular scale is the diffusion-ordered spectroscopy (DOSY) NMR, a 2D NMR technique that permits to correlate ^1H NMR signals of a mixture of compounds with its diffusion coefficients, and thus to its hydrodynamic radius through the Stoke-Einstein equation.

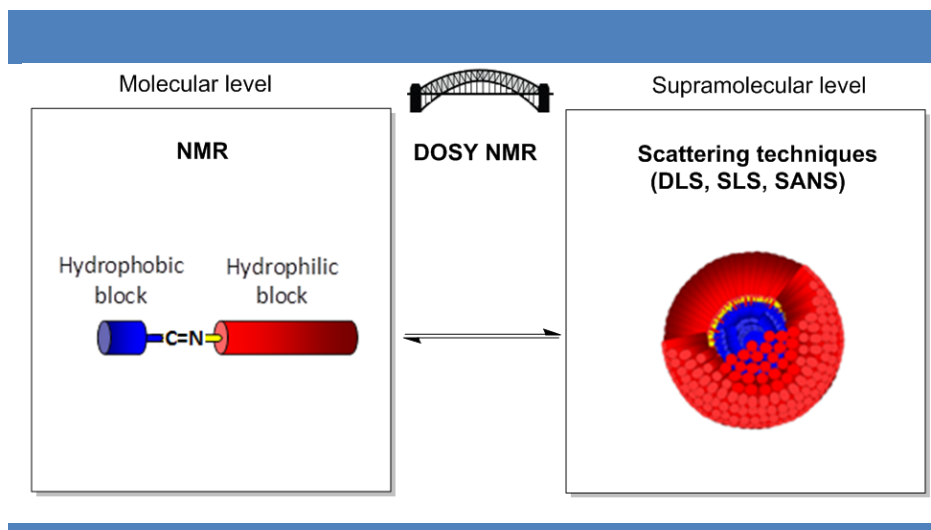


Figure 120 | Representation of the two levels of organisation of dynablocks and characterisation tools for the determination of their structures.

In the following sections, a brief presentation of the theory of scattering techniques and DOSY NMR will be exposed.

Concept

Small angle scattering (SAS) is the name given to the techniques of small angle neutron (SANS), X-ray (SAXS) and light scattering (SLS for static and DLS for dynamic light scattering). For all these techniques, radiation is elastically scattered by a sample and the resulting scattering pattern is analysed to provide information about the size, shape and orientation of some components of the sample. Although all these techniques use different type of radiations and probe different length scales, they also share similarities. They all use the same basic equations (Guinier, Zimm, Kratky, Porod) and are efficient for elucidating the structure, interaction, and phase transitions in micellar and colloid systems.^{[207][208]}

The way the radiation interacts with the sample depends on the electronic or nuclear structure of the considered matter and on the nature of the radiation. In a typical experiment of radiation scattering (example Figure 121 in the case of SANS), the monochromatic incident ray that go through the sample can be characterized by a wave vector k_i , and the scattered ray by a wave vector k_d . The norms of these vectors are defined as:

$$|\vec{k}_i| = \frac{2\pi n}{\lambda_i} \quad |\vec{k}_d| = \frac{2\pi n}{\lambda_d}$$

where λ_i and λ_d are the incident and scattered wavelength in vacuum, and n the refraction index of the environment.

The transfer wave vector q is defined as the vectorial difference between the incident vector and the scattered vector, and in the case of absence of energy transfer (elastic diffusion), $|\vec{k}_i| = |\vec{k}_d|$ and the modulus of the transfer wave vector is $|\vec{q}| = \frac{4\pi n}{\lambda_i} \sin \frac{\theta}{2}$ (θ is the diffusion angle, i.e. the angle between the vector k_i and k_d , see Figure 121).

^[207] Cazabat, M. A. In *Physics of Amphiphiles: Micelles, Vesicles and MEs*, Degiorgio, V.; Corti, M.; (Eds.), Amsterdam: North-Holland Physics Publishing (1985).

^[208] Chen, S. H., Small-Angle Neutron-Scattering Studies of the Structure and Interaction in Micellar and Microemulsion Systems. *Annu Rev Phys Chem*, **37**, 351-399 (1986)

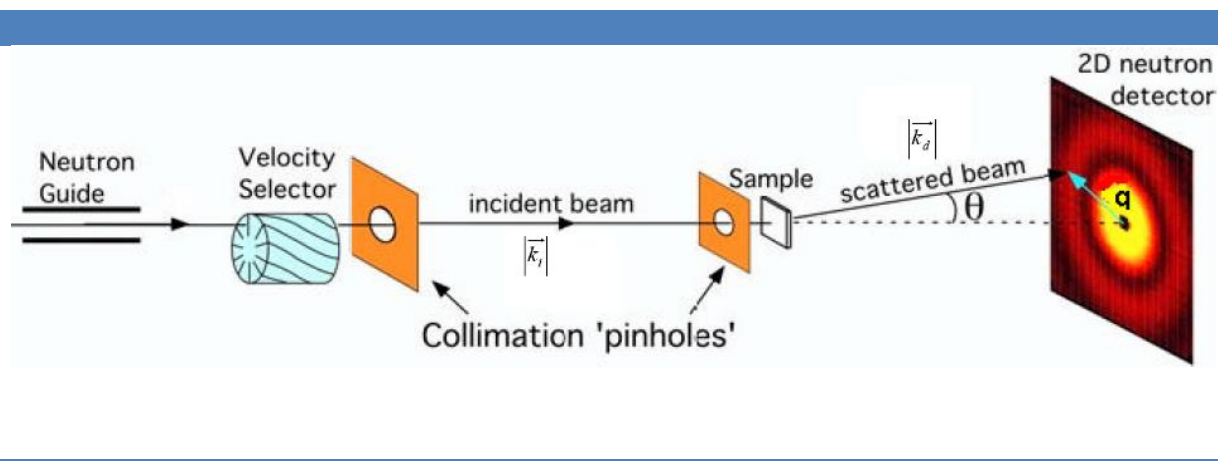


Figure 121 | Typical Small Angle neutron scattering setting.^[209]

The inverse of the modulus of the wave vector, q^{-1} , determines the observation scale of the system. This observation scale is fixed by the diffusion angle θ and the incident wavelength λ_i . Since the incident wavelength λ_i and the diffusion angle θ vary from scattering technique to another, the observation scale also varies:

$$\text{SLS: } 300 < q^{-1} (\text{\AA}) < 2000$$

$$\text{SAXS/SANS: } 2 < q^{-1} (\text{\AA}) < 300$$

In the case of a macromolecular solution, the intensity is a function of the form factor and the structure factor. For spherical symmetry particles, the intensity for N macromolecules is given by the following equation:

$$I(q) = A_0^2 f^2 NP(q)S(q)$$

The normalized structure factor of the solution $S(q)$ measures the spatial correlations between all the macromolecules and gives information on the global structure of the solution. The form factor $P(q)$ measures the correlations between the diffusers of the object and provides information on the form, the mass, and the size of the particles and gives access to the individual properties of particles, and their intramolecular correlations. According to the geometry of the objects, the form factors can be calculated.

^[209] Shukla, A. Characterization of microemulsions using small angle scattering techniques. PhD thesis, Martin-Luther-Universität Halle-Wittenberg (2003)

Light scattering

Light scattering is a technique used for the study of dynamics and structures of macromolecular and colloidal solutions. Two types of experiment can be performed:

Dynamic light scattering (DLS)

Quasi-elastic or dynamic light scattering that is a technique that measures Brownian motion of particles in suspension in a liquid and relates this to the size of these particles. This is done by measuring the size-dependent rate at which the intensity of the scattered light fluctuates when detected using a suitable optical arrangement^[210]. The small particles cause the intensity to fluctuate more rapidly than the large ones. The rate of the fluctuation of the intensity furnishes the diffusion coefficient D , and knowing the temperature T and the viscosity η , the hydrodynamic diameter d can be calculated using the Stokes-Einstein equation:

$$d(H) = \frac{kT}{3\pi\eta D}$$

The diameter that is obtained by this technique is the diameter of a sphere that has the same translational diffusion coefficient as the particle.

Small angle neutron scattering (SANS)

In SANS, it is possible to get the molecular weight, the geometry and the size of particles in a similar way that it is done with SLS, but with more detailed and with bigger wave vector q (for smaller particle sizes). The wavelength (usually of several angstroms) can be selected according to the experiment thanks to the selection of neutrons with a given speed going out of the reactor (Figure 121). For a given wavelength, the wave vector domain is chosen by changing the distance between the sample and the detector and many configurations are possible in order to have information at different scale lengths. Several measurements with different configurations can be performed and the global spectrum is obtained by combining the experiment done at all the configurations.

In neutron scattering, the diffusing particles are the core of the atoms, and as a consequence, the measured intensity has to be analysed by taking the background noise and the transmission of the samples into account.

^[210] Malvern, DLS technical note MRK656-01.

For polymer solutions, the diffused intensity is linked to the intra-chain diffusion factor $S_1(q)$ and to the inter-chain diffusion factor $S_2(q)$ through the following equation:

$$I(q)(\text{cm}^{-1}) = \frac{1}{V} \frac{d\sigma}{d\Omega} = (\Delta\rho)^2 (S_1(q) + S_2(q)) = (\Delta\rho)^2 (\Phi_{\text{vol}} V_{\text{chain}} P(q) + S_2(q))$$

with, $P(q)$ as the form factor, $(\Delta\rho)^2$ the contrast factor per unit of volume between the polymer and the solvent, Φ_{vol} the volume fraction of monomers and V_{chain} the volume occupied by the N monomers of one chain. Contrast $(\Delta\rho)^2$ is determined from the chemical composition of the system

DOSY NMR

First introduced in 1992 by K. F. Morris, DOSY NMR is a convenient technique that provides a two dimensional spectrum (2D NMR) by correlating ^1H NMR chemical shift signals of molecules in solution with the diffusion behaviour of the physical species (molecules or aggregates) in solution.^{[211][212]}

Diffusion-ordered spectroscopy (DOSY) NMR is based on a pulse-field gradient spin-echo NMR experiment, in which components experience diffusion. Consequently, the signal of each component decays with different diffusion rates as the gradient strength increases, constructing a bilinear NMR data set of a mixture. By calculating the diffusion coefficient for each component, it is possible to obtain a two-dimensional NMR spectrum: one dimension is for the conventional chemical shift and the other for the diffusion coefficient.^[213]

The diffusion coefficient is related to the Brownian motion of the species in their environment, and is dependent on their size, shape, mass, and charge. Like in the case of DLS, it is possible to calculate the hydrodynamic radius of the aggregates in solution using the Stokes-Einstein equation. DOSY NMR experiments are easy to perform, and can non-

^[211] Morris, K. F.; Johnson Jr., C. S. Resolution of discrete and continuous molecular size distributions by means of diffusion-ordered 2D NMR spectroscopy. *J. Am. Chem. Soc.* **115**, 4291–4299 (1993).

^[212] Johnson Jr., C. S. Diffusion ordered nuclear magnetic resonance spectroscopy: principles and applications. *Prog. NMR Spectrosc.* **34**, 203–256 (1999).

^[213] Huo, R.; Wehrens, R.; van Duynhoven, J.; Buydens, L. M. C., Assessment of techniques for DOSY NMR data processing. *Anal Chim Acta*, **490** (1-2), 231-251 (2003)

invasively virtually separate complex mixtures of molecules, thus explaining the success of its recent implementation in DCC.^[214]

All these elements have to stay in mind when designing new profragrances. In the next chapters, I will present the approach developed during my PhD and the results obtained to create chemical delivery systems based on imine derivatives that combine the advantages of DCC (easy *in situ* synthesis, versatility) to that of surfactants (encapsulation, catalysis and stabilisation properties).

In the next chapters, I will present the approach developed during my PhD and the results obtained to create chemical delivery systems based on imine derivatives that combine the advantages of DCC (easy *in situ* synthesis, versatility) to that of surfactants (encapsulation, catalysis and stabilisation properties).

^[214] Giuseppone, N.; Schmitt, J.-L.; Allouche, L.; Lehn, J.-M. DOSY NMR experiments as a tool for the analysis of constitutional and motional dynamic processes: implementation for the driven evolution of dynamic combinatorial libraries of helical strands. *Angew. Chem. Int. Ed.* **47**, 2235-2239(2008).

2/ General Procedures

a) Solvent and chemical reagents

All reagents and solvents were purchased at the highest commercial quality or graciously provided by Firmenich (for fragrance aldehydes and industrial formulations) or by other companies (Huntsman for Jeffamines) and used without further purification unless otherwise noted. Dry solvents were obtained using a double column SolvTech purification system. Water was deionized by using a milli-gradient system (Millipore, Molsheim, France). Yields refer to spectroscopically purified (^1H NMR) homogeneous materials.

b) Chromatographic methods

Thin Layer Chromatographies were performed using TLC Al foils (silica gel matrix with fluorescent indicator 254 nm, L x W 20 cm x 20 cm, thickness 500 μm , Sigma-Aldrich) or aluminium oxide on TLC-glass plates (fluorescent indicator 254 nm, L x W 20 cm x 20 cm, thickness 250 μm , particle size 11.0-14.0 μm , 60 Å medium pore diameter, Sigma-Aldrich). In all cases, irradiation using a *Bioblock VL-4C* UV-Lamp (6 W, 254 nm and 365 nm) as well as Ce-molybdate and Iodine stainings were used for visualization. *Preparative Adsorption Flash Column Chromatographies* were performed using silica gel (60 Å, 230 – 400 mesh, 40 – 63 μm , Sigma-Aldrich) or aluminium oxide 90 (standardized activity II, 70 – 230 mesh, Merck).

c) Analytical methods and instruments

i) Nuclear Magnetic Resonance (NMR)

^1H NMR spectra were recorded on a *Bruker Avance 400* spectrometer at 400 MHz and ^{13}C spectra at 100 MHz. The spectra were internally referenced to the residual proton solvent signal. Residual solvent peaks were taken as reference (CDCl_3 : 7.26 ppm, D_2O : 4.79 ppm, CD_3OD : 3.31 ppm, CD_3CN : 1.94 ppm). For ^1H NMR assignments, the chemical shifts are given in ppm. Coupling constants J are given in Hz. Peaks are described as singlet (s), doublet (d), triplet (t), quartet (q), multiplet (m) and broad (br). The lists of ^{13}C peaks are not

furnished when the imines could not be fully condensed (traces of aldehydes, happens usually with aliphatic imines) and for the complex Jeffamine-based imine.

ii) Mass spectrometry

Ultra Performance Liquid Chromatographies coupled to Mass Spectroscopy (UPLC-MS) were carried out on a *Waters Acquity UPLC-SQD* apparatus equipped with a PDA detector (190–500 nm, 80Hz), using a reverse phase column (Waters, BEH C18 1.7 μm , 2.1 x 50 mm), the MassLynx 4.1 – XP software and a gradient (water acetonitrile + 0.1% TFA) as eluent.

iii) TEM

TEM was performed using a CM12 Philips microscope equipped with a MVIII (Soft Imaging System) CCD camera. Image treatments were performed by using analySIS (Soft Imaging System) software. Samples were prepared by dropping solution sample on a carbon-coated copper grid. The drop was left to adsorb for 30 seconds on the grid and the remaining solution was absorbed with a filter paper.

iv) Diffusion ordered spectroscopy NMR (DOSY NMR)

^1H NMR spectra were recorded on a *Bruker Avance 500* spectrometer at 500 MHz available at the NMR service of the Institut de Chimie de Strasbourg. Spectra were internally referenced to the residual proton solvent signal. Residual solvent peaks were taken as reference (D_2O : 4.79 ppm). The NMR probe is an Inverse Proton X equipped with a gradient Z bobbin, able to generate PFGs (pulse field gradients) of 70 Gauss/cm with a power amplifier of 10 A.

v) Small angle neutron scattering (SANS)

SANS spectra were performed on the PAXE spectrometer at the Laboratoire Leon Brillouin (LLB, CEA Saclay).

vi) Dynamic and static light scattering (DLS/SLS)

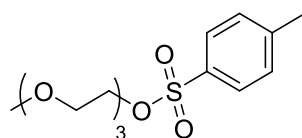
DLS and SLS spectra were performed at the University Paris Diderot on the 3D DLS spectrometer (LS Instruments, Fribourg, Switzerland) equipped with a 25mW HeNe laser (JDS uniphase) operating at 632.8 nm, a two channel multiple tau correlator (1088 channels in autocorrelation), a variable-angle detection system, and a temperature-controlled index matching vat (LS Instruments). The scattering spectrum was measured using two single mode fibre detections and two high sensitivity APD detectors (Perkin Elmer, model SPCM-AQR-13-FC). Solutions were directly filtered through 0.22 μ m Millipore filter into the scattering cell.

Particule size measurements were performed by a ZetaSizer Nano ZS (Malvern Instrument, Worcestershire, U. K.).

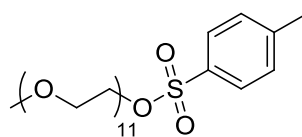
3/ Synthesis of hydrophilic amine derivatives

General procedure for the tosylation of poly(ethylene glycol)

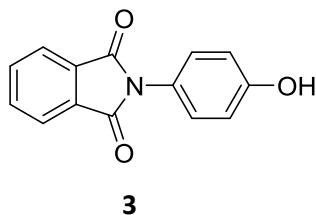
Monomethylether polyethylene glycol (1 eq.) was dissolved in pyridine (1 mL for 1 g of PEG) at 0°C. A solution of tosyl chloride (3.6 eq.) in pyridine (0.3 mL for 1 mmol of tosyl chloride) was then added slowly at -5°C. The mixture was stirred for 4 to 48 h at 0°C, and treated by adding ice with a 6N HCl solution (5 mL for 1 mL of the total volume of pyridine). The mixture was extracted three times with dichloromethane (3 mL for 1 mL of aqueous solution) and the organic layer was washed with a 2N HCl solution (1 mL for 3 mL of organic solution). The organic layer was dried with magnesium sulfate and evaporated to provide pure tosylated compounds as a clear yellow oil (89% - 97%).

Compound 1: PEG₃Tosylate**1**

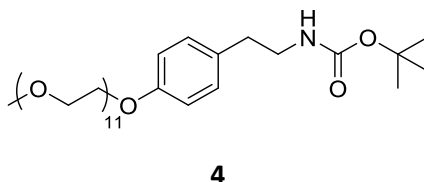
¹H NMR (CDCl₃, 400 MHz, 25°C): δ = 7.77 (d, *J* = 8.4 Hz, 2H), 7.32 (d, *J* = 8.2 Hz, 2H), 4.14 (t, *J* = 4.8 Hz, 2H), 3.67 (t, *J* = 4.8 Hz, 2H), 3.59 (m, 6H), 3.51 (m, 2H), 3.35 (s, 3H), 2.43 (s, 3H); ¹³C NMR (CDCl₃, 400 MHz, 25°C): δ = 144.81, 133.02, 129.76, 128.01, 71.90, 70.74, 70.55, 69.24, 68.67, 59.02, 21.63; ESI-MS: calcd for C₁₄H₂₂O₆S 319.11 [M+H]⁺; found 319.28.

Compound 2: PEG₁₁Tosylate**2**

¹H NMR (CDCl₃, 400 MHz, 25°C): δ = 7.76 (d, *J* = 8.4 Hz, 2H), 7.30 (d, *J* = 8.3 Hz, 2H), 4.12 (t, *J* = 4.8 Hz, 2H), 3.64 (t, *J* = 5.0 Hz, 2H), 3.62 (m, 6H), 3.60 (m, 24H), 3.57 (m, 4H), 3.54 (m, 4H), 3.51 (m, 2H), 3.34 (s, 3H), 2.41 (s, 3H); ¹³C NMR (CDCl₃, 400 MHz, 25°C): δ = 144.77, 133.02, 129.82, 127.96, 71.92, 70.72, 70.55, 70.49, 69.25, 68.67, 59.01, 21.63; ESI-MS: calcd for C₃₀H₅₄SO₁₄ 688.34 [M+H₂O]⁺; found 688.58.

Compound 3: 2-(4-hydroxyphenyl)isoindoline-1,3-dione ^[215]

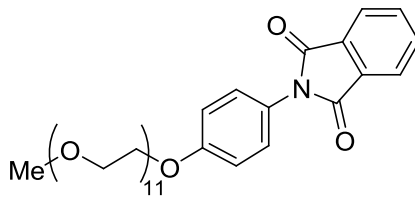
¹H NMR (CDCl₃, 400 MHz, 25°C): δ = 7.94 (m, 2H), 7.78 (m, 2H), 7.30 (d, *J* = 8.8 Hz, 2H), 6.95 (d, *J* = 8.8 Hz, 2H); ¹H NMR in DMSO: 9.77 (s, 1H), 7.93 (m, 2H), 7.88 (m, 2H), 7.21 (d, *J* = 8.7, 2H), 6.88 (d, *J* = 8.7, 2H); ¹³C NMR in DMSO: 167.43, 157.32, 134.64, 131.61, 128.84, 123.31, 122.85, 115.42; Anal. calcd. for C₁₄H₉NO₃: C 70.29, H 3.79, N 5.86; found C 67.70, H 4.06, N 5.80.

Compound 4: PEG₁₁Tyramine N-Boc

Commercially available boc-protected Tyramine (1000 mg, 1 eq., 4,216 mmol) was dissolved in acetonitrile (10 mL for 1 g of PEG₁₁Tosylate) and the solution was heated up to reflux. Potassium carbonate (932 mg, 1.6 eq., 6,746 mg) was then added followed by the tosylated polyethylene glycol (2757 mg, 1 eq., 4,216 mmol). The mixture was stirred for 12 h at reflux. The solvent was then evaporated, dichloromethane (100mL) was added and the solution was filtered. The aqueous mixture was washed three times with a saturated aqueous solution of NaHCO₃ (20mL). The resulting organic phase was then dried with sodium sulfate and further evaporation under reduced pressure afforded pure compound (2820 mg, 91%).

¹H NMR (CDCl₃, 400 MHz, 25°C): δ = 7.08 (d, *J* = 8.6 Hz, 2H), 6.85 (d, *J* = 8.6 Hz, 2H), 4.53 (s, 1H), 4.10 (t, *J* = 5.0 Hz, 2H), 3.84 (t, *J* = 5.0 Hz, 2H), 3.77-3.50 (m, 40H), 3.37 (s, 3H), 3.35-3.26 (m, 2H), 2.72 (t, *J* = 6.9 Hz, 2H), 1.43 (s, 9H); ¹³C NMR (CDCl₃, 400 MHz, 25°C): δ = 156.86, 155.36, 130.80, 129.12, 114.16, 71.39, 70.24, 70.07, 70.03, 69.93, 69.19, 66.94, 58.36, 41.55, 34.79, 27.94; ESI-MS: calcd for C₃₆H₆₅NO₁₄ 758.44 [M+Na]⁺; found 758.44.

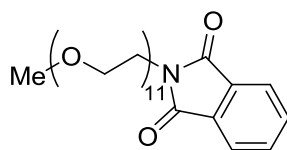
^[215] Compound synthesised and characterized by Rémi Nguyen, former Ph.D. student in the SAMS team. Rémi Nguyen, Dynamic Combinatorial Mesophases and Self-Replicating Systems, University of Strasbourg, 22 September 2010.

Compound 5: PEG₁₁Phenylphthalimide

5

2-(4-hydroxyphenyl)isoindoline-1,3-dione (952 mg, 1.4 eq.) was dissolved in acetonitrile (25 mL for 1 g of PEG₁₁Tosylate) and the solution was heated up to reflux. Potassium carbonate (627 mg, 1.6 eq.) was then added followed by the tosylated polyethylene glycol (2000mg, 1 eq.). The mixture was stirred for 12h at reflux. The solvent was then evaporated and water was added (10 mL for 1g of PEG₁₁Tosylate). The aqueous mixture was extracted three times with dichloromethane (3 mL for 1 mL of aqueous solution). The resulting organic phase was then washed with a saturated sodium carbonate solution (1 mL for 3 mL of organic solution), dried with magnesium sulfate and further evaporation under reduced pressure afforded pure compound (1444 mg, 69%).

¹H NMR (CDCl₃, 400 MHz, 25°C): δ = 7.94 (m, 2H), 7.78 (m, 2H), 7.32 (d, *J* = 9.2 Hz, 2H), 7.03 (d, *J* = 9.2 Hz, 2H), 4.17 (t, *J* = 5.2 Hz, 2H), 3.87 (t, *J* = 5.2 Hz, 2H), 3.73 (m, 2H), 3.64 (m, 36H), 3.54 (m, 2H), 3.37 (s, 3H); ¹³C NMR (CDCl₃, 400 MHz, 25°C): δ = 167.54, 158.47, 134.31, 131.84, 127.91, 124.57, 123.68, 115.18, 71.94, 70.88, 70.65, 70.57, 69.65, 67.74, 59.05; ESI-MS: calcd for C₃₇H₅₅NO₁₄ 755.38 [M+H₂O]⁺; found 755.75.

Compound 6: PEG₁₁Phtalimide

6

Phtalimide (877,5 mg, 1.4 eq.) was dissolved in acetonitrile (30 mL for 1 g of phtalimide) and the solution was heated up to reflux. Potassium carbonate (942,1 mg, 1.6 eq.) was then added followed by the PEG₁₁Tosylate (3000 mg, 1.0 eq.). The mixture was stirred for 12 h at reflux. The solvent was then evaporated and water was added (10 mL for 1g of PEG₁₁Tosylate). The aqueous mixture was extracted three times with dichloromethane (3 mL for 1 mL of aqueous solution). The resulting organic phase was then washed with a saturated sodium carbonate

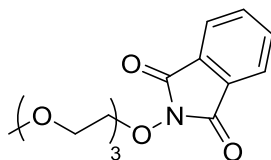
solution (1 mL for 3 mL of organic solution), dried with magnesium sulfate and further evaporation under reduced pressure afforded pure compound (1981 mg, 72%).

^1H NMR (CDCl_3 , 400 MHz, 25°C): δ = 7.83 (m, 2H), 7.70 (m, 2H), 3.88 (t, J = 5.8 Hz, 2H), 3.73 (t, J = 5.8 Hz, 2H), 3.63 (m, 40H), 3.37 (s, 3H); ^{13}C NMR (CDCl_3 , 400 MHz, 25°C): δ = 168.24, 133.92, 132.14, 123.24, 71.94, 70.57, 70.09, 67.92, 59.05, 37.28; ESI-MS: calcd for $\text{C}_{31}\text{H}_{51}\text{NO}_{13}$ 663.34 $[\text{M}+\text{H}_2\text{O}]^+$; found 663.68.

General procedure for the substitution of the tosylate with *N*-hydroxyphthalimide

N-hydroxyphthalimide (1.2 eq.) was dissolved in acetonitrile (20 mL for 1 g of *N*-hydroxyphthalimide) and the solution was heated up to reflux. Triethylamine (1.2 eq.) was then added followed by the tosylated polyethylene glycol (1.0 eq.). The mixture was stirred for 12 h at reflux. The solvent was then evaporated and water was added (10 mL for 1g of $\text{PEG}_{11}\text{Tosylate}$). The aqueous mixture was extracted three times with dichloromethane (3 mL for 1 mL of aqueous solution). The resulting organic phase was then washed with a saturated sodium carbonate solution (1 mL for 3 mL of organic solution), dried with magnesium sulfate and further evaporation under reduced pressure afforded pure compound (70% - 80%).

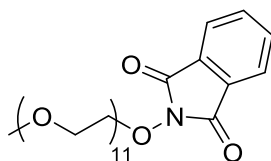
Compound 7: $\text{PEG}_3\text{Hydroxyphthalimide}$



7

^1H NMR (CDCl_3 , 400 MHz, 25°C): δ = 7.84 (m, 2H), 7.74 (m, 2H), 4.37 (t, J = 4.4 Hz, 2H), 3.86 (t, J = 4.4 Hz, 2H), 3.67 (m, 2H), 3.57 (m, 4H), 3.49 (m, 2H), 3.35 (s, 3H); ^{13}C NMR (CDCl_3 , 400 MHz, 25°C): δ = 163.44, 134.44, 129.03, 123.49, 77.21, 71.89, 70.81, 70.54, 70.49, 69.31, 59.01; ESI-MS: calcd for $\text{C}_{15}\text{H}_{19}\text{NO}_6$ 310.13 $[\text{M}+\text{H}]^+$; found 310.25.

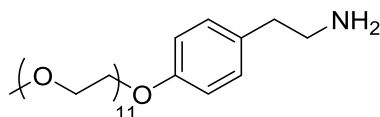
Compound 8: $\text{PEG}_{11}\text{Hydroxyphthalimide}$



8

^1H NMR (CDCl_3 , 400 MHz, 25°C): δ = 7.82 (m, 2H), 7.74 (m, 2H), 4.36 (t, J = 4.6 Hz, 2H), 3.85 (t, J = 4.6 Hz, 2H), 3.63 (m, 40H), 3.36 (s, 3H); ^{13}C NMR (CDCl_3 , 400 MHz, 25°C): δ = 163.43, 134.44, 129.01, 123.49, 77.22, 71.94, 70.79, 70.57, 70.51, 69.31, 59.00; ESI-MS: calcd for $\text{C}_{31}\text{H}_{51}\text{NO}_{14}$ 679.34 $[\text{M}+\text{H}_2\text{O}]^+$: found 679.71

Compound 9: PEG₁₁Tyramine



9

PEG₁₁Tyramine Boc-protected (2000 mg) was dissolved in a $\text{CH}_2\text{Cl}_2/\text{TFA}$ 3:1 mixture (50 mL) and stirred at room temperature. After 2 hours, the mixture was evaporated, dichloromethane (100 mL) was added and the solution was washed with a saturated aqueous solution of NaHCO_3 (3*20 mL).

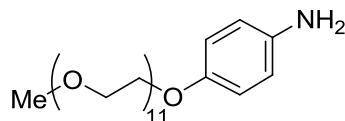
The solution was dried with sodium sulfate and further evaporation under reduced pressure afforded pure compound (1228 mg, 87%).

^1H NMR (CDCl_3 , 400 MHz, 25°C): δ = 7.10 (d, J = 8.6 Hz, 2H), 6.85 (d, J = 8.6 Hz, 2H), 4.11 (t, J = 5.0 Hz, 2H), 3.84 (t, J = 5.0 Hz, 2H), 3.76 – 3.50 (m, 40H), 3.37 (s, 3H), 2.96 (t, J = 7.1 Hz, 2H), 2.71 (d, J = 7.1 Hz, 2H); ^{13}C NMR (CDCl_3 , 400 MHz, 25°C): δ = 157.01, 131.68, 129.40, 114.39, 71.65, 70.52, 70.34, 70.31, 70.29, 70.21, 69.49, 67.21, 58.70, 43.34, 38.58; ESI-MS: calcd for $\text{C}_{31}\text{H}_{57}\text{NO}_{12}$ 636.39; $[\text{M}+\text{H}]^+$; found 636.46.

General procedure for deprotection of phtalimide groups

Phtalimide protected polyethylene glycol (1 eq.) was dissolved in THF (30 mL for 1 g of phtalimide protected PEG) and aqueous hydrazine (40 eq.) was added. The mixture was stirred for 4 h at room temperature. The solvent was evaporated and water was added (10 mL for 1 g of phtalimide protected PEG). The aqueous phase was extracted three times with chloroform (3 mL for 1 mL of aqueous solution) and the combined organic layer was dried with magnesium sulphate. Further evaporation under reduced pressure afforded pure hydrophilic amines as yellow-brown oils (76% - 95%).

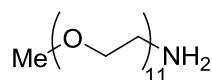
Compound **10**: PEG₁₁Aromatic amine



10

¹H NMR (CDCl₃, 400 MHz, 25°C): δ = 6.73 (d, *J* = 8.0 Hz, 2H), 6.62 (d, *J* = 8.0 Hz, 2H), 4.05 (t, *J* = 4.8 Hz, 2H), 3.80 (t, *J* = 4.8 Hz, 2H), 3.65 (m, 40H), 3.37 (s, 3H); ESI-MS: calcd for C₂₉H₅₃NO₁₂ 608.36 [M+H]⁺; found 608.67.

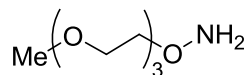
Compound **11**: PEG₁₁Amine



11

¹H NMR (CDCl₃, 400 MHz, 25°C): δ = 3.64 (m, 40H), 3.52 (m, 2H), 3.37 (s, 3H); 2.89 (t, *J* = 4.8 Hz, 2H); ¹³C NMR (CDCl₃, 400 MHz, 25°C): δ = 72.9, 72.0, 70.05, 70.06, 70.3, 59.0, 41.7; ESI-MS: calcd for C₂₃H₄₉NO₁₁ 516.34 [M+H]⁺; found 516.66.

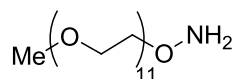
Compound **12**: PEG₃Hydroxyamine



12

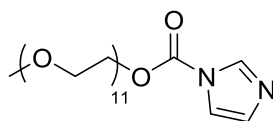
¹H NMR (CDCl₃, 400 MHz, 25°C): δ = 3.83 (m, 2H), 3.66 (m, 8H), 3.54 (m, 2H), 3.37 (s, 3H); ¹³C NMR (CDCl₃, 400 MHz, 25°C): δ = 74.79, 72.57, 71.93, 70.60, 70.53, 69.61, 59.04; ESI-MS: calcd for C₇H₁₇NO₄ 180.13 [M+H]⁺; found 180.21.

Compound **13**: PEG₁₁Hydroxyamine



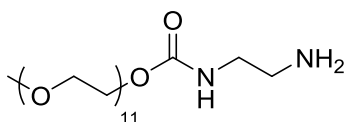
13

¹H NMR (CDCl₃, 400 MHz, 25°C): δ = 3.83 (t, *J* = 5.0 Hz, 2H), 3.66 (m, 40H), 3.54 (m, 2H), 3.37 (s, 3H).

Compound 14: PEG₁₁Imidazole Carboxylate**14**

1,1'-Carbonyldiimidazole (1769 mg, 3 eq., 10,91 mmol) was dissolved in CHCl₃ (10 mL) with PEG₁₁OH (2000 mg, 1 eq., 3,64 mmol) and stirred at room temperature. After 2 hours, brine (5 mL) was added and the mixture was stirred for 15 minutes. Layers were separated and the organic phase was dried with sodium sulfate and evaporated. (2342 mg, quant.)

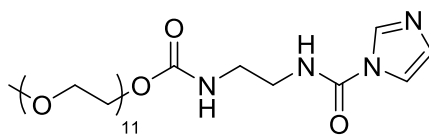
¹H NMR (CDCl₃, 400 MHz, 25°C): δ = 8.15 (t, *J* = 1.0 Hz, 1H), 7.44 (t, *J* = 1.5 Hz, 1H), 7.06 (dd, *J* = 1.5, 1.0 Hz, 1H), 4.55 (t, *J* = 4.7 Hz, 2H), 3.83 (t, *J* = 4.7 Hz, 2H), 3.75 – 3.49 (m, 40H), 3.37 (s, 3H).

Compound 15: PEG₁₁Carbamate Amine**15**

1,1'-Carbonyldiimidazole (1769 mg, 3 eq., 10,91 mmol) was dissolved in CHCl₃ (5 mL) with PEG₁₁OH (2000 mg, 1 eq., 3,64 mmol) and stirred at 0°C. After 2 hours, brine (5 mL) was added and the mixture was stirred for 15 minutes. Layers were separated and the organic phase was dried with sodium sulfate. This mixture was then added to ethylene diamine (21 mL, 100 eq.) in CHCl₃ (2 mL) and stirred at room temperature for 12 hours. The solution was evaporated, CHCl₃ (10 mL) and brine (3*5 mL) were added, the mixture was stirred for 15 minutes and layers were separated. The solution was dried with sodium sulfate and further evaporation under reduced pressure afforded pure compound (1732 mg, 79%).

¹H NMR (CDCl₃, 400 MHz, 25°C): δ = 5.50 (s, 1H), 4.21 (t, *J* = 4.7 Hz, 2H), 3.84 – 3.40 (m, 40H), 3.37 (s, 3H), 3.24 (q, *J* = 5.9 Hz, 2H), 2.83 (t, *J* = 5.9 Hz, 2H); ESI-MS: Calcd for C₂₆H₅₄N₂O₁₃ 625.36 [M+Na]⁺; found 625.39.

Compound 16: PEG₁₁Carbamate Imidazole Carboxamide

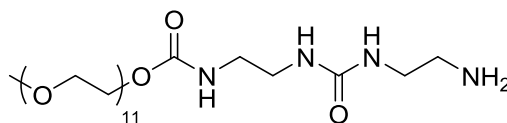


16

1,1'-Carbonyldiimidazole (347 mg, 3 eq., 2,14 mmol) was dissolved in CHCl₃ (5 mL) with PEG₁₁Carbamate amine (500 mg, 1 eq., 0,71 mmol) and stirred at 0 °C. After 2 hours, brine (5 mL) was added and the mixture was stirred for 15 minutes. Layers were separated and the organic phase was dried with sodium sulfate and further evaporation under reduced pressure afforded pure compound (512 mg, 97%).

¹H NMR (CDCl₃, 400 MHz, 25°C): δ = 8.45 (s, 1H), 8.26 (s, 1H), 7.57 (s, 1H), 7.03 (s, 1H), 6.21 (s, 1H), 4.19 (t, *J* = 4.5 Hz, 2H), 3.84 – 3.24 (m, 49H);

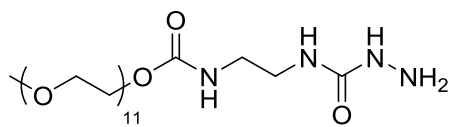
Compound 17: PEG₁₁Carbamate Urea Amine



17

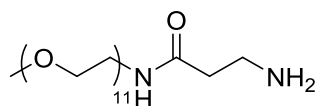
PEG₁₁Carbamate imidazole carboxamide (100 mg, 1 eq., 0,14 mmol) was dissolved in a solution of ethylene diamine (823 mg, 100 eq., 0,9 mL) in CHCl₃ (3 mL) and stirred at room temperature for 12 hours. The solvent was evaporated, CHCl₃ (10 mL) and brine (3*5mL) were added, the mixture was stirred each time for 20 minutes and layers were separated. The organic phase was dried with sodium sulfate and further evaporation under reduced pressure afforded pure compound (74 mg, 77%).

¹H NMR (CDCl₃, 400 MHz, 25°C): δ = 6.01 (s, 1H), 5.72 (s, 1H), 5.56 (s, 1H), 4.27 – 4.07 (m, 2H), 3.81 – 3.09 (m, 48H), 3.34 (s, 3H), 2.80 – 2.72 (m, 2H); ¹³C NMR (CDCl₃, 400 MHz, 25°C): δ = 159.48, 157.00, 77.48, 77.36, 77.16, 76.84, 71.97, 70.61, 70.55, 69.68, 63.83, 59.07, 42.97, 42.35, 41.90, 40.11; ESI-MS: calcd for C₂₉H₆₀N₄O₁₄ 689.41 [M+H]⁺; found 689.67.

Compound 18: PEG₁₁Carbamate Semicarbazide**18**

PEG₁₁Carbamate imidazole carboxamide (100 mg, 1 eq., 0,14 mmol) was dissolved in a solution of hydrazine in water (342 mg, 100 eq., 6,848 mmol) and stirred at room temperature for 12 hours. The solvent was evaporated, CHCl₃ (10 mL) and brine (3*5 mL) were added, the mixture was stirred each time for 20 minutes and layers were separated. The organic phase was dried with sodium sulfate and further evaporation under reduced pressure afforded pure compound (75 mg, 77%).

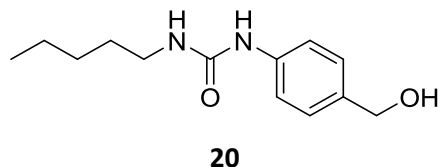
¹H NMR (CDCl₃, 400 MHz, 25°C): δ = 6.42 (s, 1H), 6.33 (s, 1H), 5.92 (s, 1H), 4.23 – 4.03 (m, 2H), 4.00 – 3.10 (m, 46H), 3.29 (s, 3H); ¹³C NMR (CDCl₃, 400 MHz, 25°C): δ = 161.15, 156.74, 77.48, 77.16, 76.84, 71.83, 70.46, 70.41, 69.53, 63.74, 58.93, 41.91, 39.38.

Compound 19: PEG₁₁Amide Amine**19**

To a solution of Boc-β-Ala-OH (103 mg, 2 eq., 0,546 mmol) dissolved in anhydrous CHCl₃ (2 mL), were added in a sequential fashion: EDC (85 mg, 2 eq., 0,546 mmol), DMAP (6,7 mg, 0,2 eq., 0,055 mmol) and PEG₁₁NH₂ (150 mg, 1 eq., 0,273 mmol). After stirring at room temperature for 1h, the reaction was diluted with CHCl₃ (5 mL) and washed with saturated NH₄Cl_{aq} (3*1 mL). The solution was then mixed with a CHCl₃/TFA solution 2:1 (5 mL) for 3 hours, washed with Na₂CO₃ (3*2 mL), dried with sodium sulfate and concentrated under reduced pressure to afford pure compound (86 mg, 51%).

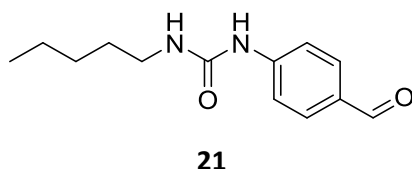
¹H NMR (CDCl₃, 400 MHz, 25°C): δ = 3.74 – 3.49 (m, 44H), 3.49 – 3.39 (m, 2H), 3.36 (s, 3H), 3.07 – 2.96 (m, 2H), 2.40 – 2.34 (m, 2H), 1.24 (s, 2H). ¹³C NMR (CDCl₃, 400 MHz, 25°C): δ = 172.30, 77.48, 77.36, 77.16, 76.84, 72.06, 70.72, 70.69, 70.66, 70.62, 70.27, 70.01, 59.13, 39.04, 38.58, 38.44, 29.80. ESI-MS: calcd for C₂₆H₅₄N₂O₁₂ 587.37 [M+H]⁺; found 587.52.

4/ Synthesis of aldehydes

Compound 20: 1-(4-(hydroxymethyl)phenyl)-3-pentylurea

Ethyl-4-aminobenzoate (1000 mg, 1 eq., 6,05 mmol) was dissolved in CHCl_3 (10mL) under argon and stirred at 0°C . Then, a solution of DIBAL-H (3444 mg, 4 eq., 24,20 mmol) in toluene was added dropwise for 45 minutes and the solution was allowed to reach room temperature. After 2 hours, the reaction was cooled to 0°C and quenched with EtOAc (150 mL). The solution was then stirred for 1 hour with a saturated solution of potassium sodium tartrate (100 mL). The organic layer was dried with magnesium sulfate and further evaporation under reduced pressure afforded a mixture of 4-aminobenzyl alcohol (60%, 3,62 mmol) and 4-nitrobenzyl alcohol (40%). In a schlenk, this mixture was dissolved in CHCl_3 (13mL) under argon and heated up to 60°C and a solution of pentyl isocyanate (410 mg, 0,6 eq., 3,62 mmol) in CHCl_3 (2 mL) was then added dropwise. After 5 days, the precipitate in the Schlenck was filtered off, cleaned with CH_2Cl_2 and dried, affording pure compound (276 mg, 19%).

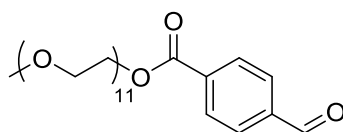
^1H NMR (CDCl_3 , 400 MHz, 25°C): δ = 7.32 (d, J = 8.0 Hz, 2H), 7.27 (d, J = 8.0 Hz, 2H), 6.24 (s, 1H), 4.65 (s, 2H), 3.24 (t, J = 7.2 Hz, 2H), 2.18 (s, 1H), 1.56 – 1.23 (m, 6H), 0.89 (t, J = 6.9 Hz, 3H); ^{13}C NMR (CDCl_3 , 400 MHz, 25°C): δ = 154.11, 146.82, 137.94, 128.19, 121.51, 64.92, 40.53, 29.77, 29.03, 22.36, 13.99;

Compound 21: 1-(4-formylphenyl)-3-pentylurea

1-(4-(hydroxymethyl)phenyl)-3-pentylurea (276 mg, 1 eq, 1,17 mmol) was dissolved in MeOH (15mL) and stirred at room temperature. Then, manganese dioxide (1523 mg, 15 eq, 17,52 mmol) was added. After 3 days, the solution was filtered through celite and further evaporation under reduced pressure afforded pure compound as a white solid (214 mg, 78%).

^1H NMR (CDCl_3 , 400 MHz, 25°C): $\delta = 9.87$ (s, 1H), 7.79 (d, $J = 8.6$ Hz, 2H), 7.51 (d, $J = 8.6$ Hz, 2H), 6.93 (s, 1H), 3.27 (dt, $J = 6.5$ Hz, $J = 6.1$ Hz, 2H), 1.58 – 1.48 (m, 2H), 1.39 – 1.23 (m, 4H), 0.88 (t, $J = 6.8$ Hz, 3H); ^{13}C NMR (CDCl_3 , 400 MHz, 25°C): $\delta = 191.20$, 154.71, 145.24, 131.52, 131.14, 118.46, 40.66, 29.84, 29.17, 22.50, 14.13; ESI-MS: calcd for $\text{C}_{13}\text{H}_{18}\text{N}_2\text{O}_2 + \text{H}^+$ 235.14 $[\text{M} + \text{H}]^+$; found 235.06.

Compound 22: PEG₁₁Benzaldehyde



22

PEG₁₁OH (10000 mg, 1 eq., 18.18 mmol) in CHCl_3 (200 mL) was added to 4-formylbenzoic acid (3276 mg, 1,2 eq., 21,82 mmol), EDC,HCl (3834 mg, 1,1 eq., 20,00 mmol), DMAP (2443 mg, 1,1 eq., 20,00 mmol), and TEA (2024 mg, 1,1 eq., 20,00 mmol) and the mixture was stirred for 12 h. The solution was then washed with HCl 0,1M (3*40mL), with NaHCO_3 (40mL) and with brine (20mL). The organic phase was dried with Sodium sulfate and evaporated under reduced pressure, affording pure compound as a slightly yellow liquid (9665 mg, 82%).

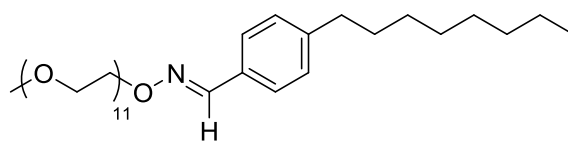
^1H NMR (CDCl_3 , 400 MHz, 25°C): $\delta = 9.83$ (s, 1H), 7.92 (d, $J = 8.2$ Hz, 2H), 7.69 (d, $J = 8.2$ Hz, 2H), 4.23 (t, $J = 4.8$ Hz, 2H), 3.58 (t, $J = 4.8$ Hz, 2H), 3.46 – 3.31 (m, 38H), 3.25 (t, $J = 4.8$ Hz, 2H), 3.07 (s, 3H); ^{13}C NMR (CDCl_3 , 400 MHz, 25°C): $\delta = 190.99$, 164.64, 138.64, 134.34, 129.55, 128.80, 71.26, 70.00, 69.96, 69.94, 69.89, 69.79, 68.34, 63.99, 58.21; ESI-MS: Calcd for $\text{C}_{31}\text{H}_{52}\text{O}_{14}$ 671.34 $[\text{M} + \text{Na}]^+$; found 671.49

5/ Synthesis of dynablocks

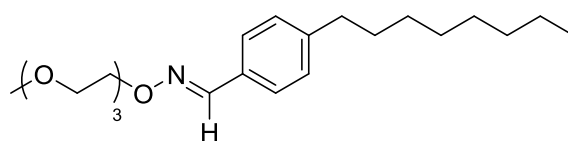
a) Oximes

General procedure for the formation of oxime from poly(ethylene glycol) hydroxylamine derivatives and aldehyde

Aldehyde (1 eq.) and Poly(ethylene glycol) hydroxylamine derivative (1 eq.) were dissolved in chloroform (2 mL for 1 g of PEG amine) under argon at room temperature. The mixture was stirred for 1 to 3 days, until full conversion. The solvent was then evaporated under vacuum for several days to remove the remaining of water, providing ready-to-use oximes and profragrances (96 - 100%).

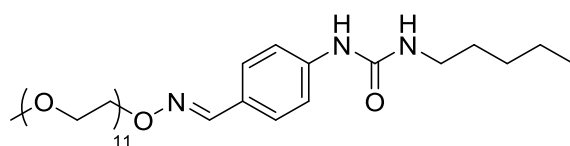
Compound 23: PEG₁₁ONH₂ 4-Octylbenzaldehyde Oxime**23**

¹H NMR (CDCl₃, 400 MHz, 25°C): δ = 8.06 (s, 1H), 7.44 (d, *J* = 8.2 Hz, 2H), 7.14 (d, *J* = 8.2 Hz, 2H), 4.28 (t, *J* = 4.9 Hz, 2H), 3.76 (t, *J* = 4.9 Hz, 2H), 3.69 – 3.48 (m, 40H), 3.35 (s, 3H), 2.57 (t, *J* = 7.5 Hz, 2H), 1.57 (p, *J* = 7.5 Hz, 2H), 1.33 – 1.18 (m, 10H), 0.85 (t, *J* = 7.0 Hz, 3H); ¹³C NMR (CDCl₃, 400 MHz, 25°C): δ = 149.06, 145.09, 129.71, 128.79, 127.03, 77.48, 77.16, 76.84, 73.47, 72.01, 70.73, 70.67, 70.64, 70.57, 70.54, 69.72, 59.05, 35.92, 31.91, 31.31, 29.48, 29.31, 29.27, 22.69, 14.13; ESI-MS: calcd for C₃₈H₆₉NO₁₂ 732.48 [M+H]⁺; found 732.87

Compound 24: PEG₃ONH₂ 4-Octylbenzaldehyde Oxime**24**

^1H NMR (CDCl_3 , 400 MHz, 25°C): $\delta = 8.09$ (s, 1H), 7.48 (d, $J = 7.9$ Hz, 2H), 7.16 (d, $J = 7.9$ Hz, 2H), 4.31 (t, $J = 5.1$ Hz, 2H), 3.79 (t, $J = 5.1$ Hz, 2H), 3.73 – 3.45 (m, 8H), 3.35 (s, 3H), 2.60 (t, $J = 7.6$ Hz, 2H), 1.60 (t, $J = 7.6$ Hz, 2H), 1.36 – 1.24 (m, 10H), 0.88 (t, $J = 6.7$ Hz, 3H); ^{13}C NMR (CDCl_3 , 400 MHz, 25°C): $\delta = 148.77$, 144.82, 129.62, 128.60, 126.87, 77.48, 77.16, 76.84, 73.30, 71.85, 70.58, 70.54, 70.44, 69.56, 58.82, 35.75, 31.76, 31.16, 29.34, 29.15, 29.13, 22.54, 13.98; ESI-MS: calcd for $\text{C}_{22}\text{H}_{37}\text{O}_4$ 380.27 $[\text{M}+\text{H}]^+$; found 380.20

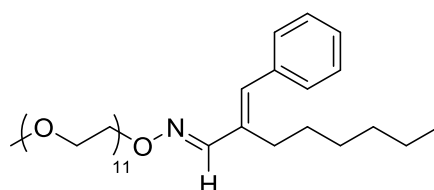
Compound 25: PEG₁₁ONH₂ 1-(4-formylphenyl)-3-pentylurea Oxime



25

^1H NMR (CDCl_3 , 400 MHz, 25°C): $\delta = 7.95$ (s, 1H), 7.83 (s, 1H), 7.50 – 7.27 (m, 4H), 5.71 (t, $J = 5.6$ Hz, 1H), 4.22 (t, $J = 4.7$ Hz, 2H), 3.81 – 3.39 (m, 40H), 3.30 (s, 3H), 3.13 (td, $J = 7.2$, 5.6 Hz, 2H), 1.42 (dt, $J = 7.2$, 6.1 Hz, 2H), 1.30 – 1.18 (m, 4H), 0.82 (t, $J = 6.8$ Hz, 3H); ^{13}C NMR (CDCl_3 , 400 MHz, 25°C): $\delta = 155.74$, 148.78, 141.87, 127.72, 125.33, 118.17, 77.45, 77.13, 76.82, 74.71, 73.18, 71.86, 71.82, 70.57, 70.52, 70.49, 70.45, 69.62, 69.55, 58.92, 39.91, 29.91, 29.08, 22.35, 14.00; ESI-MS: Calcd for $\text{C}_{36}\text{H}_{65}\text{N}_3\text{O}_{13}$ 770.45 $[\text{M}+\text{Na}]^+$; found 770.44.

Compound 26: PEG₁₁ONH₂ Hexylcinnamal Oxime

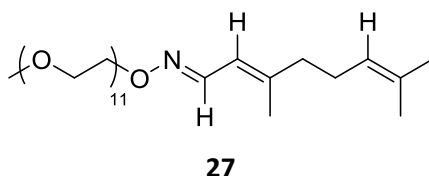


26

^1H NMR (CDCl_3 , 400 MHz, 25°C): $\delta = 7.79$ (s, 1H), 7.40 – 7.27 (m, 5H), 6.56 (s, 1H), 4.26 (t, $J = 4.8$ Hz, 2H), 3.81 – 3.51 (m, 42H), 3.38 (s, 3H), 2.52 (t, $J = 8.1$ Hz, 2H), 1.62 – 1.53 (m, 2H), 1.40 – 1.24 (m, 6H), 0.88 (t, $J = 6.8$ Hz, 3H); ^{13}C NMR (CDCl_3 , 400 MHz, 25°C): $\delta = 153.46$, 137.53, 136.75, 135.89, 129.07, 128.53, 127.60, 73.46, 72.11, 70.83, 70.78, 70.75,

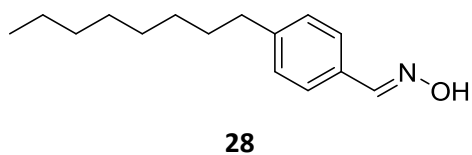
70.69, 69.84, 59.19, 31.65, 29.62, 28.78, 26.89, 22.73, 14.23; ESI-MS: calcd for $C_{38}H_{67}NO_{12}$ 732.47 $[M+H]^+$; found 732.71

Compound 27: PEG₁₁ONH₂ Citral Oxime



¹H NMR (CDCl₃, 400 MHz, 25°C): δ = 8.00 (dd, J = 12.6, 10.0 Hz, 0.7H), 7.21 (t, J = 10.0 Hz, 0.3H), 6.44 – 6.34 (m, 0.3H), 5.91 – 5.77 (m, 0.7H), 5.12 – 4.94 (m, 1H), 4.24 – 4.11 (m, 2H), 3.82 – 3.39 (m, 42H), 3.33 (s, 3H), 2.25 – 2.02 (m, 4H), 1.83 (d, J = 1.4 Hz, 0.5H), 1.81 (d, J = 1.3 Hz, 1.5H), 1.76 (d, J = 1.3 Hz, 1H), 1.66 – 1.60 (m, 3H), 1.57 – 1.52 (m, 3H); ¹³C NMR (CDCl₃, 400 MHz, 25°C): δ = 149.82, 149.61, 148.16, 147.82, 147.64, 147.52, 145.03, 144.71, 132.65, 132.51, 132.16, 123.30, 123.15, 123.03, 118.75, 117.84, 114.47, 113.67, 77.38, 77.27, 77.07, 76.75, 73.29, 73.04, 73.01, 71.91, 70.62, 70.57, 70.55, 70.48, 69.64, 69.58, 58.98, 40.23, 40.01, 32.73, 32.60, 30.87, 26.79, 26.74, 26.25, 26.11, 25.63, 25.61, 24.33, 24.19, 17.69, 17.65, 17.16, 17.02; ESI-MS: calcd for $C_{33}H_{63}NO_{12}$ 666.44 $[M+H]^+$; found 666.68

Compound 28: 4-Octylbenzaloxime

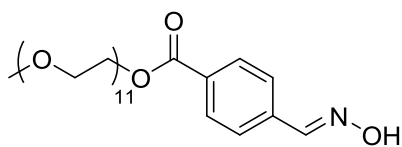


Octylbenzaldehyde (2000 mg, 1 eq., 9,16 mmol) and hydroxylamine hydrochloride (828 mg, 1,3 eq., 11,91 mmol) were dissolved in water/isopropylalcohol mixture 1:1 (50 mL) at room temperature. Sodium hydroxide (440 mg, 1.2 eq., 10,99 mmol) was then added and the mixture was stirred for 3 days. The mixture was then evaporated under vacuum, dissolved in CHCl₃ and filtered. Further evaporation afforded pure compound as a white solid (2136 mg, quant.).

¹H NMR (CDCl₃, 400 MHz, 25°C): δ = 8.12 (s, 1H), 7.47 (d, J = 8.2 Hz, 2H), 7.19 (d, J = 8.2 Hz, 2H), 2.61 (t, J = 7.6 Hz, 2H), 1.67 – 1.54 (m, 2H), 1.37 – 1.21 (m, 10H), 0.88 (t, J = 6.9

Hz, 3H); ^{13}C NMR (CDCl_3 , 400 MHz, 25°C): $\delta = 150.44, 145.46, 129.45, 128.98, 127.16, 36.01, 32.01, 31.37, 29.58, 29.41, 29.38, 22.79, 14.22$; ESI-MS: calcd for $\text{C}_{15}\text{H}_{23}\text{NO}$ 234.18 $[\text{M}+\text{H}]^+$; found 234.01.

Compound 29: PEG₁₁Benzaldoxime



29

PEG₁₁Benzaldehyde (2000 mg, 1 eq., 2,93 mmol) and hydroxylamine hydrochloride (265 mg, 1,3 eq., 0,381 mmol) were dissolved in water (10 mL) at room temperature. Sodium hydroxide (141 mg, 1.2 eq., 3,52 mmol) was then added and the mixture was stirred for 12 hours. The mixture was then evaporated under vacuum, dissolved in CHCl_3 and filtered. Further evaporation afforded pure compound (1944 mg, quant.).

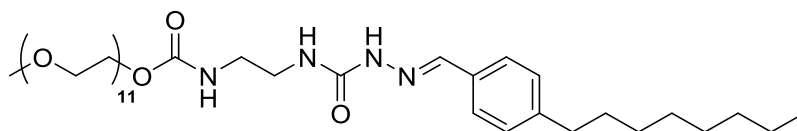
^1H NMR (CDCl_3 , 400 MHz, 25°C): $\delta = 8.97$ (s, 1H), 8.11 (s, 1H), 8.03 (d, $J = 7.2$ Hz, 2H), 7.60 (d, $J = 7.2$ Hz, 2H), 4.46 (t, $J = 4.7$ Hz, 2H), 3.90 – 3.39 (m, 42H), 3.36 (s, 3H); ^{13}C NMR (CDCl_3 , 400 MHz, 25°C): $\delta = 166.15, 148.68, 137.09, 130.91, 130.10, 126.76, 77.48, 77.36, 77.16, 76.84, 72.74, 72.01, 70.82, 70.73, 70.67, 70.64, 70.61, 70.56, 70.39, 69.26, 64.35, 61.77, 59.09$; ESI-MS: calcd $\text{C}_{31}\text{H}_{53}\text{NO}_{14}$ 664.35 $[\text{M}+\text{H}]^+$: 664.56

b) Semicarbazone

General procedure for the formation of hydrazone from poly(ethylene glycol) hydrazine derivatives and aldehyde

Aldehyde (1 eq.) and Poly(ethylene glycol) hydrazine derivative (1 eq.) were dissolved in chloroform (2 mL for 1 g of PEG hydrazine) at room temperature. The mixture was then stirred for 1 to 2 days. The solvent was then evaporated under vacuum for several days to remove the remaining water and reach full conversion, providing ready-to-use hydrazine derivatives (quant.).

Compound **30**: PEG₁₁Carbamate Semicarbazide 4-octylbenzaldehyde Semicarbazone



30

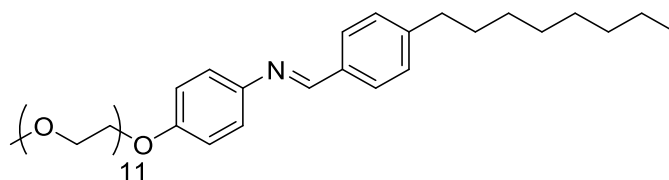
¹H NMR (CDCl₃, 400 MHz, 25°C): δ = 9.55 (s, 1H), 7.71 (s, 1H), 7.48 (d, *J* = 7.8 Hz, 2H), 7.10 (d, *J* = 7.8 Hz, 2H), 6.55 (t, *J* = 5.8 Hz, 1H), 5.78 (t, *J* = 5.6 Hz, 1H), 4.13 (t, *J* = 4.8 Hz, 2H), 3.78 – 2.75 (m, 42H), 3.29 (s, 3H), 2.52 (t, *J* = 7.6 Hz, 2H), 1.59 – 1.46 (m, 2H), 1.33 – 1.08 (m, 10H), 0.80 (t, *J* = 6.4 Hz, 3H); ¹³C NMR (CDCl₃, 400 MHz, 25°C): δ = 157.02, 156.96, 144.77, 141.65, 131.65, 128.64, 126.79, 77.48, 77.16, 76.84, 71.85, 70.50, 70.48, 70.46, 70.41, 69.47, 63.92, 58.90, 41.47, 40.01, 35.80, 31.79, 31.24, 29.37, 29.34, 29.23, 29.17, 22.57, 14.04; ESI-MS: calcd for C₄₂H₇₆N₄O₁₄ 861.54 [M+H]⁺; found 862.02.

c) Imines

General procedure for the formation of imine from poly(ethylene glycol) amine derivatives and aromatic aldehyde

Aromatic aldehyde (1 eq.) and Poly(ethylene glycol) amine derivative (1.2 eq) were dissolved in chloroform (2 mL for 1 g of PEG amine) at room temperature. The mixture was then stirred for 1 to 2 days. The solvent was then evaporated under vacuum for several days to remove the remaining water and reach full conversion, providing ready-to-use imines and profragances (98% - 100%).

Compound **31**: PEG₁₁Aromatic Amine 4-Octylbenzaldehyde Imine

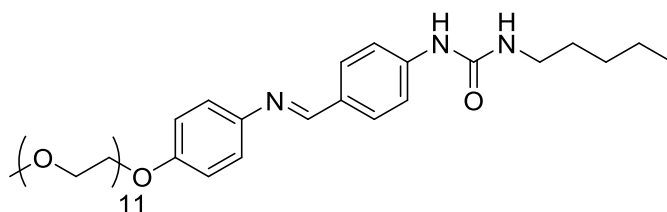


31

¹H NMR (CDCl₃, 400 MHz, 25°C): δ = 8.44 (s, 1H), 7.79 (d, *J* = 8.2 Hz, 2H), 7.26 (d, *J* = 8.2 Hz, 2H), 7.20 (d, *J* = 8.8 Hz, 2H), 6.94 (d, *J* = 8.8 Hz, 2H), 4.15 (t, *J* = 4.9 Hz, 2H), 3.87 (t, *J*

= 4.9 Hz, 2H), 3.79 – 3.43 (m, 38H), 3.38 (s, 3H), 2.66 (t, $J = 7.7$ Hz, 2H), 1.70 – 1.60 (m, 2H), 1.40 – 1.18 (m, 10H), 0.88 (t, $J = 6.6$ Hz, 3H). ESI-MS: calcd for $C_{44}H_{73}NO_{12}$ 808.51 $[M+H]^+$; found 808.76.

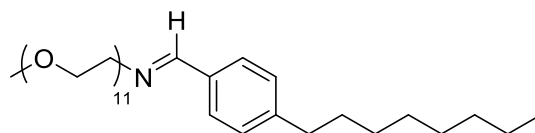
Compound 32: PEG₁₁Aromatic Amine 1-(4-formylphenyl)-3-pentylurea Imine



32

1H NMR ($CDCl_3$, 400 MHz, 25°C): $\delta = 8.31$ (s, 1H), 8.06 (s, 1H), 7.69 (d, $J = 8.2$ Hz, 2H), 7.49 (d, $J = 8.2$ Hz, 2H), 7.12 (d, $J = 8.4$ Hz, 2H), 6.86 (d, $J = 8.4$ Hz, 2H), 5.89 (s, 1H), 4.19 – 3.02 (m, 44H), 3.33 (s, 3H), 1.55 – 1.37 (m, 2H), 1.36 – 1.15 (m, 4H), 0.83 (t, $J = 6.9$ Hz, 3H); ESI-MS: calcd for $C_{42}H_{69}N_3O_{13}$ 824.48 $[M+H]^+$; found 824.99.

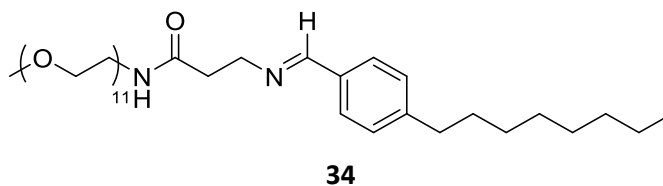
Compound 33: PEG₁₁NH₂ 4-octylbenzaldehyde Imine



33

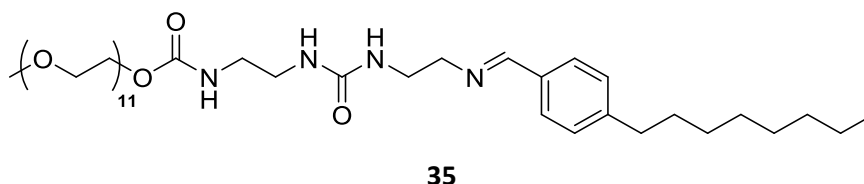
1H NMR ($CDCl_3$, 400 MHz, 25°C): $\delta = 8.24$ (s, 1H), 7.60 (d, $J = 7.8$ Hz, 1H), 7.18 (d, $J = 7.8$ Hz, 2H), 3.83 – 3.41 (m, 44H), 3.35 (s, 3H), 2.59 (t, $J = 7.6$ Hz, 2H), 1.64 – 1.53 (m, 2H), 1.35 – 1.15 (m, 10H), 0.85 (t, $J = 6.7$ Hz, 3H); ^{13}C NMR ($CDCl_3$, 400 MHz, 25°C): $\delta = 162.72, 146.00, 133.85, 128.69, 128.19, 77.48, 77.16, 76.84, 72.01, 70.92, 70.73, 70.67, 70.64, 70.60, 70.57, 70.51, 61.18, 59.07, 35.97, 31.92, 31.34, 29.49, 29.33, 29.29, 22.70, 14.15$; ESI-MS: calcd for $C_{38}H_{69}NO_{11}$ 716.49 $[M+H]^+$; found 716.90

Compound 34: PEG₁₁Amide Amine 4-octylbenzaldehyde Imine



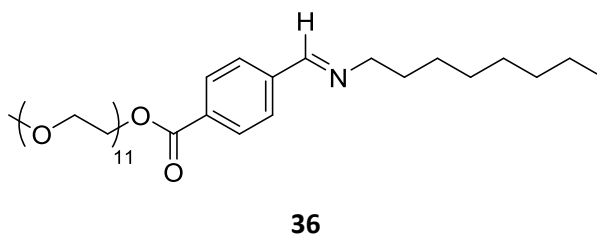
¹H NMR (CDCl₃, 400 MHz, 25°C): δ = 8.27 (s, 1H), 7.61 (d, *J* = 8.2 Hz, 2H), 7.20 (d, *J* = 8.2 Hz, 2H), 7.00 (s, 1H), 3.86 (t, *J* = 6.5 Hz, 2H), 3.73 – 3.41 (m, 44H), 3.38 (s, 3H), 2.62 (t, *J* = 7.7 Hz, 2H), 2.57 (t, *J* = 6.5 Hz, 2H), 1.61 (p, *J* = 7.7 Hz, 2H), 1.36 – 1.18 (m, 10H), 0.88 (t, *J* = 7.1 Hz, 3H). ESI-MS: calcd for C₄₁H₇₄N₂O₁₂ 787.52 [M+H]⁺; found 787.83.

Compound 35: PEG₁₁Carbamate urea Amine 4-octylbenzaldehyde Imine



¹H NMR (CDCl₃, 400 MHz, 25°C): δ = 8.24 (s, 1H), 7.60 (d, *J* = 8.2 Hz, 2H), 7.19 (d, *J* = 8.2 Hz, 2H), 5.75 (s, 1H), 5.48 (s, 1H), 5.15 (s, 1H), 4.26 – 4.13 (m, 2H), 3.86 – 3.08 (m, 50H), 3.36 (s, 3H), 2.60 (d, *J* = 7.0 Hz, 2H), 1.64 – 1.52 (m, 2H), 1.37 – 1.17 (m, 10H), 0.86 (t, *J* = 6.8 Hz, 3H); ESI-MS: calcd for C₄₄H₈₀N₄O₁₄ 890.57 [M+H]⁺; found 890.81.

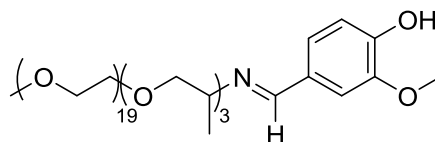
Compound 36: Octylamine PEG₁₁Benzaldehyde Imine



¹H NMR (CDCl₃, 400 MHz, 25°C): δ = 8.24 (s, 1H), 8.01 (d, *J* = 8.3 Hz, 2H), 7.71 (d, *J* = 8.3 Hz, 2H), 4.41 (t, *J* = 4.8 Hz, 2H), 3.77 (t, *J* = 4.8 Hz, 2H), 3.67 – 3.42 (m, 40H), 3.30 (s, 3H), 1.69 – 1.57 (m, 2H), 1.32 – 1.15 (m, 10H), 0.80 (t, *J* = 7.1 Hz, 3H); ¹³C NMR (CDCl₃, 400 MHz, 25°C): δ = 166.02, 159.69, 140.24, 131.53, 129.86, 127.80, 77.48, 77.16, 76.84, 71.84, 70.61, 70.55, 70.52, 70.50, 70.47, 70.40, 69.10, 64.21, 61.84, 61.42, 58.90, 31.75, 30.73,

29.30, 29.15, 27.28, 22.56, 14.02; ESI-MS: Calcd for $C_{39}H_{69}NO_{13}$ 760.48 $[M+H]^+$; found 760.58.

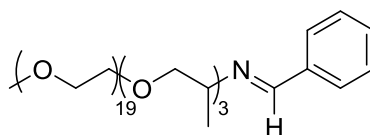
Compound 37: M1000 Vanillin Imine



37

1H NMR ($CDCl_3$, 400 MHz, 25°C): δ = 8.19 (s, 0.5H), 8.18 (s, 0.5H), 7.40 (m, 1H), 7.10 (dd, J = 8.0, 1.8 Hz, 1H), 6.91 (d, J = 8.0 Hz, 1H), 3.94 (s, 3H), 3.78 – 3.12 (m, 85H), 3.37 (s, 3H), 1.27 – 1.00 (m, 9H); ESI-MS: Calcd for $C_{56}H_{105}NO_{24}$ 1176.70 $[M+H]^+$; found 1176.90.

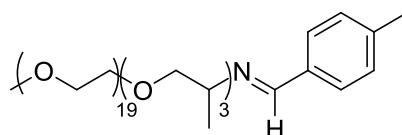
Compound 38: M1000 Benzaldehyde Imine



38

1H NMR ($CDCl_3$, 400 MHz, 25°C): δ = 8.29 (s, *trans*, 0.5H), 8.28 (s, *cis*, 0.5H), 7.75 – 7.65 (m, 2H), 7.42 – 7.32 (m, 3H), 3.86 – 3.03 (m, 88H), 1.28 – 0.92 (m, 9H); ESI-MS: Calcd for $C_{55}H_{103}NO_{22}$ 1130.70 $[M+H]^+$; found 1130.93.

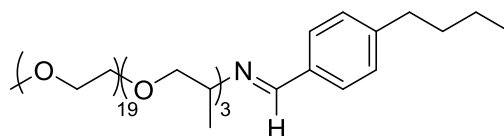
Compound 39: M1000 Tolualdehyde Imine



39

1H NMR ($CDCl_3$, 400 MHz, 25°C): δ = 8.13 (s, 1H), 7.47 (d, J = 7.9 Hz, 2H), 7.06 (d, J = 7.9 Hz, 2H), 3.71 – 3.13 (m, 85H), 2.23 (s, 3H), 1.09 (d, J = 5.7 Hz, 3H), 1.04 – 0.87 (m, 6H); ESI-MS: calcd for $C_{56}H_{105}NO_{22}$ 1145.71 $[M+H]^+$; found 1145.33.

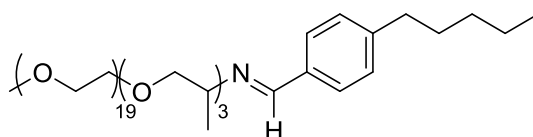
Compound **40**: M1000 4-butylbenzaldehyde Imine



40

^1H NMR (CDCl_3 , 400 MHz, 25°C): δ = 8.26 (s, 1H), 7.62 (d, J = 7.8 Hz, 2H), 7.20 (d, J = 7.8 Hz, 2H), 3.86 – 3.40 (m, 85H), 3.37 (s, 3H), 2.62 (t, J = 7.6 Hz, 2H), 1.58 (m, 2H), 1.34 (m, 2H), 1.22 (d, J = 6.1 Hz, 3H), 1.16 – 1.00 (m, 6H), 0.91 (t, J = 7.3 Hz, 3H); ESI-MS: calcd for $\text{C}_{59}\text{H}_{111}\text{NO}_{22}$ 1187.76 $[\text{M}+\text{H}]^+$; found 1187.49.

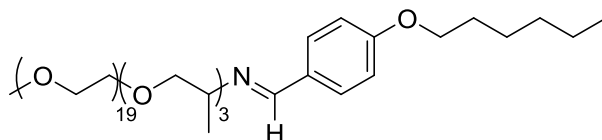
Compound **41**: M1000 4-pentylbenzaldehyde Imine



41

^1H NMR (CDCl_3 , 400 MHz, 25°C): δ = 8.29 (s, 1H), 7.65 (d, J = 7.8 Hz, 2H), 7.22 (d, J = 7.9 Hz, 2H), 3.90 – 3.27 (m, 80H), 3.40 (s, 3H), 2.64 (t, J = 7.3 Hz, 2H), 1.63 (p, J = 7.5 Hz, 2H), 1.39 – 1.04 (m, 13H), 0.91 (t, J = 6.8 Hz, 3H); ESI-MS: Calcd for $\text{C}_{60}\text{H}_{113}\text{NO}_{22}$ 1202.78 $[\text{M}+\text{H}]^+$; found 1202.47.

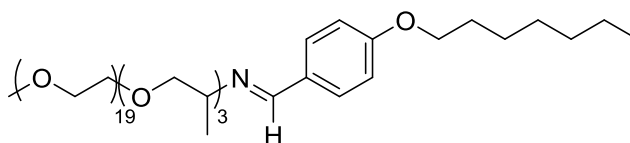
Compound **42**: M1000 4-hexyloxybenzaldehyde Imine



42

^1H NMR (CDCl_3 , 400 MHz, 25°C): δ = 8.22 (s, 1H), 7.64 (d, J = 8.8 Hz, 2H), 6.88 (d, J = 8.8 Hz, 2H), 3.97 (t, J = 6.6 Hz, 2H), 3.78 – 3.27 (m, 85H), 3.37 (s, 3H), 1.77 (m, 2H), 1.45 (m, 2H), 1.38 – 0.81 (m, 16H); ESI-MS: Calcd for $\text{C}_{61}\text{H}_{115}\text{NO}_{23}$ 1230.79 $[\text{M}+\text{H}]^+$; found 1230.85.

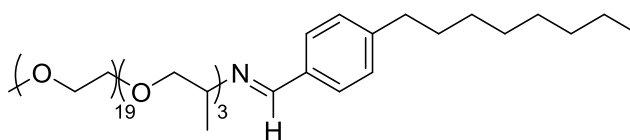
Compound 43: M1000 4-Heptyloxybenzaldehyde Imine



43

$^1\text{H NMR}$ (CDCl_3 , 400 MHz, 25°C): δ = 8.21 (s, 1H), 7.63 (d, J = 8.6 Hz, 2H), 6.87 (d, J = 8.6 Hz, 2H), 3.96 (t, J = 6.6 Hz, 2H), 3.77 – 3.24 (m, 85H), 3.36 (s, 3H), 1.76 (m, 2H), 1.50 – 0.80 (m, 20H); ESI-MS: Calcd for $\text{C}_{62}\text{H}_{117}\text{NO}_{23}$ 1244.80 $[\text{M}+\text{H}]^+$; found 1244.84.

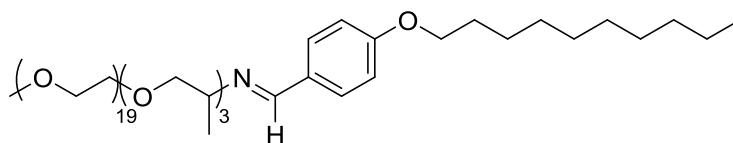
Compound 44: M1000 4-octylbenzaldehyde Imine



44

$^1\text{H NMR}$ (CDCl_3 , 400 MHz, 25°C): δ = 8.26 (s, 1H), 7.61 (d, J = 7.9 Hz, 2H), 7.18 (d, J = 7.9 Hz, 2H), 3.83 – 3.25 (m, 85H), 3.36 (s, 3H), 2.60 (t, J = 7.9 Hz, 2H), 1.59 (m, 2H), 1.38 – 0.79 (m, 21H); ESI-MS: Calcd for $\text{C}_{63}\text{H}_{119}\text{NO}_{22}$ 1242.82 $[\text{M}+\text{H}]^+$; found 1243.12.

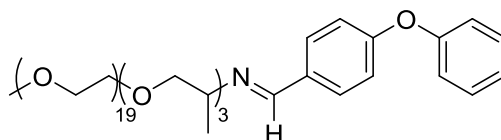
Compound 45: M1000 4-decyloxybenzaldehyde Imine



45

$^1\text{H NMR}$ (CDCl_3 , 400 MHz, 25°C): δ = 8.20 (s, 1H), 7.63 (d, J = 8.7 Hz, 2H), 6.87 (d, J = 8.7 Hz, 2H), 3.95 (t, J = 6.6 Hz, 2H), 3.82 – 3.22 (m, 85H), 3.36 (s, 3H), 1.76 (m, 2H), 1.50 – 0.96 (m, 23H), 0.86 (t, J = 6.6 Hz, 3H);

Compound 46: M1000 4-phenoxybenzaldehyde Imine

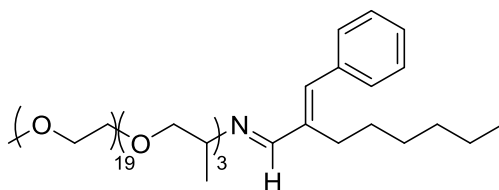


^1H NMR (CDCl_3 , 400 MHz, 25°C): $\delta = 8.18$ (s, 1H), 7.61 (d, $J = 8.5$ Hz, 2H), 7.27 (d, $J = 8.5$ Hz, 2H), 7.08 – 6.87 (m, 5H), 3.76 – 3.06 (m, 85H), 3.28 (s, 3H), 1.14 (d, $J = 5.6$ Hz, 3H), 1.09 – 0.93 (m, 6H); ESI-MS: Calcd for $\text{C}_{61}\text{H}_{107}\text{NO}_{23}$ 1222.72 $[\text{M}+\text{H}]^+$; found 1222.96.

General procedure for the formation of imine from poly(ethylene glycol) amine derivatives and aliphatic aldehyde

Aliphatic aldehyde (1 eq.) and Poly(ethylene glycol) amine derivative (1.2 eq) were dissolved in chloroform (2 mL for 1 g of PEG amine) under argon at room temperature. Sodium sulphate was then added and the mixture was stirred for 1 to 3 weeks, until the conversion has reached at least 95%. The solvent was then evaporated under vacuum for several days to remove the remaining water and reach full conversion, providing ready-to-use imines and profragrances (95% - 99%).

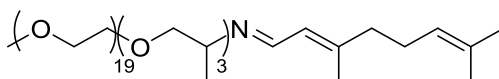
Compound 47: M1000 Hexylcinnamal Imine



47

^1H NMR (CDCl_3 , 400 MHz, 25°C): $\delta = 8.14$ (*cis*, s, 0.1H), 7.83 (*trans*, s, 0.9H), 7.29 - 7.15 (m, 5H), 6.81 (*cis*, s, 0.1H), 6.63 (*trans*, s, 0.9H), 3.75-3.25 (m, 88H), 3.29 (s, 3H), 2.51 (t, $J = 8.0$ Hz, 2H), 1.50-1.42 (m, 2H), 1.31-1.15 (m, 6H), 1.13-0.99 (m, 9H), 0.79 (t, $J = 6.9$ Hz, 3H); ESI-MS: Calcd for $\text{C}_{63}\text{H}_{117}\text{NO}_{22}$ 1240.81 $[\text{M}+\text{H}]^+$; found 1240.92.

Compound 48: M1000 Citral Imine

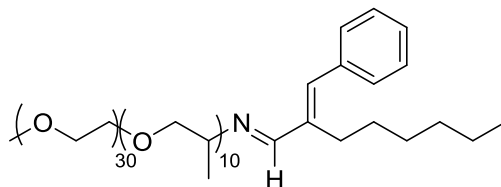


48

^1H NMR (CDCl_3 , 400 MHz, 25°C): $\delta = 8.20$ (d, $J = 9.3$ Hz, 0.5H), 8.15 (d, $J = 9.3$ Hz, 0.5H), 6.03 – 5.91 (m, 1H), 5.21 – 4.96 (m, 1H), 3.82 – 3.23 (m, 85H), 3.36 (s, 3H), 2.36 – 2.02 (m,

4H), 1.89 (s, 1,5H), 1.85 (d, $J = 1.4$ Hz, 1,5H), 1.66 (s, 3H), 1.61 – 1.55 (m, 3H), 1.19 – 0.97 (m, 9H); ESI-MS: Calcd for $C_{58}H_{113}NO_{22}$ 1176.78 $[M+H]^+$; found 1176.94.

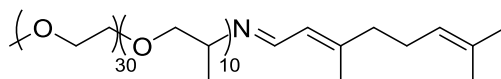
Compound 49: M2070 Hexylcinnamal Imine



49

1H NMR ($CDCl_3$, 400 MHz, 25°C): $\delta = 8.14$ (*cis*, s, 0.1H), 7.83 (*trans*, s, 0.9H), 7.43 – 7.11 (m, 5H), 6.81 (*cis*, s, 0.1H), 6.62 (*trans*, s, 0.9H), 3.85 – 3.14 (m, 150H), 3.29 (s, 3H), 2.51 (t, $J = 8.0$ Hz, 2H), 1.53-1.37 (m, 2H), 1.34 – 1.13 (m, 8H), 1.13-0.98 (m, 30H), 0.79 (t, $J = 6.7$ Hz, 3H)

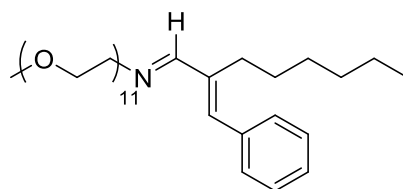
Compound 50: M2070 Citral Imine



50

1H NMR ($CDCl_3$, 400 MHz, 25°C): $\delta = 8.19$ (d, $J = 9.3$ Hz, 0.5H), 8.13 (d, $J = 9.3$ Hz, 0.5H), 6.03 – 5.93 (m, 1H), 5.15 – 5.02 (m, 1H), 3.82 – 3.23 (m, 150H), 3.36 (s, 3H), 2.37 – 1.98 (m, 4H), 1.90 (s, 1.5H), 1.85 (d, $J = 1.4$ Hz, 1.5H), 1.66 (s, 3H), 1.61 – 1.53 (m, 3H), 1.21 – 1.00 (m, 30H).

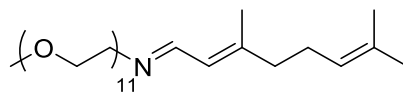
Compound 51: PEG₁₁NH₂ Hexylcinnamal



51

1H NMR ($CDCl_3$, 400 MHz, 25°C): $\delta = 7.91$ (s, 1H), 7.43 – 7.20 (m, 5H), 6.73 (s, 1H), 3.78 – 3.51 (m, 44H), 3.38 (s, 3H), 2.58 (t, $J = 8.2$ Hz, 2H), 1.59 – 1.46 (m, 2H), 1.42 – 1.21 (m, 6H), 0.87 (t, $J = 7.1$ Hz, 3H); ESI-MS: Calcd for $C_{38}H_{67}NO_{11}$ 714.47 $[M+H]^+$; found 714.46.

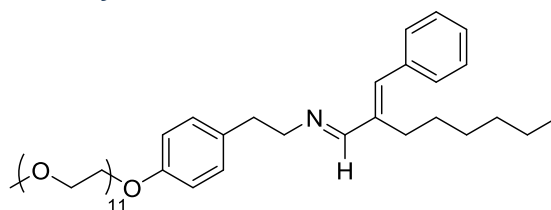
Compound **52**: PEG₁₁NH₂ Citral Imine



52

¹H NMR (CDCl₃, 400 MHz, 25°C): δ = 8.22 (d, *J* = 9.4 Hz, 0.5H), 8.17 (d, *J* = 9.4 Hz, 0.5H), 6.06 – 5.94 (m, 1H), 5.17 – 4.99 (m, 1H), 3.85 – 3.44 (m, 44H), 3.37 (s, 3H), 2.36 – 2.09 (m, 4H), 1.91 (d, *J* = 1.3 Hz, 1.5H), 1.87 (d, *J* = 1.3 Hz, 1.5H), 1.68 (s, 3H), 1.62 – 1.56 (m, 3H); ESI-MS: calcd for C₃₃H₆₃NO₁₁ 650.44 [M+H]⁺; found 650.69.

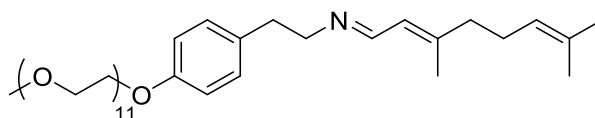
Compound **53**: PEG₁₁Tyramine Hexylcinnamal



53

¹H NMR (CDCl₃, 400 MHz, 25°C): δ = 7.74 (s, 1H), 7.44 – 6.75 (m, 5H), 7.12 (d, *J* = 8.6 Hz, 2H), 6.83 (d, *J* = 8.6 Hz, 2H), 6.67 (s, 1H), 4.10 (t, *J* = 5.0 Hz, 2H), 3.82 (t, *J* = 5.0 Hz, 2H), 3.78 – 3.47 (m, 42H), 3.37 (s, 3H), 3.01 – 2.84 (m, 2H), 2.65 – 2.39 (m, 2H), 1.59 – 1.50 (m, 2H), 1.44 – 1.18 (m, 6H), 0.88 (t, *J* = 6.9 Hz, 3H); ESI-MS: Calcd for C₄₆H₇₅NO₁₂ 834.53 [M+H]⁺; found 834.85.

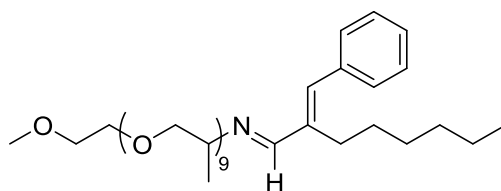
Compound **54**: PEG₁₁Tyramine Citral



54

ESI-MS: calcd for C₄₁H₇₁NO₁₂ 770.50 [M+H]⁺; found 770.67.

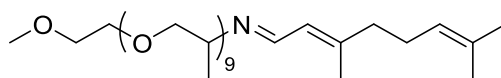
Compound 55: M600 Hexylcinnamal Imine



55

^1H NMR (CDCl_3 , 400 MHz, 25°C): δ = 8.21 (*cis*, s, 0.1H), 7.90 (*trans*, s, 0.9H), 7.39-7.22 (m, 5H), 6.88 (*cis*, s, 0.1H), 6.69 (*trans*, s, 0.9H), 3.68-3.27 (m, 40H), 3.34 (s, 3H), 2.58 (t, J = 7.7 Hz, 2H), 1.60 – 1.44 (m, 2H), 1.37 – 1.21 (m, 6H), 1.21 – 1.05 (m, 27H), 0.85 (t, J = 6.8 Hz, 3H); ESI-MS: calcd for $\text{C}_{45}\text{H}_{81}\text{NO}_{10}$ 795.59 $[\text{M}+\text{H}]^+$; 795.95.

Compound 56: M600 Citral Imine

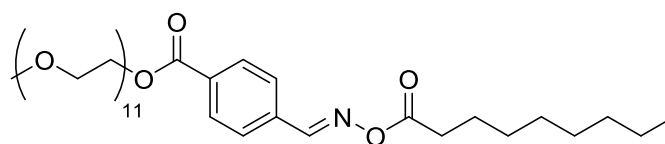


56

^1H NMR (CDCl_3 , 400 MHz, 25°C): δ = 8.21 (d, J = 9.3 Hz, 0,25H), 8.16 (d, J = 9.2 Hz, 0,25H), 6.03 – 5.94 (m, 1H), 5.14 – 5.03 (m, 1H), 3.73 – 3.04 (m, 40H), 3.35 (s, 3H), 2.39 – 2.01 (m, 4H), 1.90 (s, 1,5H), 1.85 (d, J = 1.4 Hz, 1,5H), 1.66 (s, 3H), 1.61 – 1.55 (m, 3H), 1.22 – 0.94 (m, 27H); ESI-MS: calcd for $\text{C}_{40}\text{H}_{77}\text{NO}_{10}$ 732.55 $[\text{M}+\text{H}]^+$; found 732.59.

6/ Acyloxime

Compound 57: PEG₁₁Benzaldoxime Nonanoyl chloride Acyloxime



57

Nonanoyl chloride (152 mg, 3 eq., 0,861 mmol) was added to a solution of PEG₁₁Benzaldoxime (200 mg, 1 eq., 0,287 mmol) and TEA (145 mg, 5 eq., 1,435 mmol) in CHCl_3 (2 mL) and the mixture was stirred for 30 min. The solution was filtered, evaporated, dissolved in brine (5 mL) and filtered again. Then it was dissolved in ether (5 mL), refiltered, dried with sodium sulfate and evaporated under reduced pressure, affording pure compound as a colorless oil (144 mg, 60%).

^1H NMR (CDCl_3 , 400 MHz, 25°C): δ = 8.39 (s, 1H), 8.10 (d, J = 8.4 Hz, 2H), 7.81 (d, J = 8.4 Hz, 2H), 4.49 (d, J = 4.7 Hz, 2H), 3.88 – 3.80 (m, 2H), 3.74 – 3.57 (m, 38H), 3.54 (t, J = 4.7 Hz, 2H), 3.37 (s, 3H), 2.48 (t, J = 7.5 Hz, 2H), 1.72 (m, 2H), 1.37 – 1.29 (m, 10H), 0.88 (d, J = 5.1 Hz, 3H); ^{13}C NMR (CDCl_3 , 400 MHz, 25°C): δ = 171.08, 165.73, 154.90, 134.45, 132.76, 130.17, 128.26, 77.48, 77.16, 76.84, 71.98, 70.73, 70.69, 70.67, 70.64, 70.62, 70.54, 69.17, 64.50, 59.03, 33.92, 32.79, 31.83, 31.82, 29.72, 29.25, 29.21, 29.16, 29.14, 29.12, 24.85, 24.82, 22.66, 14.11;

7/ Kinetic experiments of dynablocks hydrolysis followed by ^1H NMR

Procedure for the hydrolysis of dynablocks in deuterium oxide

A dynablock ($C = 10 \dots 500$ mM) was dissolved in deuterium oxide (0.7 mL) at room temperature (corresponding to $t=0$ of the experiment). The pH was measured and the hydrolysis of the dynablock was followed by ^1H NMR.

8/ Kinetic experiments of dynablocks hydrolysis in formulations followed by ^1H NMR

Procedure for the preparation of alkaline body-wash formulations

Freeze-dried Texapon® NSO IS (4 WT%) was dissolved in deuterium oxide (95 WT%) at room temperature. The dynamic profragrance (1 WT%) was added to the formulation at the beginning of the experiment ($t=0$), pH was measured and NMR measurements were launched.

Procedure for the preparation of neutral body-wash formulations

Freeze-dried Texapon® NSO IS (4 WT%) was dissolved in a pD 7,5 buffer solution of 100 mM HEPES in deuterium oxide (95 WT%) at room temperature. The dynamic profragrance (1 WT%) was added to the formulation at the beginning of the experiment ($t=0$), the pH was measured and NMR measurements were launched.

Procedure for the preparation and hydrolysis of dynablocks in advanced alkaline body-wash formulations

A 65°C melted solution of lauric acid (14,5 wt%), myristic acid (4,8 wt%) and stearic acid (1wt%) is slowly added to a solution of sodium deuterioxide 40% in deuterium oxide (11 wt%) under stirring at 70°C. Then, a solution of Texapon® NSO IS (4 wt%) in deuterium oxide (54,7 wt%) was added to the mixture, and the solution was allowed to reach room temperature. After this, the solid was heated under stirring slightly above the melting temperature (~50°C), and the dynamic profragrance (1 wt%) was added (t=0 of the reaction) and the solution was stirred until full dissolution of the profragrance. The solution was then cooled down to room temperature, providing a white waxy solid. The kinetics of hydrolysis of the imine was followed by NMR after dissolution of 100 mg of the formulation in 900 mg of D₂O.

Procedure for the preparation of neutral liquid detergent formulations

Freeze-dried Hostapur® SAS 60 (7 WT%) and freeze-dried Genapol® LA 70 (17 WT%) were dissolved in deuterium oxide (75 WT%) at room temperature. The dynamic profragrance (1 WT%) was added to the formulation at the beginning of the experiment (t=0), and the pH was measured and NMR measurements were launched.

Procedure for the preparation of alkaline liquid detergent formulations

Freeze-dried Hostapur® SAS 60 (7 WT%) and freeze-dried Genapol® LA 70 (17 WT%) were dissolved in deuterium oxide (75 WT%) at room temperature. Then, sodium deuterioxide 40% in deuterium oxide was added until reaching pH 10. The dynamic profragrance (1 WT%) was added to the formulation at the beginning of the experiment (t=0), the pH was measured and NMR measurements were launched.

9/ Competition experiments of dynablocks studied by ¹H NMR

General protocol for the kinetics of hydrolysis and formation of dynablocks in water

Dynablock(s) (C= 50 mM) in presence or absence of aldehydes were dissolved in deuterium oxide (0,7 mL) at room temperature (t=0 of the experiment). The pH was measured and the hydrolysis of the dynablock was followed by ¹H NMR.

Dynamic covalent surfactants for the controlled release of bioactive volatiles

Résumé

Ce projet consiste à fabriquer et à étudier des micelles à la fois biocompatibles et capables de relarguer des molécules volatiles bioactives à partir d'une solution aqueuse sous l'influence de stimuli extérieurs tel que le pH, la température ou la concentration. Pour atteindre ce but, nous avons étudiés un nouveau type d'objets micellaires qui sont formés par l'auto-assemblage d'amphiphiles covalents dynamiques (DCAs), des surfactants peu onéreux formés de l'association moléculaire réversible d'un bloc hydrophile et d'un bloc hydrophobe. Ces systèmes peuvent relarguer une large gamme de fragrances à partir d'une solution, que cela soit à partir du cœur hydrophobe de la micelle ou alors à partir de l'amphiphile (profragrance). Ils ont aussi été capables de stabiliser en solution des aldéhydes sensibles à l'hydrolyse.

MOTS-CLES: chimie supramoléculaire, amphiphiles, dynablocks, liaison imine, CCD, Tensio-actifs, relargage contrôlé.

Résumé en anglais

This project relies on the simple design and the study of biocompatible responsive micelles, capable of releasing a hydrophobic bioactive volatile from an aqueous solution and that, depending on the modulation of external factors such as pH, temperature, and concentration. To reach this goal, we have taken advantages of a new kind of micellar objects that are formed by the efficient self-assembly of biodegradable Dynamic Covalent Amphiphiles (DCAs), low cost surfactants that are made by the reversible molecular association of one hydrophilic and one hydrophobic block. These systems can release a broad variety of fragrances from solution, both

from the hydrophobic micellar core or directly from the amphiphile (profragrance). It also proved able to stabilise some sensitive aldehydes in solution.

KEYWORDS: supramolecular chemistry, amphiphiles, dynablocks, imine bond, DCC, surfactants, controlled release.